Understanding the mechanisms of *cir1* disease resistance in *Arabidopsis thaliana*

by

Maryke Carstens

Thesis Presented for the Degree of

DOCTOR OF PHILOSOPHY

in the

Department of Molecular and Cell Biology

UNIVERSITY OF CAPE TOWN

April 2008

Chapter 1

Introduction

Chapter 2

Materials and Methods

Chapter 3

Genomic mapping of *cir1*

Chapter 4

Elucidating the mechanisms of *cir1* resistance

Chapter 5

General Discussion

Chapter 6

References

Declaration

I, the undersigned, hereby declare that the work contained in this thesis is my own original work and has not in its entirety or in part been submitted to any university for a degree.

....

Signature: Maryke Carstens Date

Abstract

Understanding the mechanisms of *cir1* disease resistance in *Arabidopsis thaliana*

Maryke Carstens

Thesis presented for the degree of Doctor of Philosophy at the University of Cape Town

April 2008

Plants have evolved an elaborate and very effective defence system to curb disease caused by pathogen infections. To gain insight into the defence signalling network and defence responses deployed by plants for resistance to pathogens, the defence-related *Arabidopsis thaliana* mutant *cir1* (constitutively induced resistance 1) was further investigated. It was previously shown that *cir1* constitutively expresses salicylic acid-, jasmonic acid- and ethylene-dependent defence-related genes and exhibits increased resistance to the virulent bacterial pathogen *Pseudomonas syringae* pv. *tomato* and the virulent oomycete pathogen *Hyaloperonospora parasitica* Noco2. Through first–pass mapping experiments, it was formerly determined that the *CIR1* locus is located on the lower arm of chromosome IV.

With the aim of identifying the *CIR1* gene, comprehensive genomic mapping of *cir1* was conducted in this study. Upon the generation of a suitable mapping population, PCR-based markers were employed to narrow down *CIR1* location to 309.10 kb. This region was included in six genomic DNA clones which were tested for complementation of the *cir1* mutant. A small region in which *CIR1* resides was identified and possible candidate genes within it were investigated. It was established that *CIR1* is one of eight annotated genes.

This study also assessed which known components of the defence signalling network play a role in *cir1*-mediated resistance, to establish a possible function of *CIR1* in the Arabidopsis defence network. Epistasis analyses were performed between *cir1* and the *eds1* (enhanced disease susceptibility 1) and *pad4* (phytoalexin deficient 4) mutants which regulate the salicylic acid signalling pathway, as well as the *coi1* (coronatine-insensitive 1) mutant which functions in the jasmonic acid signalling pathway. The disease resistance profiles of *cir1 eds1*, *cir1 pad4* and *cir1 coi1* double mutants to infection by virulent *P. syringae* and virulent *H. parasitica* established that *coi1*, *pad4* and *eds1* are epistatic to *cir1*, suggesting that *CIR1* is located upstream in the defence signalling network. Through defence-related gene expression profiling, it was found that *cir1* simultaneously activates multiple signalling pathways, resulting in the induced expression of many defence-related genes and the increased expression of some of these genes was correlated to *cir1*'s enhanced resistance to virulent pathogens. Therefore, it appears that CIR1 functions as a negative regulator of the disease resistance signalling network. Furthermore, EDS1 protein accumulation may play a role in *cir1*-mediated resistance as it was found that *cir1* has a stabilizing effect on the EDS1 protein.

Acknowledgements

My sincerest gratitude to the following people and institutions for their contributions to the successful completion of this thesis:

My supervisor, **Dr Katherine Denby**, for her advice, encouragement and helpful discussions throughout my PhD as well as for the critical reading of the manuscript; **Assoc. Prof. Nicci Illing** for acting as an administrative supervisor when Katherine joined the University of Warwick;

Dr Shane Murray for all her help and suggestions during my project as well as the critical reading of the manuscript;

My **lab friends,** especially Lara, Lindsay, Nix, Rob and Linda for invaluable technical discussions, advice and assistance. Thank you for many good laughs both inside and outside of the lab;

The Max Planck Institute for Plant Breeding Research and **Dr Jane Parker** for their hospitality and the opportunity to use their excellent facilities during my research abroad. Thank you to everyone in the Parker-group for your assistance and advice. A special thank you to Enrico, Doris and Jagreet for showing me the sights of Cologne;

The **National Research Foundation**, the **UCT Conference Grant**, the **UCT Travel Grant**, **Dr Katherine Denby** and **my parents** for financial assistance during the course of this work;

My **friends outside of the lab**, especially Peti, Giselle, Reinette & Fats, Esmé, Alex, Jenni, Candide, Robyn as well as the Schulschenk and Gagiano families are warmly thanked for their friendship and constant encouragement;

A very special thank you to my loving parents, **Hennie and Olivia**, and sister, **Ena**, for believing in me. Last, but by no means least, I would like to thank **Marco** for his unconditional love and patience. Thank you for being my best friend.

Publications

Ingle, R. A., Carstens, M. and Denby, K. J. (2006) PAMP recognition and the plant–pathogen arms race. BioEssays **28**: 880–889.

List of abbreviations

°C	degree Celsius
µ	micro
$^1O_2$	singlet oxygen
ACC	1-aminocyclopropane-1-carboxylic acid
APS	ammonium persulphate
At	*Arabidopsis thaliana*
ATP	adenosine 5-triphosphate
Avr	avirulence
BAK1	BRI1-associated receptor kinase 1
Bar	phosphinothricin acetyltransferase gene
bp	base pair(s)
C	carboxy-terminal
CAPS	cleaved amplified polymorphic sequences
CC	coiled-coil
cDNA	complementary deoxyribonucleic acid
cfu	colony forming units
cir1	constitutively induced resistance 1 mutant
cm	centimetre(s)
cM	centiMorgan(s)
COI1	coronatine-insensitive 1
Col-0	*Arabidopsis thaliana* ecotype Columbia
CPR	constitutive expressor of pathogenesis-related genes
CSP	cold shock protein
DEPC	diethylpyrocarbonate
dH_2O	deionised water
DNA	deoxyribonucleic acid
dNTP	deoxynucleosidetriphosphate
dpi	days post inoculation
DTT	dithiothreitol
edr5	enhanced disease resistance 5 mutant
EDS1	enhanced disease susceptibility 1
EDTA	ethylenediamine tetraacetic acid
EFR	elongation factor Tu receptor
EF-Tu	elongation factor Tu
EIN2	ethylene insensitive 2
ERF	ethylene response factor

ET	ethylene
ETI	effector-triggered immunity
Fig.	figure
flg22	flagellin epitope
FLS2	flagellin sensitive 2
g	gram(s)
g	gravity constant (9.81 ms^{-1})
GSNO	*S*-nitrosoglutathione
GSNOR	*S*-nitrosoglutathione reductase
h	hour(s)
H_2O_2	hydrogen peroxide
HPLC	high performance liquid chromatography
HR	hypersensitive response
InDel	insertions/deletion polymorphisms
ISR	induced systemic resistance
JA	jasmonic acid
JAR1	jasmonate resistant 1
JAs	jasmonates
JAZ	jasmonate ZIM-domain
KAPP	kinase-associated protein phosphatase
kb	kilobase(s)
KB	King's broth
kDa	kiloDalton(s)
kV	kilovolt(s)
l	litre(s)
LB	Luria Bertani
L*er*	*Arabidopsis thaliana* ecotype Landsberg *erecta*
LRR	leucine-rich repeat
LUC	firefly luciferase reporter gene
Luc2	Col-0 plants harbouring a *PR-1::LUC* gene cassette
m	milli
M	molar
MAPK	mitogen-activated protein kinase
MAPKK	mitogen-activated protein kinase kinase
MAPKKK	mitogen-activated protein kinase kinase kinase
Mb	megabase(s)
MeJA	methyl jasmonate

$MgCl_2$	magnesium chloride
min	minute(s)
mm	millimetre(s)
mpk4	map kinase 4 mutant
MRC	major recognition complexes
mRNA	messenger ribonucleic acid
MS	Murashige and Skoog
N	amino-terminal
NaCl	sodium chloride
NADPH	nicotine adenine dinucleotide phosphate (reduced form)
NahG	salicylate hydroxylase gene
NBS	nucleotide binding site
ng	nanogram(s)
nm	nanometer(s)
NO	nitric oxide
NPP1	*Phytophthora* protein 1
NPR1	nonexpresser of pathogenesis-related genes 1
NR	nitrate reductase
OB	oxidative burst
OD	optical density
P	probability
PAD4	phytoalexin deficient 4
PAMP	pathogen-associated molecular pattern
PCR	polymerase chain reaction
PDF1.2	plant defensin 1.2
pH	negative decimal logarithm of the H^+ concentration
pmr4	powder mildew resistant 4 mutant
PPT	phosphinothricin
PR	pathogenesis-related
PR-1::LUC	firefly luciferase reporter gene fused to tobacco *PR-1* promoter
PRR	pattern recognition receptor
Psm ES4326	*Pseudomonas syringae* pv. *maculicola* ES4326
Pst DC3000	*Pseudomonas syringae* pv. *tomato* DC3000
PTI	PAMP-triggered immunity
pv.	pathovar
R	resistance
ref2	reduced epidermal fluorescence 2 mutant

RIN4	RPM1 interacting protein 4
RLK	receptor-like kinase
RLP	receptor-like protein
RLU	relative light units
RNA	ribonucleic acid
ROS	reactive oxygen species
rRNA	ribosomal ribonucleic acid
SA	salicylic acid
S-AdoMet	*S*-adenosylmethionine
SAG101	senescence associated gene 101
SAR	systemic acquired resistance
SDS	sodium dodecyl sulphate
sec	second(s)
SID	salicylic acid-induction deficient
siRNA	small interfering ribonucleic acid
SNC1	suppressor of *npr1-1*, constitutive 1
SNO	*S*-nitrosothiol
SNP	single nucleotide polymorphisms
SSI	suppressor of SA insensitivity
SSLP	simple sequence length polymorphisms
T-DNA	transfer deoxyribonucleic acid
TIR	*Drosophila* Toll and human interleukin-1 receptor
U	unit(s)
UV	ultraviolet
V	Volt
v/v	volume per volume
w/v	weight per volume

Table of contents

Chapter 1: Introduction

Plants are extremely important as food and energy sources for humans. Agricultural crops world-wide are plagued by various pathogens and pests including bacteria, fungi, viruses, insects and nematodes, and one of the most serious challenges in agriculture is the reduction of pre- and post-harvest crop loss (Agrios, 2005). The widespread use of pesticides and fungicides has been the most common approach in controlling disease, however disease still continues. Furthermore, the high cost and exposure of the environment to harmful chemicals are encouraging researchers to develop low cost, environmentally-friendly alternative approaches. Through plant breeding, resistance genes from wild populations have been introduced into crop cultivars, however pathogens evolve quickly to overcome this resistance (Agrios, 2005). A promising alternative to generating disease-resistant crops is probably through the manipulation of signal transduction pathways which control the expression of defence-related genes. This approach is likely to provide a stronger mode of resistance than that conferred by a single defence response gene. By activating regulatory or signalling genes, a broad range of defence responses instead of a single response can be induced, making it more difficult for pathogens to overcome. This approach however requires an understanding of plant-pathogen interactions.

1.1 *Arabidopsis thaliana* as a model system

Arabidopsis thaliana (Arabidopsis), a small diploid plant in the *Brassicaceae* family, has several traits that make it an ideal model genetic system for research in plant science (Meinke et al., 1998). Arabidopsis is easy to grow and its small plant size, short life cycle of approximately six weeks and the large amount of seed produced allow for the rapid growth of many plants in a relatively small area (Meinke et al., 1998). The 125 Mb Arabidopsis genome is organized in five chromosomes and was the first plant genome to be fully sequenced in a multinational effort (The Arabidopsis Genome Initiative, 2000). Numerous methods for research on Arabidopsis have been developed including chemical and insertional mutagenesis, efficient transformation methods, a collection of mutants with a diverse range of phenotypes (TAIR, http://www.arabidopsis.org), construction of genetic maps of each chromosome and the development of DNA markers aiding the process of map-based cloning (Jander et al., 2002).

Not only does Arabidopsis have genetic advantages as a model system, it is also host to different classes of pathogens including oomycetes, bacteria, fungi and viruses (Mauch-Mani and Slusarenko, 1993). This makes it an excellent system for studying plant defence responses to pathogen attack. The oomycete, *Hyaloperonospora parasitica* (Parker et al., 1993; McDowell et al., 2000), and bacterial pathogen, *Pseudomonas syringae* (Whalen et al.,

1991; Volko, 1998), have been particularly valuable in the dissection of the mechanisms underlying plant disease and host resistance.

Many disease resistant and enhanced susceptibility mutants to various pathogens have been identified and the ongoing analyses of these mutants are especially useful in unravelling the signal transduction networks leading to activation of defence responses (Glazebrook, 2001; Thatcher et al., 2005). The isolation and analysis of the genes responsible for these abovementioned mutant phenotypes will provide some understanding of defence signalling and responses in Arabidopsis. This knowledge could facilitate the identification of structural and functional orthologues in crop plants as well as elucidating their roles in disease resistance pathways (Hammond-Kosack and Parker, 2003). For example, by using knowledge gained from Arabidopsis-pathogen interactions, several potato homologues of Arabidopsis defence signalling genes were identified and mapped (Pajerowska et al., 2005), establishing a basis for understanding disease resistance in this major crop species. In another study, the Arabidopsis defence signalling gene, *NPR1* (nonexpresser of PR genes 1) was used to genetically engineer disease-resistance in tomato crop plants (Lin et al., 2004). The transgenic tomato lines accumulated higher levels of NPR1 proteins and exhibited enhanced resistance to various tomato diseases.

1.2 The plant immune system

Plants offer a valuable source of nutrition to various microbes and therefore our global food supply is constantly threatened by a multitude of pathogens and pests as plant diseases can considerably reduce the yield of crops (Moffat, 2001). Unlike animals, sessile plants must sense and respond to changing local environments without the advantage of mobility, and therefore all surfaces of plant organs are constantly exposed to various challengers including microbial pathogens, nematodes and insects (Gómez-Gómez, 2004). Plant pathogens can be classified as biotrophs that obtain nutrients from the living tissue of the host, as necrotrophs which derive nutrients from dead or dying host tissue cells, or as hemi-biotrophs that act as both biotrophs and necrotrophs depending on the stage of their life cycle or the existing conditions in which they are present (Agrios, 2005; Glazebrook, 2005). Even though pathogens are genetically diverse, only a relatively small proportion of these pathogens successfully invade plants and cause disease (Hammond-Kosack and Parker, 2003). Plants have evolved elaborate, multicomponent and very effective defence systems involving a combination of physical and chemical obstacles that are either preformed or induced after pathogen attack (Gómez-Gómez, 2004). Preformed defences are the first obstacle that the pathogen needs to overcome to infect the plant. These defences include both the constitutive barriers provided by the epidermis, waxes, cell wall and the cytoskeleton and preformed antimicrobial compounds including peptides, proteins and secondary metabolites

(Heath, 2000; Dixon, 2001; Nürnberger et al., 2004). In some cases, the pathogen overcomes or bypasses the preformed defence system and obtains access to the plant interior either by directly penetrating the surface, by entering through wounds or through natural openings such as gas and water pores (Jones and Dangl, 2006). It then needs to face a two-armed innate immunity system where the first arm, termed pathogen-associated molecular pattern (PAMP)-triggered immunity (PTI), recognizes and responds to the presence of a pathogen by molecules which are common to many classes of microbes. The second arm is cultivar-specific resistance, also known as effector-triggered immunity (ETI), responding to effector molecules from the pathogen in a gene-for-gene manner (Jones and Dangl, 2006).

Although general plant defence systems will be discussed in the following sections, the focus will be on the Arabidopsis immune system. Many studies are currently geared towards the understanding of the components of the plant immune system, especially that of the PAMP-triggered immunity. The aim of this study is understanding the mechanisms of resistance of the Arabidopsis defence mutant *cir1* (constitutively induced resistance 1; Murray et al., 2002). *Cir1* affects resistance to virulent pathogens and therefore it appears to be involved in basal resistance which relies on PTI. Studies have shown that *cir1* seems not to be involved in ETI, therefore the following sections will focus in detail on the various components of PTI.

1.2.1 PAMP-triggered immunity (PTI)

PAMP-triggered defence responses are induced upon the recognition of PAMPs by plant cell-surface receptors (Jones and Dangl, 2006) and its induction is associated with defence responses such as deposition of callose, production of reactive oxygen species (ROS), mitogen-activated protein kinase (MAPK) signalling and the transcriptional activation of defence-related genes which all contribute to the prevention of pathogen colonization (Nürnberger et al., 2004).

The immunity of an entire plant species to all isolates of a pathogen species is the commonest form of disease resistance and is termed “non-host” or “species level resistance” (Heath, 2000). This common and durable form of resistance is effective against most micro-organisms (Mysore and Ryu, 2004) and a pathogen that cannot cause disease on a non-host plant is referred to as a non-host pathogen. It is believed that non-host resistance relies on multiple overlapping mechanisms that include both constitutive preformed barriers as well as inducible reactions (Heath, 2000; Hammond-Kosack and Parker, 2003; Thordal-Christensen, 2003). The preformed structural or chemical barriers present on the plant surface may effectively halt pathogen colonization or the formation of infection structures by non-host pathogens. However, when a non-host pathogen overcomes the constitutive defensive obstacles, inducible defence responses triggered by the recognition of PAMPs, referred to as basal resistance, are immediately initiated by the plant (Mysore and Ryu, 2004; Nürnberger

et al., 2004; Nürnberger and Lipka, 2005). In non-host resistance, the activated basal defence responses are often successful in controlling the proliferation of non-host pathogens (Chisholm et al., 2006).

Basal defence responses are also induced in host plants in response to infection by virulent pathogens (Ingle et al., 2006). In this case, it is insufficient at controlling pathogen growth and does not result in disease resistance, however it does restrict virulent pathogen growth to some degree. The identification of "enhanced disease susceptibility" mutants pointed to the existence of this crucial protective layer as these mutants were hyper-susceptible to virulent pathogen infection and displayed even higher levels of disease development than susceptible wild-type hosts (Glazebrook et al., 1996; Parker et al., 1996; Reuber et al., 1998). A large number of Arabidopsis mutants are compromised in basal resistance to virulent pathogens indicating that many genes are involved in maintaining this protective defence layer (Glazebrook et al., 1996; Parker et al., 1996; Menke et al., 2004; Zhang and Li, 2005).

It is likely that both non-host and basal resistance rely on PTI as it is only the effectiveness of the resistance response that is varying. Furthermore, significant similarities and common characteristics in early defence responses and subsequent defence signalling (to be discussed in sections 1.2.1.3 and 1.2.1.4) have been identified in non-host and basal resistance. Therefore in this thesis, these forms of resistance are treated as one response which relies on PTI.

1.2.1.1 Pathogen-associated molecular patterns (PAMPs)

PAMP-triggered defence responses rely on the receptor-mediated recognition of ubiquitous and highly conserved molecules essential for microbial life but not necessarily for pathogenicity, and normally absent from the host (Nürnberger et al., 2004). These molecules or "general elicitors" are known as PAMPs, yet since these molecular patterns exist in pathogenic and non-pathogenic microbes, they should really be referred to as microbial-associated molecular patterns (MAMPs) (Mackey and McFall, 2006). In addition, breakdown products of the plant cell wall known as "endogenous elicitors", probably released by plant cell wall degrading enzymatic activities of the attacking phytopathogens, are also recognized as molecular patterns thereby inducing defence responses (Vorwerk et al., 2004). Numerous PAMPs which trigger basal defence responses in plants have been identified including bacterial flagellin, the necrosis-inducing *Phytophthora* protein 1 (NPP1), lipopolysaccharide (LPS), harpin, elongation factor Tu (EF-Tu), cold shock protein (CSP) and chitin, ergosterol and β-glucans from fungi (Fellbrich et al., 2002; reviewed in Nürnberger et al., 2004 and Nürnberger and Lipka, 2005). Several of these PAMPs are perceived only by a narrow range of plants species, while others trigger defence responses in many species. For example, flg22, the elicitor epitope of flagellin consisting of a highly conserved 22 amino acid stretch

from the N-terminal of the protein, induces defence responses in various plants (Felix et al., 1999), whereas the perception of bacterial CSP and EF-Tu appear to be restricted to members of *Solanaceae* and *Brassicaceae*, respectively (Felix and Boller, 2003; Kunze et al., 2004). Furthermore, it has been found that PAMPs contain short amino acid epitopes that often elicit more intense defence responses than the complete protein. For instance, flg22 is a more powerful elicitor than flagellin (Felix et al., 1999). Other eliciting epitopes include an N-acetylated peptide comprised of the first 18 amino acids from the N-terminus of EF-Tu (Kunze et al., 2004), a 15 amino acid peptide including the highly conserved RNA-binding RNP-1 motif of CSP (Felix and Boller, 2003) and Pep-13, a 13 amino acid internal peptide of a cell wall transglutaminase enzyme from *Phytophthora sojae* (Brunner et al., 2002).

It appears that PAMPs can be subject to natural selection as some microbes have developed the capacity to avoid detection by specific receptors. The efficiency of flagellin from various *Xanthomonas campestris* pv. *campestris* strains in eliciting PTI is variable in Arabidopsis (Sun et al., 2006), whereas flagellin from *Agrobacterium tumefaciens* does not trigger a defence response in Arabidopsis (Felix et al., 1999). Additionally, EF-Tu from *Pseudomonas syringae* pv. *tomato* DC3000 (*Pst* DC3000) is a less potent elicitor than EF-Tu from *A. tumefaciens* (Kunze et al., 2004).

1.2.1.2 Molecular pattern recognition

Plants have evolved molecular pattern recognition receptors (PRRs) which function in recognizing certain PAMPs (Nürnberger and Lipka, 2005; Abramovitch et al., 2006). PAMP-mediated recognition and subsequent signal transduction is believed to activate the first line of inducible plant defence responses, which may curb attempted pathogen assault (Nürnberger and Lipka, 2005). Large gene-families that encode receptor-like kinases (RLKs) (Shiu and Bleecker, 2001) and receptor-like proteins (RLPs) are present in plants and some of these act as PRRs (Fritz-Laylin et al., 2005). RLKs are transmembrane proteins with an extracellular ligand-binding domain that is often comprised of leucine-rich repeats (LRRs), a single membrane spanning domain and an intracellular serine/threonine kinase domain (Bittel and Robatzek, 2007). RLPs have a similar structure to RLKs but lack the intracellular kinase domain (Bittel and Robatzek, 2007). The Arabidopsis genome contains 610 RLKs, of which 235 carry a LRR domain also referred to as LRR-RLKs, and 56 RLPs (Shiu and Bleecker, 2001; Fritz-Laylin et al., 2005), however few of them have been functionally characterized.

The most studied PRR mediating PAMP perception is FLS2 (flagellin sensitive 2), the Arabidopsis receptor of flagellin which is the main component of the flagellar filament of eubacteria (Gómez-Gómez and Boller, 2002). FLS2 was found to be the flagellin receptor through chemical cross-linking and immunoprecipitation experiments which showed that the flg22 peptide directly bound FLS2 (Chinchilla et al., 2005). Moreover, heterologous *FLS2* expression in tomato cells was sufficient to transfer specific features characteristic of the

flg22 perception system of Arabidopsis (Chinchilla et al., 2005). The *FLS2* gene encodes an typical RLK protein consisting of an extracellular LRR domain and an intracellular kinase domain (Gómez-Gómez and Boller, 2002). A point mutation in one of the LRR of FLS2 resulted in the complete loss of flg22 binding, indicating that the extracellular LRR domain is the binding site (Bauer et al., 2001). Zipfel et al. (2004) established a link between flagellin perception and enhanced resistance to the virulent pathogen *Pst* DC3000 as wild-type plants treated with flg22 showed induced expression of several defence-related genes and displayed significantly reduced bacterial growth after subsequent *Pst* DC3000 infection. FLS2 recognition of the flg22 peptide triggers a complete MAPK cascade and WRKY transcription factors that function downstream of flg22 perception, resulting in defence responses (Asai et al., 2002). The WRKY transcription factors activate transcription by binding to WRKY DNA-binding elements (W-box) found in the promoters of many defence-related genes, including *PR-1* (pathogenesis-related protein 1). These elements are also found in the promoters of WRKY29 leading to signal amplification through a positive feedback loop (Asai et al., 2002). Furthermore, *fls2* mutant plants are insensitive to flagellin (Gómez-Gómez and Boller, 2000) and are more susceptible to bacterial growth (Zipfel et al., 2004). Once a PAMP is recognized by PRRs, the activities of many PRRs are up regulated resulting in amplified signal transduction and defence responses that restrict bacterial growth (Nürnberger and Lipka, 2005). Interestingly, *fls2* mutant plants pre-treated with an assortment of bacterial extracts which contained not only flagellin but also other PAMPs, led to enhanced resistance to subsequent growth of *Pst* DC3000. This demonstrates that the PAMPs in the bacterial extracts were recognized by the plant through receptors apart from FLS2 and that multiple PAMP receptors function to curtail microbial growth (Zipfel et al., 2004).

The EF-Tu receptor (EFR) is another RLK receptor identified in Arabidopsis (Zipfel et al., 2006). EF-Tu is one of the most abundant and conserved proteins in bacteria and has been detected in the secretomes of various bacteria (Chisholm et al., 2006; Zipfel et al., 2006). Arabidopsis *efr* mutants are insensitive to EF-Tu and the transient expression of *EFR* in *Nicotiana benthamiana*, that is normally unable to perceive EF-Tu, resulted in the binding of EF-Tu. Tobacco plants also gained responsiveness to EF-Tu after transformation with EFR as exemplified by the increase in ethylene biosynthesis and an oxidative burst (Zipfel et al., 2006). Furthermore, the transformation efficiency of *A. tumefaciens* was higher in *efr* mutants (Zipfel et al., 2006) highlighting the importance of this PAMP perception in plant defence. EFR elicited very similar signalling events and defence responses to that induced by flagellin, however it is as yet unclear whether the signalling events occur via common signalling components or by convergence at a later stage in the signalling pathway (Zipfel et al., 2006).

The tomato receptor for the fungal elicitor ethylene-inducing xylanase (EIX) is the first example of an RLP functioning as a PRR (Ron and Avni, 2004). The *LeEix* locus contains two members, *LeEix1* and *LeEix2*, which encode highly homologous proteins with a leucine zipper, an extracellular LRR domain with glycosylation signals, a transmembrane domain and a domain with a mammalian endocytosis signal at the C-terminal. Silencing of the *LeEix* gene family abolished the binding of EIX in an EIX-responsive plant and the overexpression of either *LeEix1* or *LeEix2* in EIX-nonresponsive plants mediated EIX-binding, though only *LeEix2* triggered the hypersensitive response (HR), a rapid and localized cell death that restricts the growth of the pathogen, upon EIX elicitation (Ron and Avni, 2004).

The immune system in mammals consists of adaptive and innate immunity which work jointly to protect the host from pathogen attack. Adaptive immunity is characterized by the creation of strain-specific antibodies via somatic recombination in B and T lymphocytes (Girardin et al., 2002), while innate immunity involves PAMP detection by PRRs. One of the most prominent group of mammalian PRRs is the transmembrane Toll-like receptors (TLRs), which reside in the plasma membrane and consists of an extracellular LRR domain and an intracellular TIR protein-protein interaction domain (named after *Drosophila* Toll and human interleukin-1 receptors) (Underhill and Ozinsky, 2002). In addition to TLRs, mammals have cytosolic PRRs containing a nucleotide oligomerization domain (NOD) (Athman and Philpott, 2004; Gigardin and Philpott, 2004). NOD proteins are characterized by a variable N-terminal domain, a central nucleotide-binding domain and C-terminal LRRs (Athman and Philpott, 2004) and are structurally related to plant resistance (R) proteins that function in the plant immune system (to be discussed in section 1.2.2.1).

PTI in plants corresponds theoretically to the innate immune system of animals, as both recognize conserved microbial molecular patterns and both act as an early warning system against potential pathogen attack (Ausubel, 2005). However, animals also have an adaptive branch of the immune system which involves the generation of pathogen-strain specific antibodies through somatic gene recombination. This adaptive immunity found in animals does not exist in plants (Nürnberger et al., 2004). In addition, as plants do not have a circulatory blood system, they also lack specialized cell types and therefore every plant cell is autonomously capable of perceiving the presence of microbes resulting in elicitation of defence responses (Nürnberger et al., 2004). Although the molecular components mediating PAMP-triggered signal transduction cascades are structurally similar in a broad sense, it is unclear if these similarities are due to convergent evolution or a common ancestral origin (Nürnberger et al., 2004).

1.2.1.3 Early defence responses

Some typical early defence responses to pathogen perception include phosphorylation and dephosphorylation of plasma membrane proteins, calcium and ion fluxes across the plasma

membrane and alkalization of the apoplast. Furthermore, synthesis and deposition of callose can be initiated rapidly at the site of pathogen invasion. MAPKs are activated and generation of ROS occurs within minutes of contact with the elicitor (Zhao et al., 2005). The activation of transcription factors and early expression of defence genes also occurs while the activated MAPK cascades and ROS further amplify the defence signals to downstream reactions (Dardick and Ronald, 2006). This is subsequently followed by phytoalexin accumulation and the activation of late defence-related genes such as pathogenesis-related (PR) proteins, which have antimicrobial activity and hence serve to contain the infection (Wojtaszek, 1997; Hammerschmidt, 1999; van Loon and van Strien, 1999). In some cases, programmed cell death in the form of HR occurs, however it is more frequently associated with the recognition of a specific than a general elicitor (Greenberg, 1997; Espinosa and Alfano, 2004; Greenberg and Yao, 2004).

One of the earliest events after pathogen exposure, is a change in the ion permeability of the plasma membrane resulting in influxes of calcium (Ca^{2+}) and protons (H^{+}) as well as an efflux of potassium (K^{+}) and chloride (Cl^{-}) ions (Zimmermann et al., 1997). Perception of the PAMP, flagellin, resulted in fluxes in cytosolic and nuclear Ca^{2+} (Lecourieux et al., 2005) and plasma membrane-located Ca^{2+} channels responded to the oomycete PAMP, Pep13 (Zimmermann et al., 1997), resulting in the transient elevation of cytosolic Ca^{2+} levels. Although the amplitude and duration of defence-related Ca^{2+} transients vary, the increase in cytosolic Ca^{2+} levels is essential for the elicitation of defence responses in plants (Nürnberger et al., 2004). Some of the downstream events triggered by Ca^{2+} influxes include the production of ROS, cytosol acidification, plasma membrane depolarisation (Pugin et al., 1997) and nitric oxide (NO) production (Lamotte et al., 2004).

Callose is a (1→3)-β-D-glucan which is widely distributed in higher plants where it has a role in normal growth and development (Jacobs et al., 2003). It has an additional role in plant defence during which the host cells rapidly synthesize and deposit callose in close proximity to the invading pathogen (Ryals et al., 1996; Donofrio and Delaney, 2001). Callosic deposits in the from of drops, plugs or plates are commonly referred to as papillae (Jacobs et al., 2003), which probably act as physical barriers to obstruct pathogen penetration and to impede nutrient transfer from the host to the pathogen (Brown et al., 1998; Donofrio and Delaney, 2001). By delaying pathogen growth, the host could direct other defence responses, such as antimicrobial compounds, upon the attacking pathogen (Brown et al., 1998). It has been suggested that callose further assists this process by supplying a medium for the accumulation of toxic compounds (Donofrio and Delaney, 2001).

MAPKs undergo rapid activation upon PAMP perception and amplify early responses (Peck, 2003; Ludwig et al., 2005). MAPK cascades consist of three kinase modules and involve the sequential transfer of phosphate groups from a MAPK kinase kinase (MAPKKK), to a MAP

kinase kinase (MAPKK) and to a MAPK. These cascades are linked in a variety of ways to upstream receptors and downstream targets and numerous studies have shown that plant MAPK cascades are activated by hormones, abiotic stresses, pathogens and pathogen-derived elicitors (Hirt, 2000). Furthermore, a more recent study has shown that MAPKs from tomato are involved in defence against herbivorous insects (Kandoth et al., 2007). LeMPK1, LeMPK2 and LeMPK3 function upstream of jasmonic acid where they act as essential signalling components required for the expression of certain wound-response genes, that ultimately results in resistance to herbivorous insect attack (Kandoth et al., 2007). Evidence that MAPKs regulate PTI in plants has come from several studies in different plant species. Two tobacco MAPKs, the SIPK (salicylic acid-induced protein kinase) and WIPK (wounding-induced protein kinase) and their orthologues in alfalfa and Arabidopsis, are activated by bacterial flagellin and harpin as well as by fungal cell-wall-derived elicitors such as elicitin, Pep13 and NPP1 (Zhang and Klessig, 2001). Furthermore, a complete Arabidopsis MAPK cascade was found to be activated in response to flagellin (flg22). This cascade consists of AtMEKK1 (a MAPKKK) which activates AtMKK4 and AtMKK5 (MAPKKs) that in turn phosphorylates the MAPKs, AtMPK3 and AtMPK6 (Asai et al., 2002). This MAPK cascade culminates in the activation of key transcription factor WRKY29, and the possibly functionally redundant WRKY22, which is thought to regulate the expression of defence-related genes such as *PR-1* and *PR-5* (pathogenesis-related protein 5) (Gómez-Gómez et al., 1999; Asai et al., 2002). The transient overexpression of either the AtMEKK1 kinase domain or constitutively active AtMKK4 and AtMKK5 resulted in Arabidopsis leaves with increased resistance to the bacterial pathogen *P. syringae* or the fungal pathogen *Botrytis cinerea* (Asai et al., 2002), signifying that this MAPK cascade activates defence responses which are effective against both bacterial and fungal pathogens. A more recent study by Menke et al. (2004) showed that the Arabidopsis AtMPK6 is required to maintain basal resistance to a virulent bacterial pathogen as the silencing of AtMPK6 resulted in the increased growth of *P. syringae*. Additionally, AtMPK4 and AtMPK6 are activated by bacterial harpin, indicating that certain MAPK components are involved in more than one PAMP signalling pathway necessary for basal defence responses (Desikan et al., 2001).

1.2.1.4 Defence signal transduction

Following pathogen attack, the early defence responses are often amplified through the defence signalling network which acts downstream of PRRs. Several components of the defence signalling network are shared between PAMP-triggered, non-host and basal defences which all contribute to resistance mediated by PTI. Therefore, the following sections will highlight common signalling pathways involved in these defence responses. The complex signalling network consists of distinct signalling pathways mediated by the endogenous signalling hormones salicylic acid (SA), jasmonic acid (JA) and ethylene (ET). Small,

signalling molecules such as ROS and NO also contribute to the transmission of defence signals (Karpinski et al., 2003; Crawford and Guo, 2005), thereby providing the plant with the capacity to launch multifaceted and complex defence responses. An invading pathogen has to evade or overcome several of these signalling components to cause disease in the plant.

It has been found that the SA, JA and ET signalling pathways contribute to *cir1*-mediated defence-related gene expression and resistance to pathogens (Chapter 4; Murray et al., 2002). Therefore, the significance of these signalling pathways, as well as that of ROS and NO signalling, will be discussed in the following sections. Evidence of synergistic and antagonistic interactions among these signalling pathways follows in the cross-talk section.

1.2.1.4.1 Reactive oxygen species in defence signalling

ROS consist of H_2O_2, superoxide ($O_2^{\cdot-}$), hydroxyl radical (OH·), perhydroxyl radical ($O_2H\cdot$) and singlet oxygen ($^1O_2$). Mainly apoplastic superoxide or its dismutation product, H_2O_2, are produced during the so-called oxidative burst, one of the earliest cellular responses subsequent to successful pathogen recognition (Doke, 1983; Auh and Murphy, 1995; Grant et al., 2000b; Kroj et al., 2003; Torres et al., 2006). As ROS are potentially damaging, plant cells contain several enzymatic and non-enzymatic antioxidant scavenging systems that detoxify ROS, thereby maintaining a normal redox homeostasis (Apel and Hirt, 2004). Several forms of stress, such as pathogen invasion, can disrupt the cellular redox homeostasis leading to the accelerated generation of ROS (Lamb and Dixon, 1997; Apel and Hirt, 2004).

The oxidative burst is the rapid and transient production of large amounts of ROS at the site of attempted pathogen invasion (Lamb and Dixon, 1997). During ETI, apoplastic ROS production occurs in a biphasic manner resulting in high amounts of accumulated ROS which are correlated with disease resistance (Lamb and Dixon, 1997). Although the amount of accumulated ROS are less in response to virulent pathogens, ROS accumulation also plays a role in the establishment of basal defences. Similarly, PAMP recognition triggers an oxidative burst (Torres et al., 2006) as demonstrated by induced ROS production in parsley cells treated with the PAMP, Pep13 (Kroj et al., 2003).

The ROS generated during the pathogen-mediated oxidative burst are produced by enhanced activities of the plasma membrane-bound NADPH oxidase (Torres et al., 2002), whereas apoplastic H_2O_2 can be generated by cell wall-bound peroxidases, germin-like oxalate oxidases or by apoplast-located amine oxidases (Apel and Hirt, 2004; Mittler et al., 2004). ROS have several roles in plant defence such as direct toxicity to pathogens (Bussink and Oliver, 2001) or contributing to the structural reinforcement of plant cell walls by the cross-linking of cell wall polymers (Bradley et al., 1992), thereby containing the spread of the penetrating pathogen. Furthermore, ROS have been proposed to act as important signalling molecules mediating the induction of defence-related genes (Laloi et al., 2004), such as *GST1* (glutathione *S*-transferase) (Grant et al., 2000a).

The integration of ROS into the plant defence signalling network is mostly unknown, however some key players involved in ROS signal transduction have been identified. For example, ROS signalling is intimately linked to calcium metabolism as a Ca^{2+} influx is required for ROS production by activating plant NADPH oxidases after elicitation (Blume et al., 2000; Torres and Dangl, 2005). It appears that MAPK signalling cascades also play a significant role in ROS-mediated signalling. H_2O_2 can activate the Arabidopsis AtMPK3 and AtMPK6 via the activity of the MAPKKK protein, ANP1 (NPK1-related protein kinase 1) (Kovtun et al., 2000). Another upstream mediator of AtMPK3 and AtMPK6, is the OXI1 (oxidative signal-inducible 1) protein kinase (Rentel et al., 2004). The *oxi1* null mutant is hypersensitive to infection by virulent *H. parasitica* and is compromised in H_2O_2-induced activation of AtMPK3 and AtMPK6, while the over expression of an OXI1 fusion protein in protoplasts increases the H_2O_2-induced AtMPK3 activity (Rentel et al., 2004).

ROS modulate the expression of several genes and three general modes of action regarding the effect of ROS signalling on gene expression have been proposed (Mittler et al., 2004). It is believed that ROS sensors could activate certain signalling cascades or alternatively ROS could directly inhibit phosphatases activity which might result in the activation of specific kinases thereby triggering downstream signalling events. Lastly, ROS could alter gene expression by modifying the activity of redox-sensitive transcription factors or genes, such as *NPR1* (Mou et al., 2003). Further regulatory functions for ROS in plant defence occur concurrently with other signalling molecules, such as NO.

1.2.1.4.2 Nitric oxide burst during plant-pathogen interactions

NO is a highly toxic gas with a broad chemistry that involves a range of interrelated redox forms with different chemical reactivities (Delledonne, 2005). Notably studies regarding NO synthesis and signalling are much more advanced in animals than in plants. NO can be generated enzymatically or non-enzymatically in biological systems and the most extensively described NO-producing enzyme in plants is nitrate reductase (NR). This enzyme is usually associated with the assimilation of nitrogen, however it also catalyses the NAD(P)H-dependent reduction of nitrite to NO (Yamasaki, 2000). NR could have a role in NO production during plant-pathogen interactions since potato tubers exposed to either *Phytophthora infestans* or a PAMP derived from this pathogen display NO accumulation as well as enhanced *NR* gene expression and increased NR protein levels (Yamamoto et al., 2003). Another potential NO-generating enzyme is nitric oxide synthase (NOS), but no plant homologue has been identified to date.

It appears that NO works in association with ROS in the induction of the pathogen-induced HR cell death (Delledonne et al., 2001) and many studies have established that NO accumulation is often associated with the *R* gene-mediated oxidative burst that occurs immediately before the onset of HR cell death (Delledonne et al., 1998). In this case, NO

might play a vital role as an intracellular signal that functions in the cell-to-cell spread of the HR (Zhang et al., 2003a), in addition to being involved in the induction of defence-related genes and the establishment of systemic acquired resistance (SAR) (Durner et al., 1998; Delledonne et al., 2001). However, NO accumulation also occurs in PAMP-triggered defence responses. The general PAMP elicitors, LPS and harpin, can induce a strong and rapid NO burst in Arabidopsis (Krause and Durner, 2004; Zeidler et al., 2004). Furthermore, NO accumulation occurs in tobacco leaves treated with the fungal PAMP cryptogein (Foissner et al., 2000) and has been observed in basal defence responses to virulent bacteria in soybean and Arabidopsis cell suspensions (Delledonne et al., 1998; Clarke et al., 2000a). As NO accumulates in resistant plants challenged with pathogen infection, a correlation between disease resistance responses and NO has been established (Romero-Puertas et al., 2004).

Together with ROS, NO has a significant role in triggering resistance-associated HR cell death, but it is also involved in other defence responses. NO activates MAPK signalling pathways (Kumar and Klessig, 2000; Pagnussat et al., 2004) and regulates the expression of defence-related genes. Expression profiling of Arabidopsis leaves treated with NO showed that the application of NO can increase the transcriptional activity of several genes, including *PR-1* (Polverari et al., 2003). NO also regulates the expression of a number of genes involved in the synthesis of and response to JA (Orozco-Cárdenas and Ryan, 2002; Jih et al., 2003) and ET (Polverari et al., 2003). NO also has a role in post-translational modification of proteins through *S*-nitrosylation. Intracellular NO reacts with the cysteine residues of proteins to form protein *S*-nitrosothiols (SNOs), a modification that could alter protein activity (Stamler et al., 2001). NO also reacts with glutathione to yield *S*-nitrosoglutathione (GSNO) which is thought to act both as a reservoir and donor of biologically active NO (Stamler et al., 1992; Lindermayr et al., 2005), thereby contributing to protein *S*-nitrosylation. GSNO reductase (GSNOR) metabolises GSNOs and its activity controls the intracellular levels of GSNOs and *S*-nitrosylated proteins (Liu et al., 2001). Through proteomic approaches some targets of *S*-nitrosylation have been identified including stress-related proteins, signalling or regulating proteins and metabolic enzymes (Lindermayr et al., 2005). Protein SNO levels may play a role in the regulation of defence responses, however contradicting results have been reported. According to Feechan et al. (2005), basal and non-host disease resistance was increased in the plants with enhanced GSNOR activity and compromised in plants with reduced GSNOR function. In contrast, it was established that plants with decreased amounts of GSNOR, which correlates with elevated levels of intracellular SNOs, displayed enhanced basal resistance against the virulent oomycete, *H. parasitica* Noco2 (Rustérucci et al., 2007). Interestingly, the Arabidopsis AtGSNOR1 regulates both SA biosynthesis and SA signalling, suggesting that certain nodes of the SA signalling pathway may be controlled by *S*-nitrosylation (Feechan et al., 2005).

1.2.1.4.3 Salicylic acid-mediated signalling and defence responses

It has long been acknowledged that SA plays a central role in plant defence against pathogens. SA is required for the rapid activation of local defence responses to restrict growth of virulent pathogens, for the induction of several *R* gene-mediated defence responses and for the launch of SAR (Kunkel and Brooks, 2002). SAR is activated throughout the plant following primary pathogen infection, conferring enhanced and long-lasting protection against secondary infection by a variety of pathogens (Durrant and Dong, 2004). The activation of SA signalling and SAR is associated with the accumulation of PR proteins which are thought to contribute to pathogen resistance (van Loon, 1997) and serve as molecular markers for the onset of the defence response (van Loon, 1997; Durrant and Dong, 2004). Interestingly, SAR against subsequent virulent pathogen infection can also be achieved by infiltrating plants with PAMPs (Mishina and Zeier, 2007), indicating that PAMP-based recognition events are not only involved in activating local defence responses but also in the establishment of systemic defence responses. Furthermore, the levels of SA increase in response to pathogen infection and through the exogenous application of SA to plants, the resistance to a variety of pathogens can be enhanced (Ryals et al., 1996; Dempsey et al., 1999). Based on previous studies, it was believed that SA is synthesized from phenylalanine (Mauch-Mani and Slusarenko, 1996) however the presence of an alternative biosynthesis pathway which seems to be especially important in plant-pathogen interactions, has been discovered. Similar to certain bacteria, plants can also synthesize SA from chorismate via isochorismate (Serino et al., 1995). Chorismate is derived from the shikimate pathway of which several components are notably up regulated in response to pathogen challenge (Truman et al., 2006). Isochorismate synthase and isochorismate pyruvate lyase catalyse the two-step reaction from chorismate to SA (Serino et al., 1995) and the overexpression of these bacterial enzymes in Arabidopsis resulted in increased levels of SA and enhanced resistance to pathogens (Verberne et al., 2000; Mauch et al., 2001).

Two genes important in the SA signalling pathway, *EDS1* (enhanced disease susceptibility 1) and *PAD4* (phytoalexin deficient 4), are essential for the activation of SA accumulation following exposure to certain SA-inducing stimuli (Zhou et al., 1998; Falk et al., 1999). The phenotypes of *eds1* and *pad4* mutant plants regarding *PR-1* expression positioned EDS1 and PAD4 upstream of SA accumulation. The pathogen induced expression of *PR-1* is abolished in *eds1* and strongly suppressed in *pad4,* but is fully rescued in both mutants after treatment with SA or its active analogue (Parker et al., 1996; Zhou et al., 1998; Falk et al., 1999; Jirage et al., 1999; Feys et al., 2001). Furthermore, the *eds1* and *pad4* mutant alleles compromise SA synthesis in plant-pathogen interactions (Jirage et al., 1999; Feys et al., 2001) as well as in constitutive SA signalling mutants (Jirage et al., 1999; Clarke et al., 2000a). Additionally, the expression of these two genes is enhanced through

SA-application, signifying that *EDS1* and *PAD4* are regulated by an SA-dependent positive feedback loop in the defence network (Falk et al., 1999; Jirage et al., 1999; Feys et al., 2001). The *EDS1* and *PAD4* genes have been cloned and both display homology to triacyl glycerol lipases (Falk et al., 1999; Jirage et al., 1999). Not only are EDS1 and PAD4 important activators of SA signalling, they have additional roles in regulating antagonism between the SA and JA/ET defence pathways (Wiermer et al., 2005).

Both EDS1 and PAD4 are essential in basal defences to biotrophic and hemi-biotrophic pathogens and have fundamental roles in ETI mediated by the TIR-NBS-LRR class of R proteins (Zhou et al., 1998; Feys et al., 2001). Analysis of the *eds1* and *pad4* mutant phenotypes has shown that EDS1 exerts an early activity in TIR-NB-LRR type *R* gene-mediated resistance that is necessary for the oxidative burst and expression of the HR, whereas the combination of EDS1 and PAD4 are required for the amplification of defence responses around infection sites through the increased accumulation of SA (Feys et al., 2001; Rustérucci et al., 2001). Consistent with the combined role of EDS1 and PAD4 in defence signal amplification, it was established that both proteins are indispensable components of basal resistance in curbing the growth of virulent pathogens (Aarts et al., 1998; Reuber et al., 1998; Feys et al., 2001; Xiao et al., 2005). The *eds1* mutant shows enhanced susceptibility to virulent isolates of *H. parasitica* and to the virulent bacterial strains *Pst* DC3000 and *P. syringae* pv. *maculicola* ES4326 (*Psm* ES4326) (Parker et al., 1996; Aarts et al., 1998). Similarly, *pad4* mutant plants display enhanced susceptibility to virulent *Psm* ES4326 but the loss of resistance is normally not as absolute as in *eds1* (Zhou et al., 1998). In addition, *Psm* ES4326-infected *pad4* plants exhibit lower SA levels, reduced *PR-1* expression and a reduction in the production of camalexin, an Arabidopsis phytoalexin (Zhou et al., 1998).

Another important component of SA signalling and SAR is *NPR1* which encodes an ankyrin repeat-containing protein that plays a central role in SA signal transduction, operating downstream of SA accumulation (Delaney et al., 1995; Glazebrook et al., 1996). *Npr1* (nonexpresser of PR genes 1) mutant alleles were identified in mutational screens for defects in *PR* gene expression or disease resistance in response to SA or SA analogues (Cao et al., 1994) aimed at finding components involved in SA signal transduction. The *npr1* mutant accumulates SA after pathogen challenge, but is unable to induce SAR-marker genes. These SA-insensitive mutants also exhibit increased susceptibility to virulent pathogen infection and are impaired in certain *R* gene-mediated resistance responses (Cao et al., 1994; Delaney et al., 1995; Glazebrook et al., 1996). Overexpression of *NPR1* does not constitutively activate the expression of SAR markers, but does enhance resistance in Arabidopsis to *H. parasitica*, *P. syringae* and *Erysiphe cichoracearum* (Cao et al., 1998; Friedrich et al., 2001), indicating that activation of the NPR1 protein is a prerequisite for the establishment of SAR even if it is expressed at high levels (Cao et al., 1998).

Elevated SA levels triggered either by pathogen recognition or the application of SA, affect NPR1 activity in two parallel ways. First, the transcription of *NPR1* is up regulated by SA which requires WRKY transcription factors that interact with the W boxes in the *NPR1* promoter (Yu et al., 2001). The regulation of NPR1 is important for its function in SA signal transduction as its expression levels are correlated with the level of resistance and *PR* gene expression (Cao et al., 1998). Secondly, the elevated SA levels also stimulate a change in the redox status of the NPR1 protein (Mou et al., 2003). During an uninduced state when SA levels are low, the constitutively synthesized NPR1 protein exists as cytosolic, disulphide-bound oligomers. An increase of SA levels induce a change in the cellular redox status by increasing the reduction potential in the plant cells. Under these conditions, the NPR1 oligomers are reduced to active monomers which translocate to and accumulate in the nucleus, where they physically interact with members of the TGA transcription factor family (Despres et al., 2003; Mou et al., 2003). The interactions of NPR1 with TGA factors stimulate TGA-binding to SA-responsive elements in the promoters of *PR* genes resulting in gene expression (Zhang et al., 2003c). Notably, the interactions between NPR1 and TGA1 and/or TGA4 also appear to be regulated by the cellular reduction potential (Fobert and Després, 2005). Furthermore, genetic studies of TGA2, TGA5 and TGA6 revealed that these factors also play an important and redundant role in SAR induction (Zhang et al., 2003c). It has been suggested that in addition to TGA factors, WRKY transcription factors act as regulatory nodes in SAR. Wang et al. (2006) showed that the expression of several WRKY genes is directly regulated by NPR1, functioning as either positive or negative regulators of SAR. Expression profiling established that, besides controlling the expression of *PR* genes, NPR1 also directly up regulates the expression of the protein secretory pathway genes (Wang et al., 2005). This is vital for SAR since the disruption of this pathway resulted in reduced secretion of PR proteins, including *PR-1*, and subsequently in decreased resistance. It is likely that NPR1 controls these secretion-related genes through a novel transcription factor which is translocated into the nucleus once SAR is induced (Wang et al., 2005; Wang et al., 2006).

In contrast to the positive feedback regulation of *EDS1* and *PAD4*, it is believed that *NPR1* is involved in a negative feedback loop to regulate SA accumulation. SA accumulation is higher in infected *npr1* mutants than in infected wild-type plants (Shah et al., 1997). Uncontrolled SA synthesis may result in dwarfing of plants (Mauch et al., 2001) and could compromise other defence signalling pathways which are inhibited by SA (Kunkel and Brooks, 2002; Glazebrook, 2005), highlighting the importance of regulating SA synthesis and signalling. In addition, NPR1 also plays a role in other defence signalling pathways. NPR1 is an essential component of another induced resistance response, known as induced systemic resistance (ISR) (Pieterse et al., 1998). ISR is elicited by non-pathogenic root-colonizing bacteria and confers resistance to bacteria and fungi in aerial parts of the plant (Pieterse et

al., 1996; Pieterse et al., 1998). Notably, this resistance response occurs independently of SA but requires JA and ET signalling (Pieterse et al., 1998).

Some SA-dependent defence responses occur independently of *NPR1* (Glazebrook et al., 1996; Uguillas et al., 2004). The existence of another branch of the SA signalling pathway is supported by studies of various Arabidopsis constitutive defence signalling mutants (Dong, 2001). The broad spectrum disease resistance observed in these mutants is abolished by either the SA-deficient *sid1* (salicylic acid-induction deficient 1; Nawrath and Metraux, 1999) mutation or by *NahG* which is unable to accumulate SA, but is retained in the *npr1* mutant background (Shah et al., 1999; Clarke et al., 2000b; Devadas et al., 2002). Furthermore, the Arabidopsis transcription factor, AtWhy1, has been implicated in the regulation of the SA-dependent, NPR1-independent defence mechanism (Desveaux et al., 2004). AtWhy1 is induced by *H. parasitica* infection and SA treatments in both wildtype and *npr1* mutant plants, whereas *AtWhy1* mutants with reduced DNA binding activity, display reduced *PR-1* expression and an enhanced susceptibility to pathogens. These results suggest that both the NPR1-dependent and –independent branches of the SA signalling pathway contribute to SA-induced *PR-1* expression.

SA has been implicated in playing a role in PAMP-triggered, non-host and basal resistance through the analyses of accumulated SA levels in various disease resistance mutants and mutants with defects in SA accumulation. The infiltration of Arabidopsis leaves with NPP1, a PAMP purified from *H. parasitica*, resulted in the induction of *PR-1* expression. This NPP1-mediated accumulation of *PR-1* transcripts is dependent on SA since no *PR-1* expression could be detected in the salicylate-deficient *NahG* or *pad4* plants (Fellbrich et al., 2002). The *eds1*, *pad4* and *npr1* mutants displayed increased growth of a wheat powdery mildew, which is a non-host pathogen of Arabidopsis (Yun et al., 2003). The simultaneous loss of EDS1 and actin cytoskeleton function especially reduced non-host resistance as the wheat pathogen could undergo asexual reproduction accompanied by conidiophore formation and hyphae proliferation (Yun et al., 2003). Furthermore, *eds1* mutants displayed significant increases in penetration and hyphal elongation of a barley powdery mildew compared to wildtype (Zimmerli et al., 2004). The Arabidopsis *sid2* (salicylic acid-induction deficient 2; Nawrath and Metraux, 1999) mutant is defective in an enzyme necessary for SA biosynthesis. The non-host pathogen, cowpea rust fungus, was able to cause disease on *sid2* (Mellersh and Heath, 2003) indicating that SA is important in regulating non-host resistance. The *eds1* and *pad4* mutant plants infected with virulent *P. syringae* and *H. parasitica* pathogens display "enhanced disease susceptibility" phenotypes suggesting that their basal defence responses are severely compromised (Parker et al., 1996; Aarts et al., 1998; Zhou et al., 1998). In addition, *sid1* and *sid2* also showed increased susceptibility to virulent strains of *P. syringae*

and *H. parasitica* (Nawrath and Metraux, 1999), demonstrating a significant role for SA in basal defence.

1.2.1.4.4 Jasmonic acid-mediated signalling and defence responses

The plant hormone JA and its biologically active derivatives known as jasmonates (JAs), are widely distributed throughout the plant kingdom (Gfeller and Farmer, 2004). These compounds are important cellular regulators involved in diverse physiological and developmental processes, such as fruit ripening, root growth, seed germination, tendril coiling and senescence (Turner et al., 2002; Cheong and Choi, 2003). Furthermore, JAs activate plant defence responses to wounding, various pathogens and insects, and environmental stresses including drought, low temperature and salinity (Creelman and Mullet, 1997). In addition, it has been suggested that JAs could have a possible role as the initiating signals in SAR and therefore JAs are also integral to systemic defence (Truman et al., 2007). JA biosynthesis occurs via the octadecanoid lipid pathway from the substrate linoleic acid which is catalysed to linolenic acid by ω-3 fatty acid desaturase in the chloroplasts (Leon and Sanchez-Serrano, 1999). Linolenic acid is subsequently converted to 12-oxo-phytodienoic acid in a multi-step enzymatic process involving lipoxygenase, allene oxide synthase and allene oxide cyclase. JA synthesis continues in the cytoplasm with the action of 12-oxo-phytodienoic acid reductase and is followed by three rounds of β-oxidation in the peroxisomes (Leon and Sanchez-Serrano, 1999). The transcription of the abovementioned genes that synthesize JA is also induced by JA, allowing for feed-back regulation of the biosynthetic pathway (Devoto and Turner, 2003). Evidence suggests that developmentally regulated JA biosynthesis varies from, but overlaps with, the biosynthetic pathway that regulates wound and/or pathogen-induced JA formation (Turner et al., 2002). Despite its importance during plant defence responses, the molecular components of the JA signalling pathway remain largely undefined. The isolation and characterization of the JA insensitive mutant *coi1* (coronatine-insensitive 1; Feys et al., 1994) as well as the analysis of other mutants defective in JA biosynthesis and signalling highlighted the broad role of JAs as signalling compounds (Berger, 2002; Turner et al., 2002).

COI1 is required for all of the abovementioned JA-dependent responses and has a vital role as a principal control in JA signalling (Devoto et al., 2005; Lorenzo and Solano, 2005). It is also required for the initiation of the expression of several secondary metabolite genes as well as for the transcription of JA- and wounding-induced genes (Devoto et al., 2005). *COI1* encodes an F-box protein (Xie et al., 1998) which forms an integral part of the SCF^{COI1} (SKP1-CDC53p/CUL1-F-box) complex and functions as a receptor that selectively recruits repressor proteins as substrates for ubiquitin-mediated degradation in response to jasmonate (Turner et al., 2002). The SCF^{COI1} complex is one of six families of Arabidopsis E3 ubiquitin-ligases and is composed of SKP1 (S-phase kinase associated protein 1), CUL1 (cullin), Rbx (ring-box

protein 1) and COI1, the F-box containing protein (Devoto and Turner, 2005). The repressors of jasmonate signalling have recently been identified as members of the jasmonate ZIM-domain (JAZ) protein family, which are direct targets of the SCF^{COI1} complex (Chini et al., 2007; Thines et al., 2007). COI1 is therefore involved in the degradation of JAZ proteins resulting in the transcriptional activation of jasmonate responses (Chini et al., 2007; Thines et al., 2007). The JA-insensitive *coi1* mutant (Feys et al., 1994) exhibits a defect in pollen development rendering it male-sterile, it is unresponsive to growth inhibition by methyl jasmonate (MeJA) and fails to express several JA-responsive genes including *PDF1.2* (plant defensin 1.2), *PR-3* (pathogenesis-related protein 3) and *PR-4* (pathogenesis-related protein 4) upon MeJA treatment or pathogen infection (Feys et al., 1994; Thomma et al., 1998).

Other components in Arabidopsis and tomato JA signalling include the conserved MYC transcription factors (Boter et al., 2004; Lorenzo et al., 2004). *JIN1* (jasmonate insensitive 1) encodes AtMYC2, a basic helix-loop-helix leucine zipper transcription factor localized in the nucleus, whose expression is rapidly induced by JA in a COI1-dependent manner (Lorenzo et al., 2004). More recently it has been found that JA also negatively regulates *AtMYC2* expression through the AtMKK3-AtMPK6 cascade. This kinase cascade is activated by JA, functions upstream of AtMYC2 and plays a pivotal role in the JA-dependent regulation of *AtMYC2* expression and the JA signal transduction pathway. It is believed that by fine-tuning the expression of *AtMYC2* through positive as well as negative JA-regulation, the plant ultimately controls JA signalling (Takahashi et al., 2007). AtMYC2 is involved in a negative feedback regulatory loop with JAZ proteins. The JAZ proteins, JAI3 (jasmonate-insensitive 3) and JAZ1, interact with and repress AtMYC2. Upon the SCF^{COI1}-dependent proteasome degradation of the JAZ proteins, the suppression of AtMYC2 is lifted, allowing for the transcriptional activation of jasmonate responses (Chini et al., 2007). It appears that AtMYC2 differentially regulates the expression of two groups of JA-induced genes. A mutation in this locus inhibits the activation of *VSP* (vegetative storage protein), which is involved in JA-mediated responses to insects and herbivores, whereas the expression of JA-induced genes involved in pathogen defence is increased. Accordingly, *jin1/AtMYC2* mutant plants show enhanced resistance to *B. cinerea* and *Plectosphaerella cucumerina* (Lorenzo et al., 2004).

The involvement of JAs in the regulation of plant defence responses is based on the observations that accumulation of JAs occurs in response to pathogen attack, that plants affected in JA biosynthesis or signalling display altered susceptibility or resistance to infection and that the exogenous application of JAs has an effect on plant resistance (Pozo et al., 2005). In addition, JA-dependent responses are linked to increased expression of several defence-related genes including *VSP* and *Thi2.1* (thionin 2.1) used as markers for JA-dependent defence responses (Penninckx et al., 1998; Pieterse and van Loon, 1999; Devoto

and Turner, 2003). Some defence-related genes, such as *PDF1.2*, *CHI-B* (chitinase B) and *HEL* (hevein-like protein) are induced co-operatively by the JA and ET signalling pathways in Arabidopsis (Penninckx et al., 1998; Norman-Setterblad et al., 2000).

Arabidopsis mutants impaired in the synthesis or perception of JA display enhanced susceptibility to a variety of pathogens, including *Alternaria brassicicola*, *B. cinerea*, and the bacterium *Erwinia carotovora* (Thomma et al., 1998; Norman-Setterblad et al., 2000). In general, JA defence responses are considered effective against necrotrophic pathogens (Turner et al., 2002; Farmer et al., 2003), however in some cases JA-dependent signalling seems to also contribute to resistance against biotrophs. For example, the Arabidopsis *cev1* (constitutive expression of *vsp1*) mutant exhibits constitutive JA signalling and enhanced defences against the bacterium *Psm* ES4326 (Ellis et al., 2002). In addition, the *coi1* mutant also shows resistance to virulent *P. syringae* pathogens (Kloek et al., 2001; Ellis et al., 2002).

Evidence for the role of JAs in non-host and basal resistance resulted from genetic studies of JA-biosynthesis or JA-perception mutants. The virulent pathogen *Pst* DC3000 reached higher levels of growth in the leaves of the Arabidopsis JA-insensitive mutant, *jar1* (jasmonate resistant 1; Staswick et al., 1992) indicating that JA-dependent defence responses contribute to basal resistance (Pieterse et al., 1998). Moreover JAs have a role in non-host resistance as both *jar1* and the *fad3 fad7 fad8* triple mutant (McConn and Browse, 1996) that is defective in JA biosynthesis, displayed susceptibility to the soil-borne oomycetes of the genus *Pythium* which are non-host pathogens of Arabidopsis (Staswick et al., 1998; Vijayan et al., 1998). Expression profiling of Arabidopsis after challenge with the non-host potato late blight pathogen indicated that the JA-signalling pathway was activated and the pattern of gene expression was most similar to that of MeJA treatment (Huitema et al., 2003).

Besides genetic studies, experiments investigating the effect of exogenous JA application on plant resistance also provide evidence that JAs have important roles in plant defence. The most frequently used treatment is the application of MeJA, a naturally occurring and key compound of the JA signalling pathway (Pozo et al., 2005). MeJA treatment of the *fad3 fad7 fad8* triple mutant reduced its susceptibility to *Pythium mastophorum*, resulting in infection levels similar to wildtype (Vijayan et al., 1998). Furthermore, MeJA reduced disease caused by *B. cinerea* (Thomma et al., 2000) and has been shown to be effective against *P. syringae* (Pieterse et al., 1998; van Wees et al., 1999).

1.2.1.4.5 Ethylene-mediated signalling and defence responses

ET is a simple gaseous phytohormone that affects myriad physiological and developmental processes. Although most commonly associated with fruit ripening, ethylene is also a regulator of seed germination, seedling growth, flower and leaf senescence as well as organ abscission. It also mediates plant responses to environmental stress conditions and pathogen

attack (Schaller and Kieber, 2002; Guo and Ecker, 2004; van Loon et al., 2006). ET is derived from the amino acid methionine which is converted to *S*-adenosylmethionine (*S*-AdoMet) via *S*-AdoMet synthase. The first committed and rate-limiting step in ET biosynthesis is the conversion of *S*-AdoMet into 1-aminocyclopropane-1-carboxylic acid (ACC) by the enzyme ACC synthase (Adams and Yang, 1979). In the final step, ACC is oxidized to ET by ACC oxidase (Kende, 1993). Both ACC synthase and ACC oxidase enzymes are encoded by multigene families whose members are differentially regulated by external stimuli such as pathogen infection and wounding (Wang et al., 2002).

Considerable progress has been made in the genetic and molecular dissection of the ET-response pathway. A well-known effect of ET on plant growth is known as the "triple response", a series of dramatic morphological changes undergone by etiolated seedlings grown in the presence of ET under dark conditions. Genetic screens based on this phenotype have led to isolation of many unique Arabidopsis mutants which either display a constitutive triple response from ET overproduction or are insensitive to ET. Characterization of these mutants has largely defined the Arabidopsis ET signal transduction pathway which acts in a linear manner (Wang et al., 2002; Ecker, 2004; Guo and Ecker, 2004). ET is perceived by a family of membrane-associated ET receptors that including ETR1, ETR2, ERS1, ERS2 and EIN4 (Chang et al., 1993; Hua et al., 1995; Hua et al., 1998; Sakai et al., 1998). Downstream of the ET receptors is CTR1, a negative regulator of the ET response which has similarity to the Raf family of MAPKKKs (Kieber et al., 1993). In the absence of ET, the receptors maintain CTR1 in an active state thereby repressing ET responses possibly through unidentified MAPKKs and MAPKs (Chang, 2003). The binding of ET inactivates receptors and, in turn, CTR1. As a result, the central regulator EIN2 is activated (Alonso et al., 1999) and signals downstream to the transcription factors EIN3 and EIL1 that activates the expression of direct target genes, such as the transcription factor ERF1 (Solano et al., 1998; Guo and Ecker, 2004). The *ein2* mutant (ethylene insensitive 2; Alonso et al., 1999) displays the strongest ethylene-insensitive phenotype of all ethylene-insensitive mutants isolated in Arabidopsis, corroborating the critical role of EIN2 in ET signalling. Consequently, ERF1 binds to the GCC box found in the promoters of many ET-inducible genes such as β-1,3-glucanase, *PDF1.2* and *CHI-B* (Ohme-Takagi and Shinshi, 1995; Solano et al., 1998). Therefore, the transcriptional cascade mediated by EIN3/EIL1 and ERF1 eventually leads to an ET-dependent defence response. Furthermore, EIN5 and EIN6 are positive regulators of ET responses acting downstream of CTR1 (Roman et al., 1995).

The availability of mutants affected in their response to ET allowed for the study of the role of ET during pathogen infection. In general, increased ET production is an early response to the perception of pathogen attack and is linked with the activation of defence reactions (Boller, 1991). However, the role of ET in plant resistance seems somewhat

ambiguous as it contributes to resistance in some cases but promotes disease development in others. For example, the Arabidopsis *ein2* mutant displays increased susceptibility to *B. cinerea* (Thomma et al., 1999a) and *E. carotovora* (Norman-Setterblad et al., 2000) but increased tolerance to virulent strains of both *Pst* DC3000 and *X. campestris* pv. *campestris* (Bent et al., 1992). Results from several studies have suggested that ET contributes to resistance to necrotrophs more than it does in resistance to biotrophic pathogens by acting in concert with the JA signalling pathway (Thomma et al., 2001; Ton et al., 2002). However, it has also been shown that the SA- as well as the JA and/or ET-dependent pathways provide resistance to pathogens with diverse lifestyles (van Wees et al., 2000; Devadas et al., 2002; O'Donnell et al., 2003). Moreover, several plant pathogens are capable of producing ET as a virulence factor, thereby improving their ability to colonize plant tissues (Chagué et al., 2006). It therefore appears that ET production during certain plant-pathogen interactions promotes disease development instead of reducing it (van Loon et al., 2006).

Instances exist where ET plays a role in non-host and basal resistance. It has been reported that several ET insensitive mutants of Arabidopsis exhibit enhanced susceptibility to infection by virulent *Pst* DC3000 (Pieterse et al., 1998) and *E. carotovora* (Norman-Setterblad et al., 2000), demonstrating that ET-dependent defence responses contribute to basal resistance. Knoester et al. (1998) transformed tobacco with the mutant Arabidopsis ET receptor *etr1*, rendering it unable to perceive ET. These plants were susceptible to the non-host pathogen *Pythium sylvaticum*, indicating that ET also has a role in non-host resistance. In addition, global gene expression patterns of Arabidopsis infected with the non-host pathogen, barley powdery mildew, indicated that the induced genes were dependent on the JA/ET signalling pathway (Zimmerli et al., 2004).

Generally, ET treatment promotes fruit ripening and leaf senescence which could make plant tissues either more susceptible or resistant to disease (Panter and Jones, 2002). Disease development of *B. cinerea* is promoted by ET treatment (Elad, 1993) whereas the resistance of Arabidopsis seedlings to *Pst* DC3000 is enhanced by ACC treatment (van Loon and Bakker, 2005). It has been suggested that the timing of ET exposure can determine whether resistance is increased or inhibited. It appears that ET treatment before pathogen inoculation reduces disease development, whereas disease expansion is expedited if ET treatment occurs after pathogen infection (van Loon et al., 2006). In addition, the role of ET seems to be dramatically different depending on the plant species and type of pathogen (van Loon et al., 2006).

1.2.1.4.6 Cross-talk between defence signalling pathways

Often when signal transduction pathways operating in defence signalling are studied, they are considered as independent units to simplify interpretation. However, signal transduction is not mediated through isolated, linear pathways but consists of a network of pathways,

influencing each other through regulatory interactions known as "cross-talk" (Kunkel and Brooks, 2002; Bostock, 2005). Cross-talk is often referred to as the specific interactions between components of different signalling pathways and the influences of those pathways on one another through positive or negative interactions resulting in either positive, negative or neutral functional outcomes (Kunkel and Brooks, 2002; Rojo et al., 2003; Bostock, 2005). Plant defences are tightly regulated by multiple signalling pathways involving various signal molecules such as NO, ROS, SA, JA and ET. Both synergistic and antagonistic interactions among these signalling pathways have been observed and in response to an invading pathogen, the biological output is generated by the combination of functions of various regulatory components (Devoto and Turner, 2005). The results of studies conducted primarily on Arabidopsis, that provide evidence for cross-talk between the SA, JA and ET signalling pathways, are summarized in Fig. 1.1. Further details and references are noted in the text. Cross-talk between these pathways is probably necessary to allow plants to fine-tune their defence responses, thereby adjusting defence to a protective level while minimizing associated costs (Kunkel and Brooks, 2002).

In most cases, the relationship between SA and JA seems to be mutually antagonistic (Fig. 1.1; Kunkel and Brooks, 2002; Devoto and Turner, 2005). SA and its functional analogues have been shown to have an inhibitory effect on the JA biosynthesis and JA-dependent gene expression (Peña-Cortés et al., 1993; Gupta et al., 2000). The *eds4* and *pad4* mutants which are impaired in the pathogen-induced accumulation of the SA, display enhanced responses to inducers of JA-dependent gene expression (Gupta et al., 2000). Spoel et al. (2003) demonstrated that NPR1, a central and positive regulator of the SA signalling pathway, is an important modulator of the antagonistic effect of SA on JA-dependent gene expression. The *npr1* mutant alleviated the SA-mediated suppression of pathogen-induced JA production and the expression of JA-responsive genes including *PDF1.2*. Interestingly, the nuclear localization of NPR1 appears not be required for its the negative effect on the JA-dependent gene expression, indicating that the cytosolic form of the regulatory NPR1 protein is responsible for the SA-mediated suppression of JA-dependent signalling (Spoel et al., 2003). However, a more recent model has been formulated that proposes that NPR1 is required for the suppression of *PDF1.2* as it is necessary for the transcriptional activation of *GRX480*. In turn, GRX480 forms an inhibitory complex with TGA factors that interferes with the transcription of *PDF1.2* (Ndamukong et al., 2007). GRX480 is a member of the glutaredoxin family and was identified in a screen to find regulatory proteins of the SA-dependent signalling pathway. The transcription of *GRX480* is SA-inducible and relies on NPR1, indicating that GRX480 has a role in the cross talk between SA and JA (Ndamukong et al., 2007). An additional key element in cross-talk between SA and JA has been identified as the Arabidopsis transcription factor, WRKY70 (Fig. 1.1). WRKY70 act as both an activator of

SA-dependent genes and a repressor of JA-responsive genes, thereby acting as a node of convergence between these antagonistic pathways (Li et al., 2004).

Besides the antagonistic effect of SA on JA signalling, JA is also reported to negatively regulate SA signalling. For example, JA signalling negatively regulates the activation of the SA-mediated defences in the JA-signalling mutants *coi1*, *mpk4* (map kinase 4) and *ssi2* (suppressor of SA insensitivity 2) (Petersen et al., 2000; Kachroo et al., 2001; Kloek et al., 2001). While *coi1* plants do not exhibit constitutive expression of the SA-mediated defences, the SA-dependent signalling pathway is hypersensitized in response to invading pathogens as evidenced by the enhanced expression of SA-mediated *PR-1* and by the increased resistance to virulent *P. syringae* (Feys et al., 1994; Kloek et al., 2001). The *mpk4* and *ssi2* mutants do not only display impaired JA signalling, but constitutively express SA-dependent defences and have increased resistance to virulent *P. syringae* and *H. parasitica* (Petersen et al., 2000; Kachroo et al., 2001; Shah et al., 2001). MPK4 is required for JA-dependent gene expression and may act as a regulator of the negative cross-talk between JA and SA in the activation of defences by simultaneously repressing SA biosynthesis and promoting the perception of or response to JA in Arabidopsis (Fig. 1.1; Petersen et al., 2000). Furthermore, this function of MPK4 involves EDS1 and PAD4, as mutations in these defence regulatory genes resulted in the inhibition of the de-repression of the SA signalling pathway and of the block of the JA pathway in *mpk4* (Fig. 1.1; Brodersen et al., 2006). The *SSI2* gene encodes a stearoyl-acyl carrier protein, which catalyses the synthesis of a fatty acid-derived signal that is involved in the negative cross-talk between the JA and SA pathways (Fig. 1.1; Kachroo et al., 2001). Furthermore, expression profiling of various Arabidopsis lines including wildtype and several mutants defective in SA and JA signalling pathways, provided additional evidence for the mutual antagonism between these pathways (Glazebrook et al., 2003).

Despite clear antagonism between SA- and JA-dependent pathways, synergistic interactions between SA and JA have also been documented. Global gene expression studies demonstrated that numerous defence-related genes were co-induced or co-repressed by SA and JA (Schenk et al., 2000; Glazebrook et al., 2003), suggesting that the two pathways co-ordinately regulate these genes. Interestingly, it appears that the effects of SA and JA on gene expression is dependent on the concentration of the signals. Transient synergistic enhancement in gene expression associated with either the SA- or JA-dependent signalling pathway was observed when both signals were applied to the plant at low concentrations, whereas prolonged application or higher concentrations of SA and JA resulted in antagonism. These results could explain some of the discrepancies observed in different mutants since the trends observed could either be dependent on the relative concentration of SA and/or JA or it could be due to the modifications of the respective signalling pathway (Mur et al., 2006). In addition, simultaneous activation of the SA and JA signalling pathways has been shown to

enhance the rhizobacteria-induced systemic resistance of Arabidopsis to *Pst* DC3000 (van Wees et al., 2000).

Data suggest both positive and negative regulatory interactions between the SA and ET signalling pathways. The development of the disease symptoms in Arabidopsis and tomato following infection by *P. syringae*, *X. campestris* or *Fusarium oxysporum* (Lund et al., 1998; O'Donnell et al., 2001; O'Donnell et al., 2003) seems to require cooperative actions of SA and ET. In addition, infection by *X. campestris* pv. *vesicatoria* induce ET-dependent accumulation of SA in tomatoes (O'Donnell et al., 2001). Results from the aforementioned expression profile analysis of Arabidopsis indicated that SA and ET may function together to induce several defence-related genes (Schenk et al., 2000). Even though SA-mediated induced expression of *PR* genes (or SAR markers) in Arabidopsis occurs independently of an intact ET signalling pathway (Ryals et al., 1996), it has been shown that ET treatment potentiate the SA-dependent induction of *PR-1* (Lawton et al., 1994). However, the ET signalling pathway also negatively affects SA-dependent responses as suggested by the considerably elevated levels of *PR-1* mRNA in *ein2* mutant plants (Lawton et al., 1994; Lawton et al., 1995). These results seem contradictory, but may merely be indicative of the complexity of the cross-talk between the SA and ET signalling pathways.

Results from certain plant-pathogen interactions suggest that SA appears to suppress ET-dependent defence responses (Penninckx et al., 1998; Diaz et al., 2002; Gu et al., 2002). In tomato plants, the exposure to SA inhibited ET-dependent expression of defence-related genes (Gu et al., 2002) and the simultaneous treatment with ET and SA diminished their ET-induced resistance to *B. cinerea* (Diaz et al., 2002).

Limited evidence suggests antagonistic interactions between the JA and ET signalling pathways. In tobacco nicotine biosynthesis, a direct defence against some herbivores, the JA-induction of certain nicotine biosynthetic genes was successfully suppressed by the simultaneous treatment with ET (Shoji et al., 2000). It has also been shown that ET negatively regulates JA-dependent expression of glucosinolate biosynthetic genes as well as glucosinolate accumulation. Glucosinolates are secondary metabolites in the *Brassicaceae* family that function in defence against microbial pathogens and herbivores (Mikkelsen et al., 2003; Halkier and Gershenson, 2006).

ET often acts synergistically with JA in activating the expression of defence-related genes, for example the parallel activation of both the JA and ET signalling pathway are required for the pathogen-induced expression of *PDF1.2*, *CHI-B* and *HEL* in Arabidopsis (Fig. 1.1; Penninckx et al., 1996; Penninckx et al., 1998; Norman-Setterblad et al., 2000) and *PR-5* in tobacco (Xu et al., 1994). Arabidopsis microarray experiments (Schenk et al., 2000;

Glazebrook et al., 2003) revealed that nearly half of ET-inducible genes were also induced by JA treatment, indicating that JA and ET co-ordinately regulate several other defence-related genes. Furthermore, both JA and ET signalling pathways are required for the SA-independent systemic resistance, ISR (Fig. 1.1; Pieterse et al., 1998).

Support also exists for the synergistic interaction between the SA, JA and ET signalling pathways. The constitutive expression of *PDF1.2* and the NPR1-independent expression of *PR-1* in the *ssi1* mutant (suppressor of SA insensitivity 1; Shah et al., 1999) requires the SA, as well as JA and ET signalling pathways (Shah et al., 1999; Nandi et al., 2003). In addition, NPR1-independent resistance in the *cpr5* (constitutive expresser of PR genes 5; Bowling et al., 1997) and *cpr6* (constitutive expresser of PR genes 6; Clarke et al., 1998) mutants requires SA and components of the JA and ET signalling pathways (Fig. 1.1; Clarke et al., 2000b).

ROS and NO signalling interact with several other regulatory components of the defence network. It has been proposed that ROS functions synergistically in a signal amplification loop with SA, while the interaction of NO with ROS and SA plays a central role in the activation of defence responses. All three signals seem to act synergistically in inducing the HR and defence-related gene expression (Fig. 1.1; Shirasu et al., 1997; Delledonne et al., 1998; Delledonne et al., 2001). The addition of low concentrations of exogenous SA to pathogen-infected soybean cells potentiates ROS production and HR cell death (Shirasu et al., 1997). Likewise, NO potentiates the ROS-triggered HR in soybean cells (Delledonne et al., 1998). It has also been shown that both ROS and NO modulate each other's accumulation (Tada et al., 2004; Zeier et al., 2004) and the biosynthesis of SA. In turn, SA induces the production of ROS and NO-mediated responses (van Camp et al., 1998). While H_2O_2 is a weak inducer of *PR* gene expression, the combined applications of H_2O_2 and SA enhance tobacco *PR-1a* expression and provide greater defence against subsequent infection by virulent *P. syringae* pv. *tabaci* than only SA treatments could provide (Blee et al., 2004). The exposure of Arabidopsis and tobacco plants to exogenous NO resulted in an increase in endogenous SA (Durner et al., 1998; Huang et al., 2004), while in tobacco it also activated *PR* gene expression that is dependent on SA accumulation (Durner et al., 1998). Together EDS1 and PAD4 are required for potentiation of pathogen defence responses and certain abiotic stress responses which involves either the direct or indirect processing of ROS-derived molecules around the site of infection (Feys et al., 2001; Rustérucci et al., 2001; Mateo et al., 2004). In a study on the Arabidopsis conditional *flu* (fluorescent) mutant, a distinct link between the SA- and $^1O_2$-mediated signalling pathways through EDS1 was demonstrated (Ochsenbein et al., 2006). *EDS1* expression in *flu* is rapidly induced following the release of $^1O_2$ and is required for the subsequent accumulation of SA and the activation of *PR* gene expression (Ochsenbein et al., 2006). However, SA can also down-regulate ROS scavenging

systems resulting in an increase in the overall ROS levels following pathogen recognition (Klessig et al., 2000). Limited data suggest positive regulatory interactions between the ROS or NO and JA/ET signalling pathways. Genome-wide analysis of tobacco plants deficient in catalase, a H_2O_2 scavenging enzyme, revealed that H_2O_2 induces some genes involved in the biosynthesis of JA and ET (Vandenabeele et al., 2003). Increased accumulation of H_2O_2 in the *ocp3* (overexpressor of cationic peroxidase 3) mutant is correlated with the constitutive expression of *GST1* and *PDF1.2* and enhanced resistance to *B. cinerea* and *P. cucumerina* in a COI1-dependent manner (Coego et al., 2005). The ET receptor, ETR1, may represent a node in cross-talk between ET and H_2O_2 since it can act as ROS sensor, thereby regulating stomatal closure in response to H_2O_2 (Desikan et al., 2005). The treatment of Arabidopsis epidermal cells with JA resulted in the production of NO while exogenous NO application induced all JA biosynthetic genes (Huang et al., 2004).

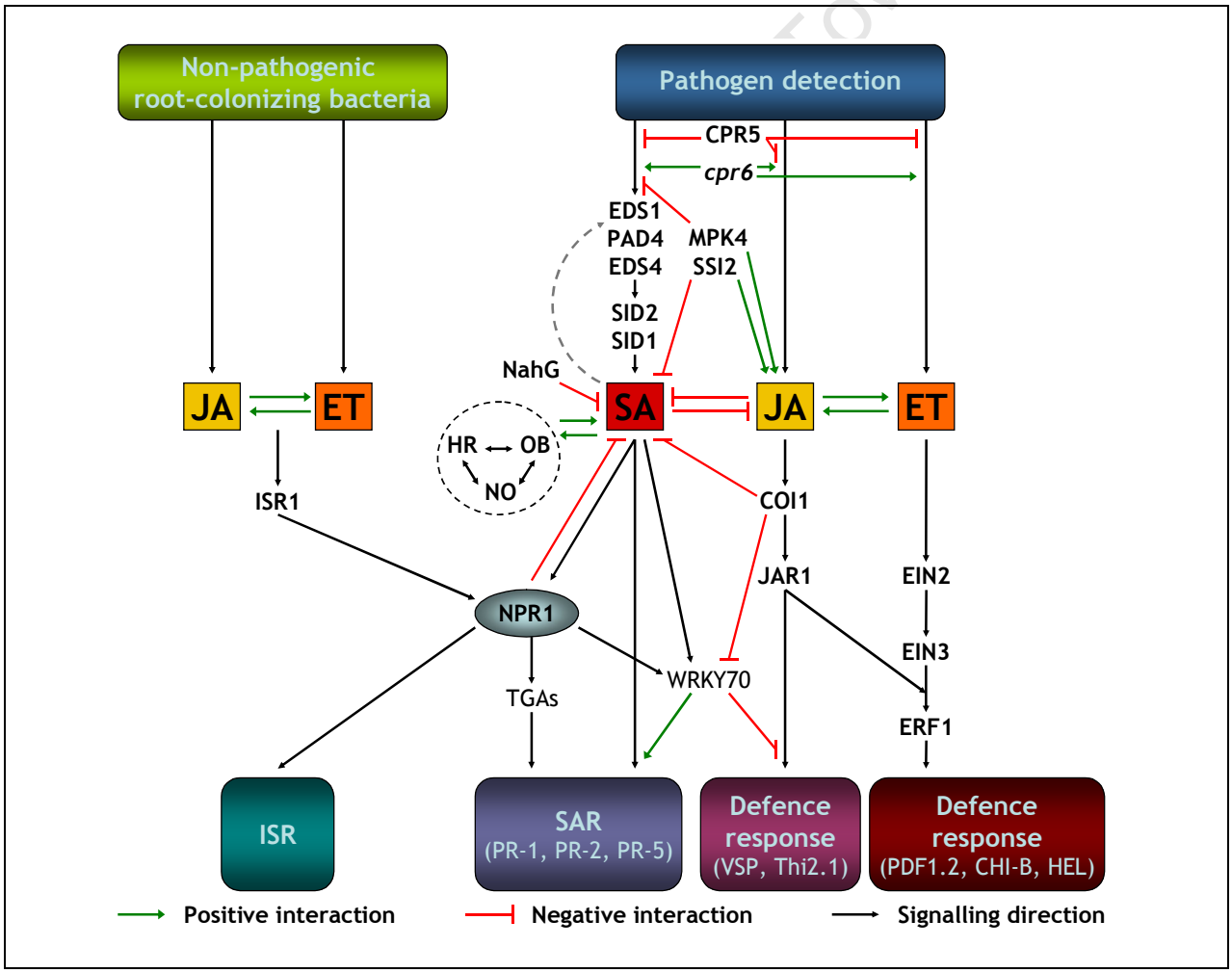

Figure 1.1. Overview of cross-talk in the signalling network controlling activation of defence responses in Arabidopsis.

In the SA signalling pathway, EDS1, PAD4 and EDS4 regulate SA synthesis, SID2 and SID1 are involved in SA biosynthesis whereas the *NahG* transgene reduces accumulated SA levels. The expression of *EDS1* and *PAD4* are regulated by a positive feedback loop indicated by the grey dashed line. NPR1 operates

downstream of SA accumulation where it is involved in a negative feedback loop to regulate SA accumulation. NPR1 interacts with WRKY70 and TGA transcription factors to induce the expression of *PR* genes. The NPR1–independent branch of the SA signalling pathway also contributes to SA-induced *PR* gene expression. In general, the SA and JA pathways seem to be mutually antagonistic. The signalling proteins, MPK4 and SSI2, have roles in the negative cross-talk between the JA and SA pathways by repressing SA biosynthesis and promoting the JA signalling pathway. In the case of MPK4, this occurs in an EDS1- and PAD4-dependent manner. WRKY70 is an additional key element in cross-talk between SA and JA as it activates SA-dependent gene expression and represses JA-dependent defence responses. NO (nitric oxide) can potentiate both the HR (hypersensitive response) and OB (oxidative burst). OB can potentiate SA-mediated signalling directly and via the induction of various MAPK cascades (not shown). Reactive oxygen species (ROS) produced during OB, and NO has been shown to stimulate biosynthesis of SA and in turn, SA induces the production of ROS and NO-mediated responses. COI1 and JAR1 are necessary for JA-dependent defence responses, resulting in the expression of *VSP* (vegetative storage protein) and *Thi2.1* (thionin 2.1). Furthermore, COI1 also antagonizes SA-dependent pathogen defence responses. The transduction of the ET signal requires EIN2 and generally synergism exists between the JA and ET signalling pathways. This is demonstrated by the expression of *PDF1.2* (plant defensin 1.2), *CHI-B* (chitinase B) and *HEL* (hevein-like protein) which are induced co-operatively by the JA and ET signalling pathways. Synergism between SA, JA and ET signalling pathways also exist as indicated by CPR5 and *cpr6*. ISR (induced systemic resistance) is caused by non-pathogenic root-colonizing bacteria and requires both the JA and ET signalling pathways as well as the NPR1 protein. ISR1 functions upstream of NPR1 and ISR does not require SA or involve the accumulation of PR proteins. For simplicity, not all known mutants are represented in this model and any potential positive interactions between the SA and JA pathways, interactions between the SA and ET pathways and possible negative interactions between the JA and ET pathways are not shown. Positive regulatory interactions between signalling pathways are indicated by green arrows, whereas negative interactions are presented by red lines. Black arrows indicate the signalling direction. Capitals represent wildtype alleles while italics indicate mutant alleles. Refer to text for more details and relevant references. (Adapted from Kunkel and Brooks, 2002; Hammond-Kosack and Parker, 2003; Thatcher et al., 2005).

1.2.1.4.7 Transcriptional regulatory network

The transcriptional regulation of a large number of plant defence-related genes is a pivotal feature of inducible defence responses (Eulgem, 2005). Pathogen perception triggers multiple defence signalling cascades where signals lead to the activation of a diverse set of transcription factors, resulting in major transcriptional reprogramming. Transcription factors are not only indispensable components of the signalling cascades but have also been implicated in modulating cross-talk between different defence signalling pathways (Anderson et al., 2004; Boter et al., 2004; Lorenzo et al., 2004). Furthermore, transcription factors regulate the temporal or spatial expression patterns of genes and it is thought that such comprehensive transcriptional reprogramming must function under a transcriptional

regulatory network (Eulgem, 2005). Several members of the Arabidopsis WRKY, Whirly, Myb and ERF transcription factor families have been implicated in the regulation of defence-related genes (Rushton and Somssich, 1998; Eulgem et al., 1999; Jakoby et al., 2002; Mengiste et al., 2003; Desveaux et al., 2004; Desveaux et al., 2005).

WRKY transcription factors are important regulators of the defence transcriptome and subsequent disease resistance responses as they modulate the expression of many defence-related genes (Eulgem and Somssich, 2007). The expression of several Arabidopsis *WRKY* genes are up regulated in reaction to pathogen infection or treatment with PAMPs (Eulgem, 2005). For example, *WRKY11*, *WRKY22*, *WRKY25*, *WRKY29*, *WRKY33* and *WRKY53* displayed high induction values after stimulation with flg22 (Navarro et al., 2004; Zipfel et al., 2004) and chitin induced a group of *WRKY* genes including *WRKY22* and *WRKY29* (Wan et al., 2004). The overexpression *WRKY18* or *WRKY29* also reduced the susceptibility of transformed plants to both bacterial and fungal pathogens (Asai et al., 2002; Chen and Chen, 2002). Furthermore, antisense suppression of *WRKY70* reduced the responsiveness of *PR-1* to SA, whereas *WRKY70* overexpression resulted in increased *PR-1*, *PR-2* (pathogenesis-related protein 2) and *PR-4* expression levels, as well as increased resistance to virulent *P. syringae* and *E. carotovora* (Li et al., 2004). *WRKY70* has been shown to be required for full basal resistance to the virulent pathogen, *H. parasitica* (Knoth et al., 2007). These studies suggest that WRKY transcript levels are important for efficient pathogen defence whereas some WRKY factors have been implicated in the establishment of SAR. As previously mentioned, direct targets of NPR1 include WRKY transcription factors such as WRKY18 and WRKY58 which operating downstream of NPR1, act as a positive and negative regulators of basal defences and SAR, respectively (Wang et al., 2006). Additional targets of NPR1 are WRKY53, WRKY54 and WRKY70 and it was established that WRKY54 and WRKY70 contribute to NPR1-mediated suppression of SA accumulation (Wang et al., 2006). In contrast, several WRKY factors act as negative regulators of basal resistance. For instance, *wrky7* and *wrky7 wrky11* insertional mutants displayed enhanced resistance to infection by virulent *P. syringae* (Journot-Catalino et al., 2006; Kim et al., 2006). *WRKY* genes positively or negatively influence the expression of themselves or of other *WRKYs* through either auto- or cross-regulatory mechanisms (Kalde et al., 2003; Journot-Catalino et al., 2006). WRKYs are believed to be the hub of the transcriptional network and together with additional signalling components are essential in controlling PTI (Eulgem and Somssich, 2007).

Additional transcription factors also have important roles in PTI. The expression of several genes encoding Myb transcription factors are induced upon *P. syringae* infection as well as other defence-related stimuli (Stracke et al., 2001) and it has been shown that certain Myb factors bind to the promoters of defence-related genes (Rushton and Somssich, 1998). A T-DNA insertion in the Arabidopsis gene encoding Myb factor *BOS1* (Botrytis susceptible 1)

resulted in increased susceptibility to *Botrytis* infection (Mengiste et al., 2003). In addition, *BOS1* is required to inhibit the growth of the necrotroph, *A. brassicicola*, and *bos1* mutant plants displayed enhanced disease symptoms after infection with the biotrophic virulent pathogens, *Pst* DC3000 and *H. parasitica* (Mengiste et al., 2003). Ethylene response factors (ERFs) have been implicated in defence-related gene regulation as the GCC boxes to which they bind, mediate gene expression in response to various virulent pathogens and PAMPs (Rushton and Somssich, 1998; Eulgem et al., 1999; Gutterson and Reuber, 2004). Additionally, the expression of several ERFs are up regulated after treatment with ET, wounding or *P. syringae* infections (Lorenzo et al., 2003). *ERF1* is induced synergistically by ET and JA as well as virulent *Pst* DC3000 (Onate-Sanchez and Singh, 2002; Lorenzo et al., 2003) and the overexpression of *ERF1* results in enhanced resistance to *B. cinerea* and *P. cucumerina* (Berrocal-Lobo et al., 2002). In addition, expression profiling indicated that ERF1 regulates, either directly or indirectly, various known defence-related genes (Lorenzo et al., 2003). As discussed previously, TGA factors also have important roles in the regulation of SA-dependent transcriptional reprogramming by physically interacting with NPR1 which results in the expression of *PR* genes (Zhang et al., 2003c).

1.2.1.5 Flagellin perception in plants: an illustration of PTI

To illustrate PAMP detection, subsequent early defence responses and PAMP-triggered signal transduction, a model of our current understanding of flagellin perception in plants (Asai et al., 2002; Gómez-Gómez and Boller, 2002; Gómez-Gómez, 2004) is presented in Fig. 1.2.

The surfaces of plants are densely colonized by bacterial flora and through the propelling action of flagellae, bacteria can enter the plant through stomata, wounds or hydathodes. Once inside the apoplast, the flagellin peptide (or flg22) interacts with the extracellular LRR domain of the FLS2 receptor (Chinchilla et al., 2005). During this interaction, the FLS2 kinase domain is activated through autophosphorylation. This process is not only required for ligand binding and subsequent signal transduction, but is also essential for the assembly of a functional flagellin receptor complex (Gómez-Gómez et al., 2001; Chinchilla et al., 2005).

To ensure both effective defence and survival, it is important for the host to dispose of some activated PRRs to ultimately control pathogen-induced signalling. However, it is not clear exactly how FLS2 activation and signalling is controlled. One possible mechanism to down-regulate FLS2 activation involves the kinase-associated protein phosphatase (KAPP). KAPP has been shown to interact with the kinase domain of FLS2 and studies with KAPP-overexpressing plants suggest that it acts as a negative regulator of the flagellin signal transduction pathway by keeping the FLS2 kinase domain dephosphorylated and therefore in an inactive state (Gómez-Gómez et al., 2001). Another FLS2 regulatory method has been identified as ligand-mediated receptor endocytosis (Robatzek et al., 2006). Upon the specific binding of the flg22 ligand, FLS2 accumulates in mobile, intracellular vesicles. This

ligand-induced endocytosis of FLS2 is followed by receptor degradation which possibly occurs via lysosomal and/or proteasomal pathways. It has been shown that FLS2 mutated in a potential phosphorylation site could bind flg22 normally, but is diminished in endocytosis and downstream signalling. This suggests that the two processes are closely linked, but it is yet unknown if the actual internalisation is required for signalling (Robatzek et al., 2006).

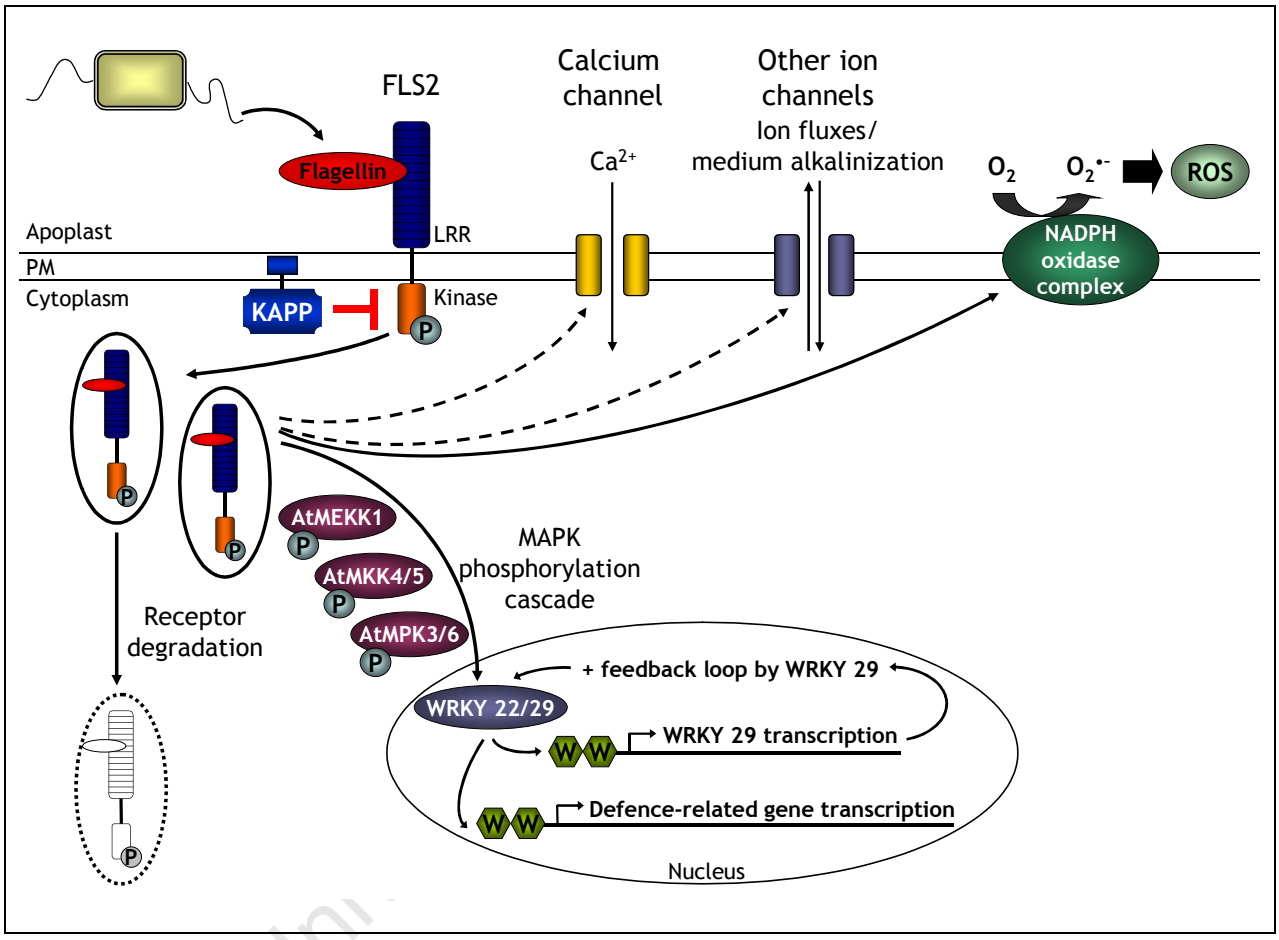

Figure 1.2. Proposed model of the perception, early defence responses and triggered signal transduction in response to flagellin in plants.

Flagellin is released from bacterial flagellae and interacts with the extracellular LRR domain of the FLS2 receptor. The autophosphorylation of the intracellular FLS2 kinase domain is not only crucial for ligand binding, but also has a role in signalling. The kinase-associated protein phosphatase (KAPP) acts as a negative regulator of the flagellin signal transduction pathway (indicated by red lines) by keeping the FLS2 kinase domain in an inactive dephosphorylated state. After binding of flagellin, FLS2 accumulates in mobile intracellular vesicles and is then degraded. The calcium fluxes in response to flagellin include increases in free calcium concentrations in the nucleus and in the cytosol, but the Ca^{2+} sources contributing to these elevations have not yet been determined. Other cellular responses to flagellin include medium alkalinization and the production of ROS through the NADPH oxidase complex. The cellular responses for which the requirement of flagellin binding has not been directed shown, are indicated by dashed arrows. The FLS2 kinase activity is necessary for the activation of a flagellin-responsive MAPK phosphorylation cascade. The phosphorylated AtMEKK1 phosphorylates

AtMKK4 and AtMKK5 that in turn phosphorylate AtMPK3 and AtMPK6 resulting in the expression of the transcription factors WRKY22 and WRKY29. WRKY22 and WRKY29 regulate the expression of flagellin-induced defence genes and WRKY29 is also involved in signal amplification through positive feedback on its own expression. (Ingle et al., 2006; © 2006 Wiley Periodicals, Inc.; Reprinted with permission of Wiley-Liss, Inc. a subsidiary of John Wiley & Sons, Inc.).

Recently it has been shown that a LRR-RLK known as BAK1 (BRI1-associated receptor kinase 1) has a role in FLS2 and EFR signalling (Chinchilla et al., 2007). It has been previously reported that BAK1 regulates the brassinosteroid receptor BRI1 (brassinosteroid-insensitive 1) (Li et al., 2002; Nam and Li, 2002). Arabidopsis *bak1* mutants exhibited normal binding of flagellin, but subsequent flagellin-triggered responses were abnormal. The mutants displayed reduced induction of an oxidative burst as well as the absence of or delayed and reduced activation of MAPKs (Chinchilla et al., 2007). The *bak1* mutation therefore affected signalling and early responses to flg22, suggesting that BAK1 acts as a positive regulator PAMP signalling in Arabidopsis. It was also established that FLS2 and BAK1 form a complex *in vivo* that is ligand-induced and specific for flg22, forming within minutes after treatment with flagellin. Therefore, the activation of the FLS2 receptor by its ligand flagellin involves the rapid formation of a complex with BAK1 (Chinchilla et al., 2007). BAK1 has an additional function to its role in plant development through the plant hormone receptor BRI1 (Li et al., 2002; Nam and Li, 2002) by acting as a positive regulator of PRR-dependent signalling, thereby influencing PTI.

Cellular responses induced by flagellin through yet unknown pathways include cytosolic and nuclear calcium fluxes (Lecourieux et al., 2005), medium alkalinization (Felix et al., 1999) and the production of ROS through the NADPH oxidase complex (Felix et al., 1999), which is the only response that has been shown to require flg22 binding to a functional FLS2 receptor (Robatzek et al., 2006). Furthermore, the FLS2 kinase activity is directly or indirectly responsible for the phosphorylation and activation of a flagellin-responsive MAPK phosphorylation cascade and the expression of defence-related genes as previously discussed.

In recent years, significant advances have been made in our knowledge about PAMP perception which ultimately results in PTI consisting of PAMP-triggered, non-host and basal defences. A significant number of PAMPs have been identified, but the identification bacterial PRRs, fungal PAMPs and their corresponding receptors as well as initial transducers of the PRR signal has lagged behind. Downstream of PAMP detection, many signalling components are required for the activation of plant defence systems and although several of these have been identified, numerous unknowns still exist. Through genetic studies of defence mutants such as *cir1* and others, defence signalling pathways and responses can be further dissected to contribute to our understanding of PAMP-triggered immunity.

1.2.2 Effector-triggered immunity (ETI)

Even though PTI provides plants with relatively robust protection from pathogen growth through the basal defence system (Fig. 1.3A), pathogens have evolved mechanisms to overcome PTI. Some pathogens have evolved non-eliciting PAMPs (e.g. *Agrobacterium*, Fig. 1.3B) and others have developed the ability to deliver effector proteins into plant cells (Espinosa and Alfano, 2004; Chisholm et al., 2006). These effector proteins are thought to suppress defence signalling (Fig. 1.3C), hence resulting in enhanced pathogen growth and disease development (Abramovitch and Martin, 2004; Nomura et al., 2005; da Cunha et al., 2006). In response, plants evolved ETI, also known as "cultivar-specific" or "*R* gene-mediated resistance", which is described by the "gene-for-gene hypothesis" (Flor, 1971) and genetically determined by complementary pairs of pathogen-encoded effector proteins and plant-derived R proteins (Bonas and Lahaye, 2002; Hammond-Kosack and Parker, 2003). Therefore, certain cultivars of an otherwise susceptible plant species display resistance to a given pathogen depending if they possess the appropriate *R* gene to detect a specific pathogen-derived effector molecule (Fig. 1.3D). The recognition of an effector, or of its activity, by a suitable R protein results in ETI and the limitation of pathogen proliferation whereas the lack of either protein leads to a breakdown of resistance and ultimately in disease (Flor, 1971; Dangl and Jones, 2001). The recognized effector is often termed an avirulence (Avr) protein. ETI is believed to be a more accelerated and amplified version of PTI (Tao et al., 2003; Thilmony et al., 2006; Truman et al., 2006), often resulting in the HR (Fig. 1.3D; Greenberg and Yao, 2004).

1.2.2.1 Effector-triggered signalling and defence responses

Upon the direct or indirect recognition of a pathogen effector molecule by the corresponding R protein, effector-triggered signalling and defence responses, collectively referred to ETI, ensues. ETI appears to be super-imposed upon PTI, acting as an additional layer of the plant immune system.

Considerable overlap has been observed between components involved in PTI and those involved in ETI. Only some of the overlapping components are highlighted in the following section. For example, ROS are produced during ETI and PTI although the amount and timing might vary slightly between the two systems (Hückelhoven et al., 2001; Able et al., 2003). NO is another common component since it is also rapidly produced in Arabidopsis after infection with an avirulent strain of *P. syringae* (Zeier et al., 2004). The role of MAPK cascades in the transduction of PAMP-triggered signals has already been discussed, but these cascades also transduce R protein-mediated signals. MAPKs are activated by certain R-effector protein interactions (Romeis et al., 1999) and AtMPK6 is required for the activation of cultivar-specific resistance (Menke et al., 2004).

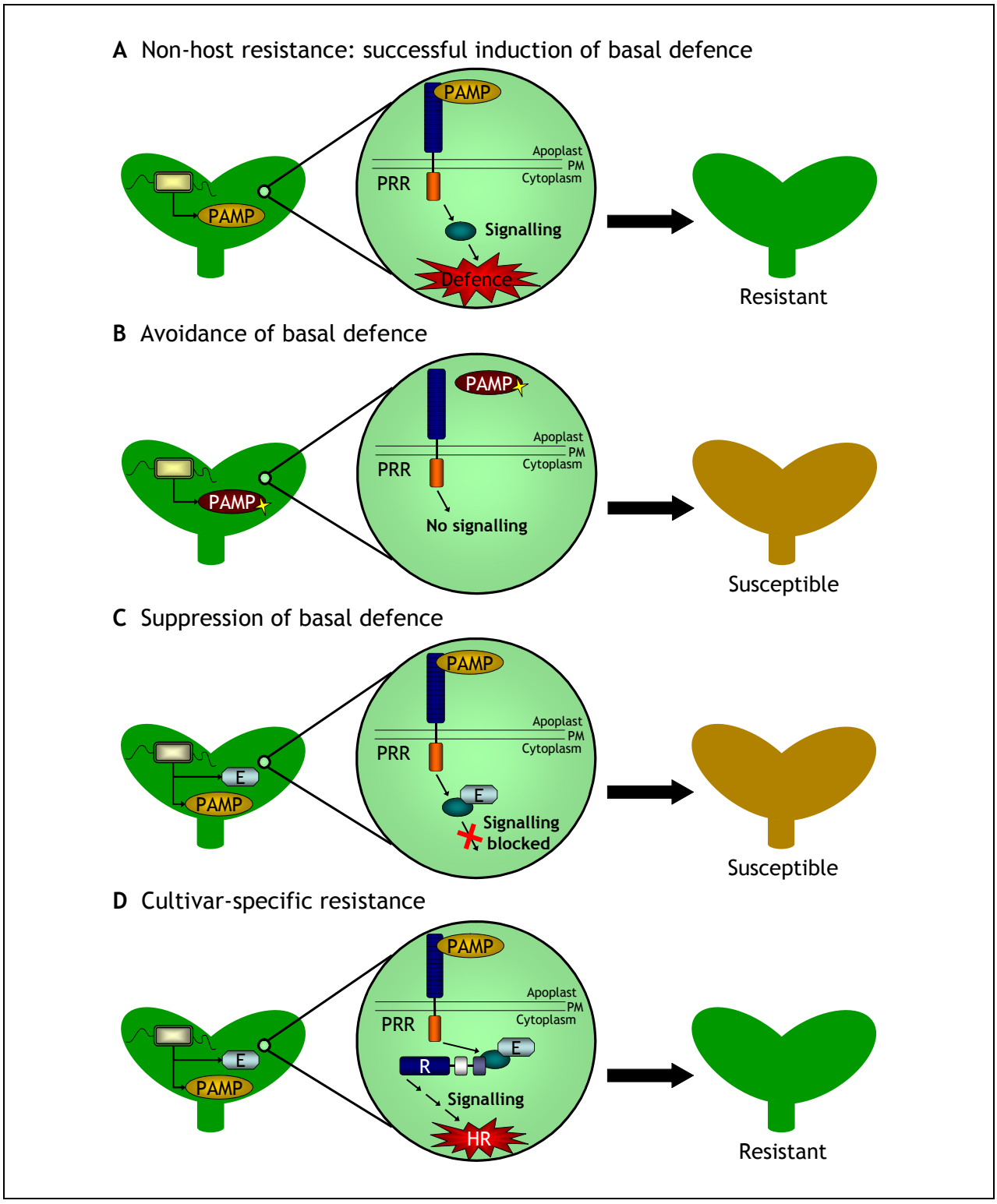

Figure 1.3. The proposed relationship between PTI and ETI in the evolution of plant disease resistance.

(**A**) Recognition of the bacterial PAMP by the matching PRR results in downstream signalling and the subsequent activation of the basal defence responses. The successful induction of PTI results in non-host resistance and renders the plant resistant to pathogen colonization. (**B**) A possible mechanism for overcoming PTI is the evolution of non-eliciting PAMPs which have the capacity to avoid detection by the relevant PRRs. PTI is not activated and the plant is susceptible to infection. (**C**) An alternative strategy for overcoming PTI, is the evolution of effector ("E") proteins. Certain signalling components

of the basal defence system are targeted by effectors to suppress defence responses downstream of PAMP recognition. This causes the plant to be susceptible to disease. (**D**) The evolution of effectors in pathogens consequently led to the evolution of cultivar-specific resistance (or ETI) in plants. To overcome the suppression by effectors, certain cultivars of a susceptible plant species evolved R proteins which recognise the activity of the corresponding effector. Recognition of the effector leads to the HR preventing further pathogen proliferation. (Ingle et al., 2006; © 2006 Wiley Periodicals, Inc.; Reprinted with permission of Wiley-Liss, Inc. a subsidiary of John Wiley & Sons, Inc.).

In addition, the SA, JA and ET signalling pathways are well-documented as playing important roles in PAMP-triggered as well as effector-triggered immunity (Pozo et al., 2005; Thatcher et al., 2005; van Loon et al., 2006). Further evidence for similar mechanisms in PTI and ETI comes from studies of the Arabidopsis *nho1* (nonhost 1; Lu et al., 2001) mutant. *NHO1*, which encodes a glycerol kinase, is not only required for resistance against the non-host pathogen *P. syringae* pv. *phaseolicola* and *B. cinerea*, but also for ETI mediated by several *R* genes (Lu et al., 2001; Kang et al., 2003; Li et al., 2005). Additionally, gene expression profiling were conducted after infection with either the non-host pathogen *P. syringae* pv. *phaseolicola* or an avirulent *P. syringae* strain carrying the AvrRpt2 effector (Tao et al., 2003). Both defence systems targeted largely overlapping sets of genes suggesting that they use some common regulatory mechanisms.

1.2.2.2 Pathogen effector proteins and host recognition thereof

Emerging evidence suggest that during infection, pathogens actively suppress the host's PAMP-triggered defences. It is believed that effectors have developed to interfere with the components of PTI or to confer a selective advantage to the pathogen by acting as virulence factors (Chisholm et al., 2006). Effector proteins use several biochemical activities including protein modification, transcriptional regulation and hormone mimicry to control host cell functions (da Cunha et al., 2007). For instance, *P. syringae* strains produce coronatine, a JA mimic that contributes to virulence by suppressing SA-mediated defence responses (Zhao et al., 2003; Brooks et al., 2005) and by inducing stomatal opening assisting pathogens to gain access to the plant apoplast (Melotto et al., 2006). Although many effector proteins have been cloned, most show little or homology to one another and the biochemical function of most remains unknown (Chisholm et al., 2006).

One of the main differences between PTI and ETI is the manner in which pathogens are recognized. *R* genes have been isolated from several plant species and their isolation has revealed that most are structurally related (Thatcher et al., 2005). The majority of R proteins contain a nucleotide binding site (NBS) and LRRs, and these cytoplasmic R proteins are further subdivided into coiled-coil (CC) or TIR according to their N-terminal domain (Martin et al., 2003; Nimchuk et al., 2003). Another major class of *R* genes encodes extracellular LRR proteins which have been divided into RLPs, RLKs and PGIPs

(polygalacturonase-inhibiting proteins) based on their domain structures (Fritz-Laylin et al., 2005). Although majority of *R* genes fall into the abovementioned classes, R proteins with novel domain structures exist.

The gene-for-gene interaction has often been considered to be similar to a receptor-ligand model where plant R proteins directly interact with pathogen effector molecules. However, direct binding has been found to be the exception rather than the rule as it has been rarely demonstrated (Jia et al., 2000; Deslandes et al., 2003). In addition, the simplified receptor-ligand theory does not provide a clear explanation of how plants co-ordinate resistance to a wide range of pathogens and their corresponding effectors. To answer this question, the "guard hypothesis" was formulated by van der Biezen and Jones (1998). Instead of developing receptors for every possible effector, plants have evolved mechanisms to monitor common host targets. Therefore, R proteins might "guard" a set of key cellular targets of the pathogen effector proteins by forming complexes with these targets. Upon modification or degradation of the targets, the R proteins indirectly detect the activities of multiple effector molecules, subsequently resulting in ETI (van der Biezen and Jones, 1998; Dangl and Jones, 2001).

1.3 Conclusion

Here we have focused only on some findings which have contributed to the understanding of the plant immune system. The study of plant defence mechanisms against pathogen infection is one of the fastest moving fields within plant science and advances are being made in the understanding of plant-pathogen interactions. These include the diversity of pathogen infection, mechanisms utilized by invading pathogens, the isolation of *R* genes and the complexity of plant defence systems involving multiple signalling pathways leading to defence responses (Nomura et al., 2005; Nürnberger and Lipka, 2005; Abramovitch et al., 2006). Furthermore, studies to elucidate the phenomenon known as "priming" which appears to be an additional aspect of the plant immune system (Conrath et al., 2002), are ongoing. Priming offers protection against a wide range of biotic and abiotic stresses by accelerating and increasing the plant's ability to activate defence responses best adapted to the specific stress situation (van Hulten et al., 2006). As priming relies on the potentiation of cellular defence responses as opposed to the direct upregulation of defence signalling pathways, primed plants might not suffer from costly energy investments as the defence responses are only activated once stress exposure occurs (Conrath et al., 2002; van Hulten et al., 2006). Therefore, priming provides an efficient mechanism to obtain broad-spectrum stress resistance (Ton et al., 2005) and better comprehension of the molecular mechanisms underlying priming will also provide valuable insight into the plant immune system, thereby contributing to the possible development of new concepts for disease control.

Considerable progress has been made in identifying key molecular components of the various signalling pathways in the plant defence network, however many gaps in the comprehension of the plant defence signalling network remain. Defence signalling pathways interact extensively with each other and the identification and characterization of potential convergence points where pathway cross-talk occurs, is especially needed. However, defining the roles of signals in this integrated defence network is further complicated by the abundance of signals and interactions within the network. Therefore, concurrent studies employing post-genomic approaches including systems biology, are needed to ultimately reveal all genes and proteins that are simultaneously expressed in a plant during the defence response. This would contribute significantly to unravelling the plant defence network.

Even though the mechanisms of pathogen perception are unique, it has become clear that there is a significant overlap between PTI and ETI, as both systems require common signal transduction molecules and generate similar transcriptional and cellular responses (da Cunha et al., 2006). Furthermore, the suppression of PTI by effector molecules are now well recognized, however it remains a challenge to elucidate the mechanisms by which these diverse effectors link to, and interfere with basal defence signalling. It is possible that certain common signalling components may be the targets of pathogen effectors and are so guarded by R proteins. Therefore, these components only act as true signalling components in PTI (Ingle et al., 2006). Further investigations into identifying effector host targets may resolve this question and further elucidate the molecular basis of PTI.

Single dominant *R* genes can be transferred to agronomically useful crop species to provide resistance to pathogens. However, resistance conferred by a single *R* gene is specific to a particular pathogen strain carrying the corresponding effector protein and since effectors can be easily eliminated, this from of protection is not durable (Mysore and Ryu, 2004). In contrast, PTI contributing to non-host and basal resistance, can be more robust. Therefore, a complete understanding of the molecular basis of plant disease resistance, specifically PTI, could ultimately result in the application of this knowledge in the construction of agronomically important crop plants that display durable resistance by recognizing a wide spectrum of pathogens.

1.4 Specific project aims

The overall aim of this project is to gain insight into the defence signalling network resulting in resistance to pathogen infection in Arabidopsis. For this purpose, the Arabidopsis defence resistance mutant *cir1* was investigated.

Two overriding goals were set in this study. The first involved the genomic mapping of *cir1* with the final aim of identifying the *CIR1* gene. The identification of the *CIR1* gene could explain the mode of action utilized by *cir1* in conferring increased resistance to the

plant. As *cir1* affects PTI which provides resistance to a broad range of different plant pathogens, *CIR1* might greatly benefit the development of efficient and durable applications for plant protection in agricultural biotechnology. First–pass mapping experiments had established that the *CIR1* locus is on the lower arm of chromosome IV (Murray, 2000; Murray et al., 2002).

To summarise, the specific aims and approaches of the first overriding goal of the study included the following:

(i) generation of a suitable mapping population based on constitutively high luciferase activity;
(ii) fine mapping of *cir1* on chromosome IV utilizing newly designed PCR-based markers;
(iii) complementation of the *cir1* mutation through the transformation of the mutant plant with overlapping wild-type genomic DNA fragments;
(iv) identification and investigation of possible *CIR1* candidate genes.

These approaches and their results are presented in Chapter 3 of this thesis.

The second overriding goal of this study was to assess the function of *cir1* in the Arabidopsis defence network. *Cir1* is resistant to infection by virulent *Pst* DC3000 and *H. parasitica* Noco2 (Murray et al., 2002), suggesting the *cir1* mutation results in the induction of basal defence responses resulting in enhanced PTI. To establish what components of the defence signalling network play a role in *cir1*-mediated resistance, the response to pathogen infections and defence-related gene expression patterns in *cir1* double mutant lines was examined.

To summarise, the specific aims and approaches of the second overriding goal of the study included the following:

(i) generation and isolation of homozygous *cir1 coi1*, *cir1 eds1* and *cir1 pad4* double mutant lines;
(ii) investigation of the disease resistance profiles of *cir1* and *cir1* double mutant lines to *B. cinerea*, virulent *P. syringae* and virulent *H. parasitica*. The disease severity profile of *cir1* to *Golovinomyces orontii* infection was also examined;
(iii) defence-related gene expression profiling of *cir1* and *cir1* double mutant lines;
(iv) examining the outputs of the signalling pathways in the *cir1* defence network.

These approaches and their results are presented in Chapter 4 of this thesis.

Chapter 2: Materials and Methods

2.1 Antibiotics, chemicals and kits

All antibiotics, chemicals and kits were purchased from one of the following companies:

Amersham Pharmacia Biotech, Little Chalfont, UK
Applied Biosystems, Foster City, USA
Bioline Ltd., London, UK
BioRad Laboratories, Inc. Hercules, USA
Biosynth AG, Staad, Switzerland
Duchefa Biochemie BV, Haarlem, The Netherlands
Fermentas lnternational Inc., Ontario, Canada
Invitrogen, Carlsbad, USA
Lehle Seeds, Round Rock, USA
Merck & Co. Inc., Whitehouse Station, USA
New England Biolabs, Hitchin, UK
Pierce, Rockford, USA
Promega Corporation, Madison, USA
Qiagen, Crawley, UK
Quantace Ltd., London, UK
Roche Molecular Biochemicals, Basel, Switzerland
Santa Cruz Biotechnology Inc., Santa Cruz, USA
Sigma-Aldrich Inc., St Louis, USA

2.2 Plant material and growth conditions

Arabidopsis thaliana (Arabidopsis) seeds of the Columbia (Col-0) or Landsberg *erecta* (L*er*) ecotypes were used. Most seed were obtained from either the European Arabidopsis Stock Centre (NASC) or from Plant Bioscience Limited (Norwich, UK). All Arabidopsis mutant strains and transgenic lines used are listed in Table 2.1.

2.2.1 Sterilization of Arabidopsis seeds

Seeds were treated with 70% (v/v) ethanol for 5 min with vigorous shaking. After the ethanol had been removed, the seeds were incubated in a bleach solution (containing 10% (v/v) household bleach, 0.02% (v/v) Triton-X) for 15 min with continuous shaking. Subsequently, the seeds were washed five times with sterile water and suspended in 0.1% (w/v) agar. The sterilized seed were stratified for 4 days in the dark at 4°C prior to plating on Murashige and Skoog (MS) basal media.

2.2.2 Growth on MS media

Sterilized seed were plated under sterile conditions on 1 x MS media (Murashige and Skoog, 1962) with macro and micro nutrients (Duchefa Biochemie BV, Haarlem, The Netherlands). Each plate contained 50 – 100 seed spaced equally apart. The plates were incubated at 21°C under fluorescent light (80 – 100 µmol photon/sec/m^2) with a 16 h light and 8 h dark regime for two weeks or until seedlings reached a suitable size to transfer to soil.

Table 2.1 Arabidopsis mutants and transgenic lines used in this study

Strains/ lines	*Ecotype*	*Description*	*Source/reference*
Col-0	n/a	Wild-type	NASC
L*er*	n/a	Wild-type	NASC
Luc2	Col-0	*PR-1::LUC* transgenic line	S. L. Murray, University of Cape Town; Murray et al., 2002
cir1	Col-0	constitutive induced resistance 1	S. L. Murray, University of Cape Town; Murray et al., 2002
coi1-1	Col-*gl1*	coronatine insensitive 1	J. G. Turner, University of East Anglia; Feys et al., 1994
edr5-1	Col-0	enhanced disease resistance 5	J. Dewdney, Harvard Medical School; Volko, 1998
eds1-2	L*er*	enhanced disease susceptibility 1	Plant Bioscience Limited; Aarts et al., 1998
ein2-1	Col-0	ethylene insensitive 2	NASC; Guzman and Ecker, 1990
pad4-1	Col-0	phytoalexin deficient 4	NASC; Glazebrook et al., 1996
pmr4	Col-0	powdery mildew resistant 4	NASC; Vogel and Somerville, 2000
npr1-1	Col-0	nonexpresser of PR genes 1	X. Dong, Duke University; Cao et al., 1994
cir1 ein2	Col-0	Double mutant: *cir1 ein2-1*	S. L. Murray, University of Cape Town; Murray et al., 2002
cir1 npr1	Col-0	Double mutant: *cir1 npr1-1*	S. L. Murray, University of Cape Town; Murray et al., 2002
cir1 coi1	Col-0/ Col-*gl1*	Double mutant: *cir1 coi1-1*	S. L. Murray, University of Cape Town; this study
cir1 eds1	Col-0/ L*er*	Double mutant: *cir1 eds1-2*	This study
cir1 edr5	Col-0	Double mutant: *cir1 edr5-1*	This study
cir1 pad4	Col-0	Double mutant: *cir1 pad4-1*	This study

2.2.2.1 Methyl jasmonate plates

For selection of homozygous *coi1-1* mutant seedlings, MeJA (Sigma-Aldrich Inc., St Louis, USA) was added to MS agar plates at a final concentration of 30 µM. Sterilized seed were plated under sterile conditions and the plates were incubated at 21°C under fluorescent light (80 – 100 µmol photon/sec/m^2) with a 16 h light and 8 h dark regime for one week. Seedlings which displayed the root-elongation phenotype typically associated with MeJA-insensitivity were scored as homozygous *coi1-1* mutant plants.

2.2.2.2 Phosphinothricin plates

For selection of transgenic *Arabidopsis* plants carrying the phosphinothricin acetyltransferase (*Bar*) gene, phosphinothricin (PPT; Duchefa Biochemie BV, Haarlem, The Netherlands) was added to MS agar plates at a final concentration of 10 µg/ml. Sterilized seed were plated under sterile conditions and the plates were incubated at 21°C under fluorescent light (80 – 100 µmol photon/sec/m^2) with a 16 h light and 8 h dark regime for one week. The seedlings which survived on PPT were scored as successfully transformed plants.

2.2.3 Soil-grown Arabidopsis

Seeds were hydrated in 0.1% (w/v) agar and stratified at 4°C in the dark for 1 to 3 days. Thereafter, the seeds were placed on potting medium consisting either of peat (Jiffy Products, International AS, Norway) or of a mixture of peat and vermiculite (1:1). The pots were covered to ensure 100% humidity and were placed at 21°C under fluorescent light (80 – 100 µmol photon/sec/m^2) under a 16 h light and 8 h dark regime unless otherwise stated. After one week, the covers were removed and the seedlings were fertilized with Phosphrogen (Bayer CropScience Group, Hertfordshire, UK).

2.3 Microbial strains

2.3.1 *Escherichia coli*

2.3.1.1 Culture conditions

Escherichia coli cultures harbouring the JAtY library clones were routinely cultured in Luria-Bertani (LB) medium (Sambrook et al., 1989) containing kanamycin (25 µg/ml) at 37°C. Solid media contained 2% (w/v) agar.

2.3.2 *Agrobacterium tumefaciens*

2.3.2.1 Culture conditions

Agrobacterium tumefaciens strain GV3101 (Holsters et al., 1980) was routinely cultured in LB medium (Sambrook et al., 1989) containing rifampicin (100 µg/ml) and gentamycin (15 µg/ml) at 28°C. Solid media contained 2% (w/v) agar.

2.3.3 *Botrytis cinerea*

2.3.3.1 Culture conditions

Botrytis cinerea isolates GLUK-1 (Kliebenstein et al., 2005b) and *Brassica oleracea* (Ferrari et al., 2003) were maintained on sugar free apricot halves incubated in the dark at 25°C until sporulation occurred.

2.3.3.2 Arabidopsis infection assay

Spores were harvested 10 to 14 days post inoculation as described (Denby et al., 2004). For the detached leaf assay (Denby et al., 2004), the spore concentration of the *B. oleracea* isolate (Ferrari et al., 2003) was adjusted to 5 x 10^3 spores/ml in half-strength grape juice. Leaves from 4-week-old soil-grown plants were excised and placed on 0.8% (w/v) agar in large plastic trays. Four microlitres of the spore suspension was drop inoculated onto the upper surface of the leaf and the tray was covered to ensure high humidity conditions. The inoculated leaves were kept at room temperature and the diameter of the developing lesions was measured at 3, 4 and 5 days post inoculation (dpi). Disease severity was expressed as lesion diameter in mm. Three leaves of similar developmental age from five plants per plant line were used.

For camalexin extractions (section 2.9.2) after *B. cinerea* infection, the spore concentration of the GLUK-1 (Kliebenstein et al., 2005b) isolate was adjusted to 1 x 10^5 spores/ml. The excised leaves from 4-week-old soil-grown plants were treated as above and inoculated with three droplets of 4 µl each. Three plants per Arabidopsis line and three leaves per plant were infected. At 2 dpi, the diameter of one representative lesion per leaf was measured resulting in three representative lesions per plant and the leaves were harvested for camalexin extractions.

2.3.4 *Pseudomonas syringae*

2.3.4.1 Culture conditions

Pseudomonas syringae pv. *tomato* DC3000 (*Pst* DC3000) (Whalen et al., 1991) was cultured in King's Broth (KB) medium (King et al., 1954) supplemented with rifampicin (50 µg/ml) at 28°C. Solid media included 2% (w/v) agar.

2.3.4.2 Arabidopsis infection assay

Bacterial cultures were grown overnight in 5 ml of selective liquid KB media. Cells from the overnight cultures were centrifuged, washed with 10 mM $MgCl_2$, and then resuspended to a final OD_{600} of 0.002 in 10 mM $MgCl_2$. An OD_{600} of 0.002 is equivalent to 1 x 10^6 colony forming units (cfu)/ml (Katagiri et al., 2002). Four-week-old soil-grown plants were infected by infiltrating the abaxial side of the entire leaf with the bacterial suspension using a 1 ml needleless syringe (Cao et al., 1994). Successful infiltrations were visualized by the

appearance of water-soaked areas on the leaf. Infected plants were covered to maintain humidity and were kept under normal growth conditions for at least 3 days. Three leaves per plant and three plants per Arabidopsis line were infiltrated.

To establish the severity of the infection, the bacterial density in the plant was analysed at 24 h, 48 h and 72 h post infection. One leaf disc of uniform size (0.5 cm^2) from each of the three infected leaves per plant was harvested and the three discs pooled to represent one sample. Therefore, three samples were collected for each *Arabidopsis* line. The samples were homogenized in 1 ml of 10 mM $MgCl_2$ and serial dilutions were made from the resulting bacterial suspension. Ten microlitres of each dilution was plated on selective solid media which were incubated at 28°C for 2 days. The number of bacterial colonies for each sample was recorded and expressed as cfu/leaf disc.

2.3.5 *Hyaloperonospora parasitica*

2.3.5.1 Culture conditions

Hyaloperonospora parasitica Noco2 (kindly provided by the research group of J. E. Parker, Max-Planck-Institute for Plant Breeding Research; Parker et al., 1993) was maintained on 2-week-old Col-0 seedlings under high humidity conditions at 16°C. New seedlings were spray-inoculated with conidiospores on a weekly basis as described (Parker et al., 1993).

2.3.5.2 Arabidopsis infection assay

Conidiospores from this oomycete were harvested by vortexing the infected seedlings in sterile water. The number of spores was counted using a haemocytometer and the suspension adjusted to 4×10^4 conidiospores/ml (Parker et al., 1996). Although 12-day-old seedlings were tested during the optimisation process, the actual infection assays were performed on four-week-old soil-grown plants, grown under short day conditions (10 h light and 14 h dark regime), which were evenly sprayed with the spore suspension (Parker et al., 1996; Reignault et al., 1996). Infected plants were maintained under humid conditions at 16°C. Assays were performed in duplicate and a total of ten plants per Arabidopsis line were infected. To establish conidiospore numbers present on the infected Arabidopsis lines, duplicate samples of at least five leaves from each of the five plants per line were weighed and harvested 6 to 7 dpi. Spores were harvested and the spore number determined as above. The infection assay was expressed as number of conidiospores/g tissue.

The extent of plant cell necrosis as well as the development and spread of *H. parasitica* intercellular mycelium within the leaf tissue were examined 6 to 7 dpi by staining whole infected leaves from each plant per line with lactophenol trypan blue as previously described (Koch and Slusarenko, 1990). The method was slightly adapted by introducing a second overnight chloral hydrate destaining step and by equilibrating the leaves in 70% (v/v) glycerol prior to mounting onto microscope slides. Stained leaves were viewed using a compound

microscope equipped with interference of phase-contrast optics. Two leaves from each of the ten plants per Arabidopsis line were examined and photographed.

2.3.6 *Golovinomyces orontii*

2.3.6.1 Culture conditions

Golovinomyces orontii (kindly provided by the research group of R. Panstruga, Max-Planck-Institute for Plant Breeding Research) was propagated on 3-week-old Col-0 plants under high humidity conditions at 21°C. New Col-0 plants were inoculated every second week by lightly dusting conidia from infected leaves onto new plants as described (Reuber et al., 1998).

2.3.6.2 Arabidopsis infection assay

Four-week-old soil-grown plants grown under a 10 h light and 14 h dark regime were infected with an inoculum of *G. orontii* by lightly dusting conidia onto all fully expanded leaves. The number of leaves of each plant initially exposed to conidia was recorded and the infected plants were covered and kept at 21°C. To determine the degree of infection, each infected leaf was scored according to a disease index at 10 dpi and an overall disease index score for each plant per plant line was established (adapted from Xiao et al., 2005). For the disease index, the following classification was used: 0 = no visible fungal mycelium, conidiophores or sporulation; 1 = low level sporulation, powdery mildew only on tip or edge of inoculated leaf; 2 = moderate sporulation, powdery mildew covers 10 – 30% of leaf surface; 3 = heavy sporulation, powdery mildew covers 30 – 60% of leaf surface; 4 = very heavy sporulation, > 60% of leaf surface covered with powdery mildew. To establish if the infection spread to other non-inoculated parts of the plant, the number of newly infected leaves which were not exposed to the initial inoculum was assessed for each plant at 14 dpi. Five plants per Arabidopsis line were tested.

2.4 DNA manipulations

2.4.1 Plasmid DNA isolations

High quality plasmid DNA was isolated using the QIAprep Miniprep Kit (Qiagen, Crawley, UK) according to the manufacturer's instructions.

2.4.2 Arabidopsis genomic DNA isolation

Genomic DNA was extracted from leaf tissue based on a standard method (Edwards et al., 1991) with some adaptations. One leaf was homogenized in 500 µl of extraction buffer (200 mM Tris (pH 7.5), 250 mM NaCl, 25 mM EDTA (pH 8.0), 0.5% (w/v) SDS) and heated at 60°C for 10 min. DNA was purified by adding an equal volume of chloroform:isoamylalcohol (24:1 v/v), mixing it well and collecting the supernatant after centrifugation. DNA was

precipitated by adding 0.7 volume of isopropanol and 1/10 volume of 3 M sodium acetate (pH 5.6). DNA was pelleted, washed in 70% (v/v) ethanol and resuspended in 50 - 100 µl of TE (10 mM Tris, 1 mM EDTA, pH 8.0).

2.4.3 Amplification of DNA

2.4.3.1 Polymerase Chain Reaction (PCR) amplification

Primers used in this study are listed in Table 2.2 and the PCR-based markers used in the genomic mapping experiments are summarized in Table 2.3. The primer sequences of the selected cleaved amplified polymorphic sequences (CAPS) and simple sequence length polymorphisms (SSLP) markers are available from databases maintained at "The Arabidopsis Information Resource" (TAIR, http://www.arabidopsis.org).

Table 2.2 Primers used in this study

Restriction enzymes (where applicable) and product sizes after amplification and/or after restriction enzyme digestion in wild-type and relevant mutants are shown.

Name	*Sequence*	*Product size*	*Source/reference*
PAD4-1 F PAD4-1 R	5'- gCgATgCATCAgAAgAg -3' 5'- TTAgCCCAAAAgCAAgTATC -3'	391 bp digest with *Bsm*FI: *PAD4-1* = 281 bp, 110 bp *pad4-1* = 391 bp	J. Glazebrook, University of Minnesota
EDS4 F EDS6 F 105/E2 R	5'- ggCTTgTATTCATCTTCTATCC -3' 5'- gTggAAACCAAATTTgACATTAg -3' 5'- ACACAAgggTgATgCgAgACA -3'	*EDS1-2* = 1500 bp, 750 bp *eds1-2* = 1500 bp, 600 bp	J. E. Parker, Max Planck Institute for Plant Breeding Research
COI1 F COI1 R	5'- ggTTCTCTTTAgTCTTTAC -3' 5'- CAgACAACTATTTCgTTACC -3'	1500 bp digest with *Xcm*I: *COI1* = ~1000 bp, ~500 bp *coi1* = 1500 bp	Xie et al., 1998
Luc F Lucint R	5'- ggTgTTgggCgCgTTATTT -3' 5'- TTCCggTAAgACCTTTCgg -3'	~1300 bp	S. L. Murray, University of Cape Town
Bar F Bar R	5'- gCACgCAACgCCTACgACTggAC -3' 5'- TCATCgCAAgACCggCAACAggA -3'	~300 bp	Patnaik and Khurana, 2003

PCR amplifications were performed in 20 µl reaction volumes using *Taq* DNA polymerase (Promega Corporation, Madison, USA). Typically the reaction consisted of 1 x thermophilic DNA polymerase PCR buffer (without $MgCl_2$), 125 µM dNTPs, 250 nM of each primer and $MgCl_2$ added to the optimal concentration determined empirically for each set of primers. Approximately 10 ng of template DNA, consisting of either Arabidopsis genomic DNA or plasmid DNA, was added to the reaction. For *E. coli* and *A. tumefaciens* colony PCR the method remained the same except that a single colony was added as template to the PCR reaction. Amplification conditions included an initial DNA denaturation step at 94°C for 2 min, followed by cycles of denaturation at 94°C for 15 sec, primer annealing according to the

specific primer melting temperatures for 30 sec and elongation at 72°C, allowing 1 min per 1 kb amplified. Reactions proceeded for 30 - 35 cycles in a GeneAmp® PCR system 2700 (Applied Biosystems, Foster City, USA). The size of the amplified PCR products was determined by agarose gel electrophoresis.

Table 2.3 PCR-based markers used in genomic mapping experiments

Markers were based on co-dominant cleaved amplified polymorphic sequences (CAPS), single sequence-length polymorphisms (SSLP), insertion-deletion polymorphisms (InDel) or single nucleotide polymorphisms (SNP) between Col-0 and L*er*. Restriction enzymes required for analysis of CAPS markers are listed.

Marker	*Sequence*	*Type*	*SNP/InDel name*[a]	*Annotation unit*[b]	*Source*
nga63	F: 5'- AACCAAggCACAgAAgCg -3' R: 5'- ACCCAAgTgATCgCCACC -3'	SSLP	N/A	N/A (I)	TAIR
nga280	F: 5'- CTgATCTCACggACAATAgTgC -3' R: 5'- ggCTCCATAAAAAgTgCACC -3'	SSLP	N/A	F14J16 (I)	TAIR
nga168	F: 5'- TCgTCTACTgCACTgCCg -3' R: 5'- gAggACATgTATAggAgCCTCg -3'	SSLP	N/A	T7F6 (II)	TAIR
nga162	F: 5'- CATgCAATTTgCATCTgAgg -3' R: 5'- CTCTgTCACTCTTTTCCTCTgg -3'	SSLP	N/A	MDC16 (III)	TAIR
nga6	F: 5'- TggATTTCTTCCTCTCTTCAC -3' R: 5'- ATggAgAAgCTTACACTgATC -3'	SSLP	N/A	T17J13 (III)	TAIR
nga8	F: 5'- gAgggCAAATCTTTATTTCgg -3' R: 5'- TggCTTTCgTTTATAAACATCC -3'	SSLP	N/A	T32A17 (IV)	TAIR
F28M11a	F: 5'- CCTCTCTTTTTCCTCCATTCC -3' R: 5'- AAAACCCgTTCCACCAAAC -3'	InDel	CER451764	F28M11 (IV)	This study
Det1.1	F: 5'- gAgCATCAACAAgATgACC -3' R: 5'- CAAAATgTgAATgTCC -3'	CAPS (*Sac*I)	N/A	T9A4 (IV)	TAIR
F24G24a	F: 5'- CAgTTgAACCCACCCATT -3' R: 5'- gATTCggTCCAAgAACCTT -3'	InDel	CER451181	F24G24 (IV)	This study
F7L13a	F: 5'- AATACTAAACACCCCCAACCA -3' R: 5'- ATggAACAggACAAgACAAgA -3'	SNP	CER432786	F7L13 (IV)	This study
T12H20a	F: 5'- TggTgTTgTCCATgCAAATg -3' R: 5'- ATTggTTCTTCCTTgTgggC -3'	SNP	CER442129	T12H20 (IV)	This study
T12H20b	F: 5'- TgTCAgAAACAAATggCCgA -3' R: 5'- gCAgCTgAgCgAgAgAggTT -3'	SNP	CER442140	T12H20 (IV)	This study
F25I24b	F: 5'- ACCAAATAgATCCACCggCA -3' R: 5'- AggTTCACTATgCgCTCggT -3'	SNP	CER429460	F25I24 (IV)	This study
F25I24c	F: 5'- TCTCAggAgCCATgAAgCg -3' R: 5'- TggACCAgAgACTgCAAAggA -3'	InDel	CER451334	F25I24 (IV)	This study
T22B4a	F: 5'- CATgAAACAAgAgAgAAg -3' R: 5'- TTCTTTTCTTACCCATAC -3'	InDel	CER459396	T22B4 (IV)	This study

Continued on next page

Table 2.3 Continued from previous page

Marker	Sequence	Type	SNP/InDel name[a]	Annotation unit[b]	Source
T22B4b	F: 5'- TgCCCTAgAAAAATgggATg -3' R: 5'- TgCAgAAgCAAAggTCTTCC -3'	SNP	CER444468	T22B4 (IV)	This study
F8L21a	F: 5'- gTgTTTATgACAATTTTCATCTC -3' R: 5'- CATCAACATgCTgTAgAATCC -3'	InDel	CER466322	F8L21 (IV)	This study
F8L21c	F: 5'- CAAAATCggCAgAAAATTCC -3' R: 5'- gTggCTCACCCATCTAAACA -3'	InDel	CER466317	F8L21 (IV)	This study
F25E4a	F: 5'- TTgAAACACAAgAgggCCA -3' R: 5'- CgAgATCCCAAATTgCTCAT -3'	SNP	CER473091	F25E4 (IV)	This study
T26M18a	F: 5'- TTgAATCTCATCgCgAAgC -3' R: 5'- CgggATgTTggAATggAA -3'	InDel	CER459855	T26M18 (IV)	This study
T4C9a	F: 5'- CAgCAATACACCATCACTCACTg -3' R: 5'- AATCCggTCATTAgCACggT -3'	InDel	CER460581	T4C9 (IV)	This study
T20K18a	F: 5'- AACTAgCATTgTggAgCTTC -3' R: 5'- gATCTgTTgAAACCAAgAgg -3'	InDel	CER459262	T20K18 (IV)	This study
CIW6	F: 5'- CTCgTAgTgCACTTTCATCA -3' R: 5'- CACATggTTAgggAAACAATA -3'	SSLP	N/A	T6G15 (IV)	TAIR
F18A5a	F: 5'- CACACACTCATTATACAAC -3' R: 5'- CAAgTATTgAgCTggATC -3'	InDel	CER466221	F18A5 (IV)	This study
CM4-3	F: 5'- gATCAATAATAAgTgTCTTCTC -3' R: 5'- TTCTgggTTCTTggTgATCTC -3'	CAPS (*Bgl*II)	N/A	FCAALL (IV)	TAIR
g4539	F: 5'- ggACgTAgAATCTgAgAgCTC -3' R: 5'- ggTCATCCgTTCCCAggTAAAg -3'	CAPS (*Hin*dIII)	N/A	FCAALL (IV)	TAIR
nga106	F: 5'- gTTATggAgTTTCTAgggCACg -3' R: 5'- TgCCCCATTTTgTTCTTCTC -3'	SSLP	N/A	N/A (V)	TAIR
nga76	F: 5'- ggAgAAAATgTCACTCTCCACC -3' R: 5'- AggCATgggAgACATTTACg -3'	SSLP	N/A	F24J2 (V)	TAIR

[a] Names of SNPs and InDels in Monsanto polymorphism collection (Jander et al., 2002).

[b] BAC or P1 vector names, according to TAIR, on which the marker is situated. The chromosome on which the annotation unit is located, are indicated in brackets.

2.4.3.2 Quantitative real-time PCR

Primers used in quantitative real-time PCR experiments are listed in Table 2.4. Two-step quantitative real-time PCR was performed. Firstly, 5 µg of total RNA of the relevant samples was reverse transcribed into first strand cDNA (see section 2.5.2 for more detail). Thereafter, real-time PCR was performed using a RotorGene RG3000A instrument (Corbett Research, Sydney, Australia). The 2 x SensiMix (dT) DNA kit (Quantace, London, UK) which contains SYBR Green, was used for quantitative real-time PCR which was performed in 25 µl reaction volumes in 0.1 ml tubes. Typically the reaction consisted of template cDNA, 1 x SensiMix (dT), 1 x SYBR® Green solution, 200 nM of each primer and $MgCl_2$ added to the

optimal concentration determined empirically for each set of primers. Amplification conditions included an initial step at 95°C for 10 min, followed by 35 – 45 cycles of 95°C for 10 sec, primer annealing according to the specific primer melting temperatures for 15 sec and elongation at 72°C for 20 sec. All PCR reactions were performed in triplicate and a biological replicate was also included.

Table 2.4 Primers used in quantitative real-time PCR experiments

The primer name, its sequence or source where relevant, the annealing temperature (°C) and $MgCl_2$ concentration (mM) used during quantitative real-time PCR experiments are shown. The well number indicates the position of the gene in the 96-well plate used for the packaging of the Arabidopsis pathogen-inducible genes primer library.

Name	*Sequence/source*	*Well #*	*Anneal. temp*	*[$MgCl_2$]*
At4g02380 (AtLEA5 or SAG21)	Arabidopsis pathogen-inducible genes primer library[a]	A3	65	3.5
At3g16530 (N/A)	Arabidopsis pathogen-inducible genes primer library[a]	A6	65	3.5
At5g44420 (PDF1.2)	Arabidopsis pathogen-inducible genes primer library[a]	A7	65	4.0
At2g31880 (N/A)	Arabidopsis pathogen-inducible genes primer library[a]	B4	65	5.0
At2g14560 (LURP1)	Arabidopsis pathogen-inducible genes primer library[a]	B10	65	3.5
At4g14400 (ACD6)	Arabidopsis pathogen-inducible genes primer library[a]	B12	65	4.0
At4g37520 (PER50)	Arabidopsis pathogen-inducible genes primer library[a]	D11	65	3.5
At3g57260 (PR-2 or BGL2)	Arabidopsis pathogen-inducible genes primer library[a]	E1	65	3.5
At3g57240 (BG-3)	Arabidopsis pathogen-inducible genes primer library[a]	E2	65	4.5
At2g14610 (PR-1)	Arabidopsis pathogen-inducible genes primer library[a]	E3	65	3.5
At3g46090 (ZAT7)	Arabidopsis pathogen-inducible genes primer library[a]	E8	65	3.5
At4g03450 (N/A)	Arabidopsis pathogen-inducible genes primer library[a]	E9	65	3.5
At5g10760 (N/A)	Arabidopsis pathogen-inducible genes primer library[a]	E11	65	4.0
At2g02930 (AtGSTF3 or GST16)	Arabidopsis pathogen-inducible genes primer library[a]	F7	65	3.5
At3g25882 (NIMIN-2)	Arabidopsis pathogen-inducible genes primer library[a]	H6	65	3.5

Continued on next page

Table 2.4 Continued from previous page

Name	Sequence/source	Well #	Anneal. temp	[$MgCl_2$]
At3g18780 (Actin-2)	Arabidopsis pathogen-inducible genes primer library[a]	H11	65	3.5
At5g25760 (Ubiquitin ligase)	F: 5'- ggACCgCTCTTATCAAAggA -3' R: 5'- CTTgAggAggTTgCAAAggA -3'	N/A	54	4.5
At1g10140 (N/A)	F: 5'- TTCACCTTCggATTCACAgA -3' R: 5'- CAgCAgAAgCAACAgAAgCA -3'	N/A	60	4.0
At3g47960 (N/A)	F: 5'- gCCTAAACCCATgAgCAgAA -3' R: 5'- CTgCCTTTCTTTgCgACACT -3'	N/A	60	4.0
At4g37430 (CYP91A2 or CYP81F1)	F: 5'- CTCCTCTCACCgTCTCATCA -3' R: 5'- AAATCgTTgCTTTCgTTggA -3'	N/A	58	3.5

[a] The Arabidopsis pathogen-inducible genes primer library was obtained from Sigma-Aldrich Inc. (St Louis, USA).

The expression level of each gene was quantified with the Corbett RotorGene analysis software (version 6.0, built 38; Corbett Research, Sydney, Australia) using a standard curve of pooled cDNA samples for the housekeeping genes and the genes of interest. Relative expression was obtained by normalizing expression of the genes of interest to those of the housekeeping genes, actin-2 (At3g18780) or ubiquitin ligase (At5g25760), which showed constant expression regardless of the infection state or the genotypes of the samples. Melt curve analysis confirmed that the individual amplified products corresponded to a single, gene-specific cDNA fragment and the amplification efficiency of each reaction was 100% ± 20%.

2.4.4 Restriction endonuclease digestion of DNA

CAPS marker PCR products were digested with 5 to 10 U of restriction enzyme supplied by either New England Biolabs (Hitchin, UK), Fermentas lnternational Inc. (Ontario, Canada) or Roche Molecular Biochemicals (Basel, Switzerland) according to the manufacturer's recommended conditions. In general, 1 U of enzyme per µg of DNA was used and the enzyme volume never exceeded 10% of the total reaction volume. All digests were carried out overnight at the appropriate temperature.

2.4.5 DNA electrophoresis

DNA fragments were separated by agarose gel electrophoresis. The DNA samples in 1 x loading buffer (0.25% (w/v) bromophenol blue, 40% (w/v) sucrose) and an appropriate DNA size marker were loaded onto the agarose gel which was electrophoresed at 100 V in 1 x TAE buffer (40 mM Tris, 1 mM EDTA, 0.11% (v/v) glacial acetic acid, 0.160 µg/ml ethidium bromide). Separated DNA fragments were visualised and photographed on a 254 nm UV

transilluminator (UVP Inc., San Gabriel, USA). See Table 3.2 (Chapter 3) for optimal % (w/v) agarose gel used for relevant PCR-based markers.

2.4.6 DNA sequencing and analysis

The primers designed for sequencing are listed in Table 2.5. PCR products to be sequenced were extracted and purified from agarose gels using the Qiagen MinElute gel extraction kit (Qiagen, Crawley, UK) according to the manufacturer's instructions. DNA sequences were determined by the DNA Sequencing Service at the University of Cape Town on an Applied Biosystems 3130 Genetic Analyzer (DNA capillary sequencer; Applied Biosystems, Foster City, USA) using Applied Biosystems Big Dye terminator v3.1 Cycle Sequencing kit (Foster City, USA) and Bioline Half Dye Mix (London, UK).

Table 2.5 Primers used for sequencing

Name	*Sequence*	*Product size*
CYP83A1_1F	5'- TTTgATgTCggTTAAgTTCggT -3'	1072 bp
CYP83A1_1R	5'- ACggTTTCTTgAAgCgCA -3'	
CYP83A1_2F	5'- TgCgCTTCAAgAAACCgT -3'	963 bp
CYP83A1_2R	5'- TTATTTAATCgAACCCgAggC -3'	

Sequence data were analysed with DNAman software (version 4.13; Lynnon Biosoft, Quebec, Canada) and Chromas freeware (version 1.45; available from www.technelysium.com.au/chromas.html).

2.5 RNA manipulations

2.5.1 Total RNA isolation from Arabidopsis

For Northern blot analysis, total RNA was routinely extracted using a guanidinium thiocyanate-phenol-chloroform extraction method adapted from Chomczynski and Sacchi, 1987. Approximately 100 mg of leaf tissue was homogenized in 500 µl of solution D (4 M guanidinium thiocyanate, 25 mM sodium citrate (pH 7.0), 0.5% (w/v) sarkosyl, 0.7% (v/v) β-mercaptoethanol). Thereafter, 500 µl of H_2O-saturated phenol (pH 4.0), 50 µl of 3 M sodium acetate (pH 4.0) and 150 µl of chloroform:isoamylalcohol (49:1 v/v) was added to the homogenate and incubated on ice for 15 min. The samples were centrifuged at 12 000 *g* for 20 min at 4°C. The RNA in the supernatant was precipitated with 500 µl of isopropanol, incubated on ice for 10 min and centrifuged at 12 000 *g* for 20 min at 4°C. The pellet was washed with 500 µl of cold 75% (v/v) ethanol, air dried for approximately 10 min and resuspended in 25 µl of deionised formamide (Sigma-Aldrich Inc., St Louis, USA).

Total RNA for reverse transcription-PCR (RT-PCR) was extracted using a modified small-scale procedure as described by Verwoerd et al. (1989). Approximately 100 mg of the leaf tissue was ground in liquid nitrogen and homogenized in 500 µl of extraction buffer consisting of 100 mM Tris (pH 9.0), 200 mM NaCl, 5 mM dithiothreitol (DTT), 1% (w/v) sarkosyl and 20 mM EDTA. RNA was extracted by adding 250 µl of phenol and 250 µl of chloroform:isoamylalcohol (24:1 v/v). Additional chloroform:isoamylalcohol (24:1 v/v) extractions were performed as required. After centrifugation, the RNA was precipitated overnight at 4°C by mixing the aqueous phase with 8 M LiCl to reach a final concentration of 2 M LiCl. Pellets were washed twice in 2 M LiCl and RNA precipitated overnight at -20°C by adding 1/10 volume of 3 M sodium acetate (pH 5.2) and 2 volumes of ethanol. After centrifugation at 12 000 *g* for 20 min at 4°C, RNA pellets were washed with 70% (v/v) ethanol, dried and resuspended in 25 µl of diethylpyrocarbonate (DEPC)-treated deionised water (dH_2O).

2.5.2 RT-PCR

Firstly, the RNA concentration of the extracted samples were determined using a Nanodrop ND-100 Spectrophotometer (Nanodrop Technologies, Inc., Montchanin, DE). The optical density of the RNA samples was determined using a wavelength of 260 nm where an OD_{260} of 1 is equal to 40 µg RNA/ml. Five micrograms of total RNA of each was reverse transcribed into first-strand cDNA using the Superscript™ III Reverse Transcriptase kit (Invitrogen, Carlsbad, USA) according to the manufacturer's instructions. The procedure was slightly adapted by incubating the reaction at 46°C for 3 h, then adding another 1 µl of Superscript™ III RT enzyme and continuing the incubation of the reaction overnight at 46°C. Thereafter, the enzymatic reaction was heat-inactivated at 70°C for 15 min. The cDNA yield of each sample was determined using a Nanodrop ND-100 Spectrophotometer (Nanodrop Technologies, Inc., Montchanin, DE). The optical density of the cDNA samples was determined using a wavelength of 260 nm where an OD_{260} of 1 is equal to 37 µg cDNA/ml.

2.5.3 Northern blot analysis

RNA yield was determined using a UV spectrophotometer (Beckman Coulter, Fullerton, USA) or the Nanodrop ND-100 Spectrophotometer (Nanodrop Technologies, Inc., Montchanin, DE). Ten micrograms of total RNA was subjected to 1.2% (w/v) formaldehyde gel electrophoresis according to standard procedures (Sambrook et al., 1989) and the ethidium bromide stained gels were photographed using a 254 nm UV transilluminator (UVP Inc., San Gabriel, USA) to be used as a loading control between RNA samples. Subsequently, the RNA was transferred onto Hybond-N nylon membranes (Amersham Pharmacia Biotech, Little Chalfont, UK) consistent with standard procedures (Sambrook et al., 1989) and the RNA was cross-linked

onto the nylon membrane with a UV illuminator (Amersham Pharmacia Biotech, Little Chalfont, UK) at 700 joules.

^{32}P-labelled probes were prepared using the Megaprime DNA labelling kit (Amersham Pharmacia Biotech, Little Chalfont, UK) according to the manufacturer's instructions by random priming of gel-purified template DNA. The *PR-1* (At2g14610) DNA template was prepared from genomic DNA using the primers 5'- gCTCTTgTTCTTCCCTCg -3' and 5'- gTgTAgTgACCACAAACTCCA -3' (Denby et al., 2005). A ~1.1 kb fragment of the *CYP83A1* (At4g13770) gene was amplified from genomic DNA by PCR with the primers 5'- TTgATgTCggTTAAgTTCggT -3' and 5'- ACggTTTCTTgAAgCgCA -3'. Radiolabelled probes were purified using Sigmaspin Post Reaction Clean-up columns (Sigma-Aldrich Inc., St Louis, USA) according to the manufacturer's instructions and the entire volume of purified probe was added to the hybridisation buffer used in Northern blot analysis.

The Church and Gilbert method was utilized for the Northern blot analysis of both *PR-1* and *CYP83A1* (Church and Gilbert, 1984). Consistent with standard procedures (Church and Gilbert, 1984; Sambrook et al., 1989), the membranes were incubated overnight at 60°C in standard hybridisation buffer containing the relevant radiolabelled probes. The following day, membranes were washed at 60°C and sealed in plastic bags. The sealed membrane was exposed to a sheet of Biomax ML film (Kodak, USA) in an autoradiography cassette with intensifying screens at -70°C. The exposure time was dependent on the total counts per second (recorded with a Geiger counter) on the membrane after the final wash. The film was developed according to the manufacturer's specifications.

2.6 Protein manipulations

2.6.1 Total protein isolation from Arabidopsis

Total protein extracts were prepared from leaves by homogenization in liquid nitrogen as described by Feys et al. (2005). Forty milligram samples were resuspended in 100 µl of 2 x SDS-PAGE sample application buffer (125 mM Tris (pH 6.8), 4% (w/v) SDS, 20% (v/v) glycerol, 0.02% (w/v) bromophenol blue, 0.2 M DTT). Samples were briefly vortexed, boiled for 5 min and centrifuged at 12 000 *g* for 10 min at 4°C. Equal volumes of the supernatant from each sample were loaded onto SDS-PAGE gels.

2.6.2 SDS Polyacrylamide Gel Electrophoresis (SDS-PAGE)

SDS-PAGE was carried out on 10% (v/v) polyacrylamide gels prepared from a 30% (w/v) acrylamide/bisacrylamide (29:1 v/v) stock solution (BioRad Laboratories, Inc. Hercules, USA) using the Mini-PROREAN® 3 system (BioRad Laboratories, Inc. Hercules, USA). The resolving gel consisted of 10% (v/v) polyacrylamide, 375 mM Tris (pH 8.8), 0.1% (w/v) SDS, 0.1% (w/v) ammonium persulphate (APS) and 0.05% (v/v) TEMED (BioRad Laboratories, Inc. Hercules,

USA). It was overlaid with a 4% (v/v) stacking gel comprised of 4% (v/v) acrylamide/bisacrylamide, 125 mM Tris (pH 6.8), 0.1% (w/v) SDS, 0.1% (w/v) APS and 0.1% (v/v) TEMED (BioRad Laboratories, Inc. Hercules, USA). Denatured protein samples and a pre-stained molecular weight marker (Precision plus protein standard dual colour; BioRad Laboratories, Inc. Hercules, USA) were electrophoresed in a running buffer (25 mM Tris, 192 mM glycine and 0.1% (w/v) SDS) at 100 V until the dye front had run off the gel.

2.6.3 Western blot analysis

Proteins were transferred at 90 V for 90 min onto Hybond™-ECL™ nitrocellulose membrane (Amersham Pharmacia Biotech, Little Chalfont, UK) using the Mini Trans-Blot® Cell blotting apparatus (BioRad Laboratories, Inc. Hercules, USA) according to the manufacturer's instructions. The transfer buffer used consisted of 25 mM Tris, 192 mM glycine and 20% (v/v) methanol. Membranes were stained with Ponceau S (Sigma-Aldrich Inc., St Louis, USA), washed with dH_2O and photographed to determine if samples were equally loaded.

Thereafter, membranes were blocked for 1 h at room temperature in TBS-T buffer (10 mM Tris, 150 mM NaCl, 0.05% (v/v) Tween 20, pH 7.5) containing 5% (w/v) blotting grade milk powder. Incubation with primary antibodies was carried out overnight at 4°C with gentle agitation under the following conditions: α-EDS1 (Feys et al., 2001), 1:500 dilution in TBS-T buffer with 2% (w/v) milk powder; α-PAD4, 1:500 dilution in TBS-T buffer with 0.9% (w/v) milk powder. The membranes were washed 3 times for 15 min each with TBS-T buffer at room temperature on a rotary shaker. The primary antibody-antigen conjugates were detected using a horseradish peroxidase-conjugated goat anti-rabbit IgG (Santa Cruz Biotechnology, Santa Cruz, USA) secondary antibody diluted 1:5000 in TBS-T buffer containing 2% (w/v) milk powder. Incubation with the secondary antibody solution occurred for 90 min at room temperature with gentle agitation and subsequently membranes were washed as described above. This was followed by chemiluminescence detection using a 7:1 (v/v) mixture for α-EDS1 and a 4:1 mixture for α-PAD4 of the SuperSignal® West Pico Chemiluminescent- and the SuperSignal® West Femto Maximum Sensitivity-kits (Pierce, Rockford, USA) according to the manufacturer's instructions. Luminescence was detected by exposing the membrane to photographic film (Biomax light film; Kodak, USA).

The intensities of the bands present on the film were quantified using ImageJ software (version 1.38x; http://rsb.info.nih.gov/ij; Abramoff et al., 2004) and were expressed relative to the EDS1 signal obtained for the wild-type samples which were set to a value of 1.0.

2.6.4 Luciferase assays

A crude protein extraction was performed by homogenizing leaf tissue from 4-week-old soil-grown plants in extraction buffer (100 mM sodium phosphate buffer (pH 7.2), 5 mM DTT). The samples were centrifuged for 5 min at 12 000 *g* to pellet cell debris. The luciferase

activity present in 100 µl of protein extract was measured using a Luminoskan TL-Plus luminometer (Labsystems, Finland). One hundred microlitres of assay buffer (60 mM Tris (pH 8.0), 20 mM $MgCl_2$, 20 mM DTT, 2 mM EDTA, 2 mM ATP) was added to 100 µl of protein extract followed by the injection of 100 µl of luciferin buffer (60 mM Tris (pH 8.0), 20 mM $MgCl_2$, 20 mM DTT, 2 mM EDTA, 1 mM luciferin (Biosynth AG, Staad, Switzerland)). Luciferase activity was measured for 20 sec after injection. The protein concentration of each sample was measured using a Bradford protein assay according to the manufacturer's instructions (BioRad Laboratories, Inc. Hercules, USA) and a bovine serum albumin standard curve was used for quantification. Luciferase activity was expressed as relative light units (RLU) per µg total protein produced during 20 sec following luciferin injection.

2.6.4.1 Salicylic acid treatment of plants

The entire abaxial side of leaves from 4-week-old plants was pressure infiltrated with 1 mM sodium salicylate (Na-SA) and harvested 24 h later. The luciferase activity of leaves treated with SA was determined as described in section 2.6.4.

2.7 *A. tumefaciens* transformation

2.7.1 Clones used for transformations

For complementation studies, seven JAtY clones namely JAtY58C12, JAtY55L22, JAtY66A23, JAtY63F16, JAtY68P03, JAtY56A02 and JAtY73H06 were obtained from GetCID, a service affiliated with the John Innes Centre Genome Laboratory (see Chapter 3 for more details). Clones were shipped as *E. coli* stab cultures transformed with the JAtY library clones, grown on solid LB media containing kanamycin (25 µg/ml). Upon arrival, the transformed *E. coli* cultures were cultivated at 37°C in 10 ml of selective liquid LB media and plasmid DNA isolations were performed as described in section 2.4.1. Additionally, an empty pSMB binary vector (Mylne and Botella, 1998) was used to transform *cir1* and *Luc2* plants to generate empty vector control plants.

2.7.2 Preparation of electro-competent *A. tumefaciens* cells

A 200 ml culture of *A. tumefaciens* GV3101 was cultured to an OD_{600} of 0.2 to 0.4 as described in section 2.3.2.1. Cells were pelleted at 4°C and resuspended in 20 ml of ice-cold 1 mM HEPES (pH 7.0). This step was repeated twice, making sure cells are kept cold at all times. After centrifugation, cells were resuspended in 2 ml ice-cold 10% (v/v) glycerol, pelleted and again resuspended in 2 ml ice-cold 10% (v/v) glycerol. Cells were then divided into 50 µl aliquots and immediately frozen in liquid nitrogen. These competent cells remained stable at -70°C for at least five months.

2.7.3 Transformation of electro-competent *A. tumefaciens* cells

Approximately 2.5 ng/µl of high quality plasmid DNA was mixed with 50 µl of electro-competent *A. tumefaciens* cells, incubated on ice for 1 min and transferred to a cold electroporation cuvette (2 mm electrode distance; Eurogentec, Seraing, Belgium). The BioRad Gene Pulse™ apparatus (BioRad Laboratories, Inc. Hercules, USA) was set to 25 µF capacitance, 2.0 kV and at 200 Ω resistance. The cells were pulsed once at the above settings and 500 µl of LB media was quickly added to the cuvette. Cells were resuspended, transferred to a microfuge tube and incubated at 28°C for 4 to 6 h. The transformation mixture was plated onto LB solid media containing rifampicin (100 µg/ml), gentamycin (15 µg/ml) as well as kanamycin (25 µg/ml) and was incubated at 28°C for 2 to 3 days. *Agrobacterium* colonies were screened by PCR to determine if the transformations were successful.

2.8 Arabidopsis transformation

2.8.1 Transformation of Arabidopsis plants (floral dip method)

Agrobacterium-mediated stable transformation of Arabidopsis is based on the floral dip protocol described by Clough and Bent (1998). Approximately 20 plants were grown on soil until primary inflorescence shoots (bolts) developed. These were removed to encourage secondary inflorescence growth and plants were fertilized with Phosphrogen (Bayer CropScience Group, Hertfordshire, UK) to maintain the health of the plant. The plants used for transformation displayed the maximum number of young flower heads, with no silique development.

A single colony of successfully transformed *Agrobacterium* was streaked on selective LB solid media and incubated at 28°C for 3 days. This was used to inoculate a pre-culture of 5 ml of selective LB liquid media grown at 28°C for 2 days. The entire 5 ml culture was used to inoculate 500 ml of selective LB liquid media which was incubated overnight at 28°C. Cells were pelleted at 3 500 *g* for 15 min at room temperature and resuspended in 250 ml of 5% (w/v) sucrose with 0.05% (v/v) Silwet L-77 surfactant (Lehle Seeds, Round Rock, USA) added just prior to use.

Plants to be transformed were inverted and dipped into the *Agrobacterium* cell-suspension ensuring all flower heads were submerged. Plants were slightly agitated to release air bubbles and left in the solution for approximately 1 min. The dipped plants were placed on their sides in a tray lined with tissue paper which was covered and returned to the growth room until the following morning. The next day, the plants were placed upright and subsequently watered from below to ensure that the *Agrobacterium* cell-suspension is not

washed off. After 1 week, dipping with the same transformed *Agrobacterium* was repeated as before to increase the efficiency of transformation.

2.8.2 Isolation of transformed lines

T_1 seed was collected from the dipped plants, surface sterilized and plated on 1 x MS media containing PPT (Duchefa Biochemie BV, Haarlem, The Netherlands). The resulting resistant heterozygous T_1 seedlings were tested by PCR to confirm the presence of the *Bar* gene, transplanted onto soil and the T_2 seed were collected separately from each of the confirmed plants after self-fertilization. Fifty seed from each of the independently transformed T_2 lines were surface sterilized and plated onto 1 x MS media containing PPT and after one week, the homozygous or heterozygous resistant T_2 plants were planted onto soil. The luciferase activity and the level of resistance to *Pst* DC3000 infection was tested at four weeks of age.

2.9 Determination of secondary metabolite levels in Arabidopsis

2.9.1 Sinapoylmalate

For the analysis of sinapoylmalate accumulation in leaves, eight leaf discs of uniform size (0.5 cm^2) were homogenized in 200 µl of 90% (v/v) methanol. Samples were centrifuged at 12 000 *g* for 10 min to remove all cell debris. The supernatant was used in high performance liquid chromatography (HPLC) analysis. HPLC analysis was performed on an LC-10 system (Shimadzu Scientific Instruments, Columbia, USA) equipped with a SPD-M6A UV-VIS photodiode array detector (Shimadzu Scientific Instruments, Columbia, USA). Samples were separated on a Prodigy RP-C18 column (250 mm x 4.6 mm, particle size 5 µm; Phenomenex, Torrance, USA) using a linear gradient of 0 to 100% acetonitrile in 0.1% trifluoroacetic acid (TFA) for 40 min at a flow rate of 0.7 ml/min. The elution of UV light–absorbing compounds was monitored at 330 nm. Sinapoylmalate compounds were identified based on their retention times and UV light spectra.

2.9.2 Camalexin

Camalexin extractions were performed as described previously (Glazebrook and Ausubel, 1994) with some modifications. For each sample, approximately 100 mg of leaf tissue was combined with 1 ml of 80% (v/v) methanol and heated at 65°C for 20 min. After centrifugation, the leaf tissue was removed and the methanol was evaporated under vacuum to approximately 100 µl. Each sample was extracted twice with 100 µl of chloroform and the pooled organic phase was evaporated under vacuum to dryness. The dried residue was dissolved in 10 µl of chloroform and loaded onto silica thin layer chromatography (TLC) plates (DC-Fertigplatten Durasil-25; Macherey-Nagel, Düren, Germany) approximately 2 cm from the bottom of the plate, leaving a 2 cm gap between each sample. The chromatogram was

allowed to develop in a tank containing chloroform:methanol (9:1 v/v) until the solvent reached 2 to 4 cm from the top of the plate. Plates were removed from the tank and allowed to dry in a fume hood for about 10 min.

The TLC plates were photographed with the Syngene Gene Genius Bio-imaging System fitted with a blue filter using GeneSnap acquistion software (version 6.05; Syngene, Frederick, USA). Once photographed, the camalexin spots on the plates were quantified with GeneTools software (version 3.06; Syngene, Frederick, USA). Camalexin accumulation was expressed as relative camalexin which is defined as the average camalexin accumulation in each plant line relative to Col-0 which was set to a value of 100.

Chapter 3: Genomic mapping of *cir1*

3.1 Introduction to genomic mapping

Genomic mapping (also called map-based or positional cloning) forms part of the forward genetics approach which aims to identify the specific sequence change that is responsible for a mutant phenotype. This process is not only useful in the genetic analysis of the mutant but is even more important in the molecular cloning of the corresponding gene.

The map position of the gene responsible for the mutation can be determined by finding linkage to markers located at precise positions in the genome. Determining linkage relies on the number of meiotic recombination events between two non-sister chromatids of each pair of homologous chromosomes. The frequency of recombinants can be used to determine the genetic map distance, expressed as centiMorgans (cM) or percentage recombination, between the gene and the marker. Alfred Sturtevant's postulation explains: the greater the distance between a gene and a marker, the greater the chance of recombination taking place in that region, thereby producing a greater proportion of recombinants (Griffiths et al., 2004). Genetic distance can range from 0 cM indicating no recombinants and absolute linkage, to 50 cM which corresponds to 50% recombination between a gene and a marker and is indicative of non-linkage.

In Arabidopsis, various genetic maps based on the same principle have been constructed. Historically, markers on genetic maps were based only on mutations with easily scorable phenotypes and defined map positions (Koornneef and Hanhart, 1983; Koornneef et al., 1983). Typically the mutant of interest was crossed with the marker phenotypic mutant and their tendency to be inherited together was used to determine the genetic distance between the two genes (Koornneef and Hanhart, 1983; Koornneef et al., 1983). Although these "classical" markers are easy to use, it requires numerous crosses and interference between the marker phenotype and the phenotype of the mutant to be mapped could pose problems (Bell and Ecker, 1994). More recently, DNA-based or molecular markers have been added to the gene map. DNA markers exploit the polymorphic differences between Arabidopsis ecotypes. The differences (or polymorphisms) in the DNA sequences are due to either base pair changes or insertions/deletions which randomly occurred in one ecotype but not in the other (Alonso-Blanco and Koornneef, 2000). DNA-based marker systems include the analysis of restriction fragment length polymorphisms (RFLP) (Chang et al., 1988; Lister and Dean, 1993; Fabri and Schaffner, 1994), random amplified polymorphic DNAs (RAPD) (Reiter et al., 1992) and amplified fragment length polymorphisms (AFLP) (Alonso-Blanco et al., 1998), but these have been lately replaced with other more widely used PCR-based markers.

The most common PCR-based markers are SSLP (Bell and Ecker, 1994) and CAPS (Konieczny and Ausubel, 1993). SSLPs amplify small genomic regions containing a polymorphic microsatellite repeat sequence, therefore the size of the amplified product

varies depending on the number of repeats present in different ecotypes (Loridon et al., 1998). CAPS rely on differences in the restriction enzyme digestion patterns of ecotypes. A genomic DNA region containing a restriction enzyme site unique to a given ecotype is amplified and digested with a diagnostic restriction enzyme to reveal the polymorphism. Both markers are co-dominant which allows for the genotyping of both chromosomes of a plant, they are abundant throughout the entire genome and can be rapidly analysed on agarose gels, making them valuable markers for genetic mapping (Lukowitz et al., 2000).

In Arabidopsis research, the Col-0 and L*er* ecotypes are among the most commonly used ecotypes and are the parental lines of the popular collection of recombinant inbred lines (Lister and Dean, 1993) used in many mapping experiments. Since the sequencing of the Col-0 genome by The Arabidopsis Genome Initiative (2000) and L*er* genome by Monsanto (Jander et al., 2002), vast amounts of information about DNA polymorphisms that can be used as molecular markers has become available. To further aid the production of molecular markers, Monsanto (previously Cereon Genomics) has made a online database available comprising most of the predicted SNP and small InDel polymorphisms identified between Col-0 and L*er* (Jander et al., 2002). SNP changes alter a single base pair at a specific location in the genome and since many SNPs modify restriction enzyme sites in either Col-0 or L*er* they can be used as CAPS markers (Konieczny and Ausubel, 1993). InDels can vary in size depending on the amount of nucleotides inserted into one ecotype and not the other, but are mostly less than 100 bp making them ideal to use as PCR-based markers. By amplifying the region of DNA spanning the InDel, the differences in the amplified product can be visualized on agarose gels and as they are co-dominant both ecoptypes can be scored (Jander et al., 2002). Both SNP and InDel markers are very abundant, inexpensive to use and have enhanced the mapping process by eliminating the problem of availability of suitable markers.

Once the markers flanking the mutant gene have been identified by the mapping process, additional steps can be taken to identify the gene of interest. A common approach involves complementation of the mutant. Complementation relies on the transformation of the mutant plant with large wild-type genomic DNA fragments which overlap and span the region of interest between the flanking markers. This is to determine which of the DNA fragments are capable of restoring the mutant phenotype to wild-type (Lukowitz et al., 2000). After the complementing fragment has been identified, the annotated Arabidopsis genome sequence can be studied for candidate genes. The relevant candidate genes are subsequently sequenced and by comparing the sequence of the mutant allele with the wild-type sequence, the exact mutation can be identified (Peters et al., 2003). Further complementation with the single candidate gene would provide definite proof that the gene of interest has been identified.

Otherwise, if the region between the flanking markers contains only a few candidate genes it might not be necessary to do complementation. It is possible to order Arabidopsis lines from various resources in which the candidate gene is knocked out either by a T-DNA or transposon (reviewed by Dinka and Raizada, 2006). The desired gene could be identified by analysing the phenotypes of such lines and, if the knockout is a phenocopy of the mutant, by ultimately conducting allelism tests (Peters et al., 2003). Alternatively, if no knockouts were available, primer pairs which amplify overlapping segments of DNA spanning the region of interest could be used to sequence the complete region in the mutant. The mutant sequence is compared to that of a wild-type plant and the mutation in the gene of interest is identified (Jander et al., 2002). The last approach is only viable if the region of interest between the flanking markers is less than 40 kb.

The advances in DNA marker methods, the sequencing of the Arabidopsis genome and the availability of the Monsanto Arabidopsis polymorphism collection (Jander et al., 2002) have contributed significantly to the process of map-based cloning. The genomic mapping of mutations is an essential tool in the process of assigning a function to the numerous annotated plant genes of which the role is still unknown.

This chapter is concerned with the genomic mapping of the disease resistance mutant, *cir1* (Murray et al., 2002), with the ultimate aim of identifying the *CIR1* gene.

3.1.1 First-pass mapping of *cir1*

In previous studies, the mutant *cir1* was isolated from ethylmethane sulfonate (EMS) mutagenized transgenic Col-0 plants harbouring a *PR-1::LUC* gene cassette (called *Luc2* as in Chapter 2). The construct consisted of the firefly luciferase (*LUC*) reporter gene fused to the tobacco *PR-1* promoter. The *LUC* gene encodes for the enzyme luciferase that catalyses the ATP-dependent oxidation of its substrate, luciferin, producing light at 465 nm (Ow et al., 1986). *Cir1* was identified based on its constitutively increased levels of luciferase activity and it was subsequently found that the mutation in *cir1* resulted in constitutive expression of both the *PR-1::LUC* transgene and the endogenous *PR-1* gene (Murray et al., 2002).

To perform the first–pass mapping experiments, *cir1* plants were crossed to L*er* plants and the F_2 progeny were analysed for constitutive *PR-1::LUC* expression. Segregation analysis established the *cir1* mutation to be recessive and that the *PR-1::LUC* transgene segregated separately as a monogenic dominant trait. Constitutive luciferase activity was therefore only found in three-quarters of F_2 homozygous *cir1* plants, demonstrating that the *cir1* to wild-type ratio is 3:13 (Murray, 2000). A total of 48 homozygous *cir1* F_2 plants displaying high luciferase activity were selected and used for mapping. The recombination frequencies indicated that the *CIR1* locus is approximately 9.40 cM below marker nga1111 on the lower arm of chromosome IV (Murray, 2000; Murray et al., 2002).

In this chapter, more comprehensive mapping experiments employing different PCR-based markers were performed to fine-map *cir1*. Once the flanking markers were determined, complementation experiments were conducted and a small region on chromosome IV in which the *CIR1* locus is situated, was identified. Furthermore, possible candidate genes in this region were investigated and it was shown that *cir1* is not allelic to *edr5* (also known as *ref2*).

3.2 High luciferase activity as selection criterion for mapping population

Once luciferase comes in contact with its substrate, luciferin, a flash of light is produced (Ow et al., 1986). Previous studies on luciferase assays found that by recording the amount of light for 20 sec after the injection of luciferin, both the initial flash as well as the stable linear production of luciferase activity was recorded (Murray, 2000). In this study, luciferase activity was therefore expressed as RLU per µg total protein produced during 20 sec following luciferin injection.

It has been found that maximum constitutive luciferase activity in *cir1* was obtained in 5-week-old plants (Murray, 2000), however this experiment was conducted under short day conditions. To determine when *cir1* plants grown under a 16 h light and 8 h dark regime acquire maximum luciferase activity, a time-course luciferase assay experiment was performed. Luciferase activity was measured in *cir1* (positive control), *Luc2* (to monitor background luciferase activity levels) and L*er* plants (negative control) after three, four and five weeks of growth (Fig. 3.1).

The luciferase assays showed that 4-week-old *cir1* plants had the most luciferase activity compared to 3- and 5-week-old plants while very little luciferase activity was measured in *Luc2* or L*er* plants of the same age (Fig. 3.1). The luciferase activity levels in the 4-week-old *cir1* plants were 15 times higher than in the 3-week-old plants (Fig. 3.1). Although 5-week-old *cir1* plants also displayed higher luciferase activity levels than 3-week-old plants, the background luciferase activity in *Luc2* plants increased to levels comparable to *cir1*. There was no significant difference in luciferase activity between these two lines in 5-week-old plants (Fig. 3.1). These high background levels would have made it difficult to distinguish *cir1* from *Luc2* plants, which could have resulted in the selection of false positives. Therefore, all luciferase assays were performed on 4-week-old plants and always included *cir1* plants as a positive control and *Luc2* plants as a background luciferase activity control.

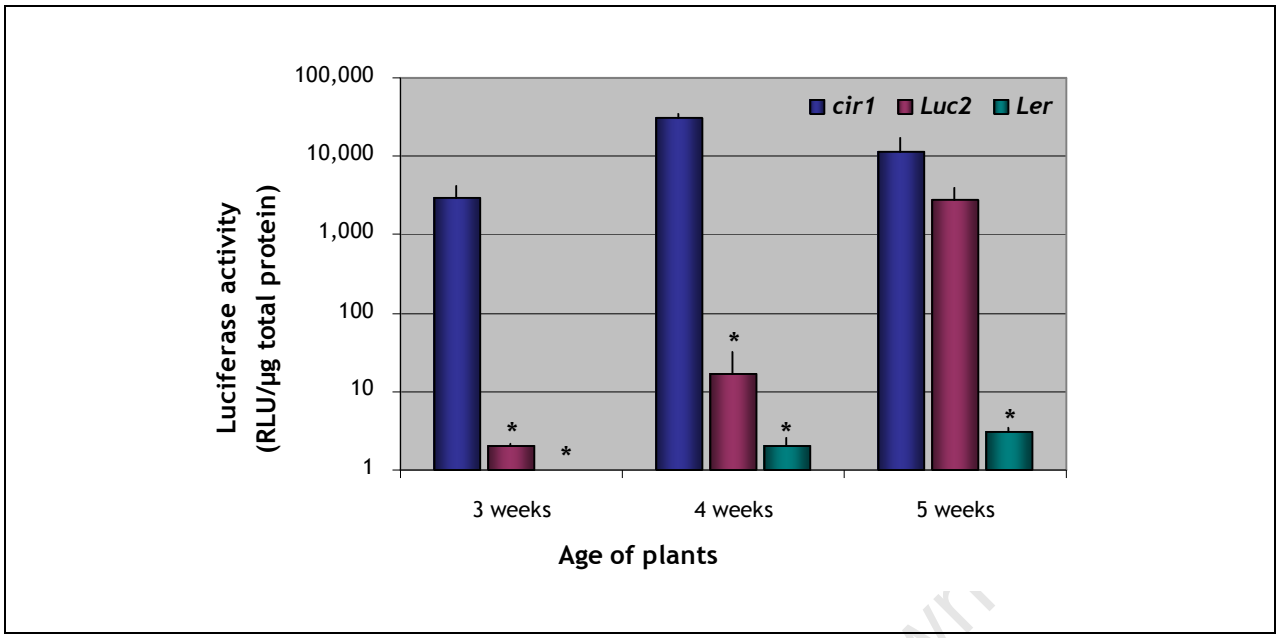

Figure 3.1. Luciferase activity of *cir1*, *Luc2* and L*er* plants at three, four and five weeks of age. Bars represent the average luciferase activity levels detected in five plants per line and are plotted on a logarithmic scale. Units of luciferase activity are defined as relative light units (RLU) per µg total protein produced during 20 sec after luciferin injection. Error bars represent the standard error between values at the 95% confidence level. Asterisks indicate significant differences in luciferase activity compared to *cir1* (Student's *t*-test, $P < 0.05$).

3.2.1 Selection and evaluation of F_2 progeny mapping population plants

The F_2 seed of the *cir1* and L*er* cross were obtained from S. L. Murray (University of Cape Town) and were screened for homozygous *cir1* plants with constitutively high luciferase activity. The relevant control plants namely *cir1*, L*er* and *Luc2* were planted with each batch of F_2 seed and all plants were assayed after four weeks to determine the level of luciferase activity. Fig. 3.2 represents the luciferase activity of certain plants selected from the F_2 progeny for inclusion in the mapping population.

All six of the F_2 and *cir1* control plants showed increased luciferase activity levels in comparison to the *Luc2* control plants, whereas L*er* control plants showed almost no luciferase activity (Fig. 3.2). Although the luciferase activity in the F_2 plants was not as high as in the *cir1* control plants, levels ranged from 4 to 29 times higher than the background luciferase activity levels in the *Luc2* plants (Fig. 3.2). These homozygous *cir1* plants were selected as part of the mapping population based on their high luciferase activity. Luciferase assays were performed on 1 860 F_2 progeny plants of which 293 plants were identified as homozygous *cir1*, increasing the mapping population to 341 plants.

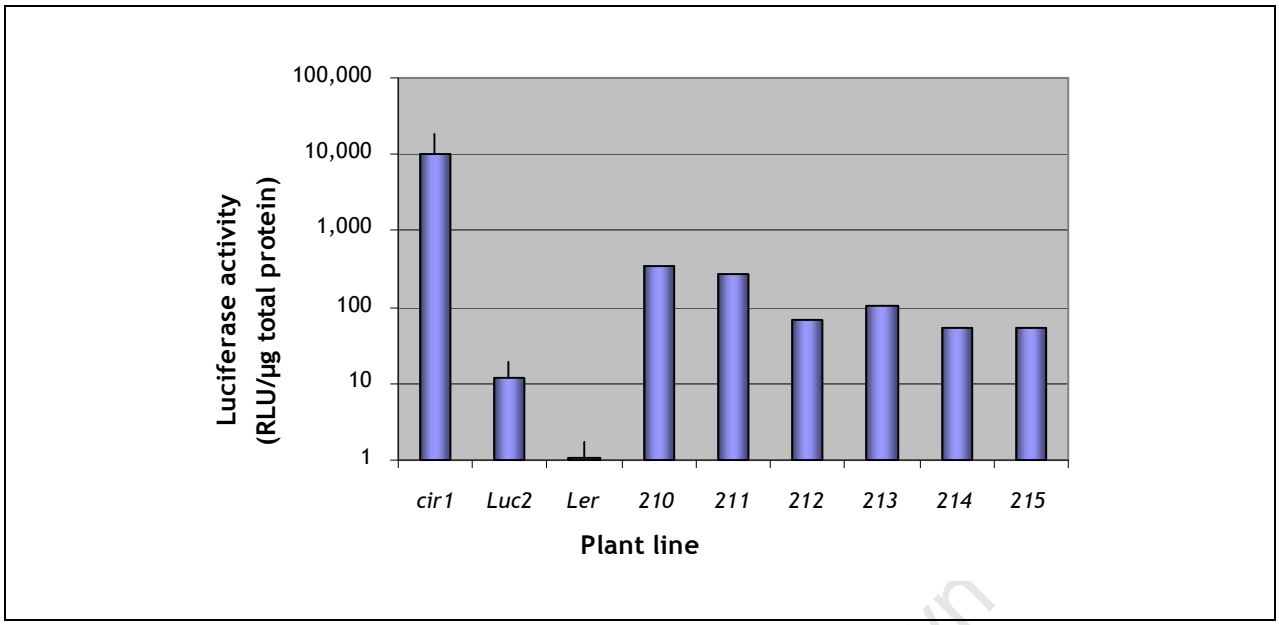

Figure 3.2. Representative graph of luciferase activity of six F_2 progeny plants selected as part of mapping population.

Four-week-old plants were assayed and *cir1* (positive control), *Luc2* (background luciferase activity control) and L*er* plants (negative control) were included as controls. Bars represent either the average luciferase activity levels detected in five plants per control line or luciferase activity levels of individual F_2 progeny plants and are plotted on a logarithmic scale. Units of luciferase activity are defined as relative light units (RLU) per µg total protein produced during 20 sec after luciferin injection. Error bars represent the standard error between values at the 95% confidence level.

The 341 mapping population plants were tested with SSLP and CAPS markers (see Table 2.3 in Chapter 2 for details) within the region of interest on chromosome IV. Linkage analysis showed that recombination frequencies at these markers were significantly greater than 9.40 cM (results not shown), contradicting results obtained during previous first-pass mapping experiments (Murray, 2000; Murray et al., 2002). Such inconsistencies are usually due to errors in the scoring of mutant phenotypes which might not be fully penetrant or could be strongly affected by growth conditions (Lukowitz et al., 2000). Therefore, these results were thought to be due to the erroneous selection of heterozygous *cir1* or wild-type plants in the F_2 progeny, thereby leading to a high proportion of recombinants in the mapping population.

Given that many false positives appear to have been selected, it was thought that the L*er* background could have an effect on the *PR-1::LUC* transgene resulting in high luciferase activity levels in heterozygous *cir1* plants. To test if the L*er* background had an effect, *Luc2* plants were crossed onto L*er* and Col-0 respectively and the F_1 progeny were tested for luciferase activity 24 h after SA treatment (Fig. 3.3).

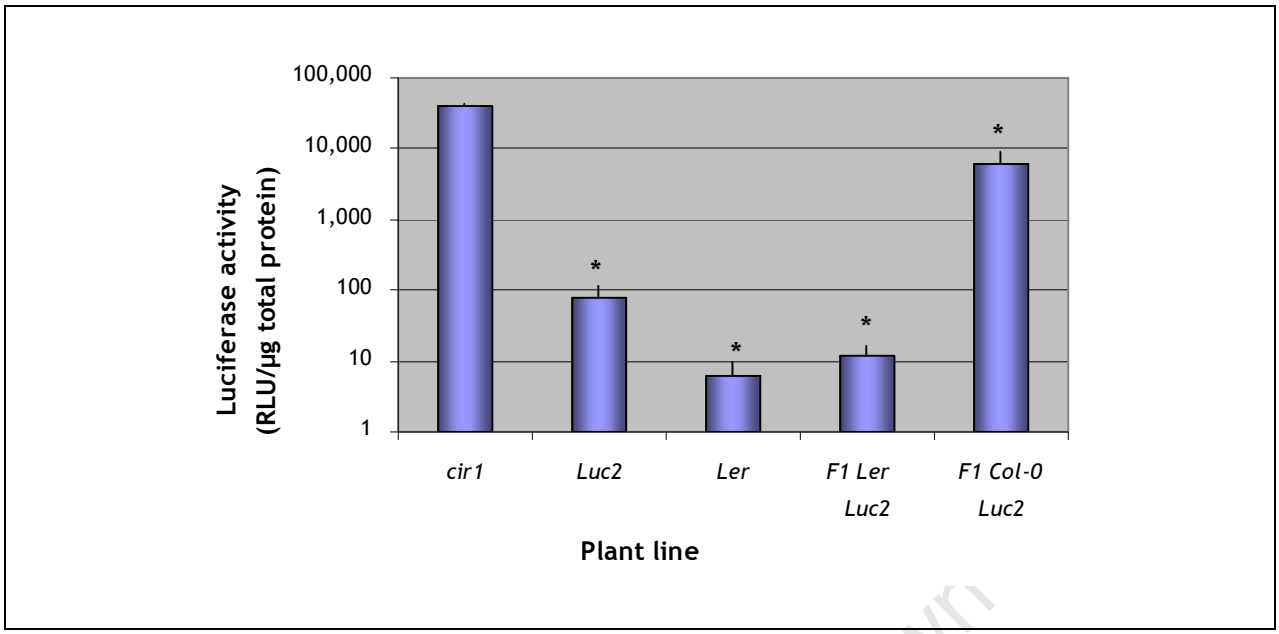

Figure 3.3. Luciferase activity of F_1 L*er Luc2* and F_1 Col-0 *Luc2* plants after salicylic acid treatment.

Four-week-old plants were assayed and *cir1* (positive control), *Luc2* (background luciferase activity control) and L*er* plants (negative control) were included as controls. F_1 progeny plants were treated with 1 mM salicylic acid and leaves were harvested 24 h after treatment. Bars represent the average luciferase activity levels detected in five plants per line and are plotted on a logarithmic scale. Units of luciferase activity are defined as relative light units (RLU) per µg total protein produced during 20 sec after luciferin injection. Error bars represent the standard error between values at the 95% confidence level. Asterisks indicate significant differences in luciferase activity compared to *cir1* (Student's *t*-test, $P < 0.05$).

We know from previous studies that treatment of Arabidopsis with SA induced *PR-1* expression after 24 h (Uknes et al., 1992) and that it induced a 350-fold increase in luciferase activity of *Luc2* plants (Murray, 2000). The F_1 Col-0 *Luc2* SA-treated plants had 83 times greater luciferase activity levels than *Luc2* plants whereas SA-treated F_1 L*er Luc2* plants resembled the L*er* control with levels 6 times lower than the *Luc2* plants (Fig. 3.3). SA-treated F_1 L*er Luc2* displayed significantly less luciferase activity than *cir1* plants and its levels were also 520 times lower than SA-treated F_1 Col-0 *Luc2* plants (Fig. 3.3). However, significantly lower luciferase levels were also detected in F_1 Col-0 *Luc2* plants compared to *cir1* (Fig. 3.3). This reduction is possibly due to the heterozygous state of the *PR-1::LUC* transgene in the F_1 progeny, yet this could only be confirmed if it is established that the luciferase activity levels of SA-treated F_1 Col-0 *Luc2* plants are significantly reduced compared to those of SA-treated, homozygous *Luc2* plants. Therefore contrary to what was expected, both the L*er* background and possibly the heterozygous state of *PR-1::LUC* reduced luciferase activity and both these factors hinder our ability to distinguish between homozygous *cir1* plants and heterozygous or wild-type plants. For instance, if a homozygous

cir1 plant contained the L*er* loci responsible for dampening luciferase activity, or a heterozygous *cir1* plant lacked these loci, levels of luciferase activity could appear similar in both.

According to the expected *cir1* to wild-type ratio of 3:13, 293 selected plants are less than the expected number of 349 plants from the 1860 tested. Together with the problems outlined above, this also indicated that the criteria for the selection of the mapping population were not optimal.

3.2.2 Confirmation of mapping population in F_3 progeny

To select a mapping population consisting only of homozygous *cir1* plants, 190 of the 341 plants were selected to be re-screened for constitutively high luciferase activity in the F_3 progeny.

The F_2 mapping plants selected in the first screening process, which were either homozygous or heterozygous for the *PR-1::LUC* transgene, underwent self-fertilization to give rise to the F_3 progeny. In the case of homozygous F_2 lines, all plants in the F_3 progeny will contain the transgene but in heterozygous plants, *PR-1::LUC* will segregate in the F_3 progeny and will only be present in a 3:1 ratio. The second screening process included stringent criteria for the selection of plants with high luciferase activity. The number of plants per line was increased to five instead of only one and ten plants of the relevant control lines were tested for luciferase activity at exactly four weeks of age. After determining the luciferase activity of each plant, the first step was to identify lines where the average luciferase activity was at least twice as high as the average for the *Luc2* control plants. Secondly, the segregation pattern of the *PR-1::LUC* gene in these specific lines was evaluated and only lines where at least 50% of the five plants showed high luciferase activity were considered to be homozygous *cir1* plants. Thus only lines with 50% of plants showing luciferase activity at least double the average of the *Luc2* plants were selected (results not shown).

Out of the 190 plants screened, 36 plants qualified based on the strict selection criteria and fine-mapping of *cir1* was continued only on these particular plants.

3.3 First-pass mapping shows *PR-1::LUC* transgene is not on chromosome IV

First-pass mapping experiments were performed to determine that the *PR-1::LUC* transgene was not also situated on chromosome IV. This needed to be established to avoid confusion and interference during the fine mapping of *cir1*. The mapping population was selected from the same F_2 seed of the *cir1* and L*er* cross used in section 3.2.1, however in this case the selection process was based on the lack of luciferase activity instead of constitutively high luciferase activity. Plants with low luciferase activity could be contributed to either the lack

of the *PR-1::LUC* transgene or the heterozygous or wild-type state of *cir1*. All low luciferase plants were tested by PCR and only plants without the transgene were selected as part of the mapping population. These plants would therefore display the L*er* ecotype at the insertion point of the *PR-1::LUC* transgene.

Eighteen plants were selected based on the absence of the *PR-1::LUC* transgene and linkage analysis was performed with PCR-based markers (see Table 2.3 in Chapter 2 for details) chosen from each of the five chromosomes. Table 3.1 outlines the recombination frequencies determined at each of the PCR-based markers used in first-pass mapping of *PR-1::LUC*.

Table 3.1 First-pass mapping of *PR-1::LUC* using PCR-based markers

Markers were selected on different chromosomes and relevant positions are shown.

Marker name	*Chromosome*	*Position (RI, AGI)*[a]	*Percentage recombination*
nga63	I	11.46 cM, unknown	61.11
nga280	I	83.83 cM, 20 877 364 bp	44.44
nga168	II	73.77 cM, 16 298 919 bp	50.00
nga162	III	20.56 cM, 4 608 284 bp	53.84
nga6	III	86.41 cM, 23 042 025 bp	47.22
nga8	IV	26.56 cM, 5 628 810 bp	58.33
F24G24a	IV	unknown, 6 422 797 bp	52.94
nga106	V	33.35 cM, unknown	63.63
nga76	V	68.40 cM, 10 418 614 bp	61.11

[a] Position based on recombinant inbred (RI) map in cM (Lister and Dean, 1993) and AGI map in bp (The Arabidopsis Genome Initiative, 2000) of each chromosome. Both maps are available from "The Arabidopsis Information Resource" (TAIR, http://www.arabidopsis.org).

It is widely accepted that a recombination frequency of less that 50% indicates linkage, however it has been suggested that when using a small mapping population, less than 30% recombination is a more accurate indication of linkage (Ponce et al., 1999). Although none of the tested markers showed recombination frequencies of less than 30%, *PR-1::LUC* was most closely linked to nga280 on chromosome I which displayed the lowest percentage recombination of 44.44 (Table 3.1). While the exact map position of *PR-1::LUC* has not been determined, this could be resolved by testing more markers smaller distances apart. However, the aim of this experiment was not to locate the exact position of transgene but to ensure that it was not located on chromosome IV. The recombination frequencies of 58% and 53% at nga8 and F24G24a respectively, strongly suggested that *PR-1::LUC* was not situated on chromosome IV (Table 3.1).

3.4 Initial mapping of *cir1*

Only PCR-based markers were used to determine linkage in all mapping experiments. During initial mapping, CAPS (Konieczny and Ausubel, 1993) and SSLP (Bell and Ecker, 1994) markers were selected from the genetic marker database available from TAIR. TAIR provides interactive physical and genetic maps complete with detailed information of the markers placed on these maps. Only five of these previously identified markers were suitably located for our purposes (see Table 2.3 in Chapter 2 for details). To fine-map and to identify the flanking markers of *cir1*, it was necessary to create new molecular markers on the lower arm of chromosome IV. These markers were based on the Monsanto SNP and InDel polymorphism collection available online (http://www.arabidopsis.org/Cereon/index.html) (Jander et al., 2002).

3.4.1 Design and generation of PCR-based markers

Primers for the new molecular markers were designed to amplify regions containing relevant SNP or InDel polymorphisms and were generated using PRIMER3 software (Rozen and Skaletsky, 2000). A list with relevant information on the designed SNP- and InDel-based markers located on chromosome IV is outlined in Table 3.2.

In the case of InDel polymorphisms, the amplified product sizes were determined by the size of the selected InDel and varied from 141 bp to 774 bp. Large InDels are usually easily detectable on agarose gels even in bigger PCR products, but InDels consisting of 20 bp or less are more obvious in small amplified products. All newly designed markers based on InDel polymorphisms, from the smallest (15 bp) to the largest (80 bp), allowed for the visualization of polymorphic Col-0 and L*er* products on high concentration agarose gels. Amplified products based on SNPs required restriction enzyme digestions and it was ensured that the differences between the lengths of the restriction fragments were sufficient to be separated on agarose gels. The restriction digested fragments ranged from 64 bp to 546 bp while uncut amplified products varied from 549 bp to 1166 bp. The agarose gel concentrations optimal for each PCR-based marker are listed in Table 3.2.

Table 3.2 Relevant information on designed PCR-based markers used in genomic mapping
The restriction enzymes for the analysis of SNP markers, optimal gel conditions and product length in bp after amplification (InDel) or restriction enzyme digestion (SNP) in genetic ecotypes Col-0 and L*er* are shown.

Marker	*Position on chromosome IV*[a]	*Type*	*InDel size (bp)*	*Enzyme*	*% gel*	*Product sizes*
F28M11a	6 342 494 bp	InDel	22/-22	N/A	3	Col-0: 221 L*er*: 199
F24G24a	6 422 797 bp	InDel	80/-80	N/A	3	Col-0: 390 L*er*: 310
F7L13a	6 452 209 bp	SNP	N/A	*Xba*I	1	Col-0: 318, 513 L*er*: 831
T12H20a	6 589 456 bp	SNP	N/A	*Kpn*I	1	Col-0: 464, 702 L*er*: 1166
F8L21a	6 898 630 bp	InDel	26/-26	N/A	3	Col-0: 210 L*er*: 184
F25E4a	6 955 144 bp	SNP	N/A	*Dra*I	2	Col-0: 64, 485 L*er*: 549
T26M18a	7 157 376 bp	InDel	59/-59	N/A	3	Col-0: 389 L*er*: 330
T4C9a	7 342 625 bp	InDel	70/-70	N/A	3	Col-0: 774 L*er*: 704
T20K18a	7 485 905 bp	InDel	61/-61	N/A	3	Col-0: 337 L*er*: 276
F18A5a	8 008 121 bp	InDel	25/-25	N/A	3	Col-0: 210 L*er*: 185

[a] Position based on AGI map (The Arabidopsis Genome Initiative, 2000) available from TAIR.

3.4.2 *cir1* is situated in ~ 309 kb region on chromosome IV

The recombination frequencies between *cir1* and the abovementioned PCR-based markers were scored in the 36 F_2 plants which were confirmed as homozygous *cir1* plants in the F_3 progeny, corresponding to a maximum of 72 analysed chromosomes. The percentage recombination between *cir1* and each molecular marker was calculated as the number of recombinant chromosomes/total number of tested chromosomes and the results are presented in Table 3.3.

The general trend in the recombination frequencies of the tested markers was a reduction from both ends of the chromosome towards the marker T22B4a situated at 6 732 662 bp. T22B4a displayed the lowest percentage recombination of 1.39 while its flanking markers, T12H20a (6 589 456 bp) and F8L21a (6 898 630 bp), both showed recombination frequencies of 2.78% (Table 3.3). This suggested that *cir1* was located between T12H20a and F8L21a, limiting the region of interest to 309.10 kb that is equivalent to roughly 1.24 cM based on the approximate calculation of 250 kb equals 1 cM (Lukowitz et al., 2000; Durrett et al., 2002).

The recombination frequencies for some markers fluctuated from the general trend observed (Table 3.3). In the case of Det1.1, the slightly higher than expected recombination frequency was due to the undetermined results of plants 16 and 94. In all likeliness these plants would have been homozygous Col-0 based on results from the flanking markers F28M11a and F7L13a (Table 3.3), thereby adjusting the percentage recombination to 2.78. It was problematic to obtain clear results for each plant using g4539 (9 631 258 bp) and CM4-3 (8 046 530 bp). Respectively, only 44 and 46 chromosomes could be analysed making the recombination frequencies at these markers high (15.91% and 6.52%, respectively) and most probably inaccurate. To determine a more precise percentage recombination for that part of chromosome IV, F18A5a (8 008 121 bp) was designed next to CM4-3 and results for 72 tested chromosomes indicated a percentage recombination of 6.94 (Table 3.3). In spite of these exceptions, the other markers for which all 72 chromosomes could be analysed followed the trend and displayed a lower percentage recombination the closer the marker was located to T22B4a (Table 3.3).

Even though plant 76 qualified for selection in the F_3 progeny, it inexplicably behaved as a heterozygous *cir1* plant at every marker tested. Its results were included in the recombination frequency calculations in Table 3.3 as even when excluding plant 76 from the calculations, the general trend remained the same. The only difference was that when excluding plant 76, the percentage recombination values were slightly lower than in Table 3.3. Plants 15, 37, 168 and 185 all showed multiple recombination events between markers nga8 (5 628 810 bp) and g4539 (9 631 258 bp). Recombination events are not uniformly distributed along chromosomes (Peters et al., 2003) and the behaviour of these plants suggested that this 4 002.44 kb region on chromosome IV was prone to recombination events.

3.5 Fine mapping of *cir1*

Once the region of interest was limited to approximately 309 kb, three different approaches were followed to fine map *cir1*.

3.5.1 Direct screening for recombination events

Plant 168 was the most informative regarding recombination frequencies of all 36 confirmed F_2 plants as summarised in Table 3.3. It showed a loss of recombination between markers T12H20a (6 589 456 bp) and F8L21a (6 898 630 bp), suggesting that these markers flanked the *CIR1* locus. Additional recombination events between these flanking markers could provide added information regarding the linkage of *cir1* to these markers and would thereby further narrow down the region containing *cir1*. To generate an alternative mapping population with additional recombination events within this 309.10 kb region, homozygous *cir1* plant 168 was crossed to L*er* and the successive F_2 progeny were screened for recombination events with markers T12H20a and F8L21a.

3.5.1.1 Finding additional recombination events between markers T12H20a and F8L21a

Fig. 3.4 is a schematic representation of the different recombination events possible in selected F_1 and subsequent F_2 progenies.

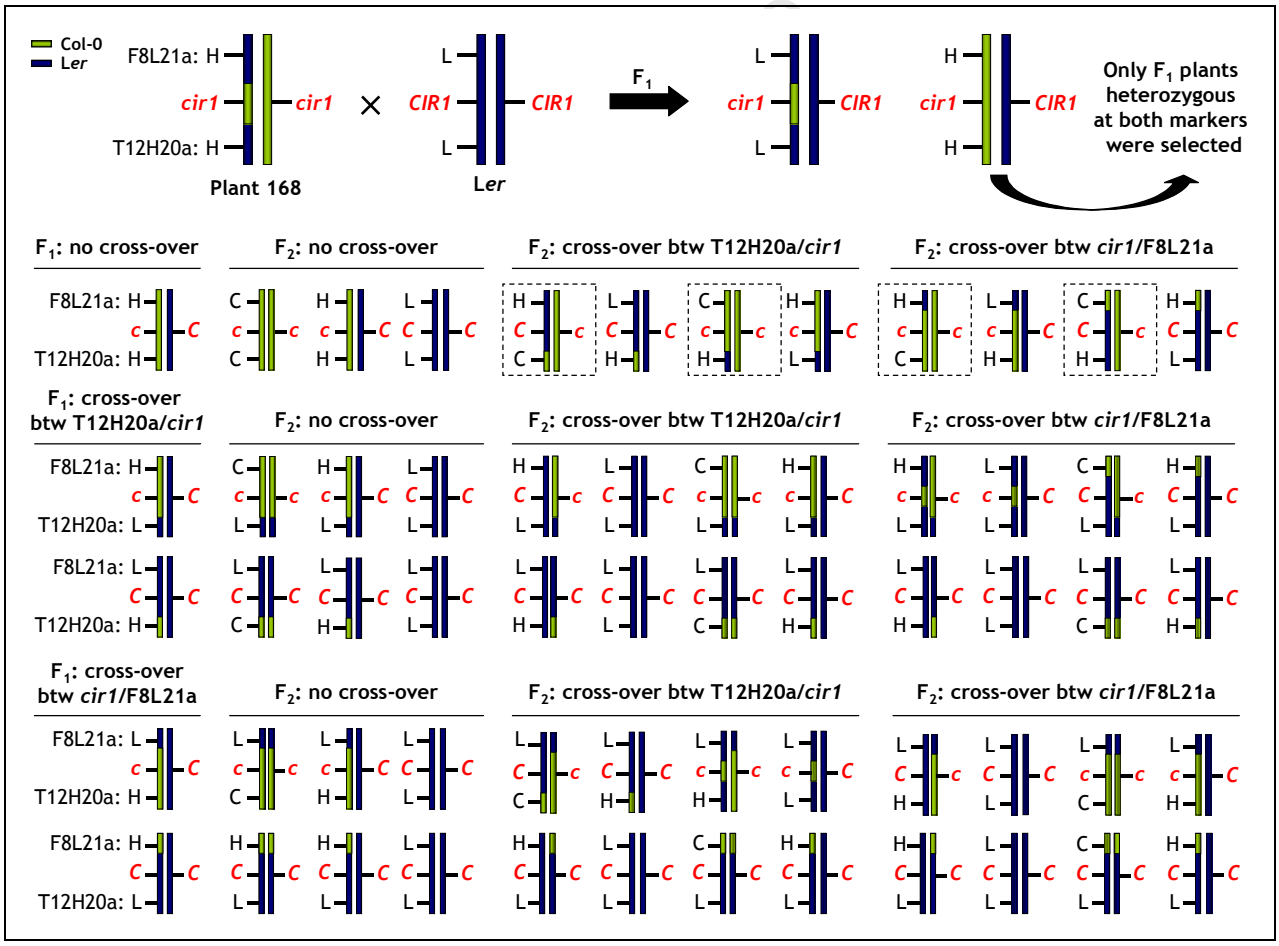

Figure 3.4. Schematic representation of possible recombination events in F_1 and F_2 progenies after plant 168 was crossed to L*er*.

Plant 168 was crossed onto L*er* and only F_1 plants heterozygous at both markers T12H20a and F8L21a were selected for self-fertilization. Subsequent F_2 progeny were screened for different recombination

events between T12H20a or F8L21a and *cir1*. Plants displaying a loss of heterozygosity to two Col-0 alleles at one of the markers (dashed boxes) were selected for luciferase activity assays and future experiments. "H" symbolizes a heterozygous genotype whereas "C" and "L" is indicative of a homozygous Col-0 and L*er* genotype at the marker, respectively. The *cir1* mutant locus is symbolised by a red "*c*" while the wild-type *CIR1* locus is indicated with a red "*C*".

The F_1 progeny was PCR-screened with T12H20a and F8L21a and only plants that were heterozygous at both markers were selected for self-fertilization. The subsequent F_2 progeny were screened for added recombination events between T12H20a or F8L21a and *cir1*. These additional recombination events can be visualized when the genotype at a specific marker changed from heterozygous to homozygous Col-0. Therefore, only F_2 plants where a loss of heterozygosity to two Col-0 alleles at one of the two markers was observed, were selected for further testing (Fig. 3.4, represented by dashes boxes). This ensured that the selected plants had additional recombination events to those present in plant 168 (Fig. 3.4) within the 309.10 kb region which could be exploited to provide more information regarding the linkage of *cir1* to T12H20a and F8L21a.

A total of 244 F_2 progeny plants were PCR-screened with T12H20a and F8L21a of which eight plants were selected based on the loss of heterozygosity to homozygous Col-0 at one of the markers (Fig. 3.5).

Plant name:	Genotype at T12H20a & F8L21a:	Luciferase activity:	Plant name:	Genotype at T12H20a & F8L21a:	Luciferase activity:
Alt 20	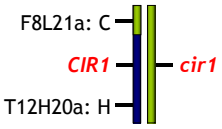	0.01	Alt 126	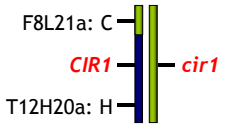	0.02
Alt 67	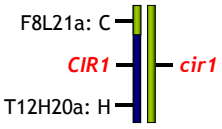	0.04	Alt 163	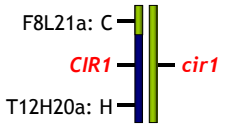	0.01
Alt 79	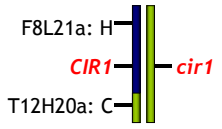	0.01	Alt 228	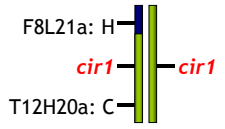	130.52
Alt 124	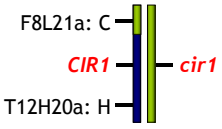	0.02	Alt 256	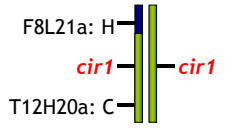	99.51

Figure 3.5. A summary of the plant name, genotype at markers T12H20a and F8L21a, and the luciferase activity of the eight selected plants.

All displayed an additional recombination event between one of the markers and *cir1*, indicated by the loss of heterozygosity to homozygous Col-0 at the relevant marker. Four-week-old plants were assayed and *cir1* (positive control), *Luc2* (background luciferase activity control) and L*er* plants

(negative control) were included as controls. Units of luciferase activity are defined as relative light units (RLU) per µg total protein produced during 20 sec after luciferin injection. Only two plants were homozygous *cir1* and displayed high luciferase activity.

The luciferase activity of these plants were measured and it was found that two of the plants, Alt 228 and Alt 256, were homozygous for *cir1* whereas the remaining six showed no constitutively high luciferase activity (Fig. 3.5). All eight plants contained the *PR-1::LUC* transgene as its presence was confirmed by PCR (results not shown).

3.5.1.2 Results from additional PCR-based markers in ~ 309 kb region

Additional PCR-based markers in the 309.10 kb region between markers T12H20a and F8L21a were designed as described in section 3.4.1. The markers relevant to this alternative mapping strategy are listed in Table 3.4.

All eight selected plants were tested with the markers listed in Table 3.4 to find the exact positions of the recombination events. According to our genotype predictions of the eight plants (Fig. 3.4 and 3.5), the *CIR1* locus would be situated in a Col-0 region in the two *cir1* plants, Alt 228 and Alt 256, and in a heterozygous region in the remaining six plants. The results obtained with each marker are presented in Table 3.5.

Table 3.4 Relevant information of additional PCR-based markers used in the direct screening for recombination events

The restriction enzymes for the analysis of SNP markers, optimal gel conditions and product length in bp after amplification (InDel) or restriction enzyme digestion (SNP) in ecotypes Col-0 and L*er* are shown.

Marker	*Position on chromosome IV*[a]	*Type*	*InDel size (bp)*	*Enzyme*	*% gel*	*Product sizes*
T12H20b	6 608 271 bp	SNP	N/A	*Dde*I	3	Col-0: 546 L*er*: 156, 389
F25I24b	6 657 086 bp	SNP	N/A	*Alu*I	2	Col-0: 324, 738 L*er*: 413, 738
F25I24c	6 732 662 bp	InDel	19/-19	N/A	3	Col-0: 433 L*er*: 414
T22B4a	6 732 662 bp	InDel	19/-19	N/A	3	Col-0: 160 L*er*: 141
T22B4b	6 781 435 bp	SNP	N/A	*Nde*I	2	Col-0: 546, 171 L*er*: 717
F8L21c	6 832 519 bp	InDel	15/-15	N/A	3	Col-0: 240 L*er*: 225

[a] Position based on AGI map (The Arabidopsis Genome Initiative, 2000) available from TAIR.

Table 3.5 Genotypes of selected plants at additional PCR-based markers within ~ 309 kb region
Markers with their corresponding annotation units and positions are shown. "C" indicates plants that are homozygous for Col-0 and "H" is indicative of heterozygous plants.

Plant name	*cir1 geno-type*	***T12H20a*** *T12H20*[a] *6589456*[b]	***T12H20b*** *T12H20* *6608271*	***F25I24b*** *F25I24* *6657086*	***F25I24c*** *F25I24* *6732662*	***T22B4a*** *T22B4* *6732662*	***T22B4b*** *T22B4* *6781435*	***F8L21c*** *F8L21* *6832519*	***F8L21a*** *F8L21* *6898630*
Alt 20	No	H	H	H	H	H	H	H	C
Alt 67	No	H	C	C	C	C	C	C	C
Alt 79	No	C	C	C	C	C	C	H	H
Alt 124	No	H	C	C	C	C	C	C	C
Alt 126	No	H	H	H	H	H	H	H	C
Alt 163	No	H	H	H	H	H	H	H	C
Alt 228	Yes	C	C	C	C	C	H	H	H
Alt 256	Yes	C	C	C	C	C	C	C	H

[a] Annotation unit which corresponds to the TAIR BAC or P1 vector names on which the marker is situated.

[b] Position based on AGI map (The Arabidopsis Genome Initiative, 2000) in bp available from TAIR.

Plants Alt 20, 126, 163 and 256 all matched their described genotype in Fig. 3.5 and recombination took place in the 66.11 kb region between F8L21c (6 832 519 bp) and F8L21a (6 898 630 bp) (Table 3.5), suggesting that the *CIR1* locus is situated to the left of F8L21a. Consistent with the abovementioned four plants, Alt 228 was similar to its illustrated genotype, but in this case recombination occurred in the 48.77 kb section between T22B4a (6 732 662 bp) and T22B4b (6 781 435 bp) (Table 3.5) which indicates that the *CIR1* locus is on the left of T22B4b. Alt 67 and Alt 124 behaved unexpectedly in that recombination arose in the 34.08 kb area between T12H20a (6 589 456 bp) and T12H20b (6 608 271 bp) (Table 3.5) and therefore the *CIR1* locus is supposed to the left of T12H20b. Alt 79 also acted differently given that recombination happened in the 51.08 kb region between T22B4b (6 781 435 bp) and F8L21c (6 832 519 bp) (Table 3.5), indicating that the *CIR1* locus is located to the right of T22B4b.

Results from Alt 20, 126, 163, 228 and 256 suggest that the *CIR1* locus is situated to the left of T22B4b (Table 3.5) but the remaining three plants had contradictory results. The genotypes at the different markers in Alt 67, 79 and 124 resembled the illustrated *cir1* plants presented in Fig. 3.4 (second and third dashed boxes), but these plants were not scored as *cir1* (Fig. 3.5). The conflicting results obtained in Alt 67, 79 and 124 were possibly due to the incorrect scoring of these plants as wild-type instead of *cir1*, again indicating that the scoring of the *cir1* mutant phenotype based on constitutively high luciferase activity was not always reliable.

Direct screening for additional recombination events within the 309.10 kb region was therefore not successful in pinpointing the position of *cir1* and other approaches were pursued.

3.5.2 Testing allelism of *cir1* to another defence related mutant, *edr5*

The *edr5* (enhanced disease resistance 5) mutant was isolated in a screen to identify mutants with altered susceptibility to *Pseudomonas syringae* pv. *maculicola* ES4326 (*Psm* ES4326) (Volko, 1998). As the name implies, this mutation causes enhanced disease resistance to the virulent bacterial pathogen *Psm* ES4326 and to the obligate fungal pathogen *Golovinomyces orontii* (Drenkard et al., 2000). The mutated *edr5* gene segregates as a recessive trait and was initially mapped to a 315 kb region on the lower arm of chromosome IV (Drenkard et al., 2000). This 315 kb region starts on the BAC T9E8, spanning across T6G15 and F18A5, and ends on FCAALL. Although the cloning of *EDR5* has not been published to date, it was established that *edr5* is allelic to the *ref2* (reduced epidermal fluorescence 2) mutant (J. Dewdney, personal communication).

The *ref2* mutant was selected in a screen for plants with reduced fluorescence in their leaves under UV light (Ruegger and Chapple, 2001) and four *ref2* mutant alleles were identified and characterised (Hemm et al., 2003). Although the disease resistance of this mutant has not been established, characterization of *ref2* revealed it contained decreased levels of several phenylpropanoid pathway-derived products in comparison to wild-type plants (Ruegger and Chapple, 2001). These products include sinapoylcholine in the seeds, syringyl lignin in the stems and most importantly for the purpose of this study, sinapoylmalate in the leaves (Ruegger and Chapple, 2001; Hemm et al., 2003). Furthermore, it was established that the reduced leaf fluorescence of *ref2* was due to the significantly decreased levels of sinapoylmalate (Ruegger and Chapple, 2001) in all four mutant alleles (Hemm et al., 2003). Sinapoylmalate is the main sinapate ester in Arabidopsis (Chapple et al., 1992) acting as a UV light protectant as it accumulates in the leaves of the plant (Landry et al., 1995; Booij-James et al., 2000). Map-based cloning localised the *REF2* locus to the BAC F18A5 and it was found to encode CYP83A1 (At4g13770), a cytochrome P450 monooxygenase (Hemm et al., 2003) which is an enzyme involved in the biosynthesis of glucosinolates (Naur et al., 2003). Glucosinolates are amino acid-derived natural plant products implicated in biological activities that range from plant-insect and plant-pathogen interactions to auxin homeostasis (Kliebenstein et al., 2005a; Woodward and Bartel, 2005; Grubb and Abel, 2006).

Based on the disease resistance phenotype of *edr5*, the initial map position of the gene on chromosome IV and the fact that the *EDR5* gene has not yet been cloned, tests were conducted to determine if *cir1* shared any phenotypes with *edr5* and to ultimately establish if *cir1* was allelic to *edr5*. These tests constituted the second approach to fine map *cir1*.

3.5.2.1 Luciferase assays and *PR-1* Northern blot analysis on F_1 *edr5 cir1* plants

For the allelism tests, *cir1* was crossed onto *edr5*. As both mutations are recessive, the subsequent F_1 progeny would be heterozygous for both genes and would normally display a wild-type phenotype, unless the genes are allelic.

It was hypothesized that if *cir1* is allelic to *edr5*, the F_1 progeny plants will have high luciferase activity levels resembling the *cir1* phenotype. If the genes are non-allelic, the F_1 plants will show the wild-type phenotype of very low luciferase activity. Therefore, five of the resulting F_1 progeny plants were tested by PCR to confirm that the *PR-1::LUC* gene was present, indicating that the cross was successful (results not shown), and their luciferase activities were analysed at four weeks to test this theory (Fig. 3.6).

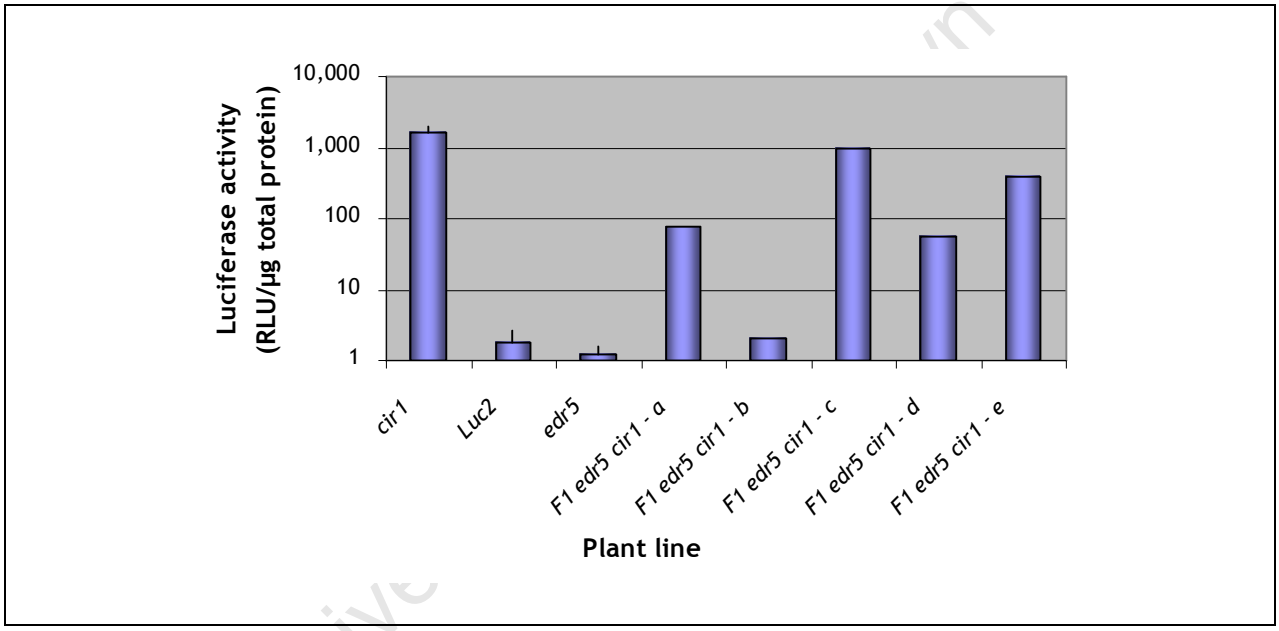

Figure 3.6. Luciferase activity of *edr5* and five individual F_1 *edr5 cir1* plants.
Four-week-old plants were assayed and *cir1* (positive control) and *Luc2* plants (background luciferase activity control) were included as controls. Bars represent either the average luciferase activity levels detected in five plants per line (*cir1*, *Luc2* and *edr5*) or the luciferase activity levels in individual plants (F_1 *edr5 cir1* -a to -e) and are plotted on a logarithmic scale. Units of luciferase activity are defined as relative light units (RLU) per µg total protein produced during 20 sec after luciferin injection. Error bars represent the standard error between values at the 95% confidence level.

Since *edr5* does not possess the *PR-1::LUC* transgene it showed very low luciferase activity levels compared to *cir1* plants, with levels even lower than the average background levels in the *Luc2* plants (Fig. 3.6). F_1 *edr5 cir1* -a, -c, -d and -e showed high luciferase activity levels, ranging from a 30- to 510-fold increase in comparison to the average background *Luc2* levels, but none reached the same high levels usually associated with *cir1* plants (Fig. 3.6). Given that all F_1 progeny plants were tested by PCR to confirm the presence of the *PR1::LUC*

transgene (results not shown), the low luciferase activity displayed by F_1 *edr5 cir1* -b (Fig. 3.6) was not due to unsuccessful crossing of *cir1* onto *edr5*. According to our theory, the F_1 plants would have resembled wild-type luciferase activity levels, as represented by *edr5* and *Luc2* plants, if the genes were non-allelic. However, the luciferase activity found in four of the five F_1 plants were much higher than wild-type levels and although it was lower than *cir1* levels, suggested that *cir1* and *edr5* could be allelic.

To confirm this result, luciferase activity assays (Fig. 3.7A) were performed on additional F_1 *edr5 cir1* plants. In addition, *PR-1* expression in *cir1*, *edr5* and F_1 *edr5 cir1* plants was determined by Northern blot analysis (Fig. 3.7B).

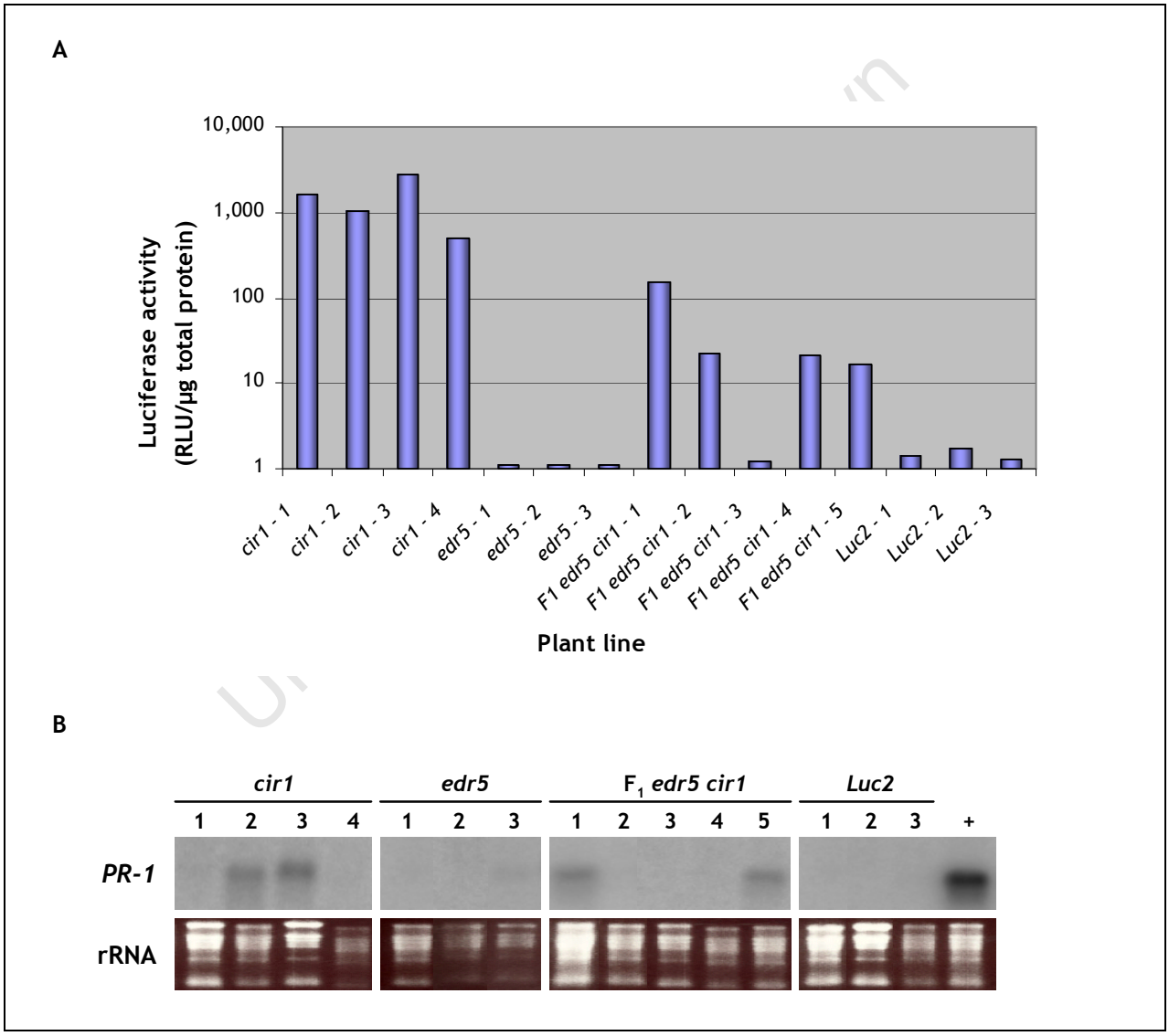

Figure 3.7. Luciferase activity and *PR-1* expression in individual *cir1*, *edr5*, F_1 *edr5 cir1* and *Luc2* plants.

(**A**) Luciferase activity levels of *cir1*, *edr5*, F_1 *edr5 cir1* and *Luc2* plants. Four-week-old plants were assayed and the units of luciferase activity are defined as relative light units (RLU) per µg total protein produced during 20 sec after luciferin injection. Bars represent the luciferase activity levels detected in individual plants and are plotted on a logarithmic scale. (**B**) Northern blot analysis of *PR-1*

expression in *cir1*, *edr5*, F_1 *edr5 cir1* and *Luc2* plants. Tissue was harvested from the same 4-week-old plants used in luciferase assays and RNA from salicylic acid-treated *Luc2* plants was used a positive control. RNA samples were probed with a *PR-1* probe. Ethidium bromide stained rRNA was used as a loading control.

The luciferase activity of individual 4-week-old plants was analysed and endogenous *PR-1* gene expression in each plant was also determined. As previously mentioned, *cir1* does not only display constitutively increased levels of luciferase activity, but also shows constitutive expression of the endogenous *PR-1* gene (Murray et al., 2002). We know from earlier studies that *edr5* has an enhanced defence resistance phenotype to bacterial and fungal pathogens (Drenkard et al., 2000) and according to an abstract by Stutius et al. (2000) this occurs in the absence of constitutive *PR* gene expression. However, to our knowledge, actual *PR-1* expression studies of this mutant have not been published. If *cir1* and *edr5* plants display similar phenotypes in the *PR-1* Northern blot analysis, corresponding *PR-1* expression in the F_1 *edr5 cir1* plants would act as additional verification of allelism between *cir1* and *edr5*. However, if *PR-1* expression in *cir1* plants are different from *edr5* plants, it would be an unsuitable allelism test.

As expected, all the *cir1* plants showed high luciferase activity beyond the background levels found in all the *Luc2* plants, whereas all the *edr5* plants displayed very low luciferase activity (Fig. 3.7A). Four out of the five tested F_1 *edr5 cir1* plants had high luciferase activity, again being higher than the *Luc2* plants but not as high as the levels found in the *cir1* plants (Fig. 3.6 and 3.7A). The high luciferase activity levels of the four plants ranged from 11 to 102 times higher than the average level of the *Luc2* plants. The low luciferase activity displayed by F_1 *edr5 cir1* -3 (Fig. 3.7A) is not due to the lack of the *PR-1::LUC* transgene since all F_1 progeny plants were tested by PCR to confirm its presence (results not shown). The behaviour of the four F_1 progeny plants (F_1 *edr5 cir1* -1, -2, -4 and -5) again suggested that *cir1* is allelic to *edr5* (Fig. 3.7A), however this result would have been more convincing if all five F_1 plants displayed high luciferase activity similar to *cir1* levels.

Results from the *PR-1* Northern blot analysis were confusing in that *cir1* normally displays constitutive *PR-1* expression (Murray et al., 2002), but in this experiment it was only expressed 50% of the time acting independently of the luciferase activity (Fig. 3.7A and B). It was previously established that the *PR-1::LUC* transgene reports endogenous *PR-1* gene expression after inoculation with *P. syringae* pv. *tomato* DC3000 carrying the AvrB effector (Murray et al., 2002) but it seems not to be the case in these uninfected plants. All four *cir1* plants had high luciferase activity confirming the constitutive expression of the *PR-1::LUC* transgene, but not all *cir1* plants expressed endogenous *PR-1* (Fig. 3.7B). For example, *cir1* -1 did not express *PR-1* whereas *cir1* -2, which had slightly less luciferase activity than *cir1* -1, expressed *PR-1* (Fig. 3.7A and B). The discrepancy could probably be contributed to

differences in the regulation of the tobacco *PR-1* promoter used in the *PR-1::LUC* construct and the endogenous Arabidopsis *PR-1* promoter, resulting in diverse expression patterns. This behaviour of *cir1* was not specific to this experiment and it has been found in other studies that *cir1* does not constantly express endogenous *PR-1* in our laboratory (results not shown).

In Fig. 3.7B, two of the three *edr5* plants did not express *PR-1* under these conditions. The faint expression of *PR-1* in *edr5* -3 might have been induced by poor growth conditions but then it would have been likely that *PR-1* expression would also have occurred in the *Luc2* plants. None of the *Luc2* plants showed *PR-1* expression (Fig. 3.7B). Two of the five F_1 progeny plants expressed *PR-1* (Fig. 3.7B), which also seemed to be unrelated to the luciferase activity levels observed in each plant (Fig. 3.7A and B). F_1 *edr5 cir1* -1 had 102 times greater luciferase activity than the average luciferase activity observed in the *Luc2* plants, whereas F_1 *edr5 cir1* -5 only had 11 times more (Fig. 3.7A). The remaining three F_1 plants which did not express *PR-1* had varying luciferase activity levels. F_1 *edr5 cir1* -2 had 15 times more, F_1 *edr5 cir1* -3 had 0.8 times less and F_1 *edr5 cir1* -4 showed 14 times higher luciferase activity than the *Luc2* average (Fig. 3.7A). The expression of *PR-1* in two of the F_1 plants suggested that these plants were prone to constitutive *PR-1* expression, like *cir1* and *edr5* -3, and again hinted at the possibility that *cir1* could be allelic to *edr5*. The *PR-1* Northern blot analysis was repeated with similar results but a definite conclusion can only be made if even more plants are tested to compensate for the variable expression of *PR-1*.

Therefore, the variable *PR-1* expression in *cir1* and F_1 progeny plants as well as the lack of *PR-1* expression in the majority of *edr5* plants, prompted the final conclusion that the *PR-1* Northern blot analysis approach was not a suitable test for allelism between *cir1* and *edr5*.

3.5.2.2 *CYP83A1* expression and sinapoylmalate levels in F_1 *edr5 cir1* plants

Thus far the phenotypic tests focussed on testing *edr5* plants for correspondence to the *cir1* phenotype and no conclusive results regarding allelism between *cir1* and *edr5* could be obtained (Fig. 3.6 and 3.7). It was therefore decided to test the *ref2* phenotype by conducting *CYP83A1* Northern blot analysis and HPLC analysis of sinapoylmalate levels in *cir1* and individual F_1 *edr5 cir1* plants. It has been established that three of the four *ref2* alleles showed substantially decreased *CYP83A1* expression and that all alleles had decreased sinapoylmalate levels compared to wild-type plants (Hemm et al., 2003). Since *edr5* is allelic to *ref2*, it is probable that *edr5* mutant plants would display reduced *CYP83A1* expression and low sinapoylmalate levels compared to wild-type plants. If *cir1* shows the same phenotype as *edr5*, F_1 progeny plants should show a decrease in *CYP83A1* expression and sinapoylmalate levels if *cir1* was allelic to *edr5*.

Leaf tissue was simultaneously harvested for the Northern blot and HPLC analysis from individual 4-week-old control and F_1 plants and the expression of *CYP83A1* (Fig. 3.8) and

sinapoylmalate levels (Fig. 3.9) was determined in each plant. *CYP83A1* expression in wild-type Col-0 plants and *Luc2* plants was similar when taking the RNA loading between the Col-0 and *Luc2* samples into account (Fig. 3.8). None of the *edr5* samples displayed a dramatic reduction in *CYP83A1* expression in comparison to the wild-type plants (Fig. 3.8). The mutant allele *ref2-4* behaved differently to the other *ref2* alleles by not exhibiting a reduction in *CYP83A1* expression (Hemm et al., 2003) and therefore it is apparent that *edr5* also falls into this class. In addition, there were no major changes in *CYP83A1* expression in the *cir1* plants compared to wild-type plants (Fig. 3.8). Since the differences in *CYP83A1* expression between *edr5* and *cir1* and wild-type plants were not significant, expression studies of *CYP83A1* in F_1 *edr5 cir1* plants were also unsuitable as an allelism test. This might have been a successful allelism test if all four of the *ref2* alleles showed decreased *CYP83A1* expression (Hemm et al., 2003) and therefore this result highlights the problem of doing allelism tests when the alleles of a mutant have different phenotypes.

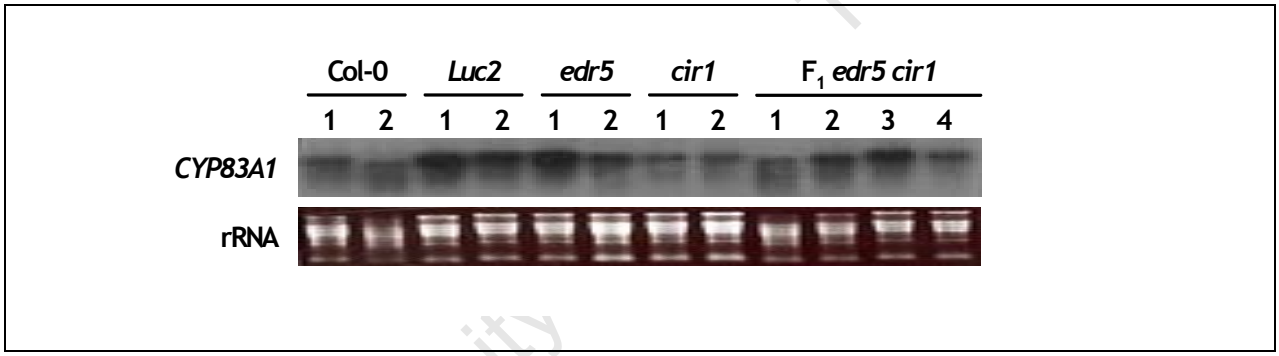

Figure 3.8. Northern blot analysis investigating *CYP83A1* expression in individual Col-0, *Luc2*, *edr5*, *cir1* and F_1 *edr5 cir1* plants.

Tissue was harvested from the same 4-week-old plants used and RNA samples were probed with a *CYP83A1* probe. Ethidium bromide stained rRNA was used as a loading control.

Although not all *ref2* alleles showed reduced *CYP83A1* expression, all showed a marked decrease in sinapoylmalate levels (Hemm et al., 2003). Therefore it was necessary to determine if *edr5*, *cir1* and the F_1 *edr5 cir1* plants also displayed reduced sinapoylmalate levels in spite of their expression of *CYP83A1*. HPLC analysis of sinapoylmalate levels in the leaf extracts of the individual plants are presented in Fig. 3.9. Peaks on the chromatograms represent sinapoylmalate levels present in leaf extracts and in the case of the Col-0 (Fig. 3.9A) and *Luc2* (Fig. 3.9B) samples, the sinapoylmalate levels were high with little variance between the two extracts. Behaving like the *ref2-4* mutant allele (Hemm et al., 2003), the *edr5* extract showed dramatically reduced accumulation of sinapoylmalate (Fig. 3.9C) in spite of not having reduced *CYP83A1* expression (Fig. 3.8) with its peak being much smaller compared to the peaks of the Col-0 and *Luc2* samples (Fig. 3.9A and B). The

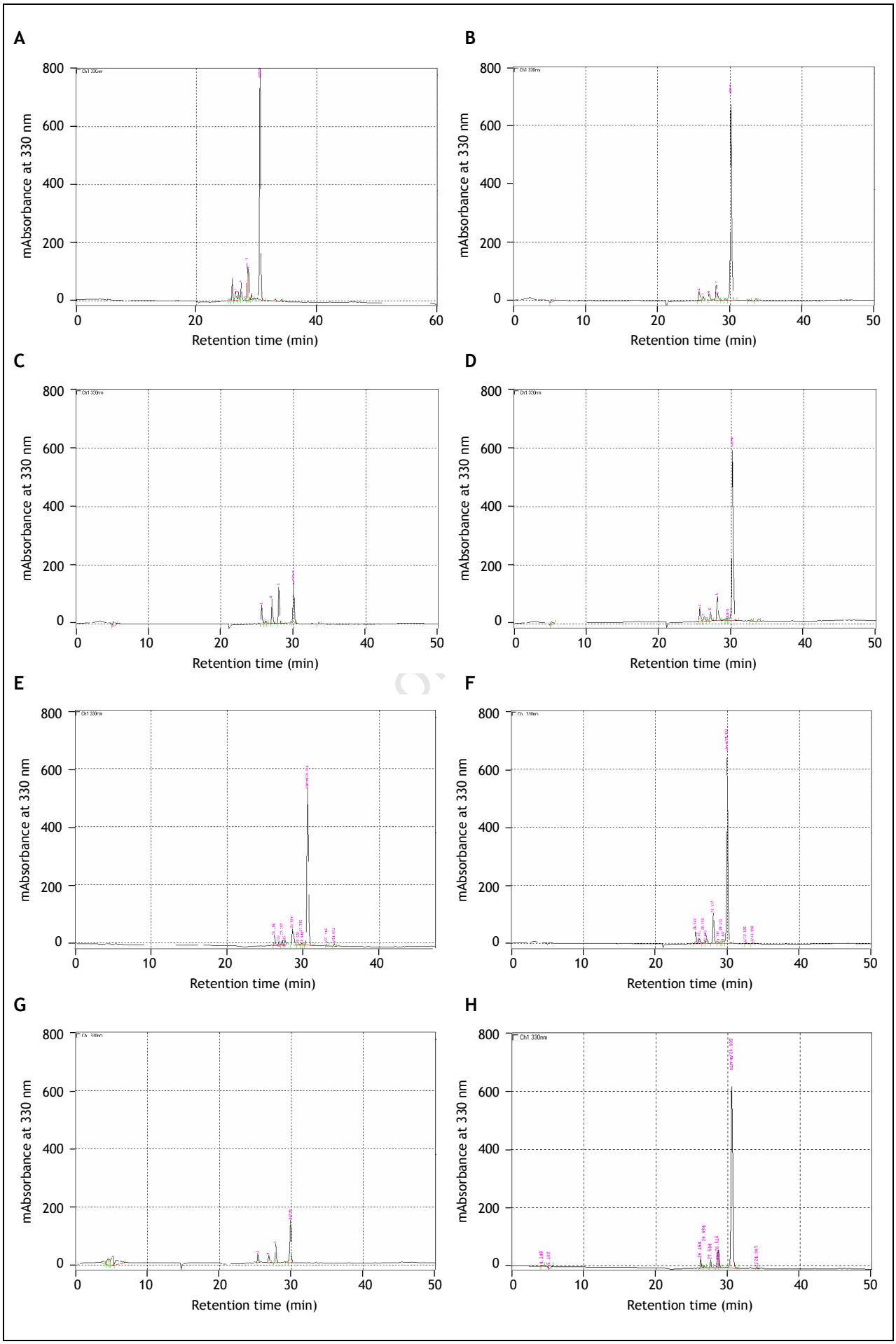
A
B
C
D
E
F
G
H
mAbsorbance at 330 nm
Retention time (min)
Ch1 330nm

Figure 3.9. High performance liquid chromatography (HPLC) analysis of sinapoylmalate accumulation in leaves of individual Col-0, *Luc2*, *edr5*, *cir1* and F_1 *edr5 cir1* plants.
Methanolic leaf extracts analysed by HPLC. Peaks on the chromatograms show sinapoylmalate levels monitored at 330 nm in (**A**) Col-0, (**B**) *Luc2*, (**C**) *edr5*, (**D**) *cir1*, (**E**) F_1 *edr5 cir1* -1, (**F**) F_1 *edr5 cir1* -2, (**G**) F_1 *edr5 cir1* -3 and (**H**) F_1 *edr5 cir1* -4 plants. Tissue was harvested from the same 4-week-old plants used in the *CYP83A1* Northern blot analysis. Only one representative chromatogram for Col-0, *Luc2*, *edr5* and *cir1* plants are shown. All peaks show a comparable retention time of 30 min indicating elution of the same compound in each samples allowing for direct comparison between samples.

sinapoylmalate accumulation in the *cir1* extract was not significantly reduced in comparison to wild-type samples (Fig. 3.9D). As *edr5* and *cir1* plants displayed variable phenotypes regarding the accumulation of sinapoylmalate, this experiment was an inappropriate test for allelism between *cir1* and *edr5* and the measurement of sinapoylmalate levels in the F_1 *edr5 cir1* extracts (Fig. 3.9E to H) proved futile.

3.5.2.3 Sequence analysis of *CYP83A1* in *cir1* background

Given that the *CYP83A1* Northern blot analysis (Fig. 3.8) and the HPLC analysis of sinapoylmalate accumulation (Fig. 3.9) proved to be inadequate as allelism tests between *cir1* and *edr5*, it was decided to search for mutations in the coding sequence of *CYP83A1* in *cir1* background. If the mutations occurred in the *CYP83A1* promoter region, we would have expected the expression of *CYP83A1* in *cir1* to be affected. *CYP83A1* expression levels in *cir1* were very similar to wild-type levels (Fig. 3.8) and therefore only the coding, and not the promoter region, was investigated.

If *cir1* was allelic to *edr5*, base pair changes in the sequence of *CYP83A1* in the *cir1* background compared to the wild-type sequence would be expected. The total length of *CYP83A1* is 1 825 bp containing two exons separated by one intron of 91 bp (details available on TAIR). The first exon consists of 912 bp of which the first 27 bp comprise the 5' untranslated region (UTR, represented by small case letters in Fig. 3.10A) and the remaining 885 bp act as the coding region. The second exon of 820 bp has a coding region of 624 bp and 3' UTR consisting of 196 bp indicated by small case letters in Fig. 3.10B.

The exons of *CYP83A1* were amplified from *cir1* genomic DNA, sequenced with forward and reverse primers (see section 2.4.5 in Chapter 2 for details) and aligned with the wild-type Col-0 *CYP83A1* sequence (Fig. 3.10). The *CYP83A1* sequence obtained from *cir1* genomic DNA exactly matched the wild-type sequence and no mutations could be found in either of coding regions of the two exons (Fig. 3.10A and B). Pooled amplified products were sequenced twice with identical results.

In comparison to all the previous experiments testing allelism between *cir1* and *edr5*, these results were the first to suggest that *cir1* was not allelic to *edr5*.

3.5.2.4 Complementation of *cir1* with *EDR5*: *cir1* was not allelic to *edr5*

The majority of the phenotypic tests conducted proved to be unsuitable in testing allelism between *cir1* and *edr5* (Fig. 3.7B, 3.8 and 3.9). However, when considering the results obtained in the suitable experiments, some implied that *cir1* could be allelic to *edr5* (Fig. 3.6 and 3.7A), while one suggested non-allelism (Fig. 3.10). These confusing findings prompted one more experiment to conclusively determine if *cir1* was in fact allelic to *edr5*. Complementation studies were done by transforming *cir1* plants with a clone containing the wild-type *EDR5* gene. The clone (JAtY58C12) was obtained from The John Innes Centre Genome Laboratory (http://jicgenomelab.co.uk/jgl) and details regarding the Arabidopsis JAtY library and vectors utilised by this facility are to follow in section 3.5.3. If the *EDR5* gene complements the *cir1* mutation, it will rescue the mutant phenotype and the transformed *cir1* plants will show a loss of constitutively high luciferase activity. It was decided to test the luciferase activity of the transformed plants as this was the only experiment where clear differences between the *cir1* and *edr5* or wild-type phenotype could be established (Fig. 3.6 and 3.7A). If the transformed *cir1* plants show wild-type luciferase activity levels, demonstrating that the *EDR5* gene has complemented the *cir1* mutation, these results would be considered as conclusive proof regarding allelism between *cir1* and *edr5*.

More details of the transformation and selection processes will be outlined in section 3.5.3. Apart from the usual controls normally included in luciferase assays, these assays also incorporated additional controls of *cir1* and *Luc2* plants transformed with an empty pSMB binary vector (Mylne and Botella, 1998). These were included to determine if the selection process to identify transformed plants had an effect on *PR-1::LUC* expression and subsequent luciferase activity. The employed vectors contained the *Bar* gene and therefore successfully transformed *cir1* and *Luc2* plants were identified through their resistance to PPT and through the PCR amplification of the *Bar* gene (results not shown). Seed from three independently transformed T_2 lines of *cir1* + pSMB, *Luc2* + pSMB and *cir1* + JAtY58C12 were plated onto MS media containing PPT and the resulting resistant plants were planted onto soil after one week. The luciferase activity of five plants from each of the three independently transformed T_2 lines of *cir1* + pSMB, *Luc2* + pSMB and *cir1* + JAtY58C12 were tested at four weeks of age (Fig. 3.11) and differences in luciferase activity levels were statistically analysed using the Mann-Whitney test ($P < 0.05$). Although luciferase activity of combined (*cir1* + pSMB and *Luc2* + pSMB) and individual T_2 lines (*cir1* + JAtY58C12) are represented in Fig. 3.11, the Mann-Whitney tests were only performed on the combined results of the luciferase activities of all fifteen plants tested per transformed line. The tests were also performed on the results from all ten plants tested in the untransformed lines.

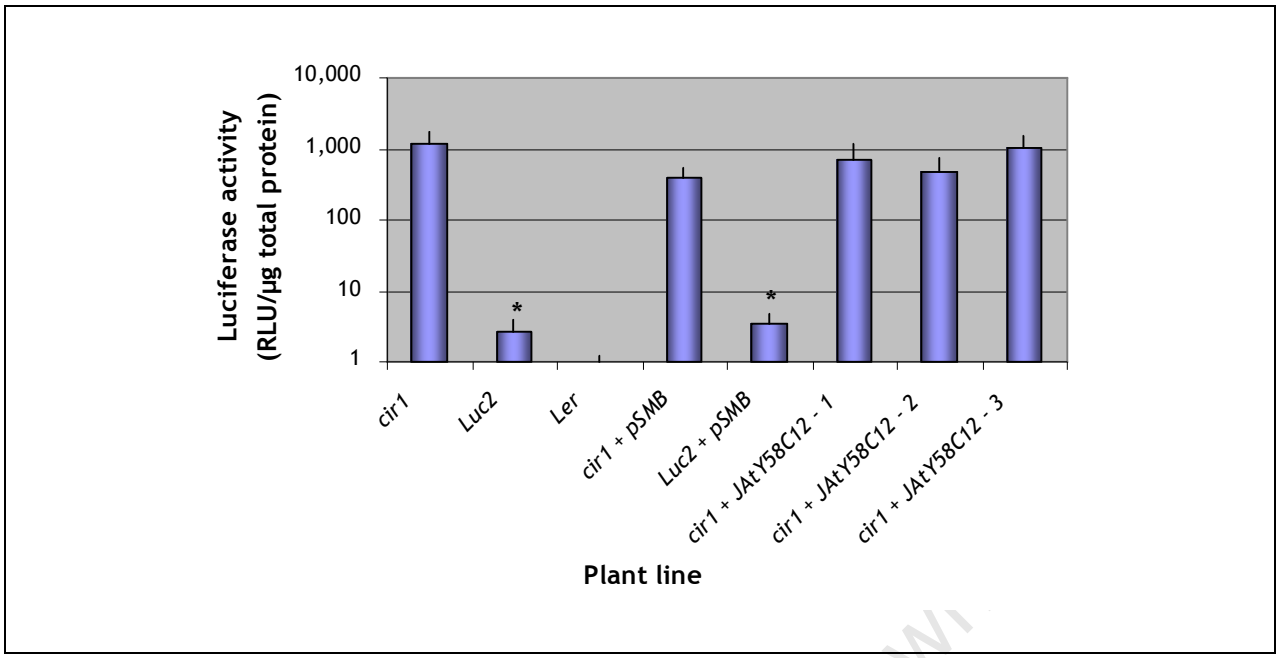

Figure 3.11. Luciferase activity of *cir1* plants transformed with the JAtY58C12 clone harbouring wild-type *EDR5*.

Four-week-old transformed *cir1* plants were assayed and untransformed *cir1* (positive control), untransformed *Luc2* (background luciferase activity control), untransformed L*er* (negative control), *cir1* + pSMB (empty vector control) and *Luc2* + pSMB plants (empty vector control) were included as controls. Bars represent the average luciferase activity levels detected in either ten (*cir1*, *Luc2* and L*er*), fifteen (*cir1* + pSMB and *Luc2* + pSMB) or five plants (*cir1* + JAtY58C12) per line and are plotted on a logarithmic scale. Units of luciferase activity are defined as relative light units (RLU) per µg total protein produced during 20 sec after luciferin injection. Error bars represent the standard error between values at the 95% confidence level. Asterisks indicate significantly less luciferase activity compared to *cir1* + pSMB (Mann-Whitney test, $P < 0.05$).

The luciferase activity levels of the transformed *cir1* + pSMB lines were not significantly different from the levels found in the untransformed *cir1* plants (Fig. 3.11). Similarly, *Luc2* + pSMB lines also showed no significant difference from the normal background luciferase activity levels in untransformed *Luc2* plants (Fig. 3.11). Both these results indicate that the selection process had no effect on the luciferase activity of transformed plants. As expected, transformed *Luc2* + pSMB lines and untransformed *Luc2* plants had significantly lower luciferase activity than untransformed *cir1* + pSMB plants (Fig. 3.11). Most importantly, there was no major decrease of luciferase activity in any of the three independent *cir1* + JAtY58C12 transformed T_2 lines in comparison to the untransformed *cir1* plants and *cir1* + pSMB lines (Fig. 3.11). This was also statistically confirmed by the Mann-Whitney test which showed that there was no significant difference in the combined luciferase activity of *cir1* + JAtY58C12 and *cir1* + pSMB plants. The statistical significant difference between the combined luciferase activity levels of *cir1* + JAtY58C12 and

Luc2 + pSMB plants (Fig. 3.11) confirmed that the transformed *cir1* plants did not display a wild-type phenotype.

Since the *cir1* + JAtY58C12 transformed lines maintained constitutively high luciferase activity levels associated with *cir1* and *cir1* + pSMB plants, it can be concluded that the JAtY58C12 clone harbouring the wild-type *EDR5* gene did not complement the *cir1* mutation proving conclusively that *cir1* is not allelic to *edr5*.

3.5.3 Complementation of the *cir1* mutation

As mentioned previously, the complementation strategy is dependent on transformation of the mutant plant with overlapping wild-type genomic DNA fragments that span the region of interest between the flanking markers. In so doing it can be determined which of the DNA fragments complement the mutation by restoring the mutant phenotype to wild-type (Lukowitz et al., 2000). Once the complementing fragment has been determined, candidate genes in that part of the Arabidopsis genome can be identified.

The last approach to fine map *cir1* involved complementation analysis of the *cir1* mutation, which was greatly facilitated by the Gene Transfer Clone Identification and Distribution (GetCID) service (http://jicgenomelab.co.uk/libraries). GetCID, which forms part of the John Innes Centre Genome Laboratory, constructed a TAC library (JAtY library) consisting of 36 864 clones using the pYLTAC17 binary vector system (Liu et al., 2002). The transformation-competent artificial chromosome (TAC) vector system can be used to clone large genomic DNA fragments and to transform plants through *Agrobacterium*-mediated methods (Liu et al., 1999) and therefore candidate clones from the JAtY library can be used to directly transform Arabidopsis plants for complementation analysis. The JAtY genomic library, which provides 14 x coverage of the Arabidopsis genome, was constructed using DNA from purified leaf nuclei from Col-0, partially digested with the restriction enzyme *Hin*dIII and ligated into the *Hin*dIII site of the pYLTAC17 vector (Liu et al., 2002). The pYLTAC17 vector contains a kanamycin-resistance gene which allows for kanamycin selection in *Escherichia coli* and *Agrobacterium tumefaciens*, as well as the *Bar* gene which confers resistance to PPT used in the selection of transformed plants (Cao et al., 1992; Liu et al., 2002). The *PR-1::LUC* gene cassette included a kanamycin selectable marker and therefore it was important to identify a library which relies on an alternative selection process to select for transformed *cir1* plants.

Many of the JAtY library clones have been end-sequenced and with the help of the *Arabidopsis thaliana* Integrated Database's (ATIDB) Genome Browser (http://atidb.org/cgi-perl/gbrowse/atibrowse; Pan et al., 2003) six overlapping JAtY clones which spanned the 309.10 kb region of interest in *cir1*, could be selected for complementation purposes. Fig. 3.12 is a schematic representation of the selected JAtY clones relative to the annotation

units and PCR markers (listed in Table 3.5) spanning the ~ 309 kb region of interest on chromosome IV.

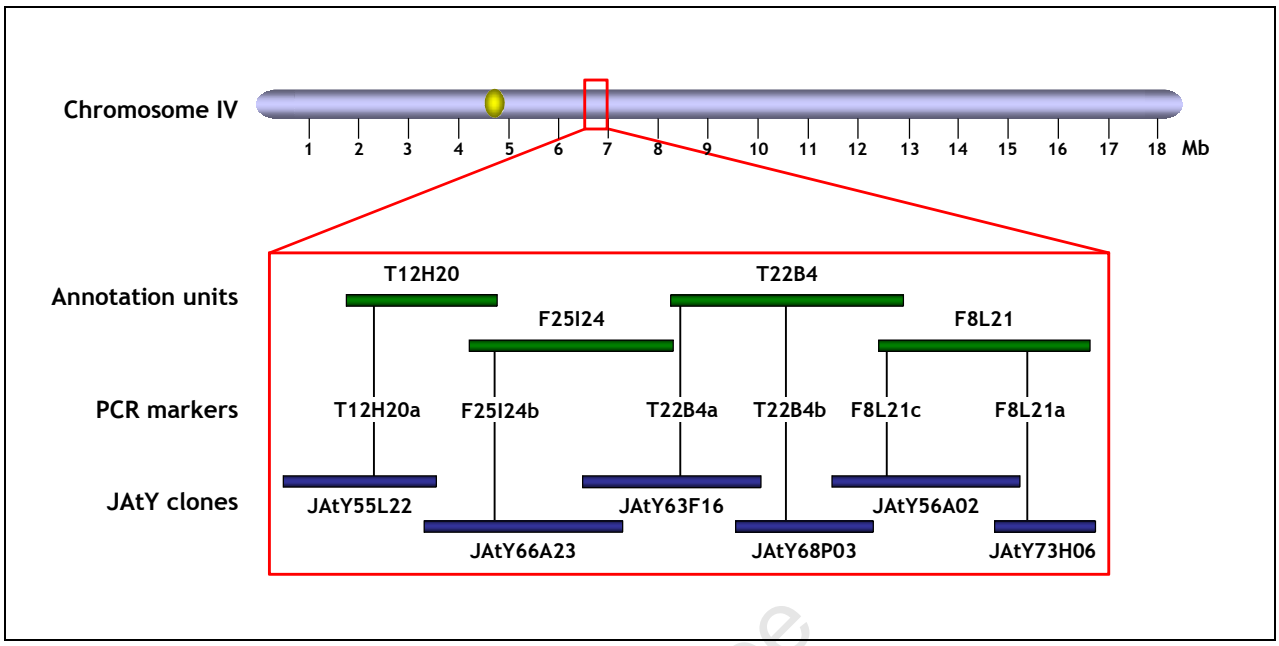

Figure 3.12. A schematic representation of the six JAtY clones selected for complementation analysis in relation to the annotation units and PCR markers spanning the ~ 309 kb region of interest on chromosome IV.

A magnified view of the ~ 309 kb region of interest on chromosome IV is boxed in red. The region spans four annotation units (indicated by green bars), starting at PCR marker T12H20a and ending at F8L21a. The positions of the six JAtY clones according to the *Arabidopsis thaliana* Integrated Database (ATIDB), relative to the annotation units and PCR markers listed in Table 3.5, are indicated by the blue bars.

Upon arrival from GetCID, the six JAtY clones were screened with the relevant PCR markers positioned on each clone (see Fig. 3.12) to confirm that their genomic inserts corresponded to the ~ 309 kb region of interest (results not shown). Five of the six clones contained the correct genomic insert and the appropriate PCR products were amplified, but no PCR product could be obtained for the JAtY55L22 clone (results not shown). After various PCR attempts and extensive troubleshooting, a second JAtY55L22 clone was ordered form GetCID but attempts to amplify part of the genomic insert in the second clone also failed (results not shown). Since it could not be confirmed that the genomic insert of JAtY55L22 corresponded to the relevant section of the ~ 309 kb region (see Fig. 3.12), it was decided to exclude this clone from the complementation analysis experiments.

3.5.3.1 Transformation of *cir1* plants with JAtY clones

The clones used in the transformation of *cir1* plants were JAtY66A23, JAtY63F16, JAtY68P03, JAtY56A02 and JAtY73H06. Additionally, an empty pSMB binary vector (Mylne and Botella,

1998) was used to transform *cir1* and *Luc2* plants. These plants acted as empty vector controls and were used to determine if PPT selection had an effect on *PR-1::LUC* expression and on the subsequent constitutively high luciferase activity in *cir1* plants and/or on the normal background luciferase activity levels in *Luc2* plants.

The JAtY clones and the empty pSMB vector were transformed into *A. tumefaciens* and the transformed colonies were confirmed by PCR (results not shown). *Cir1* plants were transformed through *Agrobacterium*-mediated methods with the individual JAtY clones or the empty pSMB vector, whereas *Agrobacterium*-mediated transformation of *Luc2* plants was only with the empty pSMB vector. Since both the pYLTAC17 vector (Liu et al., 2002) used in the JAtY clones and the pSMB vector (Mylne and Botella, 1998) contain the *Bar* gene, successfully transformed *cir1* and *Luc2* plants were identified through their resistance to PPT.

The T_1 seed from the seven transformed lines was collected and the T_1 plants were screened for resistance to PPT. The resulting resistant T_1 plants were tested by PCR to confirm the presence of the *Bar* gene (results not shown) and the T_2 seed were collected from the confirmed plants after self-fertilization. At least three T_2 lines from independent transformation events were identified for *cir1* + pSMB, *Luc2* + pSMB, *cir1* + JAtY66A23 and *cir1* + JAtY56A02, whereas only one and two independently transformed T_2 lines could be selected for *cir1* + JAtY63F16 and *cir1* + JAtY68P03, respectively. Although all T_1 seed collected from the transformation of *cir1* with JAtY73H06 were plated on MS media plates containing PPT, none of the resulting T_1 plants displayed resistance to PPT indicating that the transformation of *cir1* with the JAtY73H06 clone was unsuccessful.

The independently transformed T_2 lines of *cir1* + pSMB, *Luc2* + pSMB, *cir1* + JAtY66A23, *cir1* + JAtY63F16, *cir1* + JAtY68P03 and *cir1* + JAtY56A02 were used in the following luciferase and *Pseudomonas syringae* infection assays to identify a complementing JAtY clone.

3.5.3.2 Identification of the complementing JAtY clone based on luciferase and *Pseudomonas syringae* assays

To identify a complementing JAtY clone, it was necessary to investigate which of the clones restored the *cir1* mutant phenotype to wild-type. Thus far, the *cir1* phenotype based on constitutively high luciferase activity has been extensively described, but *cir1* has an additional phenotype based on disease resistance. The *cir1* mutation renders plants more resistant to the bacterial pathogen *Pseudomonas syringae* pv. *tomato* DC3000 (*Pst* DC3000) and the virulent oomycete *Hyaloperonospora parasitica* Noco2 (Murray et al., 2002). The c*ir1* plants transformed with the complementing JAtY clone would therefore exhibit a loss of constitutively high luciferase activity as well as a loss of resistance to *Pst* DC3000 and *H. parasitica* Noco2. For complementation analysis purposes, it was decided to initially perform luciferase assays on the transformed *cir1* plants (Fig. 3.13) and to confirm the

results of the luciferase assays, the effect of the JAtY clones on *cir1* resistance to *Pst* DC3000 was investigated (Fig. 3.14).

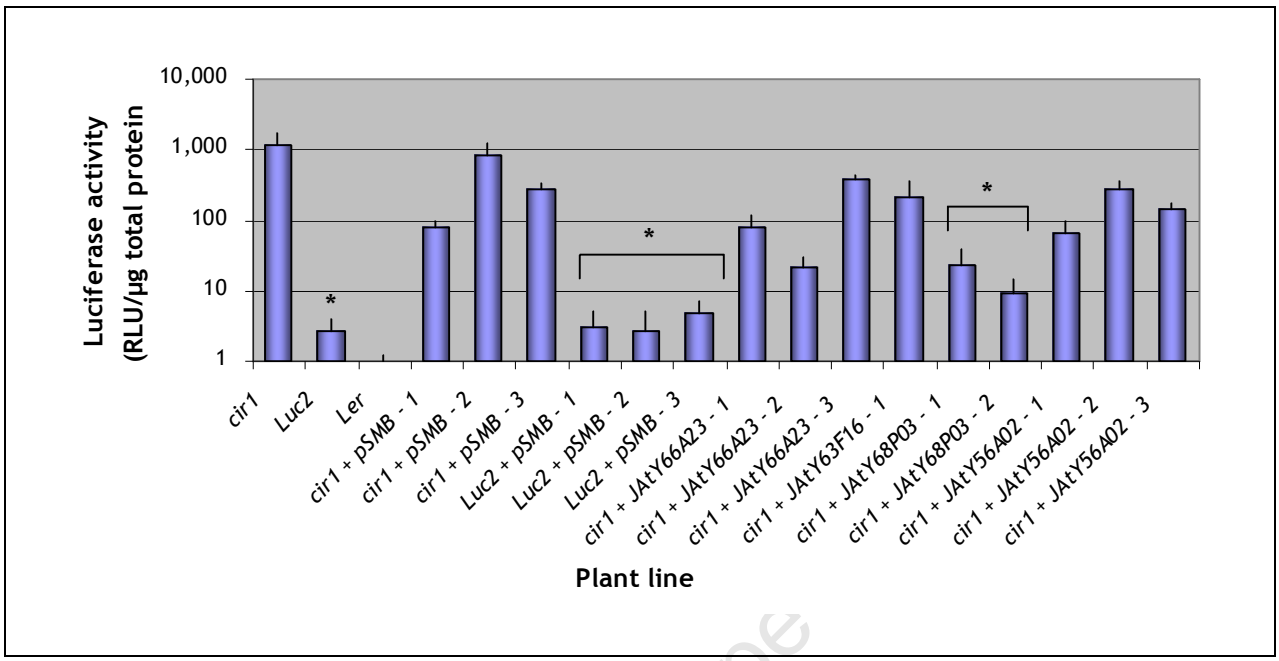

Figure 3.13. Luciferase activity of *cir1* plants transformed with individual JAtY clones.
Four-week-old transformed *cir1* plants were assayed and untransformed *cir1* (positive control), untransformed *Luc2* (background luciferase activity control), untransformed L*er* (negative control), *cir1* + pSMB (empty vector control) and *Luc2* + pSMB plants (empty vector control) were included as controls. Bars represent the average luciferase activity levels detected in ten untransformed plants (*cir1*, *Luc2* and L*er*) or in five plants per independent T_2 line of all transformed plant lines and are plotted on a logarithmic scale. Units of luciferase activity are defined as relative light units (RLU) per µg total protein produced during 20 sec after luciferin injection. Error bars represent the standard error between values at the 95% confidence level. Asterisks indicate significantly lower levels in the combined luciferase activity of all plants per plant line compared to all *cir1* + pSMB plants (Mann-Whitney test, $P < 0.05$).

Fifty seed of each of the independently transformed T_2 lines of *cir1* + pSMB, *Luc2* + pSMB, *cir1* + JAtY66A23, *cir1* + JAtY63F16, *cir1* + JAtY68P03 and *cir1* + JAtY56A02 were plated onto MS media containing PPT. After one week, the resulting resistant plants were planted onto soil and the luciferase activity of five plants per T_2 line was tested at four weeks of age (Fig. 3.13). The statistical significance of the differences in luciferase activity levels were determined with the Mann-Whitney test ($P < 0.05$) which was performed on the combined results of the luciferase activities of all plants tested per transformed line and not on the results from independent T_2 lines. Therefore, although the luciferase activity for independent T_2 lines are presented in Fig. 3.13, the indicated statistical significance was based on the results from all plants tested per transformed line. Mann-Whitney tests ($P <$

0.05) were also performed on the combined results of all plants in each of the untransformed lines.

There was no significant change in the luciferase activity levels between untransformed *cir1* and *cir1* + pSMB plants or between untransformed *Luc2* and *Luc2* + pSMB plants (Fig. 3.13). As expected, the untransformed *Luc2* and the *Luc2* + pSMB plants had significantly lower luciferase activity levels than *cir1* + pSMB plants (Fig. 3.13). Since the behaviour of the empty vector controls corresponded to the untransformed controls, the PPT selection had no effect on the constitutively high luciferase activity in transformed *cir1* plants or on the normal background luciferase activity levels in transformed *Luc2* plants. The results obtained from the different transformed lines were therefore not influenced by the PPT selection process. The *cir1* + JAtY66A23 – 2 line displayed slightly reduced luciferase activity levels in comparison to the other two *cir1* + JAtY66A23 and *cir1* + pSMB lines (Fig. 3.13), but statistically the difference in luciferase activity of all *cir1* + JAtY66A23 plants in comparison to all *cir1* + pSMB plants was insignificant. Additionally, *Luc2* + pSMB plants showed notably lower luciferase activity levels than the *cir1* + JAtY66A23 lines (Fig. 3.13) suggesting that *cir1* + JAtY66A23 did not display wild-type luciferase activity levels. Although only one T_2 line for *cir1* + JAtY63F16 could be tested, the high luciferase activity determined in this line resembled that of the *cir1* + pSMB lines more than the levels of the *Luc2* + pSMB plants (Fig. 3.13). Statistically, the distinction between this line and *cir1* + pSMB was not significant whereas luciferase activity was significantly higher than the wild-type levels displayed by the *Luc2* + pSMB plants. Interestingly, two of the five *cir1* + JAtY63F16 plants had low luciferase activity levels (results not shown) but the average luciferase activity of all five plants did not resemble wild-type levels. Both the T_2 lines of *cir1* + JAtY68P03 showed significantly reduced luciferase activity levels relative to the *cir1* + pSMB plants (Fig. 3.13). Furthermore, the luciferase activity levels of the *cir1* + JAtY68P03 plants were not statistically different from the *Luc2* + pSMB levels demonstrating that this transformed line resembled wild-type luciferase levels. All three *cir1* + JAtY56A02 lines exhibited luciferase activity levels comparable to the *cir1* + pSMB levels (Fig. 3.13) and no significant distinction in luciferase activity between these two transformed plant lines could be made. To ensure that the low luciferase activity exhibited by certain transformed plants was not due to the loss of the *PR-1::LUC* transgene, all plants of each of the transformed lines were tested with PCR to confirm the presence of the *PR-1::LUC* transgene (results not shown).

Based on the results of the luciferase assays, the JAtY68P03 clone rescued the *cir1* mutant phenotype and restored the constitutively high luciferase activity of *cir1* plants to levels similar to wild-type as represented by *Luc2* + pSMB plants. Although the *cir1* + JAtY63F16 line did not show a significant reduction in luciferase activity in comparison to the

cir1 + pSMB plants (Fig. 3.13), two of the individually tested plants displayed low wild-type luciferase activity levels (results not shown). During the screening of luciferase activity which is driven by the *PR-1* promoter of the *PR-1::LUC* construct, false results are mostly associated with plants displaying higher levels than expected. Expression of the *PR-1* gene can be induced by sub-optimal growth conditions or asymptomatic pathogen infection (Thatcher et al., 2005; Kempema et al., 2007) and hence the high luciferase activity levels observed in the three *cir1* + JAtY63F16 plants might have been misleading. Therefore, complementation by both of the JAtY63F16 and JAtY68P03 clones, instead of only by the JAtY68P03 clone, was considered as an alternative theory.

To confirm that the JAtY68P03 clone, and possibly the JAtY63F16 clone, complemented the *cir1* mutation as suggested by the low luciferase activity levels displayed by the *cir1* + JAtY68P03 lines and some *cir1* + JAtY63F16 plants, the effect of these clones on *cir1* resistance to *Pst* DC3000 was determined. If these clones complement the *cir1* mutation, it was expected that the *cir1* + JAtY68P03 and *cir1* + JAtY63F16 transformed plants would display a loss of resistance to *Pst* DC3000. A *Pst* DC3000 infection assay was conducted on plants from the same group of PPT-resistant, soil-grown plants utilized in the luciferase assays. Three plants per individual T_2 line per time point were infected with *Pst* DC3000 and the severity of the infection was determined at 48 h and 72 h post infection as presented in Fig. 3.14. Based on the results from previous *Pst* DC3000 infection assays, no significant difference in bacterial titres has been observed at 24 h post infection between *cir1* and *Luc2* plants (see Chapter 4). Therefore, the bacterial titres of infected plants were only determined at 48 h and 72 h post infection. Although Fig. 3.14 presents the bacterial titre determined in the independent T_2 lines, the indicated statistical significance was based on the combined results from all plants tested per transformed line (Student's *t*-test, $P < 0.05$).

Although there was slight variation in the bacterial growth between the three *Luc2* + pSMB lines, all displayed high bacterial titres usually associated with susceptible wild-type plants at both time points (Fig. 3.14). All three *cir1* + pSMB lines displayed similar bacterial titres which was significantly lower than the bacterial titres in the wild-type *Luc2* + pSMB plants at both 48 h and 72 h post infection (Fig. 3.14). The *cir1* + pSMB phenotype therefore corresponded to the *cir1* disease resistance phenotype. After 48 h of infection, *cir1* + JAtY63F16 exhibited bacterial titres similar to the *Luc2* + pSMB lines indicating a loss of resistance (Fig. 3.14) but statistically no significant difference between the bacterial titres of *cir1* + JAtY63F16 and *cir1* + pSMB could be established. However, it is likely that the difference between the two lines was not statistically significant due to the limited amount of plants tested in the *cir1* + JAtY63F16 line compared to the *cir1* + pSMB control line. At the later time point (72 h), the bacterial growth in *cir1* + JAtY63F16 showed a significantly lower titre than that of the wild-type plants (Fig. 3.14), suggesting that this transformed line

resembled the resistance phenotype of *cir1* + pSMB plants. Most importantly, the bacterial titre in *cir1* + JAtY68P03 was significantly higher than *cir1* + pSMB at both 48 h and 72 h post infection (Fig. 3.14) and there was no statistical distinction between the titre of the *cir1* + JAtY68P03 and wild-type *Luc2* + pSMB plants at either time point (Fig. 3.14).

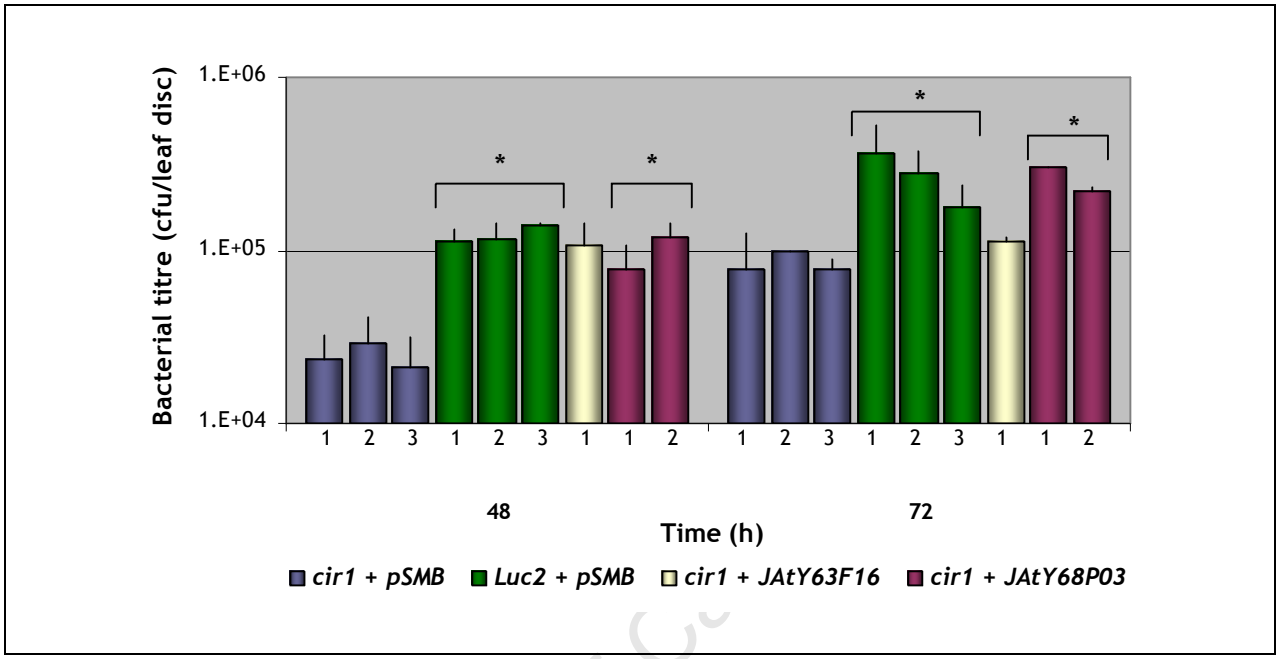

Figure 3.14. *Pseudomonas syringae* pv. *tomato* DC3000 infection assay of *cir1* plants transformed with the JAtY63F16 and JAtY68P03 clones.

Transformed *cir1* plants and the control lines *cir1* + pSMB (positive control) and *Luc2* + pSMB (negative control representing wild-type) were assayed. Bars represent the average bacterial titre of three plants per independent T_2 line at 48 h and 72 h post infection and are plotted on a logarithmic scale. Numbers on the X-axis represent the independent T_2 lines per transformed plant line. Bacterial titre is defined as colony forming units (cfu) per leaf disc of 0.5 cm^2. Error bars represent the standard error between values at the 95% confidence level. Asterisks indicate a significant increase in the combined bacterial titres in all plants per transformed line compared to all *cir1* + pSMB plants at each time point (Student's *t*-test, $P < 0.05$).

The inconsistent behaviour of the *cir1* + JAtY63F16 plants at 72 h post infection compared to the 48 h time point highlights the problem of testing only one transformed line. To conclusively establish if the JAtY63F16 clone complemented *cir1*, the luciferase and *Pst* DC3000 infection assays need to be repeated with more independently transformed *cir1* + JAtY63F16 lines. However, based on the results from the 48 h time point in the *Pst* DC3000 infection assay (where there is a greater difference between *cir1* and *Luc2* lines) and the occurrence of the two low luciferase activity plants, the possibility that the JAtY63F16 clone complemented the *cir1* mutation cannot be ignored. However, the *Pst* DC3000 infection assay results clearly demonstrated that *cir1* + JAtY68P03 plants

displayed a loss of resistance and that the *cir1* phenotype had been restored to a susceptible phenotype associated with wild-type plants. Similar results were acquired in both the independently transformed T_2 lines of *cir1* + JAtY68P03 (Fig. 3.14) confirming the results obtained in the luciferase assays. Therefore, the results of the luciferase and *P. syringae* infection assays both demonstrated that the JAtY68P03 clone complemented the *cir1* mutation. It has to be noted that the results from the luciferase and *Pst* DC3000 infection assays are preliminary and need to be repeated. In addition, although the transformed plants were selected based on resistance to PPT and the amplification of the *Bar* gene, the exact identity and status of each of the JAtY clones in the transformed lines need to be verified.

The JAtY clones selected for the complementation analysis were specifically chosen to have overlapping regions (see Fig. 3.12). The overlapping regions facilitate the identification of the exact genomic DNA fragment that is responsible for the complementation of the mutation. For instance, if both of the JAtY63F16 and JAtY68P03 clones restored the *cir1* mutant phenotype to wild-type, complementation would be attributed to the overlapping region between the two clones thereby eliminating the remaining parts of both clones from complementing region. Likewise, if only one clone complemented the mutation, only the section unique to that clone would be of interest and the overlapping regions on both sides would be excluded from the complementing region. In this case, the exclusion of the overlapping regions reduces the size of the complementing fragment, aiding in the identification of candidate genes in that region.

The JAtY68P03 clone restored both of the *cir1* phenotypes to wild-type but the alternative theory that both of the JAtY63F16 and JAtY68P03 clones complemented the *cir1* mutation, also needed to be considered. Therefore, the unique section of the JAtY68P03 clone as well as the overlapping region between the JAtY63F16 and JAtY68P03 clones was investigated for possible *CIR1* candidate genes. The overlapping region contained 11 882 bp and ranged from 6 768 913 bp to 6 780 795 bp on chromosome IV, while the unique section of JAtY68P03 was 34 155 bp in size and spanned the region from 6 780 796 bp to 6 814 952 bp.

3.6 Investigation of possible *CIR1* candidate genes

The region between 6 768 913 bp and 6 814 952 bp on chromosome IV is located on the annotation unit T22B4. During the initial mapping of *cir1*, the PCR marker T22B4a displayed the lowest percentage recombination of 1.39 (Table 3.3) suggesting that the *CIR1* locus could be located on T22B4. The initial mapping results summarised in Table 3.3 have therefore been confirmed by the complementation analysis (Fig. 3.13 and 3.14), which has demonstrated that the *CIR1* locus is situated on the annotation unit T22B4.

The 46 037 bp region on T22B4 contains eight annotated genes according to TAIR and some details of these candidate genes are summarised in Table 3.6.

Table 3.6 Details of the eight *CIR1* candidate genes in 46 037 bp region on chromosome IV

Locus	*Position on chromosome IV*[a]	*Gene model*	*Description*
At4g11100	6 768 610 – 6 770 180	At4g11100.1	Similar to unknown protein
At4g11100	6 768 709 – 6 770 155	At4g11100.2	Similar to unknown protein
At4g11110	6 771 601 – 6 777 221	*SPA2*	Member of SPA (suppressor of *phyA-105*) protein family
At4g11120	6 777 798 – 6 780 162	At4g11120.1	Putative translation elongation factor Ts
At4g11130	6 780 518 - 6 784 436	*RDR2*	RNA-dependent RNA polymerase
At4g11140	6 794 813 - 6 795 789	*CRF1*	Cytokinin response factor
At4g11150	6 799 958 - 6 801 927	*TUFF*	Vacuolar H^+-ATPases subunit E isoform 1 (*VHA-E1*)
At4g11160	6 803 615 - 6 806 871	At4g11160.1	Translation initiation factor IF-2-like protein
At4g11170	6 811 123 - 6 817 126	At4g11170.1	Putative disease resistance protein of TIR-NBS-LRR class

[a] Position based on AGI map (The Arabidopsis Genome Initiative, 2000) in bp available from TAIR.

Due to time constraints, additional experiments to determine which of these candidate genes are *CIR1* could not be performed for inclusion in this thesis, however the search for *CIR1* continues in our laboratory. To provide possible insight into which gene acts as *CIR1*, the expression of the candidate genes in a *cir1* background and the response of these genes to specific pathogen and hormone treatments, was investigated.

3.6.1 Expression analysis of candidate genes

Affymetrix DNA microarray experiments has been performed to identify differences in gene expression in *cir1* compared to wild-type *Luc2* plants (S. L. Murray, University of Cape Town). To determine if any of the eight candidate genes showed altered expression in the *cir1* mutant background, microarray data sets were analysed and the results (kindly provided by S. L. Murray) are presented in Table 3.7.

Only a 2-fold or more change in expression, presented by $\log_2$ values greater than +1 or less than –1, was considered to be significant. Of the eight genes, only At4g11120 had a significantly positive $\log_2$ ratio whereas At4g11130 (*RDR2*) and At4g11140 (*CRF1*) had $\log_2$ ratio's less than -1 (Table 3.7). Although these $\log_2$ ratio's suggest that these genes were up or down regulated respectively, all three genes had very low signal intensities in all *Luc2* and *cir1* samples (Table 3.7). The expression of genes at such low levels might be influenced by

background noise and can lead to the exaggeration of log_2 ratio's. Furthermore, the inconsistencies in the significance of the log_2 ratio's across the two experiments are probably due to the low signal intensities of each gene (Table 3.7) and therefore the changes in expression of At4g11120, At4g11130 (*RDR2*) and At4g11140 (*CRF1*) were regarded as inconclusive. No significant changes in expression of the remaining five genes could be detected in *cir1* in comparison to *Luc2* (Table 3.7). Therefore, none of the eight candidate genes displayed a drastic change in expression in a *cir1* background.

Table 3.7 Expression of eight candidate genes in *cir1* based on Affymetrix microarray experiments

The signal intensities for *Luc2* and *cir1* samples in both experiments are shown. The expression ratio represents the expression of the gene in *cir1* relative to *Luc2*. A negative log_2 ratio value indicates down regulation whereas a positive value is indicative of up regulation of a given gene in *cir1*.

Gene name	*Luc2 signal*[a]	*cir1 signal*[a]	*Expression ratio*[a]	*Log_2 ratio*[a]	*Luc2 signal*[b]	*cir1 signal*[b]	*Expression ratio*[b]	*Log_2 ratio*[b]
At4g11100	58.5	71.8	1.23	+0.3	83.3	50.8	0.61	-0.7
At4g11110	15.5	10.9	0.70	-0.5	67.0	90.6	1.35	+0.4
At4g11120	15.0	30.6	2.04	+1.0	44.8	53.0	1.18	+0.2
At4g11130	9.4	0.7	0.07	-3.7	16.4	15.2	0.93	-0.1
At4g11140	32.7	26.3	0.80	-0.3	23.6	10.1	0.43	-1.2
At4g11150	1091.1	986.8	0.90	-0.1	1653.4	1363.7	0.82	-0.3
At4g11160	31.0	24.3	0.78	-0.4	48.7	62.1	1.28	+0.4
At4g11170	0.6	0.6	1.00	0.0	28.1	15.9	0.57	-0.8

[a] Results from initial microarray experiments using an Affymetrix 8K Arabidopsis gene chips.
[b] Results from subsequent microarray experiments using an Affymetrix 22K Arabidopsis gene chips.

Although none of the genes showed altered expression in *cir1*, it does not necessarily eliminate them as candidate genes of *CIR1*. A single base pair change in a gene might not affect its expression levels but could result in an amino acid change, altering the properties of the protein or resulting in a truncated protein which is unlikely to retain any activity. Additionally, the variation between the two sets of microarray experiments might obscure any significant changes therefore additional gene expression analysis experiments based on Northern Blot or quantitative real-time PCR are required to provide conclusive results.

A bioinformatics approach was utilised to determine if any of the eight candidate genes were pathogen- and/or hormone-responsive. This approach was facilitated by the microarray database, Genevestigator (https://www.genevestigator.ethz.ch/at/; Zimmermann et al., 2004), which allows for the identification of conditions affecting the expression of specific genes. The selected Genevestigator dataset was based on microarray experiments conducted on wild-type plants with or without specific pathogen or hormone treatments and consisted of 1 860 experiments. Specifically, these experiments consisted Affymetrix DNA microarray

data comprising results for approximately 22 000 genes of the Arabidopsis genome and were sourced from the Functional Genomics Center Zurich (FGCZ) and the Gruissem laboratory as well as from other consortia such as ArrayExpress, AtGenExpress, TAIR, the European Arabidopsis Stock Centre (NASC) and the Gene Expression Omnibus (GEO).

With the help of Genevestigator, all selected microarray experiments were examined for changes in expression of the candidate genes before and after certain treatments. In this case, the gene expression data consists of combined results across all time points for a specific treatment. The following results therefore represent differences in gene expression in response to a treatment irrespective of time points and it is possible that transient gene expression might go undetected. The treatments included the infection of plants with following pathogens: *A. tumefaciens*, *Botrytis cinerea*, *Erysiphe cichoracearum*, *G. orontii*, *Phytophthora infestans* and *Pst* DC3000 or the treatment of plants with the following hormones: ABA (abscisic acid), ACC, ET, GA (gibberellic acid), IAA (indole-3-acetic acid), MeJA and SA. This is a relatively broad approach to identify differential gene expression and once the potential candidate gene has been identified, a more detailed analysis of its expression patterns could be undertaken. Genevestigator provides $\log_2$ values of the mean of signal intensities of your gene of interest in both control and treated samples across all experiments and by evaluating the $\log_2$ ratio values, treatments that cause changes in gene expression could be identified. Only treatments which resulted in a 2-fold or more induction or reduction of gene expression, presented by a $\log_2$ ratio value of above +1 or below -1, were analysed further. At4g11130 (*RDR2*) expression in response to selected treatments is presented in Fig. 3.15 which has been included as a representative graph for all eight candidate genes.

None of the treatments resulted in $\log_2$ ratio values of more than +1 or less than -1 signifying that At4g11130 (*RDR2*) expression did not display a 2-fold or more change after any of the treatments (Fig. 3.15). This suggests that At4g11130 (*RDR2*) expression is not significantly responsive to any of the selected pathogen or hormone treatments. None of the seven remaining candidate genes showed significant changes in expression after any of the listed treatments (results not shown) with the exception of two genes in response to the *A. tumefaciens* treatment. At4g11100 was down regulated as indicated by a $\log_2$ ratio value of -1.1 (results not shown) and At4g11170 was up regulated displaying a $\log_2$ ratio value of +1.3 (results not shown) in response to *A. tumefaciens* infection. The regulation of At4g11100 and At4g11170 was in response to only one pathogen and none of the other pathogen infections resulted in a considerable change in expression of these gene. Therefore in general, none of the eight candidate genes displayed drastic changes in expression after the selected pathogen infections or hormone treatments according to the data available from Genevestigator.

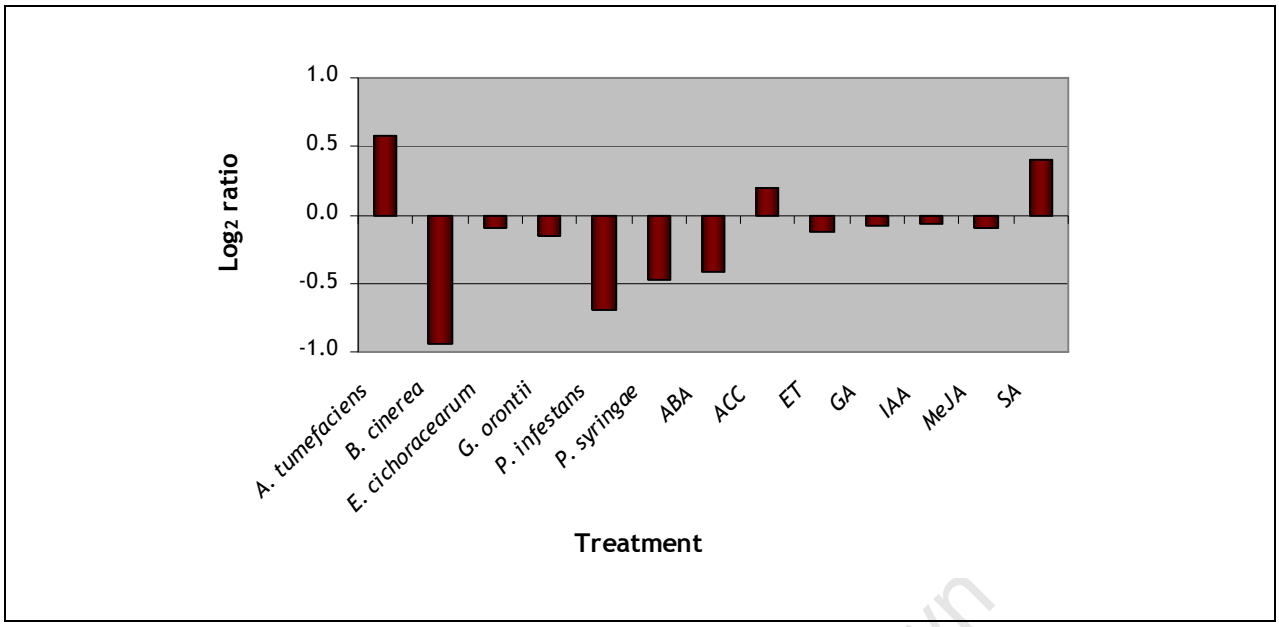

Figure 3.15. At4g11130 (*RDR2*) expression in response to pathogen or hormone treatments available from Genevestigator.

The expression of At4g11130 (*RDR2*) in response to certain treatments were analysed with Genevestigator. Treatments included the infection of plants with the pathogens *Agrobacterium tumefaciens*, *Botrytis cinerea*, *Erysiphe cichoracearum*, *Golovinomyces orontii*, *Phytophthora infestans* and *Pseudomonas syringae* pv. *tomato* DC3000 or the treating of plants with selected hormones including ABA (abscisic acid), ACC (1-aminocyclopropane-1-carboxylate), ET (ethylene), GA (gibberellic acid), IAA (indole-3-acetic acid), MeJA (methyl jasmonate) and SA (salicylic acid). Bars represent the $\log_2$ ratio of At4g11130 (*RDR2*) expression where the $\log_2$ ratio is defined as the change in gene expression after a treatment in comparison to the relevant untreated control samples. Positive $\log_2$ ratio values indicate up regulation and negative values represent down regulation of the gene.

While it seems that none of the candidate genes are transcriptionally regulated in a way that suggests they may be *CIR1*, it is perfectly possible that *CIR1* may be regulated by other means. Once *CIR1* has been identified, further investigations into its regulatory mechanisms should provide more insight.

3.7 Discussion

3.7.1 Selection of mapping population based on high luciferase activity

Ever since the sequencing of the Arabidopsis genome and the subsequent increase in available genetic markers, the amount of effort required for the map-based cloning of a gene has decreased over recent years. Although it is now believed to be a relatively straight-forward and time-efficient process, complications can occur resulting in a much more complex and time-consuming procedure. It becomes complicated to map certain mutations

when a phenotype is caused by multiple mutations or when a trait is influenced by more than one locus (Lukowitz et al., 2000; Jander et al., 2002) as in the case of flowering time, trichome density, circadian rhythms and secondary metabolism (Alonso-Blanco and Koornneef, 2000). Epigenetic mutations, where inherited changes in the function and expression of a given gene are not due to DNA sequence modifications, as well as the lack of recombination events in certain regions of a chromosome are other possible problems that could be experienced during mapping projects (Lukowitz et al., 2000). However, the most common type of complications involve the erroneous scoring of the mutant phenotype thereby contaminating the mapping population with false positives which could result in irregularities in the mapping data (Lukowitz et al., 2000).

Chemical mutagenesis performed with EMS for example, can result in loss-of-function mutations but it can also result in an allelic series producing weak, intermediate or strong mutated alleles of particular gene (Bowman et al., 1991). Weak mutant alleles often give rise to phenotypes that are not fully penetrant and therefore only some mutant plants will display a phenotype. Furthermore, mutant phenotypes might only occur in certain tissues or during specific developmental stages. Additionally, chemically induced mutations can lead to conditional phenotypes which are sensitive to variation of environmental conditions in the growth chamber (Østergaard and Yanofsky, 2004). The scoring of these phenotypes is difficult and can often result in the incorrect selection of non-mutant plants as part of the mapping population. Inconsistencies in the mapping data based on these plants are unavoidable and therefore it is best to re-examine the phenotypes of the F_2 plants in the F_3 progeny (Lukowitz et al., 2000). This additional step can prove to be very time-consuming resulting in a mapping process that is more lengthy than anticipated.

The selection of homozygous *cir1* plants based on constitutively high luciferase levels proved not to be a robust phenotype since heterozygous *cir1* or wild-type plants were often incorrectly scored as mutant plants during the selection of the mapping population (section 3.2.1) and in the direct screen for recombination events (section 3.5.1). A possible contributing factor to the irregularity of the *cir1* phenotype is the promoter selected for the *PR-1::LUC* reporter construct (Murray et al., 2002). The expression of *PR-1* has be shown to be induced in response to pathogen infections (Thatcher et al., 2005) and to the feeding of the silverleaf whitefly, a common pest of Arabidopsis (Kempema et al., 2007). Therefore, the *PR-1* promoter might have been activated by sub-optimal growth conditions leading to high luciferase activity levels in heterozygous *cir1* or non-mutant *Luc2* plants.

An additional factor that could impact on the *cir1* phenotype is the age-dependent increase in *PR-1* expression. During the time-course experiment in which the optimal age for the testing of luciferase activity of homozygous *cir1* plants was determined, a dramatic

increase of luciferase activity levels were observed between 4- and 5-week-old *Luc2* plants (Fig. 3.1). The high luciferase activity levels of the 5-week-old *Luc2* plants are probably due to the bolting of plants affecting the activity of the *PR-1* promoter of the reporter construct. *PR-1* expression has been observed in healthy leaves of bolting plants, increasing as the subsequent stages of senescence occurred in the leaves (Morris et al., 2000). Although this trend suggests that it might have been more optimal to perform the luciferase assays on plants older than 4-weeks, the background luciferase activity levels in the *Luc2* plants also increased with age, rendering *Luc2* plants indistinguishable from *cir1* plants at 5-weeks (Fig. 3.1). The use of older plants in the luciferase assays would have been just as variable and would probably also have resulted in the selection of false positives.

Although the abovementioned factors could have influenced the luciferase activity levels of *cir1*, the greatest effect on the *cir1* phenotype was probably caused by the introduction of the L*er* background when *cir1* was crossed onto L*er* for the mapping experiments. An investigation into the effect of the L*er* background on luciferase activity levels established that the levels were reduced by the L*er* background and possibly by the heterozygous state of *PR-1::LUC* transgene (Fig. 3.3). Initially it was believed that the effect of the L*er* background could result in abnormally high luciferase activity levels in heterozygous *cir1* plants, but instead our results indicated that this factor could have a reducing effect thereby obstructing the differentiation between homozygous and heterozygous *cir1* plants or wild-type plants. The effect of the L*er* background therefore played a role in the erroneous selection of false positive plants as well as in the rejection of some homozygous *cir1* plants, which resulted in a mapping population of only 293 instead of the expected 349 plants. The observed lower luciferase activity levels of the F_2 progeny mapping population plants compared to the homozygous *cir1* control plants (Fig. 3.2) are probably also due to the effect of the aforementioned factor. Other examples of L*er* suppressing the activity of transgenes could not be found, however it has been established that many expression polymorphisms between different Arabidopsis ecotypes exist (Kliebenstein et al., 2006) which could result in altered levels of gene expression between ecotypes.

While the re-screening of the mapping population in the F_3 progeny was time-consuming and prolonged the mapping process, it was necessary to confirm the phenotype of the mapping plants. Only 36 plants were selected for the fine-mapping experiments based on the strict selection criteria and although it was a small population, it was strongly believed that those plants were homozygous *cir1*.

3.7.2 Mapping of *cir1* on chromosome IV

Initial mapping results identified a 309.10 kb region on chromosome IV that contains the *CIR1* locus (Table 3.3). Interestingly, of the 36 mapping plants tested, four had multiple recombination events between markers nga8 and g4539 (Table 3.3) suggesting that this

region may contain recombination "hot spots". Studies have shown that crossover events are not evenly dispersed (Peters et al., 2003) and that regions with high rates of recombination, known as "hot spots", alternate with regions of low rates along the chromosome (Mézard, 2006). Recently it has been shown that chromosome IV contains eighteen recombination "hot spots" of which eight are clustered in the region from 5 to 8 Mb on the lower arm of the chromosome (Drouaud et al., 2006). Of the nine recombination events that occurred within the four mapping plants, seven were located in the abovementioned 3 Mb region (Table 3.3) and therefore the occurrence of these multiple recombination events could be contributed to recombination "hot spots".

In an attempt to identify the exact position of the *CIR1* locus, a direct screen for plants which had additional recombination events within the 309.10 kb region to those present in plant 168 (Fig. 3.4 and 3.5), was conducted. However, this approach proved to be unsuccessful. An additional approach to identify *CIR1* was to search for shared phenotypes between *cir1* and *edr5* (Fig. 3.6 to 3.10) to ultimately establish if *cir1* was allelic to *edr5*. The majority of phenotypic tests proved unsuitable as allelism tests since either *cir1* displayed different phenotypes to *edr5* (Fig. 3.7B and 3.9) or the phenotypes of *cir1* and *edr5* were indistinguishable from wild-type plants (Fig. 3.8). An alternative and probably better phenotypic test would have been to evaluate the disease resistance of *cir1*, *edr5* and F_1 progeny plants. The results based on the luciferase assays suggested possible allelism between the two genes (Fig. 3.6 and 3.7A) but since the other tests were inconclusive, a sequence and complementation analysis approach was pursued to conclusively determine if *cir1* was allelic to *edr5* (Fig. 3.10 and 3.11). In contrast to the results from the luciferase assays (Fig. 3.6 and 3.7A), the sequence analysis of *CYP83A1* in a *cir1* background implied that *cir1* was not allelic to *edr5* (Fig. 3.10). Furthermore, through complementation analysis it was established that *EDR5* did not complement the *cir1* mutation (Fig. 3.11).

Since the aforementioned attempts to fine-map *cir1* were unsuccessful, the complementation analysis approach proved to be paramount in reducing the size of the *CIR1*-containing region. Initially six overlapping clones were selected for complementation purposes, however the JAtY55L22 and JAtY73H06 clones proved to be problematic. The JAtY55L22 clone was excluded from the complementation experiments as it could not be confirmed that it contained the correct genomic insert. Since *E. coli* cells transformed with JAtY55L22 could be successfully cultured on selective media, it is likely that the cells either contained an empty vector or that the clone contained a different genomic insert than indicated on the ATIDB's Genome Browser. Alternatively, it is also possible that the clone harboured the correct genomic insert but that a deletion, an insertion or a sequence re-arrangement hampered the successful amplification of the relevant products. Furthermore,

no *cir1* plants transformed with the JAtY73H06 clone could be identified, signifying that transformation with this clone was unsuccessful. This result is not unanticipated since according to the GetCID website, poor transformation rates have been reported when using JAtY clones in transformation experiments. The exact reason for this is yet unclear, although it has been suggested that chromosomal integration of the TAC vector in the *Agrobacterium* or the internal rearrangement or deletion of the TAC could render the vector incapable of transforming plants.

The preliminary results from both the luciferase assays (Fig. 3.13) and the *Pst* DC3000 infection assays (Fig. 3.14) of *cir1* plants transformed with the remaining four clones, identified JAtY68P03 as a complementing clone. Although the results regarding the JAtY63F16 clone was less convincing and should be confirmed with more independently transformed lines, it suggested an alternative theory that the JAtY63F16 clone also complemented the *cir1* mutation. To avoid the omitting of possible candidate genes, both the overlapping region between the JAtY63F16 and JAtY68P03 clones as well as the unique section of the JAtY68P03 clone were investigated for *CIR1* candidate genes.

3.7.3 *CIR1* candidate genes

To understand the possible role of *CIR1*, it is necessary to regard the characteristics of *cir1* in more detail. *Cir1* constitutively expresses the SA-dependent genes *PR-1*, *PR-2* and *PR-5* (Uknes et al., 1992) as well the JA/ET-dependent *PDF1.2* gene (Penninckx et al., 1996) (Murray et al., 2002). However, in our laboratory it has been demonstrated that *cir1* does not constantly express the endogenous *PR-1* gene (Fig. 3.7B). C*ir1* also displays constitutive expression of *GST1* (Murray et al., 2002), a gene which is activated in response to reactive-oxygen intermediate accumulation produced during the oxidative burst associated with the HR (Grant et al., 2000a). Furthermore, the *cir1* mutant does not display spontaneous lesion development and therefore it operates downstream of HR activation (Murray et al., 2002). It was established that *cir1* is resistant to the bacterial pathogen *Pst* DC3000 and the virulent oomycete *H. parasitica* Noco2 (Murray et al., 2002) but it is not more resistant to the necrotrophic pathogen, *B. cinerea* (Murray et al., 2005). The *cir1*-mediated resistance against both biotrophic pathogens is NPR1-dependent, whereas only the resistance to *Pst* DC3000 requires JAR1 (jasmonate resistant 1) and EIN2 (ethylene insensitive 2) (Murray et al., 2002). Based on the expression of the mentioned defence-related genes and the disease-resistance phenotype, it was suggested that the *cir1* mutation resulted in the activation of multiple defence signalling pathways and that *CIR1* may act as a negative regulator of disease resistance functioning upstream of SA, JA and ET accumulation (Murray et al., 2002).

Since none of the candidate genes showed altered expression in *cir1* (Table 3.7) or differential expression in response to pathogen and/or hormone treatments (Fig. 3.15), only genes that could have a potential role in the signal transduction network and/or in pathogen

defence responses have been considered as likely *CIR1* candidate genes. No information on the involvement of At4g11100, At4g11110 and At4g11120 in pathogen defence responses or in the plant signalling network could be obtained during the preparation of this manuscript and therefore these genes have been excluded from the subsequent discussion. More detail on the remaining annotated genes located within the overlap of the JAtY63F16 and JAtY68P03 clones as well as the unique region of JAtY68P03 will be discussed in the following sections.

3.7.3.1 At4g11130: RNA-dependent RNA polymerase (*RDR2*)

RNA silencing provides a system of gene regulation where genes are controlled through the degradation of RNA, translational inhibition and chromatin modification (Wang and Metzlaff, 2005). These processes are facilitated by small RNAs, consisting of microRNAs and small interfering RNAs (siRNAs), of approximately 21 to 24 nucleotides produced by most eukaryotes (Lu et al., 2006).

At4g11130 or *RDR2* encodes a RNA-dependent RNA polymerase which together with the Dicer-like (DCL) protein, DCL3, has been identified as a component of the endogenous siRNA generating pathway (Xie et al., 2004). The resulting chromatin-associated siRNAs are primarily of the large-size class consisting of approximately 24 nucleotides that function through effector complexes to establish chromatin modification events (Xie et al., 2004).

An example of an endogenous siRNA that has a function in Arabidopsis disease resistance against a bacterial pathogen was reported of late (Katiyar-Agarwal et al., 2006). The biogenesis of the endogenous siRNA was specifically induced by *Pst* DC3000 possessing the effector AvrRpt2 (Katiyar-Agarwal et al., 2006). The resultant siRNA down-regulated a putative negative regulator of the *RPS2* resistance pathway and thereby contributed positively to *RPS2*-mediated disease resistance in Arabidopsis (Katiyar-Agarwal et al., 2006). However, *RDR2* expression was not responsive to virulent *Pst* DC3000 infections (Fig. 3.15) and *rdr2-1* mutant plants displayed a wild-type phenotype after infection with virulent *Pst* DC3000 (Agorio and Vera, 2007). These findings suggest that RDR2 is not essential in mounting a defence response (Agorio and Vera, 2007) and therefore it is most likely not involved in PTI, making it an improbable *CIR1* candidate.

The extent to which the RDR2-DCL3 pathway regulates gene expression is not completely understood (Xie et al., 2004; Kasschau et al., 2007). The absence of the RDR2-DCL3 pathway could result in the activation of silent chromatin but it would depend on the extent to which the transcriptionally silent loci requires the continued formation of siRNAs (Kasschau et al., 2007). However, the effect of the loss of RDR2-DCL3 pathway, and the subsequent reduction in siRNAs, resulted in developmental defects in plants (Gasciolli et al., 2005), which has not been the case in *cir1* mutant plants.

3.7.3.2 At4g11140: Cytokinin response factor (*CRF1*)

At4g11140 encodes a member of Group VI of the ethylene response factor (ERF) subfamily of the AP2/ERF family of transcription factors (Nakano et al., 2006). The ERF transcription factors regulate genes involved in disease resistance by binding to the GCC box, an element found in the promoters of some pathogenesis-related and JA/ET-induced genes (Gutterson and Reuber, 2004), acting either as activators or repressors of the target genes (Fujimoto et al., 2000; Nakano et al., 2006). Additionally, the expression of several ERF genes are regulated by plant hormones such as SA, JA and ET as well as by pathogen challenge (Cheong et al., 2002; Onate-Sanchez and Singh, 2002; Brown et al., 2003; Lorenzo et al., 2003). However, based on the results from Genevestigator, expression of At4g11140 was not significantly regulated by either pathogen infections or hormone treatments (see representative Fig. 3.15).

Of late it has been demonstrated that At4g11140 shares sequence similarity with two cytokinin up regulated genes and it has been designated as cytokinin response factor 1 (*CRF1*) (Rashotte et al., 2006). The CRF proteins accumulate in the nucleus of the plant where they mediate the transcriptional response to cytokinin, a plant hormone that has a role in many facets of plant growth and development (Brenner et al., 2005). Loss-of-function mutations revealed that CRFs have a redundant function in the regulation of embryo-, cotyledon- and leaf-development (Rashotte et al., 2006). Nevertheless, based on the phenotypic differences observed between the *crf* mutants and the cytokinin receptor mutants (Higuchi et al., 2004; Nishimura et al., 2004), CRFs may have an additional role in other signalling or developmental pathways (Rashotte et al., 2006).

It is hard to correlate *CIR1*, a negative regulator of the disease resistance signalling network to *CRF1*, a mediator of cytokinin-regulated transcriptional responses, but ET could act as the link. It has previously been shown that cytokinin acts through ET, that it regulates ET synthesis (Cary et al., 1995) and that many genes related to ET signalling were up or down regulated by cytokinin, whereas SA- and JA-related genes were less affected (Brenner et al., 2005). The regulatory links between cytokinin and ET suggests cross-talk between these two pathways.

Cross-talk, which is often still poorly understood, could be accomplished if pathways converge by making use of the same signalling components or transcription factors, or if transporters or metabolic enzymes are regulated in such a way that it subsequently affects the concentration of other signalling molecules (Brenner et al., 2005). The defence responses of *cir1* are based on the SA, JA and ET pathways (Murray et al., 2002) which are known to act together in a complex network through regulatory interactions and cross-talk (Kunkel and Brooks, 2002). Hence, the possibility of cross-talk between the plant disease

resistance signalling network and additional plant signalling pathways, such as the cytokinin pathway, can not be excluded.

3.7.3.3 At4g11150: Vacuolar H^+-ATPases subunit E isoform 1 (*VHA-E1*/*TUFF*)

Plants need to be able to adapt to environmental stresses such as excess salt or the presence of toxic metals in order to survive and through the up or down regulation of the activities of transporters, or proton pumps, they respond and adapt to the changes in the environment (Sze et al., 2002). The vacuolar H^+-ATPase (V-ATPase) is the most common proton pump located in the endomembrane compartments of all eukaryotic cells (Sze et al., 2002; Dettmer et al., 2005; Dettmer et al., 2006). V-ATPases are multi-subunit enzyme complexes composed of a membrane-bound V_0 domain involved in H^+ transport and consisting of subunits a-e, and the peripherally associated ATP-hydrolysing V_1 domain comprised of subunits A-H (Nishi and Forgac, 2002; Nelson, 2003).

Subunit E of the V_1 domain (also known as VHA-E) is encoded by three genes but for our purposes the focus will only be on the Arabidopsis *TUFF* gene (At4g11150), encoding VHA-E isoform 1 (*VHA-E1*) (Strompen et al., 2005). A decrease in At4g11150 protein has been shown during an AvrRpm1/RPM1-mediated defence response (Jones et al., 2006). The Arabidopsis resistance gene, *RPM1*, recognises both the *Pst* DC3000 effectors AvrRpm1 and AvrB (Grant et al., 1995), triggering a strong HR and preventing further pathogen colonization. Although the exact reason for the decrease in the TUFF protein is unknown, it could either be directly or indirectly modified by AvrRpm1 or the decrease could be caused by processes downstream of the activated RPM1 (Jones et al., 2006). Interestingly, based on results from Genevestigator, At4g11150 expression was unaffected by virulent *Pst* DC3000 infection (see representative Fig. 3.15).

Two different *tuff* mutant alleles, both disrupting the *VHA-E1* gene and lacking the VHA-E1 protein, display the same phenotype of embryo lethality. A third embryo-lethal *tuff* mutant allele, carrying another T-DNA insertion, has also been identified (Tzafrir et al., 2004). It is believed that the *TUFF* gene has an important task in upholding a functional secretory system required for normal embryogenesis and ultimately for normal plant development (Strompen et al., 2005). All three *tuff* mutant alleles were embryo-lethal whereas *cir1* has never displayed any significant morphological changes compared to wild-type plants (Murray et al., 2002). However, the *tuff* alleles are all null mutants while *cir1* may not be, which could explain the different phenotypes of the two mutants regarding embryo lethality.

3.7.3.4 At4g11160: Translation initiation factor IF-2-like protein

Very little information is currently available on At4g11160. This gene has not been cloned but it has been assigned a putative function as a translation initiation factor (details

available from TAIR). It is therefore involved in the initiation of the ribosome-mediated translation process where the information in the mRNA is utilised to determine the amino acid sequence of the associated protein (Dever, 2002).

The predicted function of At4g11160 is based on its protein domain similarity to the prokaryotic translation initiation factor IF-2. These two proteins share four protein domains: i) a protein synthesis factor with GTPase and GTP-binding activity; ii) a translation elongation factor EF-Tu/EF-1A domain 2 also involved with GTP binding; iii) a small GTP-binding protein domain and iv) the highly variable N-terminal domain of translation initiation factor IF-2 (details available from TAIR).

eIF5B, the plant ortholog of IF-2, also contains a GTP-binding domain and shares extensive amino acid sequence similarity and a conserved function with IF-2 (Pestova et al., 2000). Alternative roles have been assigned to some plant translation initiation factors, such as eIF3 which associate with the COP9 signalosome (Karniol et al., 1998). The COP9 signalosome is a protein complex involved in the regulation of protein ubiquitination and turnover in many plant developmental and physiological conditions such as hormone signalling, pathogen defence and light-regulated development (von Arnim, 2003). In addition to its role during translation initiation, it has been suggested that eIF3 may act as a key intracellular connection between various pathways to ultimately regulate translation (Browning, 2004).

Thus far, no information relating to the possible function of the At4g11160 protein in the Arabidopsis disease resistance signalling network could be obtained and therefore any possible roles of this protein beyond translation initiation still need to be elucidated.

3.7.3.5 At4g11170: Putative disease resistance protein of TIR-NBS-LRR class

One of the branches of the plant immune system is known as ETI which relies on the interaction between pathogen effector molecules and corresponding host R proteins (Jones and Dangl, 2006). The largest class of R proteins have a NBS domain and LRR domains (Meyers et al., 2003) and these NBS-LRR plant R proteins are further divided based on the presence of either a CC or a TIR domain at the N-terminal end (Pan et al., 2000; Dangl and Jones, 2001).

At4g11170 has not been cloned but computational analysis of its predicted protein domains has revealed that it contains a N-terminal TIR domain, a conserved NBS domain and the C-terminal LRR domains, strongly suggesting that this gene could encode an R protein of the TIR-NBS-LRR class. It is unclear how an R protein would function as a negative regulator of defence, as predicted for CIR1. However, it is intriguing that *cir1* shares some phenotypic characteristics with plants carrying an *R* gene mutation.

Examples exist where mutations in TIR-NBS-LRR-type *R* genes lead to the constitutive expression of several defence-related genes and mutant plants displaying an enhanced resistance phenotype (Li et al., 2001; Shirano et al., 2002; Zhang et al., 2003b). *Snc1*

(suppressor of *npr1-1*, constitutive 1), is an *R* gene mutant which constitutively expresses *PR-1* and *PR-2*, and displays resistance to *Psm* ES4326 and *H. parasitica* Noco2 infections (Li et al., 2001). The *snc1* point mutation renders the *R* gene constitutively active even in the absence of pathogen interactions (Zhang et al., 2003b). Similar to *cir1*, *snc1* mutant plants also do not show spontaneous lesion development, but they differ from *cir1* in that they are smaller than wild-type plants (Murray et al., 2002; Zhang et al., 2003b). Several reports have suggested that NBS-LRR proteins are under negative regulation (reviewed by Rathjen and Moffetty, 2003) and it is also the case with wild-type SNC1 (Zhang et al., 2003b). SNC1 is under negative regulation by interacting with its negative regulator BON1 (bonzai 1) (Yang and Hua, 2004). By mutating the *SNC1* gene, the binding affinity between the snc1 protein and the negative regulator is reduced, resulting in the subsequent activation of the downstream defence pathways (Zhang et al., 2003b). However, *snc1* is a dominant gain-of-function mutant whereas *cir1* is recessive and hence likely to be a loss-of-function mutation.

The activation of R proteins results in a plant defence network, comprised of cross-talking SA, JA and ET pathways that maintain a balance between the accumulation of SA and JA/ET (Glazebrook, 2005). Interestingly, it is believed that CIR1 acts upstream of SA, JA and ET accumulation (Murray et al., 2002) where it regulates these signalling molecules in its distinct defence responses to different microbial pathogens.

3.7.4 Future work

The best approach to identify which of the candidate genes are *CIR1*, involves complementation studies with the individual wild-type candidate genes. Similar to the previously described complementation analysis, transformed *cir1* plants should be tested for a loss of constitutively high luciferase activity and the loss of *cir1* resistance to *Pst* DC3000. The rescuing of the *cir1* phenotype with a wild-type candidate gene would provide conclusive proof that the *CIR1* has been identified. To identify the exact nucleotide base pair change responsible for the *cir1* mutation, it would be necessary to sequence the complementing candidate gene in the *cir1* background and by comparing the sequences of the gene in *cir1* with the wild-type Col-0 sequence, the nature of the mutation could be determined. It would be more informative to initially sequence the cDNA of *cir1*, which only incorporates the coding regions of the genes, but if no mutations are identified, sequencing of *cir1* genomic DNA should be considered.

Additionally, T-DNA insertion lines which each knock out one of the candidate genes could be analysed to determine if these mutants display the same phenotype as *cir1*. As none of the T-DNA mutant lines contain the luciferase gene present in *cir1*, the use of luciferase assays as a phenotypic test would be futile. Therefore, *Pst* DC3000 infection assays must be performed to determine if any of the mutant or knock-out lines resemble the resistance phenotype of *cir1*. However, based on the prospect that *cir1* might not be a null mutant, it

is possible that the knock-out lines may display a different disease resistance phenotype as *cir1*, hence the principal approach to identify *CIR1* should be complementation analysis with the wild-type candidate genes.

Alternatively, *cir1* could be crossed with a homozygous knock-out line and allelism tests based on luciferase activity assays and *Pst* DC3000 infection assays, could be performed. In this case, it is necessary to first establish that the knock-out line has the same phenotypes as *cir1* before any allelism tests should be conducted. Demonstrating that a specific candidate gene is allelic to *cir1*, would be sufficient proof that *CIR1* had been identified.

In summary, the aim of this chapter was to map the *cir1* mutation located on the lower arm of chromosome IV to ultimately identify the *CIR1* gene. Mapping experiments identified the flanking markers of *cir1* and reduced the *cir1*-containing region to 309.10 kb. A subsequent complementation analysis approach identified the *CIR1* gene to be one of eight candidate genes.

Chapter 4: Elucidating the mechanisms of *cir1* resistance

4.1 Introduction

Induced plant defences, which contribute to plant innate immunity, can be broadly divided into two different plant immune systems. The first and the focus of this chapter, termed PTI, contribute to PAMP-triggered, non-host as well as basal resistance responses (Jones and Dangl, 2006). PAMP-triggered defences involve the recognition of various PAMPs by PRRs (Zipfel and Felix, 2005), and this recognition leads to the activation of a series of inducible defence mechanisms. It is thought that the induction of PAMP-triggered defences, in combination with pre-formed barriers, contribute to non-host resistance (Nürnberger and Lipka, 2005). Non-host resistance renders an entire plant species resistant to infection by a specific pathogen and thereby the pathogen, termed a non-host pathogen, is unable to cause disease (Mysore and Ryu, 2004). Basal defences are activated in response to virulent pathogens on susceptible hosts (Jones and Dangl, 2006), acting as an important protective layer. Basal resistance limits the spread of pathogens to a certain extent and many Arabidopsis mutants, especially the "enhanced disease susceptibility" mutants, are compromised in basal defences to virulent pathogens, signifying that an array of genes are involved in the maintenance of this defence system (Hammond-Kosack and Parker, 2003). The second system is mediated by *R* genes encoding proteins that recognize the presence of pathogen effectors molecules, resulting in the activation of ETI (Jones and Dangl, 2006). ETI leads to a HR preventing further pathogen colonisation and ultimately renders the plant resistant to disease (Dangl and Jones, 2001). This system is also believed to prime uninfected tissues of the plant against subsequent pathogen attack in a process called SAR (Dong, 2004). However, recently it has been shown that PAMPs also contribute to the induction of SAR (Mishina and Zeier, 2007) highlighting the fact that basal resistance, which relies on PTI, and ETI have overlapping components involved in downstream signalling responses.

Several important role players in PTI have been characterized and one of these is COI1. The *coi1* (Feys et al., 1994) mutation defines a gene that functions in the JA signalling pathway necessary for defence against pathogens or insects as well as for pollen development. It also has a high impact on male fertility and root development (Xie et al., 1998). Furthermore, the *coi1* mutant is more susceptible to the fungal pathogens *Alternaria brassicicola* and *Botrytis cinerea* but shows decreased susceptibility to *Hyaloperonospora parasitica* (Thomma et al., 1998) and virulent *Pseudomonas syringae* pathogens (Kloek et al., 2001; Ellis et al., 2002). The resistance of *coi1* mutant plants to virulent bacterial pathogens demonstrate an induction of basal defences suggesting that *COI1* has a role in the PAMP-triggered immune system.

Two additional key players in Arabidopsis defence include EDS1 and its interacting partner PAD4 as discussed in Chapter 1. The "enhanced disease susceptibility" phenotypes of *eds1* and *pad4* mutant plants infected with virulent pathogens suggest that the basal defence, and therefore PTI, of these mutants is severely compromised. Therefore, it is believed that Arabidopsis basal resistance is wielded by the combined activities of EDS1 and PAD4 and it was subsequently established that both *EDS1* and *PAD4* are required for the accumulation of SA and *PR-1* expression in response to virulent *P. syringae* infections (Feys et al., 2001). Furthermore, the expression of both *EDS1* and *PAD4* is up regulated upon challenge with virulent *Pseudomonas syringae* pv. *tomato* DC3000 (*Pst* DC3000) (Feys et al., 2001). Despite their similarities, the functions of EDS1 and PAD4 in basal resistance are not redundant since mutations in either gene results in an enhanced susceptibility phenotype to virulent pathogens (Aarts et al., 1998; Zhou et al., 1998).

Another role player in PTI is the *cir1* mutant which displays enhanced basal defence phenotypes to virulent pathogens. To reiterate, the increased resistance of *cir1* to the virulent bacterial pathogen *Pst* DC3000 is NPR1-, JAR1- and EIN2-dependent whereas its resistance to the virulent oomycete *H. parasitica* Noco2 only requires NPR1. Additionally, *cir1*-induced resistance to both pathogens requires SA accumulation (Murray et al., 2002). It appears that *cir1* is not involved in *R* gene-mediated (specifically *RPM1*) resistance given that mutant plants are not significantly more resistant to infection by *Pst* DC3000 carrying the effector AvrB (S. L. Murray, personal communication). In addition, *cir1* does not display increased resistance to the necrotrophic pathogen, *B. cinerea*, (Murray et al., 2005) suggesting that *cir1*-mediated resistance is only effective against certain invading biotrophs and hemi-biotrophs. Furthermore, *cir1* shows constitutive expression of defence related genes in the SA, JA and ET defence signalling pathways. These genes include the SA-dependent *PR-2* and *PR-5* as well as the JA/ET-dependent *PDF1.2* (Murray et al., 2002). According to previous studies, *cir1* also constitutively expresses *PR-1* (Murray et al., 2002) however we have shown that this is not always the case (Fig. 3.7B). The defence-related gene expression and disease-resistance phenotypes imply that multiple defence signalling pathways contributing to basal resistance are activated in the *cir1* mutant (Murray et al., 2002).

It clear from the aforementioned information and the details discussed in Chapter 1 that COI1, EDS1 and PAD4 have distinct roles in two major signalling pathways in the plant defence network. COI1 has an important function in the JA-dependent signalling pathway (Lorenzo and Solano, 2005) whereas EDS1 and PAD4 are required for SA accumulation and therefore regulate the SA signalling pathway (Feys et al., 2001). In this chapter, these mutants were employed to help elucidate the function of *cir1* in the Arabidopsis defence network. To investigate which parts of the defence signalling network are being activated in *cir1*-enhanced resistance, the disease resistance profiles of *cir1 coi1*, *cir1 pad4* and *cir1 eds1* double mutants to *B. cinerea*,

virulent *P. syringae* and virulent *H. parasitica* were analysed. In addition, the breadth of the defence phenotype of *cir1* was investigated by determining its response to infection by an additional and previously untested fungal biotroph, *Golovinomyces orontii*. Furthermore, the outputs of the different signalling pathways in the *cir1* defence network were examined by establishing defence-related gene expression patterns as well as the accumulation of the EDS1 protein and camalexin in the single and double mutant lines.

4.2 Generation and isolation of double mutants

4.2.1 *cir1 coi1*

To determine the role of *COI1* in disease resistance and expression of defence-related genes in *cir1* plants, *cir1* was crossed with the null mutant *coi1-1* (Feys et al., 1994). Homozygous *coi1-1* mutant plants were identified by germinating a segregating family of the mutant on MeJA-containing media and selecting the plants displaying the root-elongation phenotype typically associated with MeJA-insensitivity (Feys et al., 1994). Since *coi1-1* is a recessive mutation, a quarter of the segregating plants produced roots longer than wildtype or *cir1*. As *coi1-1* plants are male-sterile, *cir1* was crossed onto an identified homozygous *coi1-1* plant. The resulting seed was germinated and the subsequent plants were allowed to set seed through self-fertilization. F_2 lines that were homozygous for *cir1* and *coi1-1* were identified by selecting for plants that displayed the constitutively high luciferase activity phenotype and the root-elongation phenotype, as well as male sterility in mature plants (results not shown). To maintain a segregating population, *cir1* was crossed onto the homozygous *cir1 coi1-1* double mutant plants (renamed to *cir1 coi1* for purposes of this study). The F_1 plants from this cross underwent self-pollination to produce F_2 seed and ultimately an F_2 *cir1*/*cir1 COI1-1*/*coi1-1* plant line was identified for future experiments. It was also established that the selected line was homozygous for the *PR-1::LUC* transgene (results not shown).

As the *PR-1::LUC* transgene segregates as a monogenic dominant trait, constitutive luciferase activity will normally only be found in three-quarters of F_2 plants containing the monogenic recessive *cir1* mutation. Therefore, the *cir1* segregation ratio to wild-type is 3:13 (Murray, 2000). In the segregating F_2 *cir1*/*cir1 COI1-1*/*coi1-1* population, the hypothesis was that the second mutation would have no influence on the constitutively high luciferase activity of *cir1* and the segregation data confirmed this hypothesis with a *P* value significantly greater than 0.05 (Table 4.1).

In addition, *cir1* had no effect on the segregation of the *coi1-1* mutation as a quarter of the F_2 *cir1*/*cir1 COI1-1*/*coi1-1* population were homozygous for *coi1-1*, displaying male sterility in mature plants (results not shown).

Table 4.1 Genetic analysis of the F_2 population of the *cir1* x *cir1 coi1* cross

The χ^2 value was calculated and compared to the relevant critical value to determine *P* value range.

Donor	*Recipient*	*Hypothesis*	*No. tested*	*Luc. activity*		*No luc. activity*		χ^2	*P value*
				Observed	Expected	Observed	Expected		
cir1	*cir1 coi1*	3:13[a]	43	9	8	34	35	0.15	>0.70

[a] The *PR-1::LUC* transgene segregates as a monogenic dominant trait whereas *cir1* segregates as a monogenic recessive trait. Therefore, constitutive luciferase (luc.) activity will normally be found only in three-quarters of F_2 plants containing the *cir1* mutation. The hypothesis was that *coi1-1* will have no effect on the luciferase activity of the F_2 plants.

4.2.2 *cir1 eds1*

To establish the function of *EDS1* in disease resistance and expression of defence-related genes in *cir1* plants, a *cir1 eds1-2* double mutant (renamed to *cir1 eds1*) was generated. The pollen from *cir1* plants in the Col-0 background was used to fertilize *eds1-2* (Falk et al., 1999) null mutant plants in the L*er* background. Both mutations are recessive and therefore no *cir1* (Table 4.2) or *eds1-2* (results not shown) phenotypes could be visualised in the resultant F_1 progeny. It was however established that the cross was successful through the amplification of the *PR-1::LUC* transgene in the F_1 plants (results not shown). The F_1 plants were allowed to self-pollinate, the F_2 seed were collected and the F_2 plants were screened for homozygous double mutant plants.

The F_2 plants were initially screened with luciferase assays to identify homozygous *cir1* plants with high luciferase activity levels. Since *EDS1* is required for *PR-1* expression (Feys et al., 2001) and the high luciferase activity of *cir1* is based on the expression of the *PR-1::LUC* transgene (Murray et al., 2002), it was believed that the introduction of the *eds1-2* mutation might affect the luciferase activity levels of the segregating F_2 population. As previously mentioned, high luciferase activity levels associated with homozygous *cir1* plants will only be visualised in a 3:13 ratio in F_2 plants. This segregation ratio would be affected if *eds1-2* impedes the luciferase activity of a quarter of the population, which would include the homozygous *cir1 eds1* double mutants. To establish if *eds1-2* affected or did not affect the luciferase activity of the F_2 progeny plants, two hypotheses were tested (Table 4.2).

Due to the low *P* values indicating these results are highly unlikely if the hypothesis were true (Table 4.2), both hypotheses had to be rejected and therefore no conclusions on the effect of *eds1-2* on the luciferase activity of the F_2 plants could be made. However, the low number of observed plants with high luciferase activity (Table 4.2) points to interference of some sort. During the screening process of the mapping population (Chapter 3), it was established that the L*er* background reduces the luciferase activity of SA-treated *Luc2* plants. Since *eds1-2* is in the L*er* background, the discrepancy between the expected and observed amount of plants with high luciferase activity could be attributed to the effect of the L*er* background and not necessarily only to the introduction of the *eds1-2* mutation. F_2 progeny

plants of *cir1* crossed with L*er* were screened as a control alongside the experimental F_2 plants, allowing us to assess the effects of the mixed genetic background on the penetrance of the *cir1* mutant phenotype. Great care was taken during the screening process to avoid the problem of selecting false positive plants as experienced in Chapter 3 and although only one plant displayed high luciferase activity levels significantly higher than background levels, there was no doubt that this plant was homozygous for *cir1*.

Table 4.2 Genetic analysis of the *cir1* x *eds1-2* cross

The χ^2 value was calculated and compared to the relevant critical value to determine *P* value range.

Gene-ration	*Donor*	*Recipient*	*Hypothesis*	*No. tested*	*Luc. activity*		*No luc. activity*		χ^2	*P value*
					Observed	Expected	Observed	Expected		
F_1	*cir1*	*eds1-2*		5	0	0	5	5		
F_2	*cir1*	*eds1-2*	3:13[a]	63	1[c]	11	62	52	11.01	<0.001
F_2	*cir1*	*eds1-2*	9:55[b]	63	1[c]	8	62	55	7.02	<0.01

[a] *cir1* segregates as a monogenic recessive trait whereas the *PR-1::LUC* transgene segregates as a monogenic dominant trait. Constitutive luciferase (luc.) activity will therefore be found only in three-quarters of F_2 plants containing the *cir1* mutation. The hypothesis in this case was that *eds1-2* does not affect the luciferase activity of the F_2 plants.

[b] The *PR-1::LUC* transgene segregates as a monogenic dominant trait whereas *cir1* segregates as a monogenic recessive trait. Therefore, constitutive luciferase (luc.) activity will normally be found only in three-quarters of F_2 plants containing the *cir1* mutation. In this case, the hypothesis was that *eds1-2* affects the luciferase activity in one quarter of the F_2 plants.

[c] This plant was PCR screened to establish whether it was homozygous for *eds1-2*. It was found to be heterozygous for *eds1-2* and was allowed to self-fertilize. A homozygous double mutant line was identified in the resultant F_3 progeny.

Thereafter, the F_2 population was PCR screened with a triple primer set (see Chapter 2 for details) to distinguish *eds1-2* homozygous plants from wild-type or heterozygous plants. As expected, one quarter of the analysed F_2 plants were homozygous for *eds1-2* (results not shown) signifying that *cir1* had no effect on the segregation of the *eds1-2* mutation. No homozygous double mutant lines could be identified in the F_2 progeny, since the only homozygous *cir1* plant was heterozygous for *eds1-2* (results not shown).

This F_2 *cir1*/*cir1 EDS1-2*/*eds1-2* plant was allowed to self-fertilize, the F_3 seed was collected and the F_3 progeny was PCR screened using the triple primer set (results not shown). Approximately one quarter of the screened plants were homozygous for *eds1-2* and consequently five homozygous *cir1 eds1* lines were selected for forthcoming experiments to compensate for the variation in the Col-0 and L*er* background affecting mutant phenotypes.

4.2.3 *cir1 pad4*

A *cir1 pad4-1* double mutant (renamed *cir1 pad4*) was constructed to determine the role of *PAD4* in the disease resistance phenotype of *cir1* as well as in the expression of defence-related genes in *cir1* plants. *Cir1* was crossed onto a homozygous null mutant *pad4-1*

(Glazebrook et al., 1996; Jirage et al., 1999) plant and the resulting F_1 progeny were tested by PCR to confirm the presence of the *PR-1::LUC* transgene, indicating that the cross was successful (results not shown). As both mutations are recessive, none of the F_1 plants displayed the *cir1* (Table 4.3) or *pad4-1* (results not shown) phenotype. The F_1 plants were allowed to self-fertilize, the F_2 seed were collected and the F_2 generation plants were analysed for homozygous double mutant plants.

Table 4.3 Genetic analysis of the *cir1* x *pad4-1* cross

The χ^2 value was calculated and compared to the relevant critical value to determine *P* value range.

Gene-ration	*Donor*	*Recipient*	*Hypothesis*	*No. tested*	*Luc. activity*		*No luc. activity*		χ^2	*P value*
					Observed	Expected	Observed	Expected		
F_1	*cir1*	*pad4-1*		5	0	0	5	5		
F_2	*cir1*	*pad4-1*	3:13[a]	80	10[c]	15	70	65	2.05	>0.10
F_2	*cir1*	*pad4-1*	9:55[b]	80	10[c]	11	70	69	0.11	>0.70

[a] The *PR-1::LUC* transgene segregates as a monogenic dominant trait whereas *cir1* segregates as a monogenic recessive trait. Therefore, constitutive luciferase (luc.) activity will normally be found only in three-quarters of F_2 plants containing the *cir1* mutation. The hypothesis in this case was that *pad4-1* does not interfere with the luciferase activity of the F_2 plants.

[b] *cir1* segregates as a monogenic recessive trait whereas the *PR-1::LUC* transgene segregates as a monogenic dominant trait. Constitutive luciferase (luc.) activity will therefore be found only in three-quarters of F_2 plants containing the *cir1* mutation. In this case, the hypothesis was that *pad4-1* interferes with the luciferase activity in one quarter of the F_2 plants.

[c] All 10 plants were PCR screened to establish if they were homozygous for *pad4-1*. None of these plants were *pad4-1* homozygous, but six were heterozygous for *pad4-1* and were allowed to self-pollinate. A homozygous double mutant line was identified in the subsequent F_3 progeny.

Firstly the F_2 progeny plants were screened for constitutively high luciferase activity to identify homozygous *cir1* plants. Similar to *EDS1*, *PAD4* is required for *PR-1* expression (Feys et al., 2001) and therefore *pad4-1* might also affect the expression of the *PR-1::LUC* transgene and consequently the luciferase activity levels of the segregating F_2 generation. Normally, high luciferase activity levels will only be found in three-quarters of F_2 plants containing the monogenic recessive *cir1* mutation in a 3:13 ratio, however if *pad4-1* interferes with the luciferase activity it would affect a quarter of the population including the homozygous *cir1 pad4* double mutants. The hypotheses that *pad4-1* interfered or did not interfere with the luciferase activity of F_2 progeny plants were tested and are summarised in Table 4.3. The *P* values indicated neither hypothesis can be rejected. However, the difference between the observed and expected numbers of the second hypothesis, which states that *pad4-1* interferes with the luciferase activity of the F_2 plants, is less than in the first hypothesis thereby also having a larger *P* value and greater significance (Table 4.3).

Subsequently, a *pad4-1* co-dominant CAPS DNA marker (details in Chapter 2) which distinguishes homozygous *pad4-1* plants from heterozygous or wild-type plants was employed to analyse the F_2 population. Approximately one quarter of the analysed F_2 plants were

homozygous for *pad4-1* (results not shown) indicating that *cir1* did not affect the segregation of the *pad4-1* mutation. However, none of the plants that were homozygous for *cir1* and displaying high luciferase activity levels, were *pad4-1* homozygous (results not shown). Therefore, no homozygous double mutant lines could be identified in the F_2 progeny.

The F_2 *cir1*/*cir1 PAD4-1*/*pad4-1* line with the highest luciferase activity levels underwent self-fertilization and the F_3 progeny were PCR screened to identify homozygous *pad4-1* plants (results not shown). About one quarter of the plants were homozygous for *pad4-1* and therefore a homozygous *cir1 pad4* double mutant line could be selected for future experiments.

4.3 Disease severity profile of double mutants to different pathogens

It is generally accepted that programmed cell death and defence responses largely regulated by SA-dependent signalling are more effective against biotrophic pathogens whereas JA/ET signalling pathways control a different set of defence responses to necrotrophic pathogens (Glazebrook, 2005). Since necrotrophs benefit from the death of host cells, programmed cell death and SA-dependent defences would be mainly ineffective against these pathogens (Glazebrook, 2005). However, exceptions to this model exist as evidence of the involvement of SA and its signalling components in combating susceptibility to necrotrophs, has surfaced (Ferrari et al., 2003).

Plant resistance is therefore controlled by a combination of defence response pathways whose activation is dependent on the nature of the pathogen and its mode of pathogenesis. Through the measurement of pathogen growth *in planta*, the disease severity caused by selected pathogens in *cir1* and the *cir1 coi1*, *cir1 pad4* and *cir1 eds1* double mutant lines was evaluated.

4.3.1 *Botrytis cinerea*

The fungal pathogen *B. cinerea* is classified as a necrotroph as it kills the host cells at an early stage of infection, causing extensive tissue damage (van Kan, 2006). Resistance to this pathogen depends on JA and ET signalling and Arabidopsis mutants altered in JA and ET signalling or biosynthesis display increased susceptibility to *B. cinerea* infection (Veronese et al., 2006).

4.3.1.1 Increased susceptibility of *coi1* to *B. cinerea* infection is independent of CIR1

Since *cir1* constitutively expresses *PDF1.2* and its resistance to *Pst* DC3000 infection is JAR1-dependent (Murray et al., 2002), it is believed that the JA-dependent defence responses are activated in *cir1*. Infection by *B. cinerea* activates the expression of *PDF1.2* in a JA- and ET-dependent manner and this activation has been correlated with resistance to *B. cinerea* (Penninckx et al., 1998), however it is known from previous studies that *cir1* is not more

resistant than wild-type plants to infection by *B. cinerea* (Murray et al., 2005). Similarly, other susceptible responses to *Botrytis* have been observed despite induction of *PDF1.2*, suggesting that increased *PDF1.2* expression is not sufficient in offering full protection to the plant (Ferrari et al., 2003; Mengiste et al., 2003).

COI1 has an important role in JA-dependent responses, is required for the expression of *PDF1.2* and *coi1-1* mutant plants display enhanced susceptibility to *B. cinerea* (Penninckx et al., 1996; Thomma et al., 1998). To determine if *cir1* has an effect on *coi1-1* susceptibility to *B. cinerea* infection and if the loss of COI1, and therefore JA signalling, would result in an altered phenotype for *cir1*, a segregating population of *cir1 coi1* double mutants were analysed using a detached leaf infection assay (Denby et al., 2004). Three leaves from five plants per plant line were inoculated with a *Botrytis* spore suspension and the diameter of the developing lesions was measured at 3, 4 and 5 dpi as presented in Fig. 4.1. As a negative control, two leaves per line were inoculated with half-strength grape juice without *Botrytis* spores. These control leaves displayed no lesion formation (results not shown). Not only homozygous double mutant (*cir1*/*cir1 coi1*/*coi1*) plants were selected for testing; based on the luciferase activity levels and male sterility of plants, plants that were homozygous *cir1* and heterozygous or wild-type *COI1-1* (c*ir1*/*cir1 COI1*/-) as well as heterozygous or wild-type *CIR1* and homozygous *coi1-1* (*CIR1*/- *coi1*/*coi1*) were also included in the infection assay.

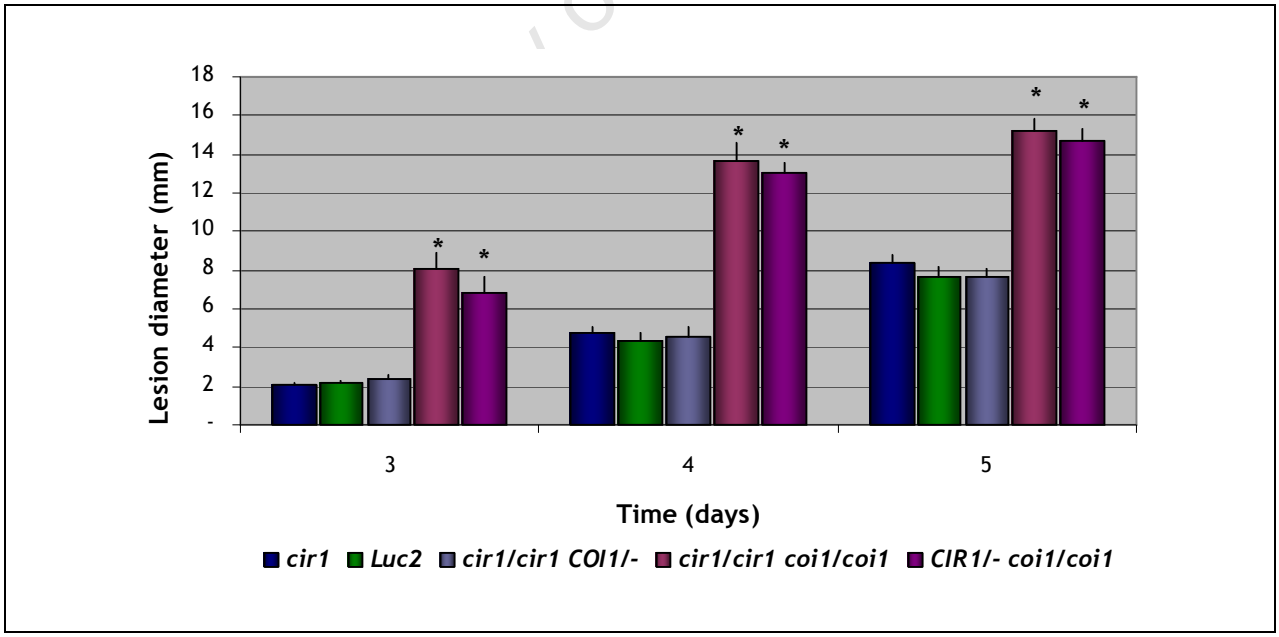

Figure 4.1. *Botrytis cinerea* detached leaf infection assay of a segregating *cir1 coi1* population. Leaves from the segregating *cir1 coi1* population and *cir1* (homozygous line not from segregating population) and *Luc2* (representing wild-type Col-0) control lines, were assayed. Bars represent the average lesion diameter measured on three leaves taken from five plants per plant line at 3, 4 and 5 days post infection. Lesion diameter is measured in mm. Error bars represent the standard error

between values at the 95% confidence level. Asterisks indicate a significant increase in lesion diameter compared to *cir1* plants at each time point (Student's *t*-test, $P < 0.05$).

It has been previously shown that plant susceptibility and disease severity could be correlated with the diameter of lesion, where a lesion with a large diameter would be indicative of a susceptible plant with enhanced fungal growth and a high degree of disease severity, whereas a lesion with a small diameter indicates resistance to infection, little fungal growth and a lesser extent of disease (Govrin and Levine, 2000; Ferrari et al., 2003; Denby et al., 2004; Murray et al., 2005). The spread of the lesions measured in this experiment was not limited by the actual size of the leaf and the experiment was repeated twice with similar results. The *cir1* control line displayed lesion diameters similar to those of the *Luc2* control plants at all three time points (Fig. 4.1), confirming previous results that *cir1* was not more resistant to *B. cinerea* infection than wild-type plants (Murray et al., 2005). The homozygous *cir1* line (*cir1*/*cir1 COI1*/-) identified from the segregating *cir1 coi1* population also did not show a significant difference in lesion diameter at all time points compared to *cir1* and the wild-type *Luc2* plants (Fig. 4.1). The presence of a homozygous mutant *coi1-1* gene resulted in a significant increase of susceptibility in the homozygous *cir1*/*cir1 coi1*/*coi1* double mutant plants compared to *cir1*, *Luc2* and *COI1-1* wild-type (*cir1*/*cir1 COI1*/-) plants at 3, 4 and 5 dpi (Fig. 4.1). Additionally, it appears that CIR1 had no effect on the susceptibility of homozygous *coi1-1* plants since no significant differences in lesion diameter between *cir1*/*cir1 coi1*/*coi1* and *CIR1*/- *coi1*/*coi1* plants could be determined irrespective of the loss of or the heterozygous state of *CIR1* (Fig. 4.1).

Previous studies established that *eds1-2* and *pad4-1* mutants did not display lesion sizes significantly different from the relevant wild-type plants after *B. cinerea* infection (Ferrari et al., 2003) and therefore the disease severity profiles of *cir1 eds1* and *cir1 pad4* lines to this pathogen were not determined.

4.3.1.2 Camalexin accumulation in *cir1* and *cir1 pad4* after *B. cinerea* infection

In response to both biotrophic and necrotrophic pathogen attack, Arabidopsis plants rapidly induce the biosynthesis and accumulation of camalexin (3-thiazol-2'-yl-indole), which is the characteristic and major phytoalexin of Arabidopsis (Glawischnig, 2007). Phytoalexins are low molecular weight secondary metabolites with antimicrobial activity *in vitro* (Hammerschmidt, 1999). Camalexin is synthesized from tryptophan via indole-3-acetaldoxime, which upon conjugation with cysteine or cysteine-metabolites forms the intermediate dihydrocamalexic acid that is ultimately metabolised to camalexin (Glawischnig et al., 2004; Glawischnig, 2007). The first reaction from tryptophan to indole-3-acetaldoxime is catalysed by CYP79B2/CYP79B3 (Hull et al., 2000; Mikkelsen et al., 2000)

whereas PAD3 (CYP71B15) converts dihydrocamalexic acid into camalexin in the final step of camalexin biosynthesis (Schuhegger et al., 2006).

Camalexin accumulation triggered by biotrophic and necrotrophic pathogens forms part of an intricate defence network, involving SA-, JA- and ET-dependent signal transduction pathways (Glawischnig, 2007). *PAD4* has an regulatory effect on camalexin synthesis (Zhou et al., 1998), but camalexin accumulation could also be regulated by a *PAD4*-independent pathway, depending on which pathogen interactions are analysed (Glawischnig, 2007). For example, the *pad4-1* mutant does not accumulate camalexin after virulent *P. syringae* infection (Glazebrook et al., 1996) but high camalexin levels accumulates after infection with avirulent *P. syringae* (Zhou et al., 1998). Furthermore, *pad4-1* is not more susceptible to *B. cinerea* infection than wild-type plants despite reduced camalexin levels (Ferrari et al., 2003). This may be contributed to the reduction in SA-dependent signalling in *pad4-1*, which in turn alleviates the inhibition of JA signalling and results in increased JA-dependent defence responses (Gupta et al., 2000). JA-dependent responses are effective against *B. cinerea* infections (Veronese et al., 2006) and therefore no increased susceptibility was observed in *pad4-1*.

B. cinerea induces the accumulation of camalexin (Thomma et al., 1999b; Govrin and Levine, 2000) and it has been found that the lesion sizes caused by *B. cinerea* infections are reduced in the presence of high camalexin accumulation, suggesting that camalexin has a potential role in defence against *B. cinerea* (Denby et al., 2004). Additionally, the *pad3* camalexin deficient mutant (Zhou et al., 1999) supported significantly more fungal growth compared to Col-0 wild-type plants (Ferrari et al., 2003; Denby et al., 2004).

Previous studies found that *cir1* accumulates higher levels of camalexin compared to *Luc2* wild-type plants after *B. cinerea* infection (S. L. Murray, personal communication) even though it displayed lesion sizes corresponding to that of wild-type plants (Murray et al., 2005). Lesion development and camalexin accumulation after *B. cinerea* infection were measured in the *cir1*, *pad4-1* and *cir1 pad4* double mutant lines to determine whether the camalexin levels are correlated with the disease severity phenotype of each line in terms of lesion diameter. In addition, the possible effects that *cir1* might have on the regulatory function of *PAD4* on camalexin synthesis was also evaluated. A modified detached leaf assay (Denby et al., 2004; see Chapter 2 for details) was employed to infect three leaves harvested from each of three plants per plant line. At 2 dpi, the diameter of three representative lesions per plant was measured as presented in Fig. 4.2A and camalexin levels were determined (Fig. 4.2B). No lesion development or camalexin accumulation was detected in uninfected or negative control leaves which were inoculated with half-strength grape juice without *Botrytis* spores (results not shown). The experiment was repeated twice with similar

results and the spread of the lesions measured in this experiment was not limited by the physical size of the infected leaves.

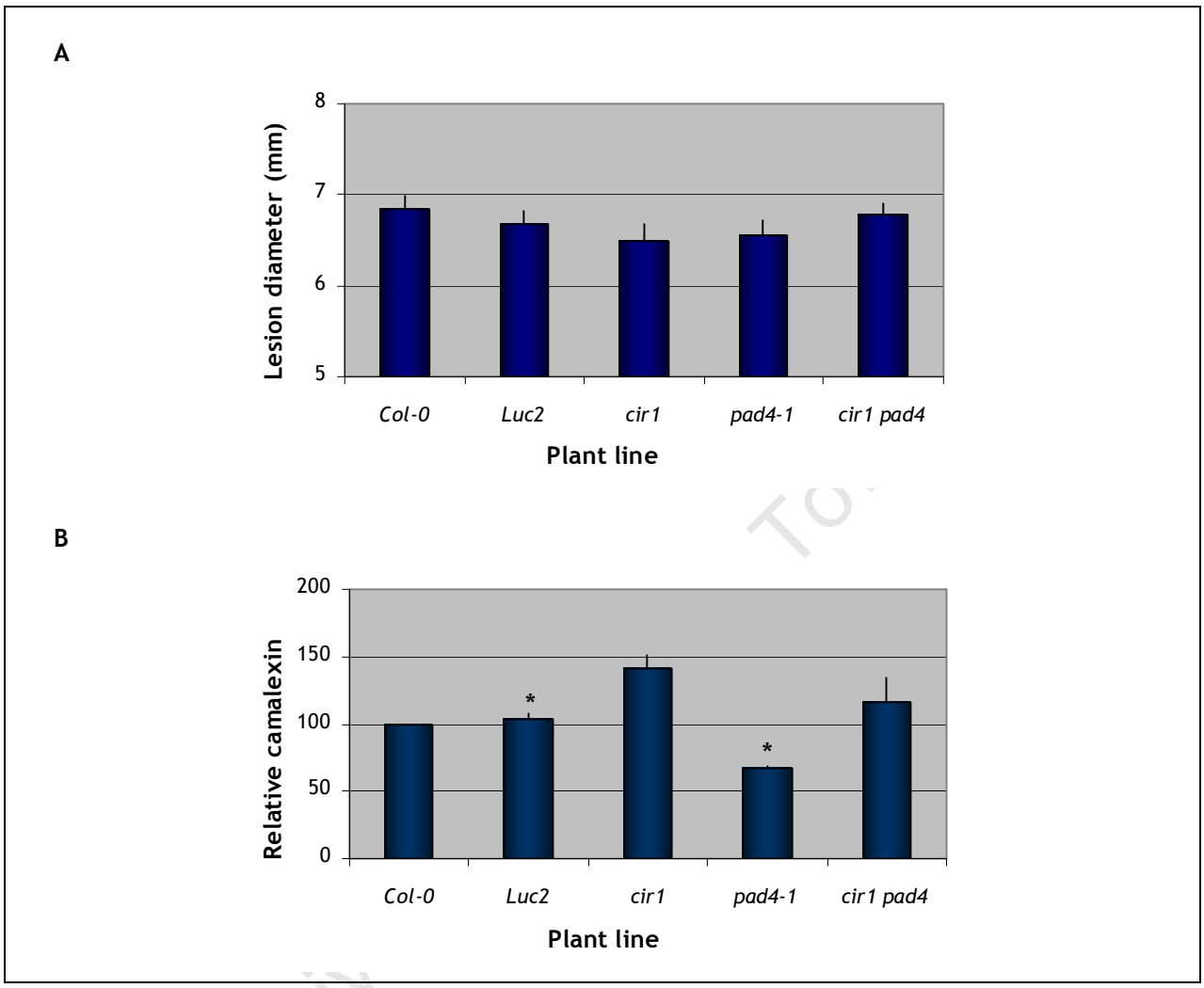

Figure 4.2. Camalexin accumulation in *cir1 pad4* in response to *Botrytis cinerea* infection.
Four-week-old Col-0 (negative control), *Luc2* (transgenic Col-0 line as negative control), *cir1* (positive control), *pad4-1* (positive control) and homozygous *cir1 pad4* plants were assayed. (**A**) Bars represent average lesion diameter measured on three leaves taken from three plants per plant line at 2 days post infection. Lesion diameter is measured in mm and represents fungal growth and the severity of the disease. Error bars represent the standard error between values at the 95% confidence level. None of the plant lines displayed significant differences in lesion diameter compared to Col-0 plants (Student's *t*-test, $P < 0.05$). (**B**) Bars represent the relative camalexin per leaf from three plants per line at 2 days post infection. Relative camalexin is defined as the average camalexin accumulation in each plant line relative to Col-0 which was set to a value of 100. Error bars represent the standard error between values at the 95% confidence level. Asterisks indicate a significant reduction in camalexin levels compared to *cir1* plants (Student's *t*-test, $P < 0.05$).

The two control lines, Col-0 and *Luc2*, displayed comparable lesion diameters indicating that the *Luc2* transgenic line had a wild-type phenotype regarding *B. cinerea* disease

symptoms (Fig. 4.2A). Confirming previous results (Fig. 4.1; Ferrari et al., 2003; Murray et al., 2005), the lesion diameters on the *cir1* and *pad4-1* plants were not significantly different from the lesions on *Luc2* and Col-0 control plants, respectively (Fig. 4.2A). The *cir1 pad4* double mutant resembled both the *cir1* and *pad4-1* phenotype as there was no significant difference in lesion diameters between any of the three plant lines (Fig. 4.2A). Therefore, none of the tested lines were more susceptible or resistant to *B. cinerea* infection than wildtype.

The *Luc2* transgenic line displayed a wild-type phenotype regarding camalexin accumulation by exhibiting similar relative camalexin levels as the Col-0 wild-type control line (Fig. 4.2B). As in previous studies, *cir1* accumulated significantly higher relative camalexin levels than *Luc2*, reaching approximately 40% higher levels than *Luc2* (Fig. 4.2B). Camalexin levels in *pad4-1* were moderately decreased compared to Col-0, accumulating to around 70% of wildtype (Fig. 4.2B). This correlates with previous findings where *pad4-1* plants displayed approximately 60% of wild-type camalexin levels after *B. cinerea* infection (Ferrari et al., 2003). The *cir1 pad4* double mutant line exhibited relatively high camalexin levels with an increase of 15% compared to the Col-0 control (Fig. 4.2B). It therefore appears that *cir1* partially suppressed the camalexin deficiency caused by *pad4-1*, however there was no statistical difference between levels reached in the double mutant and the *cir1* or *pad4-1* single mutant lines. In addition, the *pad4-1* mutation did not significantly reduce camalexin levels in *cir1 pad4*, suggesting that PAD4-independent regulation of camalexin synthesis occurred in this line in response to the necrotroph, *B. cinerea*.

Even though significant differences in relative camalexin levels were observed between *cir1* and *Luc2* and between *cir1* and *pad4-1*, the lesion diameters of all four lines were comparable (Fig. 4.2). In contrast to Denby et al. (2004), these results suggest that higher camalexin accumulation, as in *cir1*, is not associated with reduced lesion diameter. These phenotypes could be due to defence responses other than camalexin accumulation involved in establishing the extent of susceptibility of these lines to *B. cinerea* infection or that the camalexin accumulation in the *cir1* and *pad4-1* lines did not display a sufficient increase or decrease respectively, to have any noteworthy effects on *B. cinerea* growth. Alternatively, the increase in camalexin accumulation could have occurred after the infection already became established, which would have been too late to affect *B. cinerea* growth. A time-course experiment would be able to establish if this was indeed the case.

4.3.2 *Pseudomonas syringae* pv. *tomato* DC3000

P. syringae infects the host tissue through natural openings or wounds and multiplies in the intercellular spaces (Katagiri et al., 2002). The infected leaves of a susceptible plant initially display water-soaked patches without the occurrence of cell death, but in the later stages of infection the host tissue becomes necrotic and chlorotic (Katagiri et al., 2002).

Thus it has been suggested that *P. syringae* be classified as a hemi-biotrophic pathogen although is still often considered as a biotroph (Glazebrook, 2005). Resistance to virulent *P. syringae* infection largely relies on SA-dependent defence responses, but the *Pst* DC3000 pathogen seems to exploit the inhibition of SA signalling through the activation of JA-dependent defences (Glazebrook, 2005). *Pst* DC3000 produces a toxin, coronatine, which affects JA and/or ET signalling (Bender et al., 1999) and it is believed that coronatine contributes to bacterial virulence by activating JA signalling, thereby repressing the SA-dependent defences necessary to limit *P. syringae* proliferation (Kloek et al., 2001).

Previous studies have shown that *cir1* is not involved in *RPM1*-gene mediated defence responses, as *cir1* mutant plants were not more resistant to the avirulent *Pst* DC3000 AvrB strain compared to wild-type plants (S. L. Murray, personal communication). Consequently, only virulent *Pst* DC3000 was employed in the disease severity studies of the double mutant lines.

4.3.2.1 *cir1*-mediated resistance to *Pst* DC3000 infection is COI1-dependent

Bacterial infection assays on *cir1 jar1* double mutant plants established that *cir1*-induced resistance to *Pst* DC3000 is dependent on JAR1 (Murray et al., 2002), which is required for JA-dependent defences (Staswick et al., 1992; 2002). JAR1 encodes a JA-amino synthetase that conjugates JA to several amino acids, including isoleucine (Staswick et al., 2002; Staswick and Tiryaki, 2004). The JA-isoleucine conjugate is a more active form of JA and is necessary for optimal JA-dependent signalling in certain jasmonate responses (Staswick and Tiryaki, 2004). Unlike *coi1-1* mutants, all known alleles of *jar1* are fertile even though male fertility is dependent on JA (Stintzi and Browse, 2000), indicating that *JAR1* is not required for all jasmonate responses (Staswick et al., 2002). It is believed that only COI1 is necessary to regulate pollen and stamen development whereas both COI1 and JAR1 are required for the regulation of JA-dependent defence responses (Turner et al., 2002). To ascertain if *cir1*-mediated resistance is reliant on JA-dependent signalling through both COI1 and JAR1, the disease severity of *Pst* DC3000 infection on *cir1 coi1* double mutant plants were analysed. To identify homozygous *cir1 coi1* double mutant, homozygous *coi1-1* and wild-type *COI1-1* control plants, the *cir1*/*cir1 COI1-1*/*coi1-1* segregating population and a heterozygous *coi1-1* population were PCR screened utilising the *coi1-1* co-dominant CAPS DNA marker (details in Chapter 2) at 2 weeks of age (result not shown). Subsequently, three plants per line per time point were infected with *Pst* DC3000 at 4 weeks of age. The severity of the infection was photographed at 72 h post infection and the bacterial titre *in planta* was determined at 24 h, 48 h and 72 h post infection as presented in Fig. 4.3. No bacterial titre was observed for the control leaves of each plant line which were infiltrated with the $MgCl_2$ buffer without *Pst* DC3000 (results not shown).

Based on a visual assessment, in wildtype the water-soaked patches associated with *Pst* DC3000 infection have become chlorotic (Fig. 4.3A) and some leaves display early stages of necrosis after 72 h post infection (Fig. 4.3A; *COI1-1*). The infected leaves from the *cir1* single mutant, *coi1-1* single mutant and *cir1 coi1* double mutant seem to be less chlorotic than that of the wild-type *Luc2* and *COI1-1* plants (Fig. 4.3A). As confirmation, the extent of the disease severity was established by analysing the bacterial titres *in planta* (Fig. 4.3B).

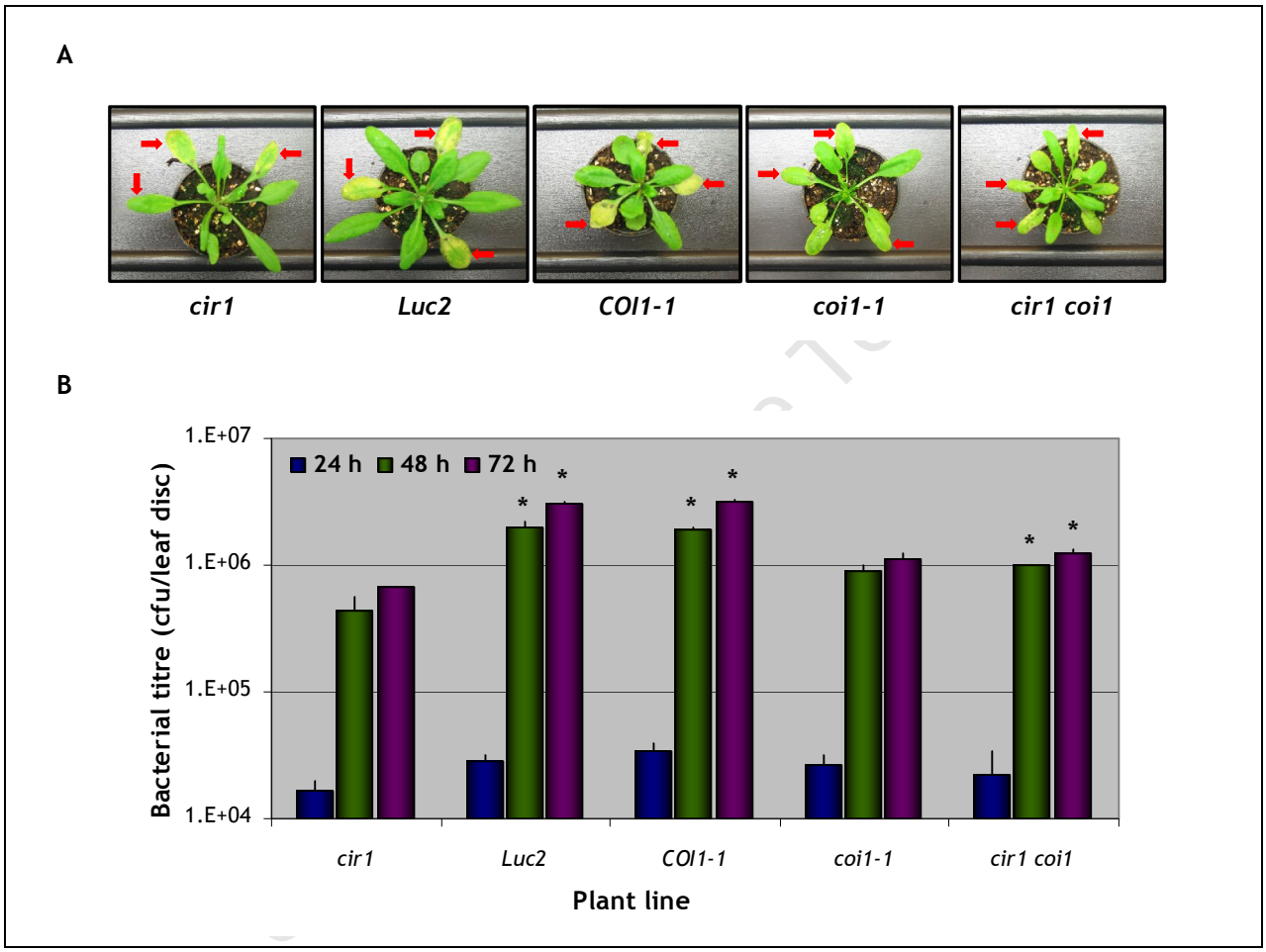

Figure 4.3. *Pseudomonas syringae* pv. *tomato* DC3000 infection assay of *cir1 coi1* plants.
Four-week-old *cir1* (positive control), *Luc2* (negative control; background control of *cir1*), *COI1-1* (negative control; background control of *coi1-1*), homozygous *coi1-1* (positive control) and homozygous *cir1 coi1* plants were assayed. (**A**) Visual symptoms of infected plants photographed at 72 h post infection. Red arrows point to infected leaves. (**B**) Bars represent the average bacterial titre in three leaves from three plants per line at 24 h, 48 h and 72 h post infection and are plotted on a logarithmic scale. Bacterial titre is defined as colony forming units (cfu) per leaf disc of 0.5 cm^2. Error bars represent the standard error between values at the 95% confidence level. Asterisks indicate a significant increase in the bacterial titres compared to *cir1* plants at each time point (Student's *t*-test, $P < 0.05$).

No noteworthy differences in bacterial titres between any of the lines were detected at 24 h post infection (Fig. 4.3B). As expected, the bacterial titres in *cir1* single mutants were significantly reduced in comparison to the wild-type *Luc2* plants at both 48 h and 72 h post infection (Fig. 4.3B; Murray et al., 2002). Similar to previous results (Kloek et al., 2001; Ellis et al., 2002), the homozygous *coi1-1* single mutant plants were more resistant to *Pst* DC3000 infection and displayed significantly lower bacterial titres than *COI1-1* wild-type plants at both time points (Fig. 4.3B). Although the bacterial titres in the homozygous *cir1 coi1* double mutant plants were reduced compared to wild-type *Luc2* and *COI1-1* plants, they were notably higher than *cir1* single mutant plants (Fig. 4.3B). The bacterial titres of the double mutant plants were similar to those of the homozygous *coi1-1* single mutant plants (Fig. 4.3B), suggesting that *cir1*-mediated resistance to *Pst* DC3000 was dependent on *COI1-1* and JA signal transduction. Therefore, the JA-dependent signalling involved in *cir1* basal resistance functions through JAR1 (Murray et al., 2002), as well as COI1. In addition, the reduced bacterial titres in the *cir1* single mutant, *coi1-1* single mutant and *cir1 coi1* double mutant plants confirmed the visual assessment of the *Pst* DC3000 infection in Fig. 4.3A.

4.3.2.2 *cir1*-induced resistance to *Pst* DC3000 is dependent on both EDS1 and PAD4

The signal molecule SA plays an important role in the activation of disease resistance responses and it has been established that SA-dependent signalling is pivotal for resistance to *P. syringae* infections (Glazebrook, 2005). The *cir1* mutation causes the constitutive expression of SA-dependent genes and mutant plants display enhanced resistance, dependent on SA accumulation, to virulent pathogens (Murray et al., 2002). SA-dependent signalling is therefore essential for *cir1*-induced resistance to *Pst* DC3000. As previously mentioned, genetic analysis of SA signalling established that SA accumulation in response to certain types of pathogens is dependent on both EDS1 and PAD4 (Feys et al., 2001). Additionally, EDS1 and PAD4 have an important cooperative role in basal defence; they interact in yeast two-hybrid assays and coimmunoprecipitate in soluble leaf extracts of Arabidopsis (Feys et al., 2001). Therefore, the severity of *Pst* DC3000 infection in *cir1 eds1* and *cir1 pad4* double mutant plants were analysed to determine the role of EDS1 and PAD4 in the signal transduction network leading to the SA-dependent activation of defence responses in *cir1*. Three plants per line per time point were infected with *Pst* DC3000 at 4 weeks of age and each assay was repeated at least twice with similar results. The visual symptoms of the infection were photographed at 72 h post infection and the bacterial titre *in planta* was determined at 24 h, 48 h and 72 h post infection for the *cir1 eds1* (Fig. 4.4) and *cir1 pad4* (Fig. 4.5) double mutant lines. As a control, leaves of each plant line which were infiltrated with the $MgCl_2$ buffer without *Pst* DC3000 and no bacterial titre was observed in these leaves (results not shown).

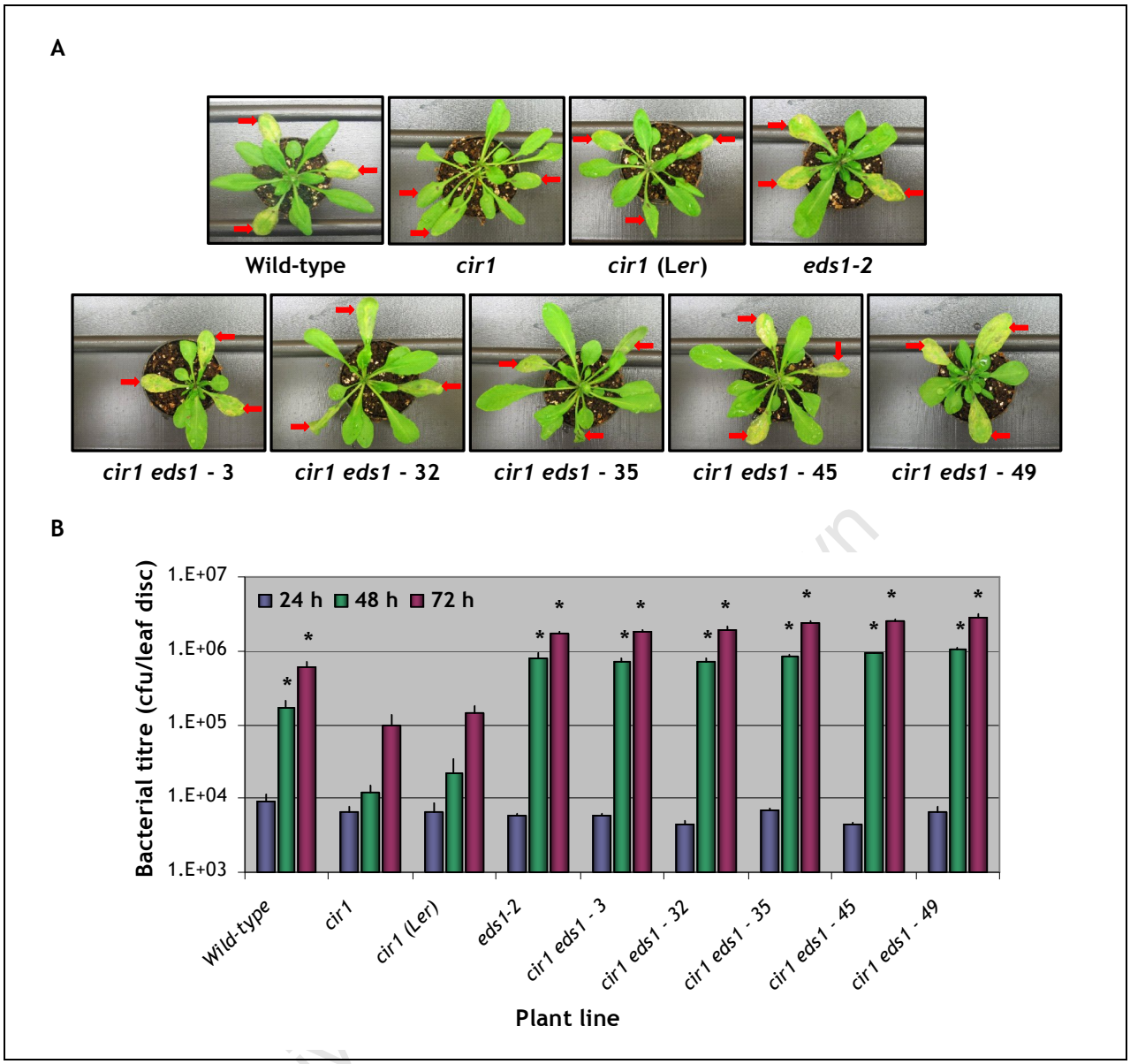

Figure 4.4. *Pseudomonas syringae* pv. *tomato* DC3000 infection assay of *cir1 eds1* plants.
Four-week-old *cir1* (positive control), *cir1* (L*er*) (*cir1* in L*er* background control), wild-type (*Luc2* transgenic Col-0 line as negative control), *eds1-2* (positive control) and five homozygous *cir1 eds1* lines were assayed. (**A**) Visual symptoms of infected plants photographed at 72 h post infection. Red arrows point to infected leaves. (**B**) Bars represent the average bacterial titre in three leaves from three plants per line at 24 h, 48 h and 72 h post infection and are plotted on a logarithmic scale. Bacterial titre is defined as colony forming units (cfu) per leaf disc of 0.5 cm^2. Error bars represent the standard error between values at the 95% confidence level. Asterisks indicate a significant increase in the bacterial titres compared to *cir1* plants at each time point (Student's *t*-test, $P < 0.05$).

The infected leaves of the *cir1* and *cir1* (L*er*) single mutant plants appear less chlorotic than those of the wild-type plant (Fig. 4.4A), suggesting that both *cir1* and *cir1* (L*er*) single mutant plants were more resistant to *Pst* DC3000 infection. The *cir1* (L*er*) plants were selected from the F_2 progeny of a *cir1* and L*er* cross and contain the wild-type *EDS1-2* allele in addition to being homozygous for *cir1* (results not shown). These plants were included as

a control to establish if a mixed Col-0 and L*er* genetic background has an effect on *cir1*-induced resistance to *Pst* DC3000. No differences in the visual symptoms between the infected leaves of *cir1* and *cir1* (L*er*) were observed (Fig. 4.4A), signifying that the mixed background has a negligible effect on *cir1*-induced resistance to *Pst* DC3000. In contrast, the infected leaves of the *eds1-2* single mutant plant displayed chlorosis similar to the wild-type plant (Fig. 4.4A). All five *cir1 eds1* double mutant lines exhibited severe chlorosis in their infected leaves with the disease severity appearing similar to that of the *eds1-2* single mutant plant (Fig. 4.4A). Additionally, certain leaves of the *cir1 eds1* double mutant lines displayed early stages of necrosis (Fig. 4.4A; *cir1 eds1* – 35). The bacterial titre *in planta* (Fig. 4.4B) was determined to confirm the visual assessment of the extent of the disease severity.

No statistically significant differences in bacterial titres between wild-type plants and the single or double mutant lines could be determined at 24 h post infection (Fig. 4.4B). The titres of *Pst* DC3000 were significantly reduced at 48 h and 72 h post infection in the *cir1* and *cir1* (L*er*) single mutant plants compared to wild-type (Fig. 4.4B), confirming the visual assessment in Fig. 4.4A and previous results (Fig. 4.3; Murray et al., 2002). There were no significant differences in bacterial titres between the *cir1* single mutant in the Col-0 background and the *cir1* (L*er*) single mutant plant (Fig. 4.4B), thereby confirming that the mixed Col-0 and L*er* genetic background had no effect on *cir1*-mediated resistance to infection by *Pst* DC3000. Similar to previous results (Parker et al., 1996) and the visual assessment (Fig. 4.4A), the *eds1-2* single mutant plants had significantly higher bacterial titres at both time points than that of wild-type and *cir1* (L*er*) plants possessing wild-type *EDS1-2* allele (Fig. 4.4B). Five homozygous *cir1 eds1* double mutant lines were included in the assays to determine if the mixed Col-0 and L*er* background of these plants caused notable variation in the severity of *Pst* DC3000 infection. The removal of EDS1 resulted in increased susceptibility to *Pst* DC3000 infection in all *cir1 eds1* double mutant lines, which displayed bacterial titres significantly higher than those of the *cir1* and *cir1* (L*er*) single mutant plants but indistinguishable from the levels attained in the *eds1-2* single mutant plants at 48 h and 72 h post infection (Fig. 4.4B). These results correspond to the severity of *Pst* DC3000 disease symptoms captured in Fig. 4.4A. Since all five double mutant lines displayed similar bacterial titres (Fig. 4.4B), the disease susceptibility was not due to the mixed genetic background of these plants but could be contributed to the *eds1-2* mutation and the complete loss of EDS1 function (Falk et al., 1999). Since the double mutant plants were as susceptible as *eds1-2* (Fig. 4.4B), it suggests that *eds1* is epistatic to *cir1* and likely to act downstream of *cir1*. Therefore, the enhanced basal resistance observed in *cir1* plants was EDS1-dependent.

The results from the *Pst* DC3000 infection assays of *cir1 pad4* double mutant plants are summarised in Fig. 4.5. The majority of the infected leaves of the *cir1* single mutant plant were less chlorotic than the infected leaves of the wild-type plant, whereas the leaves of the *pad4-1* single mutant plant displayed disease symptoms more severe than the wild-type plant (Fig. 4.5A). The *pad4-1* leaves have become completely chlorotic and have, in some cases, progressed to the early stages of necrosis (Fig. 4.5A). The *Pst* DC3000 infected leaves of the *cir1 pad4* double mutant display high levels of disease severity with necrosis occurring in the majority of the leaves (Fig. 4.5A). This signifies that the *cir1 pad4* plant resembles the *pad4-1* single mutant phenotype in being more susceptible to infection than wild-type and *cir1* plants (Fig. 4.5A). The full extent of the disease severity was established by analysing the bacterial titres *in planta* (Fig. 4.5B).

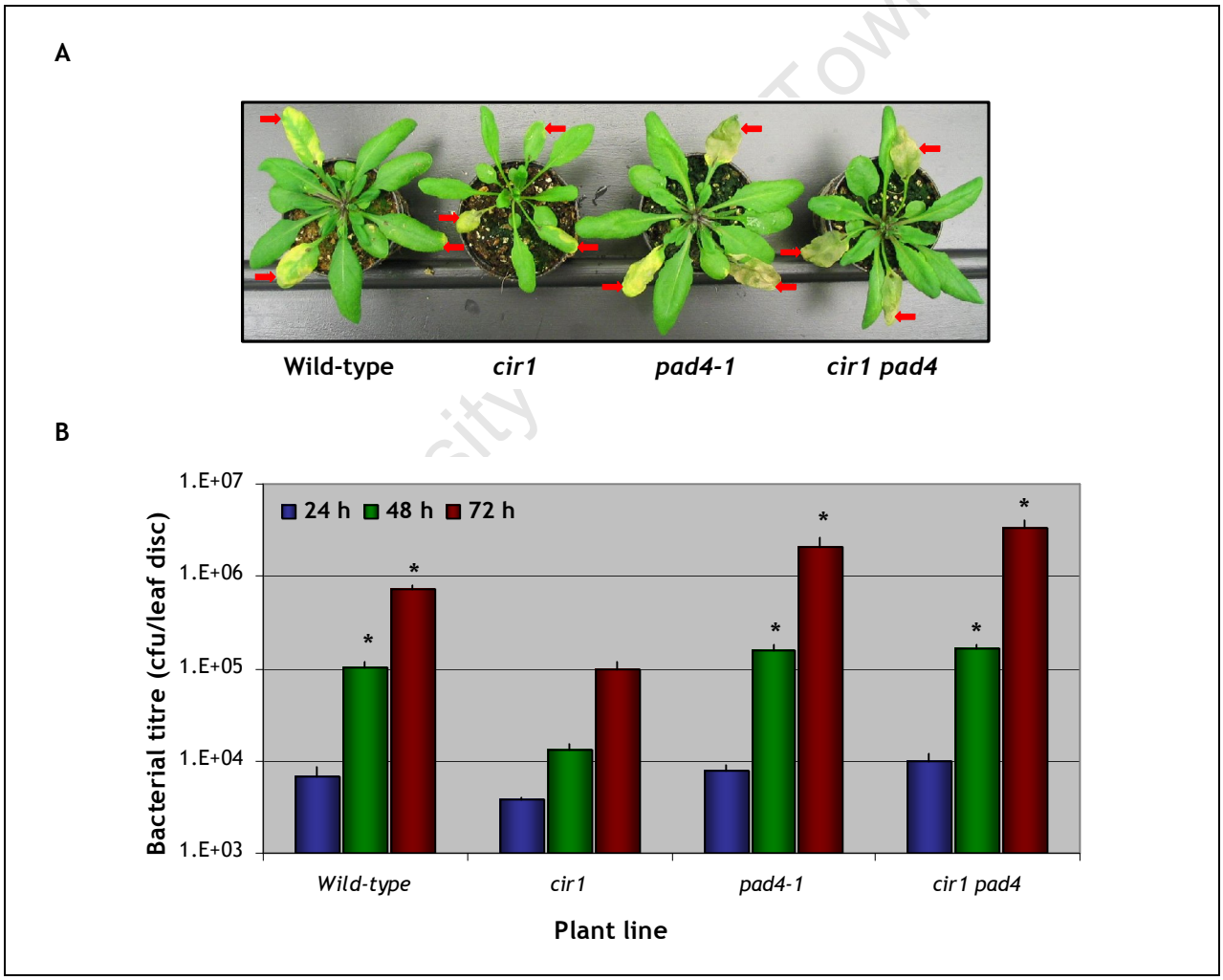

Figure 4.5. *Pseudomonas syringae* pv. *tomato* DC3000 infection assay of *cir1 pad4* plants.
Four-week-old wild-type (*Luc2* transgenic Col-0 line as negative control), *cir1* (positive control), *pad4-1* (positive control) and homozygous *cir1 pad4* plants were assayed. (**A**) Visual symptoms of infected plants photographed at 72 h post infection. Red arrows point to infected leaves. (**B**) Bars represent the average bacterial titre in three leaves from three plants per line at 24 h, 48 h and 72 h post infection and are plotted on a logarithmic scale. Bacterial titre is defined as colony forming units

(cfu) per leaf disc of 0.5 cm^2. Error bars represent the standard error between values at the 95% confidence level. Asterisks indicate a significant increase in the bacterial titres compared to *cir1* plants at each time point (Student's *t*-test, $P < 0.05$).

The differences in bacterial titre between wildtype and single or double mutant plants were not significant at 24 h post infection (Fig. 4.5B). Corresponding to the visual symptoms observed in Fig. 4.5A and previous results (Fig. 4.3; Fig. 4.4; Murray et al., 2002), the bacterial titre in the *cir1* plants was notably reduced in comparison to the wild-type plants at both 48 h and 72 h post infection (Fig. 4.5B). The *pad4-1* single mutant was more susceptible to *Pst* DC3000 infection, with significantly higher bacterial titres at both time points than that of wild-type plants (Fig. 4.5B). These results confirm previous studies (Feys et al., 2005) and are analogous to the severity of the infection symptoms in Fig. 4.5A. The bacterial titres in the *cir1 pad4* double mutant plants were equal to those in the *pad4-1* single mutant plants (Fig. 4.5B), demonstrating that *cir1* had no effect on the susceptibility to *Pst* DC3000 infection caused by the *pad4-1* mutation. The similar bacterial titres in *pad4-1* single mutant and the *cir1 pad4* double mutant plants confirms the visual assessment of the extent of infection in Fig. 4.5A. The *pad4-1* mutation, and the subsequent loss of PAD4 function, resulted in the increased susceptibility of *cir1 pad4* double mutant plants to *Pst* DC3000 infection, indicating that PAD4 was required for the enhanced basal resistance of *cir1* mutant plants.

The disease severity phenotypes of the *cir1 eds1* double mutants were very similar to those of the *cir1 pad4* double mutants (Fig. 4.4 and 4.5). EDS1 and PAD4 have similar positions upstream from SA accumulation in the defence signal transduction network and therefore the phenotypic similarities between *eds1* and *pad4* in the *cir1* background is not unexpected. The role of EDS1 and PAD4 in the plant defence signalling networks could be further elucidated through the examination of their molecular associations and biochemical functions in the *cir1* mutant.

4.3.2.3 Camalexin accumulation in *cir1* and *cir1 pad4* after *Pst* DC3000 infection

It is known that the *P. syringae* pathogen induces the accumulation of camalexin in plants (Tsuji et al., 1992; Zhao and Last, 1996) but since the camalexin deficient mutant *pad3* is not more susceptible to *Pst* DC3000 infection compared to wild-type plants (Glazebrook and Ausubel, 1994), it has been suggested that camalexin does not have an effect on the growth this bacterial pathogen (Glazebrook and Ausubel, 1994). However, *in vitro* studies established that high concentrations of camalexin (200 µg/ml) did have an inhibitory effect on *P. syringae* (Schuhegger et al., 2007). The lack of increased susceptibility of *pad3* plants after *P. syringae* infection could therefore be due to the Col-0 ecotype not accumulating such high camalexin levels *in situ* (Glawischnig, 2007). The camalexin levels of *cir1* after

Pst DC3000 infection were measured to establish if *cir1* defence responses important in limiting growth of this biotrophic pathogen, function through camalexin accumulation. Additionally, camalexin levels in the *cir1 pad4* double mutant line were determined after *Pst* DC3000 infection to establish if *PAD4* was required to activate camalexin accumulation in the *cir1* mutant. Three *cir1*, *pad4-1* and *cir1 pad4* plants were infected with *Pst* DC3000 and three infected leaves per plant were harvested at 2 dpi for camalexin extractions. The camalexin levels accumulated in each line are represented in Fig. 4.6. No camalexin accumulation was detected in uninfected or negative control leaves which were infiltrated with a $MgCl_2$ buffer without *Pst* DC3000 (results not shown). The experiment was repeated twice with similar results.

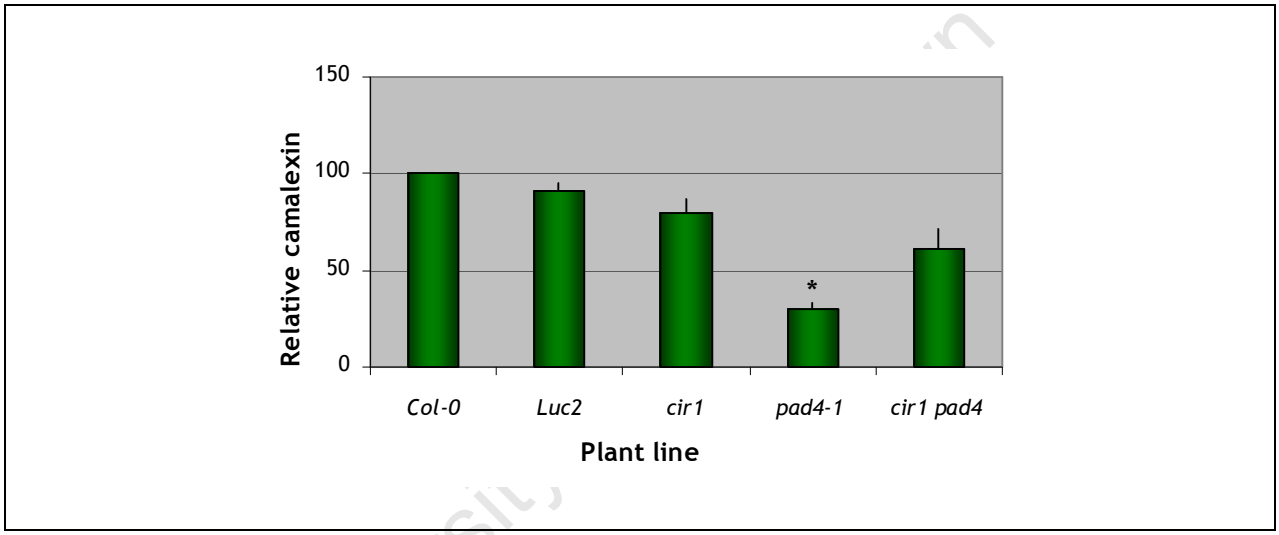

Figure 4.6. Camalexin accumulation in *cir1* and *cir1 pad4* in response to *Pseudomonas syringae* pv. *tomato* DC3000 infection.

Four-week-old Col-0 (negative control), *Luc2* (transgenic Col-0 line as negative control), *cir1*, *pad4-1* (positive control) and homozygous *cir1 pad4* plants were assayed. Bars represent the relative camalexin per leaf from three plants per line at 2 days post infection. Relative camalexin is defined as the average camalexin accumulation in each plant line relative to Col-0 which was set to a value of 100. Error bars represent the standard error between values at the 95% confidence level. Asterisks indicate a significant reduction in camalexin levels compared to *cir1* plants (Student's *t*-test, $P < 0.05$).

Although relative camalexin levels appear less in *cir1*, there was no significant difference in relative camalexin levels between *cir1* and *Luc2* or Col-0 wild-type plants (Fig. 4.6), suggesting that *cir1*-mediated resistance to *Pst* DC3000 is not dependent on camalexin accumulation. Similar to previous results (Glazebrook et al., 1996; Zhou et al., 1998), after virulent *P. syringae* infection *pad4-1* displayed a significant reduction in relative camalexin levels compared to *Luc2* wild-type and *cir1* plants (Fig. 4.6). These findings confirm that *PAD4* is necessary for camalexin accumulation in response to infection by *Pst* DC3000. The

relative camalexin levels in *cir1 pad4* were not significantly different from levels present in either the *cir1* or *pad4-1* single mutants (Fig. 4.6), suggesting that the *cir1 pad4* double mutant has an intermediate phenotype regarding camalexin accumulation after *Pst* DC3000 infection. If camalexin accumulation in the *cir1 pad4* double mutant was fully dependent on *PAD4*, the *pad4-1* mutation would have caused a more significant reduction in camalexin levels. These results suggest that the regulation of camalexin synthesis in *cir1 pad4* in response to *Pst* DC3000 infection is mediated independently of *PAD4*. In addition, it is possible that the camalexin defect of *pad4-1* plants was partially suppressed by the *cir1* mutation in the *cir1 pad4* double mutant.

4.3.3 *Hyaloperonospora parasitica* Noco2

Crucifer downy mildew is caused by the obligatory biotrophic oomycete *H. parasitica*, formerly known as *Peronospora parasitica*, which has also been described as a biotrophic pathogen of Arabidopsis (Holub et al., 1994; Glazebrook, 2005). Briefly, infection starts on the leaf surface with the germination of the conidia and appressoria formation, followed by hyphal penetration of epidermal cells and subsequent haustoria formation within the cells. The pathogen spreads throughout the leaf as the intercellular mycelium grow and eventually the pathogen undergoes asexual and sexual reproduction. In the former case, sporulation occurs with the emergence of conidiophores and the development of mature conidiospores whereas oospores are formed during sexual reproduction (Koch and Slusarenko, 1990). SA signalling and its defence responses have been shown to be effective against virulent *H. parasitica* infection, as mutants with defects in SA signalling display increased susceptibility to infection (Nawrath and Metraux, 1999). Unless JA/ET-dependent defence responses are induced prior to *H. parasitica* infection, it seems that these responses do not have a key role in resistance to *H. parasitica* (Thomma et al., 1998). Studies of the *cir1* phenotype correlated with these findings in that the induced resistance to *H. parasitica* Noco2 caused by the *cir1* mutation occurs independently of JAR1 and EIN2 (Murray et al., 2002). For this reason, the severity of *H. parasitica* infection utilising a virulent strain, Noco2, was determined only in the *cir1 eds1* and *cir1 pad4* double mutant lines.

4.3.3.1 Optimisation of *H. parasitica* Noco2 infection assay

The initial *H. parasitica* infection assays of *cir1* and relevant double mutant lines were conducted on 4-week-old plants and it was established that *cir1* plants were more resistant to *H. parasitica* infection than wild-type plants (Murray et al., 2002). However, published *H. parasitica* infection studies are frequently performed on the true leaves of 14-day-old seedlings (Clarke et al., 2001; Jirage et al., 2001; van der Biezen et al., 2002; Feys et al., 2005) and therefore it was determined if *cir1* plants displayed altered resistance to *H. parasitica* infection in 14-day-old seedlings compared to 4-week-old plants.

Ten 14-day-old and 4-week-old wild-type, *cir1*, L*er* and *eds1-2* plants were infected with the Noco2 strain of *H. parasitica*. The Noco2 strain is virulent on the Col-0 ecotype while being avirulent on the L*er* ecotype (Parker et al., 1993; Parker et al., 1996). Therefore it would result in a virulent infection on both wild-type and *cir1* plants, whereas L*er* plants harbouring the *RPP5* resistance gene would be resistant to infection. Since the *eds1* mutation suppresses *RPP5* gene-mediated resistance (Parker et al., 1996), *eds1*-2 mutant plants are susceptible to infection by the Noco2 strain and were included in the assay as a positive control. The extent of plant cell necrosis and the development of the *H. parasitica* mycelium was microscopically assessed 6 dpi by staining each of the ten infected seedlings or two infected leaves from each of the ten older plants with lactophenol trypan blue (Aarts et al., 1998). Following destaining of the infected tissue, *H. parasitica* mycelium and dead or dying plants cells (including vascular xylem) in the leaves can be identified by the blue dye it retains. Fig. 4.7 portrays the pathogen mycelium and necrotic plant cells visualized in the stained leaves collected from 14-day-old and 4-week-old infected plants. Only representative microscopic photographs taken at the same magnification have been included.

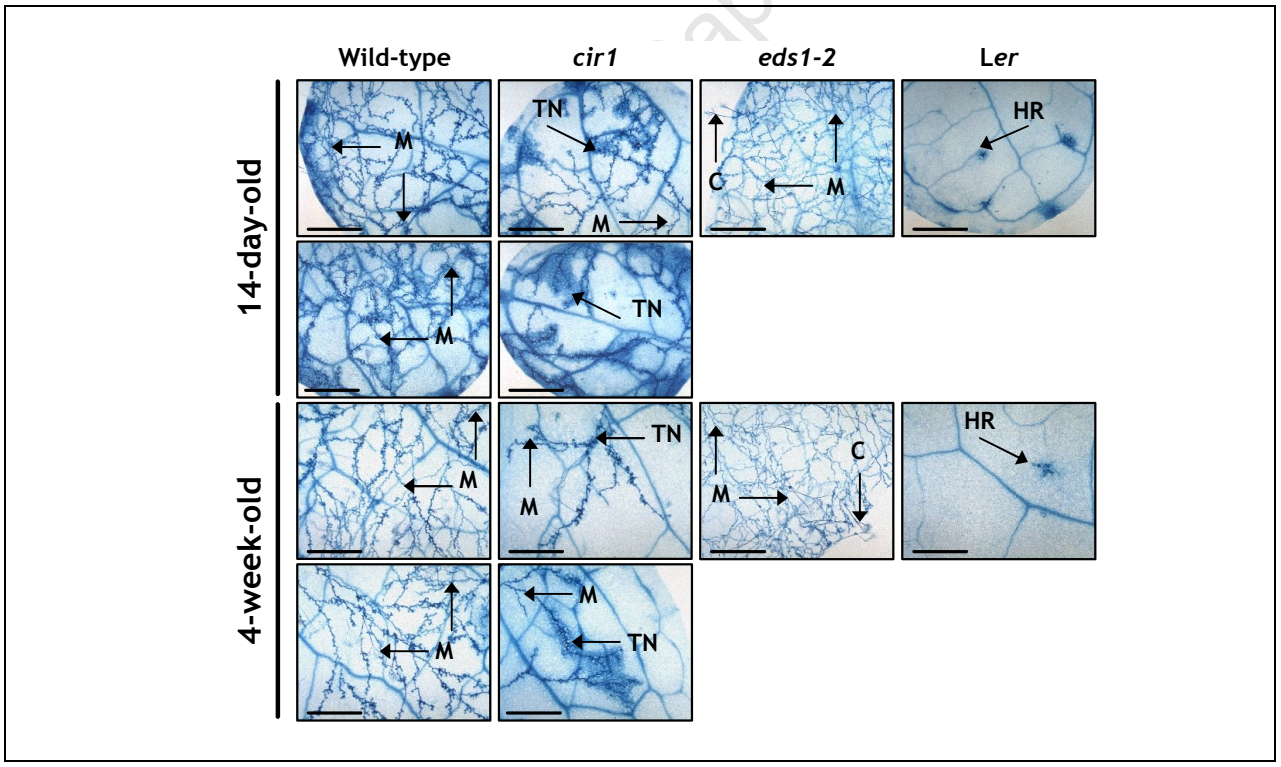

Figure 4.7. Comparison of *Hyaloperonospora parasitica* Noco2 infection phenotypes between 14-day-old and 4-week-old *cir1* plants.

Fourteen-day-old and 4-week-old wild-type (*Luc2* transgenic Col-0 line), *cir1*, *eds1-2* (positive control) and L*er* (negative control) plants were assayed. Leaves were stained with lactophenol trypan blue 6 days post infection to visualize pathogen mycelium and necrotic plant cells which retain the blue dye. Arrows point to conidiophores (C), hypersensitive response (HR), mycelium (M) or trailing necrosis

(TN). All photographs were taken under a light microscope at the same magnification. The scale bars in the bottom left corner of each photo represent 500 µM.

The Col-0 wild-type plants supported extensive intercellular mycelium growth in the mesophyll tissue of the infected leaves in both the 14-day-old and 4-week-old plants (Fig. 4.7), indicative that they were susceptible to the virulent infection. The mycelium growth of Noco2 was less widespread and lower amounts were observed in the *cir1* mutant compared to wildtype in both the young and older plants (Fig. 4.7). Confirming previous results (Murray et al., 2002), both the 14-day-old and 4-week-old *cir1* plants were more resistant to Noco2 infection than the Col-0 wild-type plants. In the *cir1* plants, the *H. parasitica* intercellular mycelium was surrounded by dead or dying mesophyll cells that retained the lactophenol trypan blue stain (Fig. 4.7). This is commonly referred to as trailing necrosis and it suggests that the HR was elicited but that it was not sufficient to fully restrict pathogen growth (Rustérucci et al., 2001). It is possible that trailing necrosis could contribute to the resistant phenotype of *cir1* plants as according to the visual assessment it seems that this form of HR restricted pathogen growth in the infected leaves (Fig. 4.7). As reduced mycelium growth and trailing necrosis occurred in both the 14-day-old and 4-week-old *cir1* plants, it appears that no notable difference in *cir1*-induced resistance could be observed between the different age plants (Fig. 4.7). Unlike the *cir1* plants, no trailing necrosis were observed in the *eds1-2* plants and therefore Noco2 colonization was unrestricted, allowing for the rapid spread of intercellular mycelium and the visualization of conidiophores indicative of asexual sporulation (Fig. 4.7). As assessed by the amount of visible mycelium observed, the *eds1-2* mutant supported higher levels of *H. parasitica* growth than the wild-type plants (Fig. 4.7) which is consistent with its "enhanced disease susceptibility" phenotype. L*er* plants displayed an HR at the points of pathogen penetration and the mycelium did not grow beyond the area of necrotic cells (Fig. 4.7). L*er* plants, utilized here as a negative control, were therefore fully resistant to *H. parasitica* Noco2 infection.

Cir1 plants were slightly impaired in growth compared to wild-type Col-0 plants (results not shown) and therefore it was a concern that the cotyledons instead of the true leaves of *cir1* plants would be exposed to the pathogen during the infection process. However, no clear difference in resistance to *H. parasitica* Noco2 infection was observed between 14-day-old and 4-week-old *cir1* plants. All further *H. parasitica* infection assays were performed on 4-week-old plants.

4.3.3.2 *cir1*-mediated resistance to *H. parasitica* Noco2 is EDS1- and PAD4-dependent

Resistance to virulent *H. parasitica* infection requires SA-dependent activation of defence responses and in turn SA accumulation in response to virulent pathogens depends on EDS1

and PAD4 (Feys et al., 2001). SA signalling plays an important role in the resistance of *cir1* to *Pst* DC3000 and *H. parasitica* Noco2 (Murray et al., 2002) and results have shown that *cir1*-induced resistance to the *Pst* DC3000 is dependent on EDS1 and PAD4 (Fig. 4.4 and 4.5). To determine if the resistance phenotype of *cir1* to *H. parasitica* Noco2 is also dependent on EDS1 and PAD4, the severity of *H. parasitica* Noco2 infection in *cir1 eds1* and *cir1 pad4* double mutant plants was analysed. Five plants per line were infected in duplicate with *H. parasitica* Noco2 at 4 weeks of age and the assay was repeated at least twice with similar results. The growth of the *H. parasitica* mycelium and the extent of plant cell necrosis was microscopically assessed by staining two leaves from each plant per line with lactophenol trypan blue (Aarts et al., 1998) of which representative photographs are presented in Fig. 4.8A. In addition, the sporulation levels of the pathogen were determined in duplicate on at least five leaves from each of the five plants per line (Fig. 4.8B) and both assessments were conducted 6 dpi.

Based on the visualization of pathogen growth and necrotic plant cells in the mesophyll tissue of infected leaves, widespread intercellular mycelium growth was observed in the susceptible wild-type Col-0 plants (Fig. 4.8A). Both *cir1* and *cir1* (L*er*) displayed less extensive pathogen growth than the wild-type plants and trails of necrotic plant cells surrounding the intercellular mycelium of the pathogen was observed in both lines (Fig. 4.8A). As expected, the L*er* plants were resistant to infection by *H. parasitica* Noco2 and therefore only HR at the penetration points and no mycelium growth were observed (Fig. 4.8A). The *pad4-1* plants displayed extensive mycelium growth similar to wild-type levels which was notably more rampant than the growth in *cir1* plants but less than that present in *eds1-2* plants (Fig. 4.8A). Corresponding to previous findings (Feys et al., 2001; Feys et al., 2005), trailing plant cell necrosis was observed in *pad4-1* mutant plants, however it was not as effective in controlling the spread of the pathogen as was the case in the *cir1* plants (Fig. 4.8A). The homozygous *cir1 pad4* double mutant plants resembled the *pad4-1* infection phenotype by supporting similarly high amounts of intercellular mycelium which was markedly more widespread than that observed in the *cir1* plants (Fig. 4.8A). *H. parasitica* Noco2 colonization of *eds1-2* was unrestricted and the mycelium multiplied promptly throughout the plant reaching higher levels of pathogen growth than wild-type Col-0 plants (Fig. 4.8A). The oospores, visualised as dark blue round structures, indicated that sexual sporulation had taken place in this line (Fig. 4.8A). All five of the homozygous *cir1 eds1* lines displayed mycelium growth similar to that of the *eds1-2* plants and drastically higher levels of pathogen growth was observed in all *cir1 eds1* plants compared to *cir1* and *cir1* (L*er*) plants (Fig. 4.8A). The visible conidiophores (Fig. 4.8A *cir1 eds1* – 3; *cir1 eds1* – 45) and oospores (Fig. 4.8A *cir1 eds1* – 3) were also indicative of the rapid proliferation of the pathogen in these lines. In addition to confirming the visual assessment of the infection, the

severity of the disease was quantified by counting the conidiospores produced on the infected leaves (Fig. 4.8B).

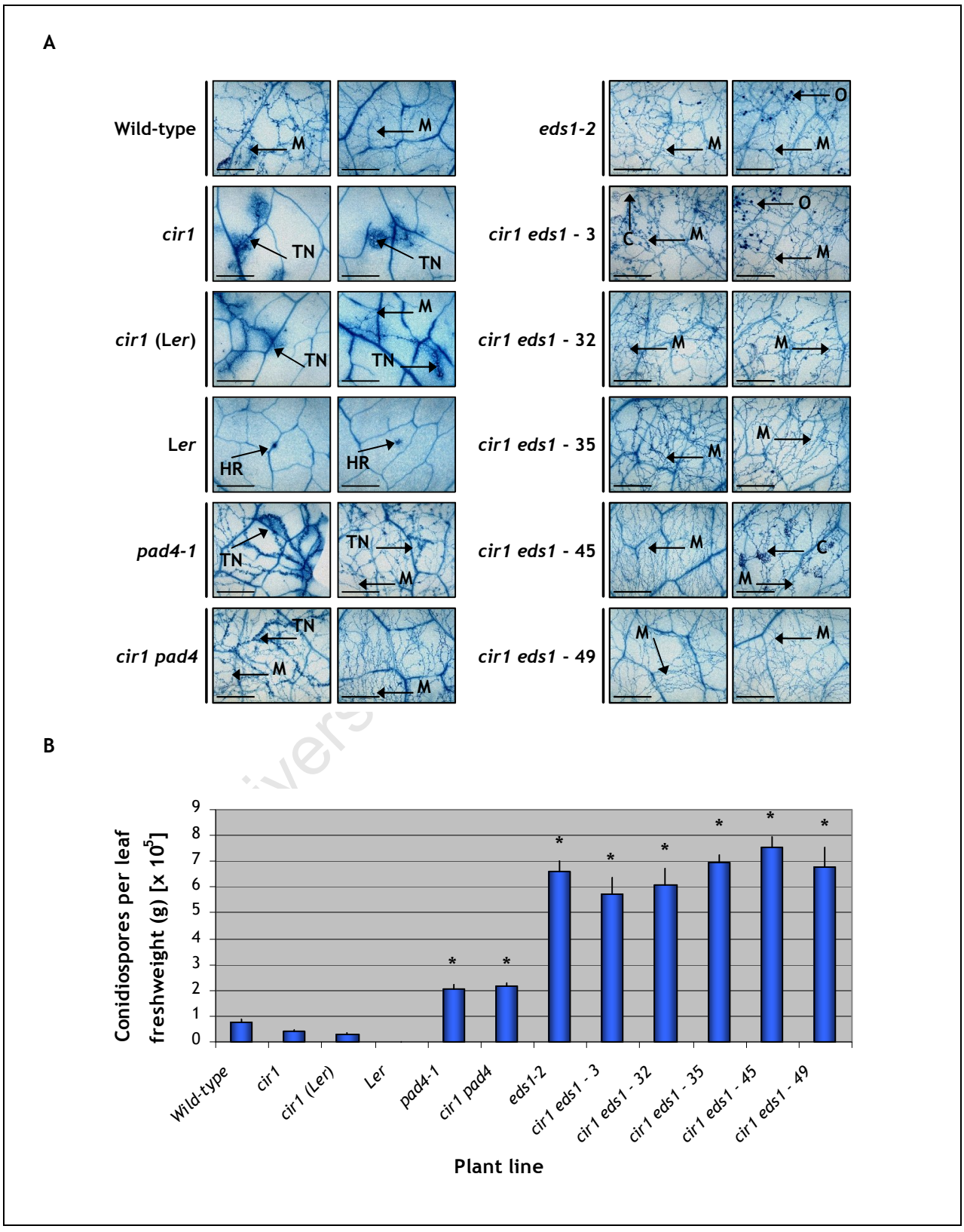

Figure 4.8. ***Hyaloperonospora parasitica*** **Noco2 infection assay of 4-week-old** ***cir1 pad4*** **and** ***cir1 eds1*** **plants.**

Four-week-old wild-type (*Luc2* transgenic Col-0 line), *cir1* (positive control), *cir1* (L*er*) (*cir1* in L*er* background control), L*er* (negative control), *pad4-1* (positive control), homozygous *cir1 pad4* line, *eds1-2* (positive control) and five homozygous *cir1 eds1* lines were assayed. (**A**) Infection phenotypes of inoculated leaves stained with lactophenol trypan blue 6 days post infection to visualize pathogen mycelium and necrotic plant cells which retain the blue dye. Arrows point to conidiophores (C), hypersensitive response (HR), mycelium (M), oospores (O) or trailing necrosis (TN). All photographs were taken under a light microscope at the same magnification. The scale bars in the bottom left corner of each photo represent 500 µM. (**B**) Sporulation levels of *H. parasitica* Noco2 on infected plants. Bars represent the average number of conidiospores harvested and counted from the leaves of the duplicate samples 6 days post inoculation. The number of conidiospores for each sample was determined on leaf tissue of equal freshweight. Error bars represent the standard error between values at the 95% confidence level. Asterisks indicate a significant increase in pathogen sporulation compared to *cir1* plants at each time point (Student's *t*-test, $P < 0.05$).

Both the *cir1* and *cir1* (L*er*) lines were more resistant than wild-type plants to infection by *H. parasitica* Noco2 (Fig. 4.8B). In this case, the number of conidiospores on *cir1* was not significantly reduced relative to the wild-type plants based on a Student's *t*-test ($P = 0.055$) (Fig. 4.8B), even though the microscopic assessment clearly showed more extensive mycelium growth in wild-type compared to *cir1* plants (Fig. 4.8A). The low quantity of conidiospores on the wild-type plants observed during the conidiospore count did not correlate with the extent of the infection visualized in the corresponding lactophenol trypan blue stained leaves and might have underestimated the severity of the infection in wild-type plants. Hence, based on the microscopic assessment (Fig. 4.8A) and confirming previous results (Fig. 4.7; Murray et al., 2002), it was concluded that the *cir1* plants were more resistant than wild-type plants to infection by *H. parasitica* Noco2. In addition, the number of conidiospores on *cir1* (L*er*) was significantly lower than on the wild-type plants (Fig. 4.8B). As mycelium growth was restricted in the resistant L*er* plants (Fig. 4.8A), no conidiospores were present on the infected leaves (Fig. 4.8B). The conidiospore count confirmed the microscopic evaluation that *pad4-1* was susceptible to infection by *H. parasitica* Noco2 (Fig. 4.8A) and similar to previous results, the pathogen displayed notably higher sporulation levels on *pad4-1* in comparison to wild-type (Fig. 4.8B; Feys et al., 2005) and *cir1* plants (Fig. 4.8B). Consistent with the microscopic evaluation of the disease severity (Fig. 4.8A), the loss of PAD4 function resulted in increased susceptibility of the *cir1 pad4* double mutant plants which displayed conidiospore numbers greatly elevated compared to the *cir1* plants and insignificantly different from the levels on the *pad4-1* single mutant plants (Fig. 4.8B). These results suggest that *cir1* has no effect on the susceptibility of *pad4-1* plants and that the basal resistance of *cir1* mutant plants to *H. parasitica* Noco2 infection was dependent on PAD4. The quantity of conidiospores on the *eds1-2* single mutant plants was considerably higher than that of wild-type (Feys et al., 2001), *cir1* and *cir1* (L*er*) plants possessing the

wild-type *EDS1-2* allele (Fig. 4.8B), confirming the visual assessment of the infection in Fig. 4.8A. The removal of EDS1 resulted in increased susceptibility of the *cir1 eds1* double mutant lines to *H. parasitica* Noco2 infection since all five double mutant lines displayed comparable conidiospore numbers which were significantly higher than those of the *cir1* and *cir1* (L*er*) plants, while being indistinguishable from the *eds1-2* single mutant plants (Fig. 4.8B). These results were analogous to the microscopic evaluation of the infection in Fig. 4.8A. Since all five *cir1 eds1* double mutant lines displayed similarly high conidiospore numbers, it is believed that the disease susceptibility was due to the *eds1-2* mutation and the complete loss of EDS1 function (Falk et al., 1999) and was not caused by the mixed genetic background of these plants. The comparable sporulation levels of *eds1-2* and double mutants plants signify that *cir1* did not suppress the enhanced susceptibility caused by *eds1-2* and consequently the enhanced basal resistance observed in *cir1* plants was EDS1-dependent.

Again the disease severity phenotypes of the susceptible *cir1 pad4* and *cir1 eds1* double mutant lines to *H. parasitica* Noco2 infection were similar and corresponded to the double mutant phenotypes observed during the *Pst* DC3000 infection assays (Fig. 4.4 and 4.5). The loss of PAD4 and EDS1 function, acting in similar positions upstream of SA accumulation, eradicated *cir1*-mediated resistance to these biotrophic pathogens.

4.3.4 *Golovinomyces orontii*

G. orontii, previously known as *Erysiphe orontii* (Braun, 1999), is a fungal pathogen that causes powdery mildew on wild-type Col-0 Arabidopsis plants (Plotnikova et al., 1998; Reuber et al., 1998). Powdery mildew fungi are obligate biotrophic and parasitic, requiring living plant host tissue for survival (Glazebrook, 2005). This fungi infects the epidermal plant cells, develops haustoria and ultimately forms a white mat of mycelium and conidiophores visible to the naked eye at ten days post inoculation, which is followed by prolific sporulation. To maintain the obligate parasitic life cycle, infection does not cause host cell death (Reuber et al., 1998; Vogel and Somerville, 2000). SA signalling and its defence responses are required for resistance against virulent *G. orontii* since mutants defective in SA signalling are more susceptible to powdery mildew infection (Reuber et al., 1998). The role of JA signalling and related defence responses are less clear as contradicting results regarding *coi1* susceptibility to *G. orontii* have been reported (Zimmerli et al., 2004; Xiao et al., 2005). *G. orontii* infection did not induce *PDF1.2* expression signifying that JA signalling is not activated by this infection (Reuber et al., 1998), however a mutant that displays constitutive activation of JA and ET signalling is more resistant to infection by *G. orontii* (Ellis and Turner, 2001). Therefore, once JA-dependent responses are induced either by mutation or by exogenous JA treatment, it appears to be effective against powdery mildew infection (Glazebrook, 2005).

4.3.4.1 *cir1* has an intermediate resistant phenotype to *G. orontii* infection

The *pmr4-1* (powdery mildew resistance 4; Vogel and Somerville, 2000) mutant is not only resistant to the fungal pathogen *G. orontii* but also to infection by a virulent isolate of the biotrophic pathogen *H. parasitica* (Vogel and Somerville, 2000). It has been shown that the *pmr4-1* mutation causes the hyper-activation of SA response genes and it was concluded that *pmr4*-induced resistance signals through the SA signalling pathway (Nishimura et al., 2003). Since *cir1* exhibits constitutive expression of defence related genes in the SA defence signalling pathway and its enhanced basal resistance to *Pst* DC3000 and *H. parasitica* Noco2 requires SA accumulation (Murray et al., 2002), the basal resistance response of *cir1* to virulent *G. orontii* infection was analysed. Five *pmr4-1*, *Luc2* and *cir1* plants were infected with *G. orontii* at 4 weeks of age and the assay was repeated at least twice with similar results. The severity of the *G. orontii* infection was visually assessed at 10 dpi and representative photographs of the disease symptoms are presented in Fig. 4.9A. Additionally, the disease symptoms and colonization of leaf surfaces of each plant per line were scored based on an adapted disease index (see Chapter 2 for details; Fig. 4.9B) and the spread of the infection was monitored at 14 dpi by assessing the number of newly infected leaves for each plant as summarized in Table 4.4.

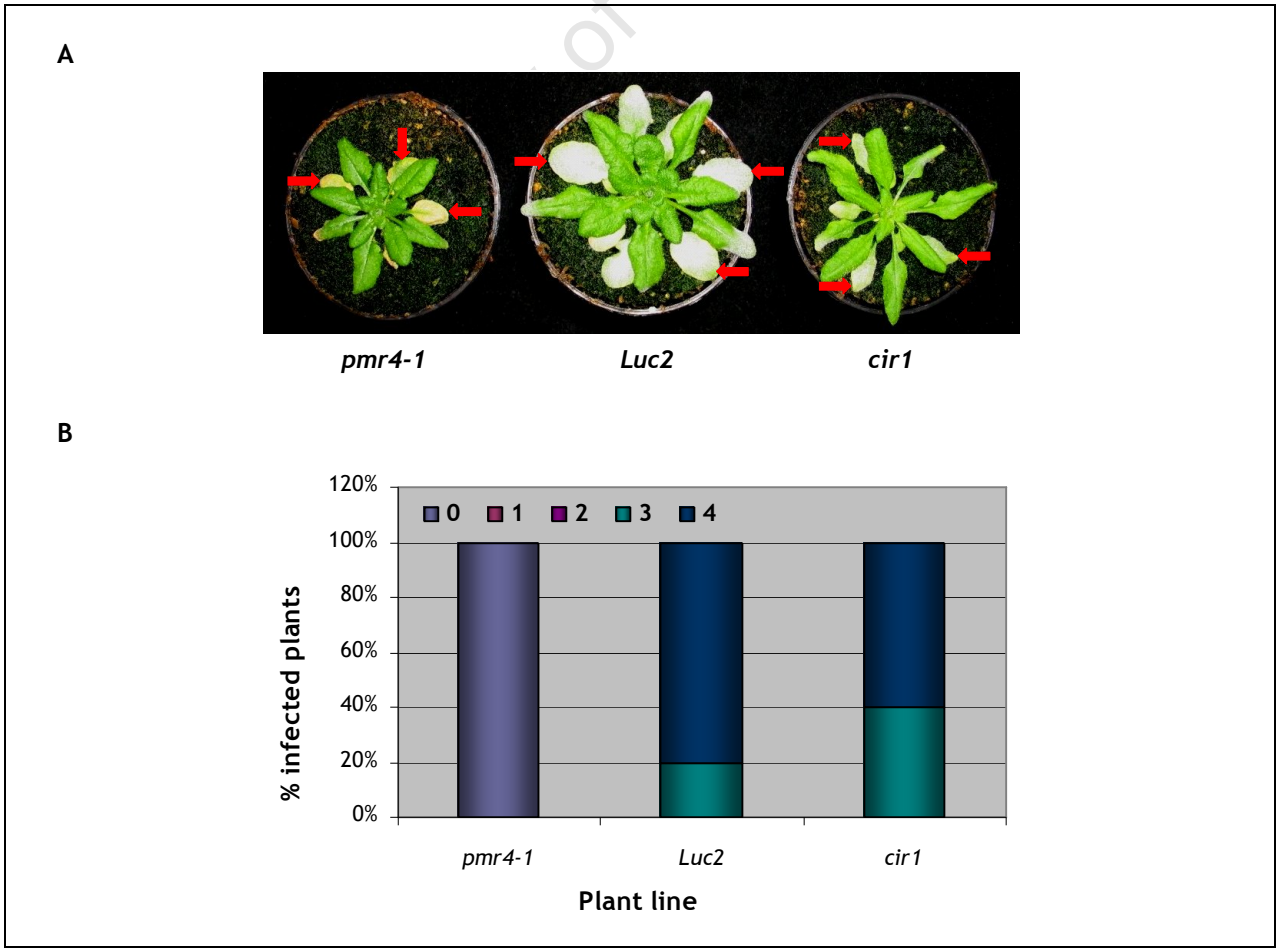

Figure 4.9. *Golovinomyces orontii* infection assay on *cir1*.

Four-week-old *pmr4-1* (negative control), *Luc2* (transgenic Col-0 line as positive control) and *cir1* were assayed. (**A**) Representative photo's of the disease symptoms on infected plants were photographed 10 days post infection. Red arrows point to selected infected leaves. (**B**) Disease symptoms from five plants per line were scored 10 days post infection using the following classification: 0 = no visible fungal mycelium, conidiophores or sporulation; 1 = low level sporulation, powdery mildew only on tip or edge of inoculated leaf; 2 = moderate sporulation, powdery mildew covers 10 – 30% of leaf surface; 3 = heavy sporulation, powdery mildew covers 30 – 60% of leaf surface; 4 = very heavy sporulation, > 60% of leaf surface covered with powdery mildew.

After 10 days, the powdery mildew colonies on the resistant *pmr4-1* mutant produced no visible mycelium and/or conidiophores denoted by the absence of the white mycelial mat usually associated with a successful powdery mildew infection (Fig. 4.9A; Vogel and Somerville, 2000). Although the infected leaves of *pmr4-1* turned light yellow, no visible mycelium, conidiophores or sporulation could be detected on any of the five plants (Fig. 4.9A) and therefore the disease symptoms of *pmr4-1* were classified as 0 (Fig. 4.9B). In contrast, the colonies on the wild-type *Luc2* plants produced a mat of mycelium, conidiophores and conidiospores as the infected leaves were covered with white powdery mildew (Fig. 4.9A). One of the five *Luc2* plants was classified as 3, whereas the remaining plants were grouped into 4 as they displayed very heavy sporulation with widespread powdery mildew growth (Fig. 4.9B). The infected *cir1* leaves were covered in patches of white powdery mildew suggesting that the mycelium and/or conidiophores did not spread as rapidly as on the infected *Luc2* leaves (Fig. 4.9A). Two of the five *cir1* plants displayed heavy sporulation with up to 60% of the leaf surface covered in powdery mildew and were classified as 3 (Fig. 4.9B). The remaining three plants shared disease symptoms with *Luc2* and were also classified as 4 (Fig. 4.9B).

Based on the visual assessment, the inoculated leaves of *cir1* did not display a significantly more resistant phenotype than *Luc2* wild-type plants, however the spread of infection appeared moderately delayed on *cir1* plants compared to wildtype. Therefore the spread of infection was monitored and the number of newly infected leaves, which were not exposed to the initial inoculum as they were not yet developed at 0 dpi, was determined at 14 dpi (Table 4.4).

Although *cir1* was not significantly more resistant to powdery mildew growth on infected leaves compared to wild-type plants (Fig. 4.9), it was established that the *cir1* mutation had an inhibitory effect on the spread of the fungus to distal plant parts (Table 4.4). Consequently, the *cir1* phenotype to *G. orontii* infection was described as "intermediate-resistance". To confirm the *cir1* phenotype and these preliminary results, additional quantified *G. orontii* infection assays should be conducted on *cir1* by counting the number of

conidiophores produced in discrete powdery mildew colonies or by measuring the hyphal length in each colony (Vogel and Somerville, 2000).

Table 4.4 The % spreading of *Golovinomyces orontii* infection at 14 days post infection

All values are the totals of numbers captured for five plants per plant line.

Plant line	*No. infected leaves (10 dpi)*	*No. new infected leaves (14 dpi)*	*Total no. infected leaves*	*% spreading*[a]
pmr4-1	32[b]	0[b]	32[b]	0.0 ± 0.0
Luc2	34	24	58	41.3 ± 1.9
cir1	33	6	39	15.4 ± 2.4

[a] The % spreading equals the number of newly infected leaves at 14 dpi divided by the total number of infected leaves ± standard error between values at the 95% confidence level.

[b] The number of leaves on *pmr4-1* plants which turned light yellow after powdery mildew inoculation. These leaves did not support fungal growth.

4.4 Gene expression patterns in *cir1* and *cir1* double mutants

The basal resistance phenotype of *cir1* relies on the activation of multiple defence signalling pathways resulting in the constitutive expression of defence related genes in the SA (*PR-1*, *PR-2* and *PR-5*) and JA/ET (*PDF1.2*) defence signalling pathways (Murray et al., 2002). In an attempt to gain a clearer understanding of what defence signalling pathways are activated in *cir1* prior to pathogen infection, additional selected gene profiles were examined in *cir1* and the *cir1* double mutants.

4.4.1 Selection of genes for quantitative real-time PCR analyses

Specific genes were selected for quantitative real-time PCR analyses and the rationale behind the selection process is outlined in the following sections. Details of each gene are listed in Table 4.5 at the end of section 4.4.1.

4.4.1.1 Differentially expressed genes based on microarray results

Through microarray expression profiling, the expression of genes in defence-related mutants can be analysed to ultimately identify novel components of defence signalling pathways (Glazebrook et al., 2003). Previously, various oligonucleotide DNA microarray experiments, including Affymetrix microarrays, were performed to highlight differential gene expression between wild-type *Luc2*, *cir1* and *cir1* double mutant plants and identify additional components of basal resistance (S. L. Murray, personal communication; Murray et al., 2007). In these experiments, the gene expression patterns of *cir1* and the double mutant lines consisting of *cir1 coi1*, *cir1 ein2* and *cir1 npr1* were compared to those of *Luc2*. Several genes with more than a 2-fold difference in expression were identified during these comparisons (S. L. Murray, personal communication). Some of these genes were selected for quantitative real-time PCR analyses based on their potential upregulation in *cir1*. The

behaviour of these genes was therefore analysed to verify the differential expression patterns observed in *cir1* and to determine their expression patterns in the previously untested *cir1 pad4* and *cir1 eds1* double mutant lines.

Based on the microarray results (S. L. Murray, personal communication), several genes were significantly up regulated in *cir1* but not in *cir1 ein2*, *cir1 coi1* or *cir1 npr1* compared to wild-type *Luc2*. These genes included *LURP1* (Knoth et al., 2007), *ZAT7*, *BG-3* (Dong et al., 1991), *PR-2* (Uknes et al., 1992), *AtLEA5* (Mowla et al., 2006), *PR-1* (Uknes et al., 1992) and a putative leucine-rich repeat transmembrane protein kinase (*At2g31880*). Additionally, the microarray experiments established that the expression of some genes was significantly up regulated in *cir1 ein2* and/or *cir1 coi1* but not in *cir1* when compared to *Luc2* (S. L. Murray, personal communication). Two of these genes were selected for quantitative real-time PCR analyses, namely *ACD6* (Lu et al., 2003) and a member of an aspartyl protease family protein (*At5g10760*).

4.4.1.2 Defence-related and marker genes of different defence signalling pathways

An array of marker genes for different defence regulation pathways was selected for quantitative real-time PCR analysis to investigate their expression patterns in *cir1* and *cir1* double mutants.

To assist in our selection process, we consulted previous global expression phenotyping studies where co-regulated defence-related genes situated in the different signalling pathways, were identified and clustered into four distinct groups (Glazebrook et al., 2003). To determine how *cir1* acts in the plant defence network, we therefore selected specific genes from each of the four clusters. The positions of the gene clusters in the main defence signalling pathways are indicated in Fig. 4.10, which is a schematic representation of the defence signal transduction network adapted from Glazebrook et al. (2003).

The genes in Cluster A are regulated by the SA signalling pathway (Fig. 4.10) and therefore show reduced expression in mutants defective in SA-dependent signalling such as *pad4-1* and *npr1-1* (Glazebrook et al., 2003). As JA/ET signalling acts antagonistically to SA signalling, some members of Cluster A displayed increased expression in the *coi1-1* and/or *ein2-1* mutants where the JA and/or ET signalling pathways have been blocked (Glazebrook et al., 2003). The genes selected from Cluster A include *PR-1* (Uknes et al., 1992), a putative LLR transmembrane protein kinase (*At2g31880*), an ankyrin repeat family protein (*At4g03450*) and *NIMIN-2* (Weigel et al., 2001). As presented in Fig. 4.10, genes in Cluster B are regulated by the JA and ET signalling pathways. The expression of Cluster B genes are usually reduced in the *coi1-1* and *ein2-1* mutants but in general they are expressed more strongly in the SA signalling mutants (Glazebrook et al., 2003), indicating that the SA signalling pathway has a repressive effect on these genes. A lectin-like protein (*At3g16530*), an unknown protein (*At1g10140*) and *PDF1.2* (Penninckx et al., 1996) were selected from Cluster B. Cluster C

genes are regulated by the JA and ET pathways as well an unknown signalling pathway. Although this unknown signalling pathway involves PAD4 and NPR1, it acts separately from the SA signalling pathway (Fig. 4.10). The expression of these genes is reduced in the *coi1-1*, *ein2-1*, *npr1-1* and *pad4-1* mutants (Glazebrook et al., 2003), however any possible effect that the *eds1-2* mutation might have on the expression of these genes has not yet been determined. *PER50* and *AtGSTF3* (Wagner et al., 2002) were selected from Cluster C. Cluster D genes are regulated in a JA-dependent manner which acts separately to ET (Fig. 4.10) and consequently these genes require COI1 but not EIN2 for enhanced expression. The expression of Cluster D genes was up regulated in the SA signalling mutants, again demonstrating the inhibitory effect of the SA signalling pathway on the JA signalling pathway (Glazebrook et al., 2003). The two genes selected from Cluster D include a proton-dependent oligopeptide transport family protein (*At3g47960*) and *CYP91A2* (Mizutani et al., 1998).

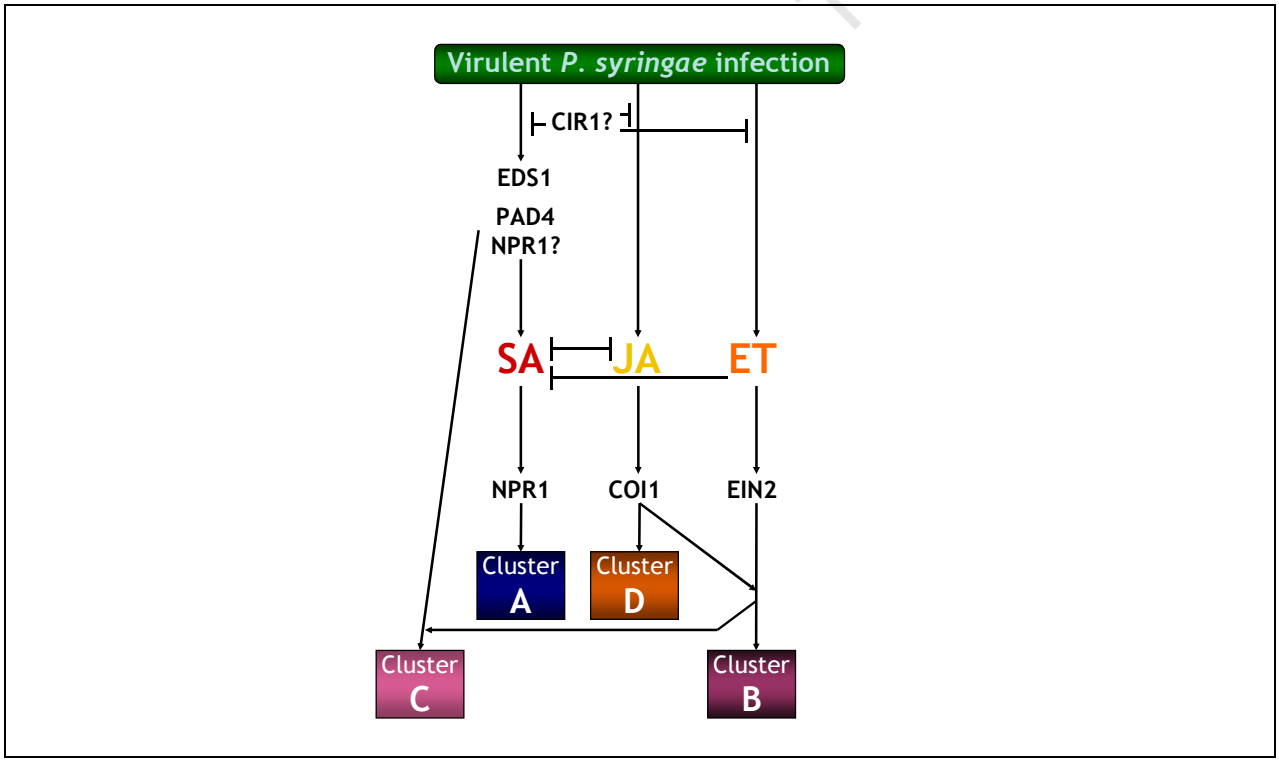

Figure 4.10. Schematic representation of the plant defence signal transduction network (adapted from Glazebrook et al. (2003)).

This model proposes that virulent *Pseudomonas syringae* infection activates EDS1, PAD4 and possibly NPR1 which in turn activates the SA signalling pathway. In addition, PAD4 and NPR1 activates an unknown signalling pathway. It has been suggested that the *npr1-1* (nonexpresser of PR genes 1; Cao et al., 1994) allele interferes with more than one function of NPR1 and therefore it has been tentatively placed with PAD4. The effect of EDS1 on the unknown signalling pathway is yet to be determined. SA signalling leads to SA accumulation which activates NPR1 and subsequently the expression of Cluster **A** genes. The JA and ET signalling pathways are also activated upon pathogen

perception. JA-dependent defence responses are mediated by COI1 and leads to Cluster **D** gene expression, whereas EIN2 regulate ET-dependent responses. The expression of Cluster **B** genes is the result of the combined effect of JA and ET signalling. The JA, ET and unknown signalling pathways collectively lead to Cluster **C** gene expression. It is believed that CIR1 acts as a negative regulator of disease resistance (Murray et al., 2002) however the exact point of inhibition has not been conclusively established. The inhibition bars between SA, JA and ET represent selected antagonistic behaviour of these signalling pathways. Only regulatory genes represented by mutants used in this study were included in this model. Arrows indicate activation whereas bars indicate repression.

To summarise, all genes selected for quantitative real-time PCR analyses are listed in Table 4.5.

Table 4.5 Genes selected for quantitative real-time PCR analyses

Certain genes displaying differential expression in DNA microarray experiments as well as known defence-related and marker genes of defence signalling pathways were selected.

Locus	*Gene model*	*Description*	*Reason for selection*	*Reference*
At2g14560	*LURP1*	Late up regulation in response to *H. parasitica* infection	Up regulated in *cir1* microarray	Knoth et al., 2007
At3g46090	*ZAT7*	Zinc finger protein ZAT7	Up regulated in *cir1* microarray	N/A
At3g57240	*BG-3*	β-1,3-glucanase	Up regulated in *cir1* microarray	Dong et al., 1991
At3g57260	*PR-2* (*BGL2*)	Pathogenesis-related protein 2	Up regulated in *cir1* microarray; known SA marker	Uknes et al., 1992
At4g02380	*AtLEA5* (*SAG21*)	Late embryogenesis abundant-like protein 5	Up regulated in *cir1* microarray	Mowla et al., 2006
At4g14400	*ACD6*	Accelerated cell death 6	Up regulated *cir1 ein2* and/or *cir1 coi1* microarray	Lu et al., 2003
At5g10760	N/A	Aspartyl protease family protein	Up regulated *cir1 ein2* and/or *cir1 coi1* microarray	N/A
At2g14610	*PR-1*	Pathogenesis-related protein 1	Up regulated in *cir1* microarray; known SA marker; known defence-related gene in Cluster A[a]	Uknes et al., 1992
At2g31880	N/A	Putative leucine-rich repeat transmembrane protein kinase	Up regulated in *cir1* microarray; known defence-related gene in Cluster A[a]	N/A
At4g03450	N/A	Ankyrin repeat family protein	Known defence-related gene in Cluster A[a]	N/A
At3g25882	*NIMIN-2*	NIM1-interacting protein 2	Known defence-related gene in Cluster A[a]	Weigel et al., 2001
At3g16530	N/A	Lectin-like protein	Known defence-related gene in Cluster B[a]	Ramonell et al., 2005

Continued on next page

Table 4.5 Continued from previous page

Locus	Gene model	Description	Reason for selection	Reference
At1g10140	N/A	Unknown protein	Known defence-related gene in Cluster B[a]	N/A
At5g44420	*PDF1.2*	Plant defensin protein 1.2	Known JA/ET marker	Penninckx et al., 1996
At4g37520	*PER50*	Peroxidase 50	Known defence-related gene in Cluster C[a]	N/A
At2g02930	*AtGSTF3* (*GST16*)	Glutathione *S*-transferase in Phi class of GSTs	Known defence-related gene in Cluster C[a]	Wagner et al., 2002
At3g47960	N/A	Proton-dependent oligopeptide transport family protein	Known defence-related gene in Cluster D[a]	N/A
At4g37430	*CYP91A2* (*CYP81F1*)	Cytochrome P450 monooxygenase 91A2	Known defence-related gene in Cluster D[a]	Mizutani et al., 1998

[a] Co-regulated defence-related genes situated in the different defence signalling pathways were identified and clustered into four distinct groups (Cluster A, B, C and D) (Glazebrook et al., 2003).

4.4.2 Relative expression of selected genes in *cir1* and *cir1* double mutants

Quantitative real-time PCR analyses were carried out to determine the relative expression levels of the selected genes in Col-0, *Luc2*, *cir1*, *pad4-1*, *cir1 pad4*, *eds1-2*, *cir1 eds1*, *coi1-1*, *cir1 coi1*, *ein2-1*, *cir1 ein2*, *npr1-1* and *cir1 npr1* plants. Additionally, Col-0 plants infected with *Pst* DC3000 and harvested 24 h post infection were included to determine if the selected genes were pathogen-inducible and therefore potentially defence-related. The gene-specific primers utilised in the real-time PCR analyses were obtained from Sigma-Aldrich Inc. (St Louis, USA) as a Primer Library for Arabidopsis Pathogen-Inducible Genes. The pathogen-inducible and housekeeping genes in the library were selected based on searches of an Arabidopsis database and publicly available microarray analyses (Tao et al., 2003 amongst others). For genes absent from the primer library, primers were designed with the help of PRIMER3 software (Rozen and Skaletsky, 2000) to span an intron resulting in distinguishable amplicon sizes from cDNA and genomic DNA to monitor putative contamination. Two different RNA samples were isolated per plant line and cDNA was synthesized from the total RNA derived from the respective samples. The cDNA was checked for genomic DNA contamination (results not shown) and equal amounts were used as templates for the real-time PCR analyses. Each sample was run in triplicate and melt curve analysis confirmed that the individual amplified products corresponded to a single, gene-specific cDNA fragment (results not shown). The expression level of each gene was quantified with the Corbett RotorGene software (version 6.0, built 38) using a standard curve of pooled cDNA samples. Relative expression was obtained by normalizing expression of the genes of interest to those of the housekeeping genes, actin-2 (At3g18780) and ubiquitin ligase (At5g25760), which showed constant expression regardless of the infection state or the genotypes of the

samples. The amplification efficiency of each reaction was 100% ± 20%. Data shown in the two graphs for each gene were obtained in separate experiments and hence cannot be directly compared.

Based on the obtained quantitative real-time PCR results, it has been established that *cir1* affects several regulatory defence pathways and hence it is believed that *cir1* operates either fairly high up or at cross-talk points in the Arabidopsis defence signalling network. Furthermore, gene expression in *cir1* supports the previous findings from the double mutant phenotypes described in this chapter. A model of induced gene expression in the *cir1* mutant background which highlights these central themes is presented in Fig. 4.22. The quantitative real-time PCR results of the genes will be discussed in the following sections where relevant genes were arranged in different clusters according to which signalling pathways were activated by *cir1* to regulate their expression.

SA-dependent gene expression in *cir1*

Of all the selected genes that were up regulated in *cir1*, only one was regulated solely by the SA signalling pathway with its expression being dependent on EDS1, PAD4 and NPR1 (presented in blue, Fig. 4.22). *At5g10760* encodes an aspartyl protease family protein with a possible role in plant-microbe interactions since it was up regulated after *H. parasitica* infection, where it forms part of the *RPP4*-mediated defence response (Eulgem et al., 2004). The quantitative real-time PCR results for *At5g10760* are summarised in Fig. 4.11

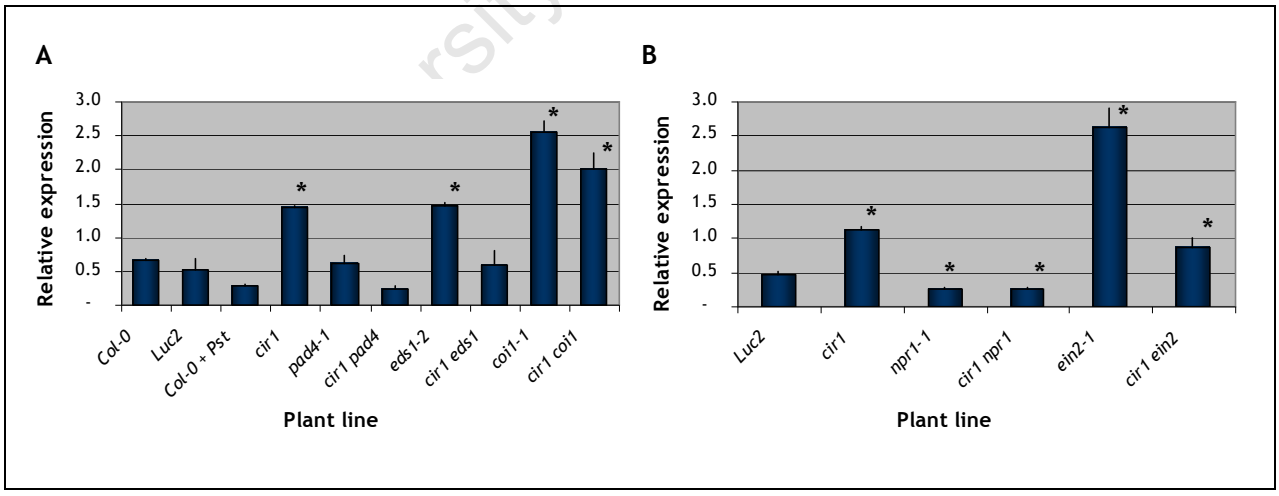

Figure 4.11. Relative expression of *At5g10760* in *cir1* and *cir1* double mutant lines.
Total RNA was extracted from leaves of four-week-old (**A**) Col-0, *Luc2*, Col-0 infected with *Pst* DC3000 and harvested 24 h post infection, *cir1*, *pad4-1*, *cir1 pad4*, *eds1-2*, *cir1 eds1*, *coi1-1*, *cir1 coi1* and (**B**) *Luc2*, *cir1*, *npr1-1*, *cir1 npr1*, *ein2-1*, *cir1 ein2* plants. cDNA was reverse transcribed from total RNA and equal amounts were used as templates for quantitative real-time PCR. The level of expression was quantified with Corbett RotorGene software (version 6.0, built 38) using a standard curve of pooled cDNA samples. Bars represent the relative expression obtained by normalizing expression to that of actin-2 (At3g18780) or the ubiquitin ligase (At5g25760). Error bars represent the standard

error between values at the 95% confidence level. Asterisks indicate a significant difference in relative gene expression compared to expression levels in *Luc2* plants (Student's *t*-test, $P < 0.05$).

Interestingly, it seems that *At5g10760* does not play a significant role in defence responses to *P. syringae* infection as expression was not induced in the Col-0 sample treated with *Pst* DC3000 (Fig. 4.11A). The microarray results indicated that *At5g10760* was not up regulated in *cir1* but showed increased expression in *cir1 ein2* and/or *cir1 coi1* compared to *Luc2* (S. L. Murray, personal communication). In addition to *cir1 coi1* (Fig. 4.11A) and *cir1 ein2* (Fig. 4.11B) displaying amplified *At5g10760* expression compared to *Luc2*, this gene was also up regulated in the *cir1* mutant in these experiments (Fig. 4.11A and B). The wild-type levels of expression in *cir1 pad4* and *cir1 eds1* (Fig. 4.11A) suggest that the augmented expression in *cir1* is dependent on PAD4 as well as EDS1. Furthermore, expression levels markedly lower than that of *Luc2* were observed in both the *npr1-1* and *cir1 npr1* samples (Fig. 4.11B). As *At5g10760* expression in both these samples was significantly lower than that of *cir1* (statistics not shown), it suggests that the induced expression in *cir1* relies on NPR1. In addition, the relative expression levels in *cir1 coi1* were not significantly different from levels present in either the *cir1* or *coi1-1* single mutants (statistics not shown), suggesting that pertaining to the *cir1* mutation, *At5g10760* expression occurs independently of COI1. Similarly, the expression levels in *cir1* and *cir1 ein2* (Fig. 4.11B) are statistically comparable (statistics not shown) and therefore increased expression of *At5g10760* in *cir1* is independent of EIN2.

cir1 regulates the SA and ET signalling pathways concurrently

The regulation of gene expression in this cluster requires the combination of the SA and ET signalling pathways (presented in red, Fig. 4.22). However, the genes are further divided in two groups based on the effect of the JA signalling pathway on their expression in the *cir1* background. COI1, and hence the JA signalling pathway, has no effect on the expression of the first group of genes, whereas the expression of the second group of genes is suppressed by COI1 in the *cir1* background.

The regulation of *At2g31880*, *At4g03450*, *NIMIN-2* and possibly *AtGSTF3* expression in *cir1* classifies these genes in the first group within this cluster (presented in red, Fig. 4.22). The relative expression levels of these genes obtained through quantitative real-time PCR analyses are presented in Fig. 4.12. Even though they did not display the same level of up regulation, their expression levels were significantly higher in *cir1* than in *Luc2* suggesting that their induced expression might be correlated with the disease resistance phenotype of *cir1* (Fig. 4.12). The up regulation of *At2g31880*, *At4g03450* and *AtGSTF3* in *cir1* was similar to that observed in the *Pst* DC3000-treated Col-0 samples (Fig. 4.12A, C and G) whereas the induction of *NIMIN-2* expression were noticeably lower in *cir1* than in the Col-0 samples

infected with *Pst* DC3000 (Fig. 4.12E). In general, the relative expression levels of the genes in *cir1 pad4*, *cir1 eds1*, *cir1 npr1* and *cir1 ein2* were similar to wildtype (Fig. 4.12) and reduced in comparison to *cir1*, whereas no significant differences between the expression levels in *cir1* and *cir1 coi1* could be established (Fig. 4.12A, C, E and G). Consequently, the increased expression of these genes in *cir1* is dependent on PAD4, EDS1, NPR1 and EIN2 but independent of COI1. It therefore appears that *cir1* regulates the SA and ET signalling pathways in concert resulting in amplified expression of the abovementioned genes which are unaffected by antagonistic effect of the JA-dependent signalling pathway.

At2g31880 encodes a putative LRR transmembrane protein kinase which has also been classified as a member of the LRR class of RLK encoding genes (Diévart and Clark, 2003). The expression of *At2g31880* was rapidly induced in samples treated with the PAMP, flg22, suggesting that At2g31880 may have a role in PAMP-triggered and basal defence (Navarro et al., 2004). Despite a notable increase in expression, the expression levels of *At2g31880* were not significantly higher in the *Pst* DC3000-infected sample than wildtype (Fig. 4.12A). Although the higher expression levels are not significant in this case, it correlates with the increased *At2g31880* expression previously observed after virulent *P. syringae* treatment (Glazebrook et al., 2003).

At4g03450 encodes an ankyrin repeat family protein with a possible role as an ankyrin-transmembrane protein (Becerra et al., 2004). Although its exact function is still unknown, it could have a role in plant defence to necrotrophs as its expression was induced in wild-type plants treated with *B. cinerea* (AbuQamar et al., 2006). The significant increase in expression of *At4g03450* in response to virulent *P. syringae* treatment (Fig. 4.12C) confirms that *At4g03450* is an SA-dependent defence-related gene (Glazebrook et al., 2003).

NPR1, also known as NIM1, is a crucial positive regulator of SA-induced *PR* gene expression and SAR (Cao et al., 1994; Delaney et al., 1995). NIM1-interacting protein 2 (NIMIN-2) was found to interact with NPR1 in a yeast two-hybrid system (Weigel et al., 2001) and it was therefore suggested that NIMIN proteins are involved in the signalling pathway resulting in SAR (Weigel et al., 2001). The expression of *NIMIN-2* was considerably up regulated in the *Pst* DC3000–treated sample (Fig. 4.12E) corresponding to findings that *NIMIN-2* is a defence related gene induced upon virulent *P. syringae* infection (Glazebrook et al., 2003). *NIMIN-2* expression in *cir1 ein2* was the exception to the expression patterns of the other genes in this cluster as it was significantly higher than wildtype (Fig. 4.12F). However, statistically *NIMIN-2* expression in *cir1 ein2* was still drastically lower than in *cir1* (statistics not shown).

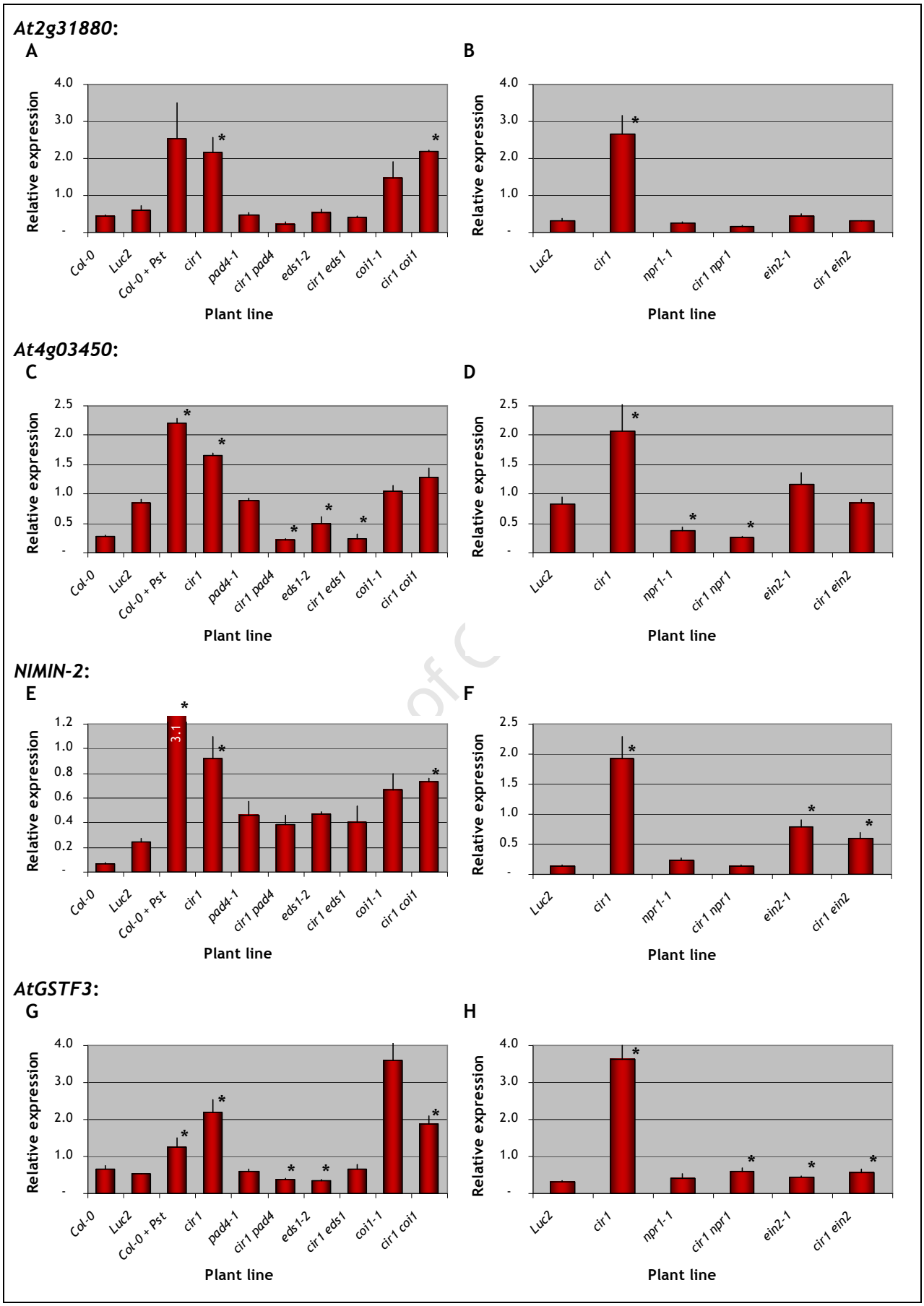

Figure 4.12. Relative expression of *At2g31880*, *At4g03450*, *NIMIN-2* and *AtGSTF3* in *cir1* and *cir1* double mutant lines.

Total RNA was extracted from leaves of four-week-old (**A**, **C**, **E**, **G**) Col-0, *Luc2*, Col-0 infected with *Pst* DC3000 and harvested 24 h post infection, *cir1*, *pad4-1*, *cir1 pad4*, *eds1-2*, *cir1 eds1*, *coi1-1*, *cir1 coi1* and (**B**, **D**, **F**, **H**) *Luc2*, *cir1*, *npr1-1*, *cir1 npr1*, *ein2-1*, *cir1 ein2* plants. cDNA was reverse transcribed from total RNA and equal amounts were used as templates for quantitative real-time PCR. The level of expression was quantified with Corbett RotorGene software (version 6.0, built 38) using a standard curve of pooled cDNA samples. Bars represent the relative expression obtained by normalizing expression to that of actin-2 (At3g18780) or the ubiquitin ligase (At5g25760). Error bars represent the standard error between values at the 95% confidence level. Asterisks indicate a significant difference in relative gene expression compared to expression levels in *Luc2* plants (Student's *t*-test, $P < 0.05$).

Another gene that possibly requires the combination of the SA and ET signalling pathways for regulation, is *AtGSTF3* (presented in red, Fig. 4.22). Previously known as *GST16*, it belongs to the Phi class of GSTs which is often differentially regulated in response to biotic and abiotic stresses (Wagner et al., 2002). *AtGSTF3* was induced after infection with virulent *P. syringae* (Glazebrook et al., 2003) but showed no increased expression in response to *Pst* DC3000 AvrRpt2 (Lieberherr et al., 2003) which could suggest that it has a role in basal defence responses. *AtGSTF3* was categorized as a Cluster C gene which is regulated by an unknown pathway that functions separately from the SA signalling pathway, and by the JA/ET pathways (Fig. 4.10; Glazebrook et al., 2003). It is known that PAD4 and NPR1 are involved in the regulation of Cluster C genes through the unknown signalling pathway (Fig. 4.10; Glazebrook et al., 2003), however the role of EDS1 in this pathway has not yet been determined. The expression of *AtGSTF3* in *cir1* was dependent on PAD4, NPR1 and EDS1 (Fig. 4.12G and H) indicating that EDS1 is involved in regulation of this Cluster C gene. However, the *pad4-1* and *npr1-1* mutations in the *cir1* background also affect the expression of the SA-regulated genes in Cluster A (Fig. 4.12A to F; Glazebrook et al., 2003) making it difficult to distinguish between the expression patterns of Cluster A and C genes in *cir1*. To conclusively establish if EDS1 has a role in the unknown signalling pathway and hence if the unknown signalling pathway has a regulatory role in the expression of *ATGSTF3*, additional experiments need to be conducted. By comparing the expression of Cluster A and C genes in mutants that distinguish between the two pathways such as *sid2*, which affects only Cluster A genes, and *pad2*, which affects genes in both Cluster A and C (Glazebrook et al., 2003), the possible role of EDS1 in the unknown pathway could be further elucidated.

Thus, based on the obtained quantitative real-time PCR results, it is not possible to establish if PAD4, NPR1 and EDS1 functioned in the unknown signalling pathway (dashed lines, Fig. 4.22) or in the SA-dependent signalling pathway (blue lines, Fig. 4.22) during the expression of the *AtGSTF3* in *cir1*. The expression of *AtGSTF3* in the *cir1* background is therefore regulated by the ET signalling pathway in combination with either the SA (red

lines, Fig. 4.22) or unknown signalling pathway (dashed lines, Fig. 4.22). Both scenarios have been incorporated in the *cir1* regulation model with *AtGSTF3* presented in red and in black (Fig. 4.22) where it might belong to a potential fourth cluster.

The second group genes in this cluster are regulated through simultaneous activation of the SA and ET pathways by *cir1* but their expression is inhibited by COI1 in the *cir1* background. *Cir1* activates the SA signalling pathway to regulate the expression of *ZAT7*, *AtLEA5* and *PR-1* while the ET signalling pathway has a role in the maximal expression of these genes in the *cir1* background (presented in red, Fig. 4.22). Fig. 4.13 presents the relative expression levels of these genes in *cir1* and the *cir1* double mutant lines.

All genes were significantly up regulated in *cir1*, whereas the expression pattern of these genes in *cir1 pad4*, *cir1 eds1*, *cir1 npr1* and *cir1 ein2* generally displayed wild-type levels (Fig. 4.13), demonstrating that the amplified expression of these genes in *cir1* is dependent on PAD4, EDS1, NPR1 and EIN2. However, in contrast to the other double mutants lines, *cir1 coi1* showed expression levels significantly higher than that of *cir1* (Fig. 4.13A, C and E). This suggests that COI1 suppresses *ZAT7*, *AtLEA5* and *PR-1* expression in *cir1* and through the *coi1-1* mutation the inhibitory effect is lifted. Since JA signalling has an antagonistic effect on the SA signalling pathway (Glazebrook, 2005; Thatcher et al., 2005), the lack of JA signalling in the *cir1 coi1* mutant presumably resulted in the induction of the SA signalling pathway and therefore an increase in expression. In summary, the increased expression of these genes in *cir1* occurs through the simultaneous activation of the SA and ET signalling pathways, with activation of the JA signalling pathway dampening expression.

The zinc finger protein ZAT7 has an important role in Arabidopsis defence responses to abiotic stress conditions such as salinity stress (Ciftci-Yilmaz et al., 2007) but it is also involved in biotic stress responses as its expression is induced in wild-type plants following *B. cinerea* infection (AbuQamar et al., 2006). Interestingly, *ZAT7* was drastically induced in response to infection by virulent *P. syringae* (Fig. 4.13A) suggesting that ZAT7 might not only be involved in defence responses to *Botrytis* infections, but could also play a role in basal defence against biotrophic pathogens.

The Arabidopsis late embryogenesis abundant-like protein 5, AtLEA5, was recently identified in a screen to detect genes involved in plant tolerance to oxidative stress (Mowla et al., 2006). AtLEA5 is also known as senescence-associated gene 21 (SAG21), a potential genetic target of Whirly transcription factors which regulate the expression of various defence-related genes (Desveaux et al., 2005). It appears that AtLEA5 does not only have a role in protection against oxidative stress (Mowla et al., 2006), but could possibly be involved in basal defence since *AtLEA5* expression is considerably up regulated after virulent *Pst* DC3000 treatment (Fig. 4.13C).

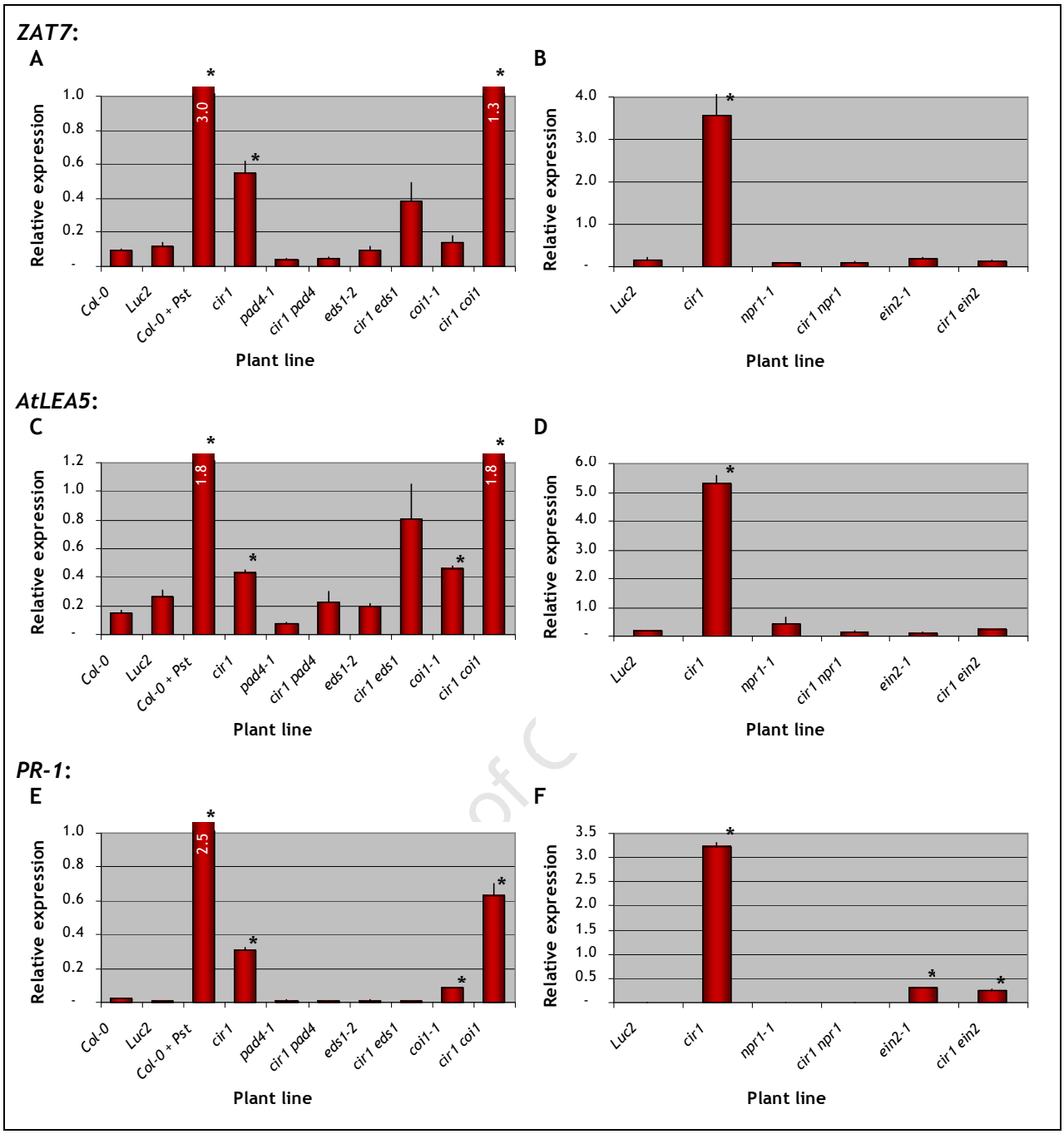

Figure 4.13. Relative expression of *ZAT7*, *AtLEA5* and *PR-1* in *cir1* and *cir1* double mutant lines. Total RNA was extracted from leaves of four-week-old (**A**, **C**, **E**) Col-0, *Luc2*, Col-0 infected with *Pst* DC3000 and harvested 24 h post infection, *cir1*, *pad4-1*, *cir1 pad4*, *eds1-2*, *cir1 eds1*, *coi1-1*, *cir1 coi1* and (**B**, **D**, **F**) *Luc2*, *cir1*, *npr1-1*, *cir1 npr1*, *ein2-1*, *cir1 ein2* plants. cDNA was reverse transcribed from total RNA and equal amounts were used as templates for quantitative real-time PCR. The level of expression was quantified with Corbett RotorGene software (version 6.0, built 38) using a standard curve of pooled cDNA samples. Bars represent the relative expression obtained by normalizing expression to that of actin-2 (At3g18780) or the ubiquitin ligase (At5g25760). Error bars represent the standard error between values at the 95% confidence level. Asterisks indicate a significant difference in relative gene expression compared to expression levels in *Luc2* plants (Student's *t*-test, $P < 0.05$).

The expression of *PR-1* is dependent on SA and it is commonly used as marker of SA-dependent defence responses (Uknes et al., 1992; Glazebrook et al., 2003). As expected *PR-1* was considerably up regulated in the sample infected with virulent *P. syringae* (Fig. 4.13E). The expression of *PR-1* was induced in *cir1* according to microarray (S. L. Murray, personal communication) and other results (Murray et al., 2002), however it has been found that not all *cir1* plants display augmented expression of *PR-1* (Fig. 3.7B). In this case, *PR-1* was constitutively expressed in *cir1* (Fig. 4.13E and F). *PR-1* expression in *cir1 ein2* was the exception to the expression profile of this cluster as expression levels were higher compared to wildtype (Fig. 4.13F). However, similar to the findings of Murray et al. (2002), *PR-1* expression in *cir1 ein2* remained significantly lower than that of *cir1* (result not shown). In previous studies, it was established that JAR1 contributes to augmented *PR-1* expression in *cir1* since the *jar1* mutation reduced *PR-1* expression in *cir1 jar1* (Murray et al., 2002). Interestingly, *coi1-1* had the opposite effect suggesting that COI1 suppresses *PR-1* expression in *cir1*. These opposing effects could be due to JAR1 not being required for all jasmonate responses (Staswick et al., 2002) resulting in different behaviour to COI1 in the *cir1* background, which highlights the complexity of gene regulation in the plant defence network.

At3g16530 was classified in the second group of this cluster as it is also regulated by the SA and ET signalling pathways and its expression is inhibited by COI1. *At3g16530*, which encodes a lectin-like protein, is up regulated in response to chitin addition (Zhang et al., 2002) where chitin acts as a general elicitor that has been linked to defence responses in plants, especially against fungal pathogens (Ramonell et al., 2005). It appears therefore that this gene might have role in plant defence against certain fungal pathogens. The quantitative real-time PCR results for this gene are summarised in Fig. 4.14.

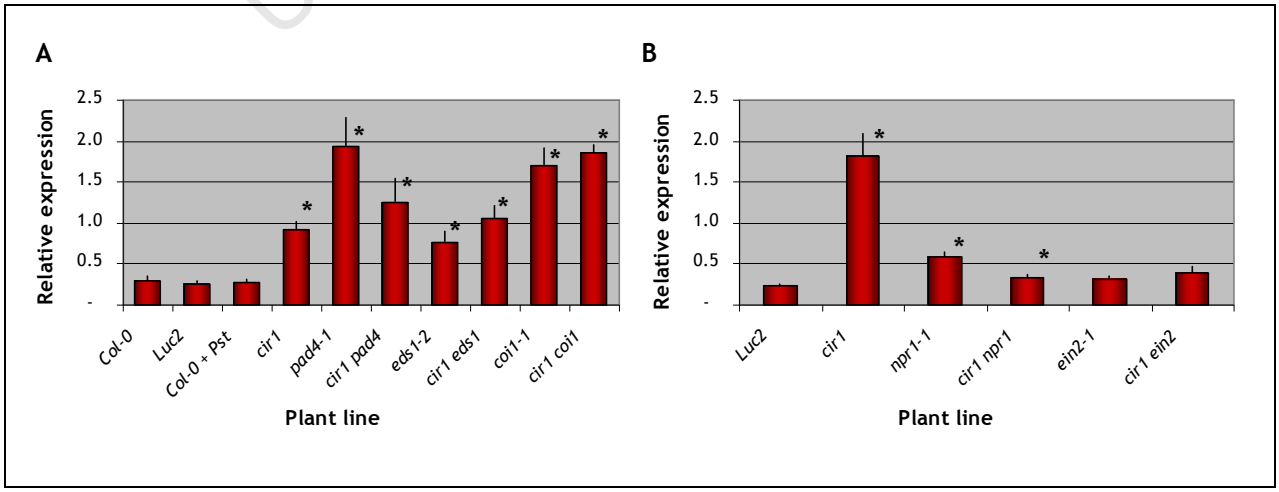

Figure 4.14. Relative expression of *At3g16530* in *cir1* and *cir1* double mutant lines.
Total RNA was extracted from leaves of four-week-old (**A**) Col-0, *Luc2*, Col-0 infected with *Pst* DC3000 and harvested 24 h post infection, *cir1*, *pad4-1*, *cir1 pad4*, *eds1-2*, *cir1 eds1*, *coi1-1*, *cir1 coi1* and (**B**)

Luc2, *cir1*, *npr1-1*, *cir1 npr1*, *ein2-1*, *cir1 ein2* plants. cDNA was reverse transcribed from total RNA and equal amounts were used as templates for quantitative real-time PCR. The level of expression was quantified with Corbett RotorGene software (version 6.0, built 38) using a standard curve of pooled cDNA samples. Bars represent the relative expression obtained by normalizing expression to that of actin-2 (At3g18780) or the ubiquitin ligase (At5g25760). Error bars represent the standard error between values at the 95% confidence level. Asterisks indicate a significant difference in relative gene expression compared to expression levels in *Luc2* plants (Student's *t*-test, $P < 0.05$).

Although *At3g16530* has been previously described as a defence-related gene (Glazebrook et al., 2003), there was no induction in expression after treatment with *Pst* DC3000 (Fig. 4.14A). *At3g16530* expression is also regulated through the activation of the SA and ET signalling pathways and its expression is inhibited by COI1 in the *cir1* background. However, the regulation of this gene varies from the abovementioned genes concerning the SA signalling pathway since its expression is dependent on NPR1 but not on EDS1 or PAD4. Hence, instead of displaying wild-type expression levels in *cir1 pad4* and *cir1 eds1* as was the case with the other genes in this group, *At3g16530* expression was induced in *cir1 pad4* and *cir1 eds1* (Fig. 4.14A) similar to levels observed in *cir1*. This suggests that the induced expression of *At3g16530* in *cir1* occurs independently of EDS1 and PAD4. Therefore, the expression of *At3g16530* is dependent on EIN2 while NPR1, but not necessarily the SA signalling pathway, also contribute to the augmented expression levels observed *cir1*.

Simultaneous activation of the SA,ET and JA signalling pathways by *cir1*

PR-2 (also known as *BGL2*) encodes pathogenesis-related protein 2, an acidic and apoplastic form of β-1,3-glucanase which is considered as one of the *PR* gene markers of SA-dependent defences in Arabidopsis (Uknes et al., 1992). The expression of *PR-1*, *PR-2* and *PR-5* is mostly regulated by the SA-dependent transduction pathway (Dong, 1998; Glazebrook, 1999), however *PR-2* expression is occasionally uncoupled from *PR-1* expression and SA (Reuber et al., 1998; Nawrath and Metraux, 1999). Previous studies established that *cir1* shows constitutive expression of *PR-1*, *PR-2* and *PR-5* (Murray et al., 2002), however we found that not all *cir1* plants constantly express the endogenous *PR-1* gene (Fig. 3.7B). To determine how *PR-2* expression is regulated in the *cir1* mutant, the expression levels of *PR-2* were determined by quantitative real-time PCR methods (Fig. 4.15).

Corresponding to the microarray data, *PR-2* expression was significantly up regulated in *cir1* (Fig. 4.15A and B). The *cir1 pad4*, *cir1 eds1* and *cir1 npr1* double mutant samples displayed *PR-2* expression levels that resembled wildtype (Fig. 4.15A and B) and was notably lower than that of *cir1* (statistics not shown), indicating that the increased *PR-2* expression in the *cir1* mutant is dependent on PAD4, EDS1 and NPR1. Unexpectedly, the reduced expression levels in *cir1 coi1* and *cir1 ein2* compared to *cir1* indicate that COI1 and EIN2 are required for the induction of *PR-2* in *cir1*. The regulation of *PR-2* expression in *cir1* is

therefore different to that of *PR-1*, with some aspects of its regulation being uncoupled from the SA signalling pathway. It therefore appears that the SA, JA and ET signalling pathways contribute in combination to constitutively induced *PR-2* expression in *cir1*.

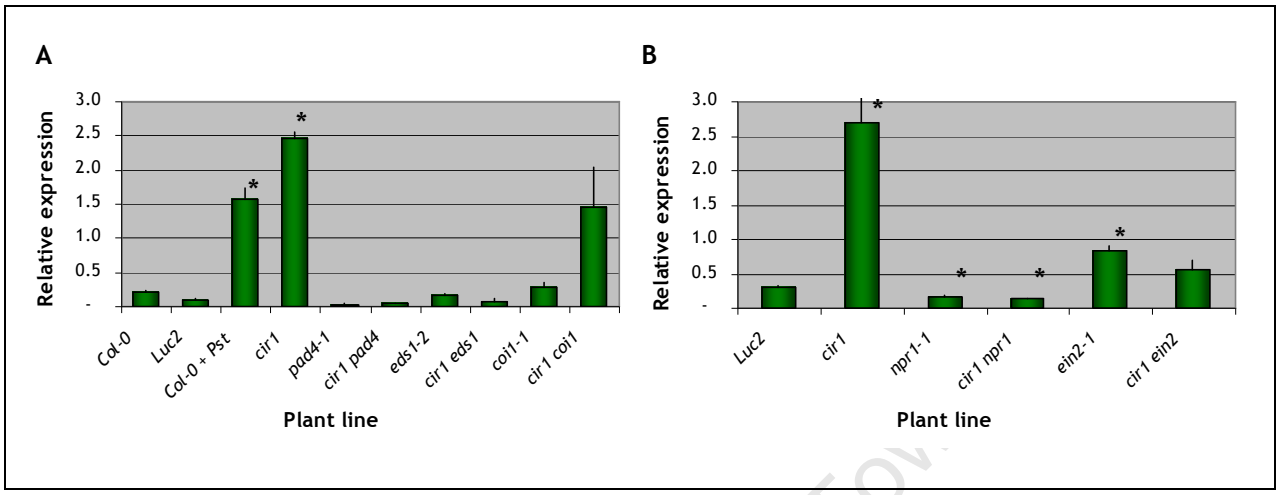

Figure 4.15. Relative expression of *PR-2* in *cir1* and *cir1* double mutant lines.
Total RNA was extracted from leaves of four-week-old (**A**) Col-0, *Luc2*, Col-0 infected with *Pst* DC3000 and harvested 24 h post infection, *cir1*, *pad4-1*, *cir1 pad4*, *eds1-2*, *cir1 eds1*, *coi1-1*, *cir1 coi1* and (**B**) *Luc2*, *cir1*, *npr1-1*, *cir1 npr1*, *ein2-1*, *cir1 ein2* plants. cDNA was reverse transcribed from total RNA and equal amounts were used as templates for quantitative real-time PCR. The level of expression was quantified with Corbett RotorGene software (version 6.0, built 38) using a standard curve of pooled cDNA samples. Bars represent the relative expression obtained by normalizing expression to that of actin-2 (At3g18780) or the ubiquitin ligase (At5g25760). Error bars represent the standard error between values at the 95% confidence level. Asterisks indicate a significant difference in relative gene expression compared to expression levels in *Luc2* plants (Student's *t*-test, $P < 0.05$).

Even though *PDF1.2* was not originally included in Cluster B (Glazebrook et al., 2003), *PDF1.2* is a known marker of the JA/ET-dependent signalling pathways (Murray et al., 2002; Mengiste et al., 2003; Veronese et al., 2004). In addition, *PDF1.2* expression is induced by *B. cinerea* and thought to mediate resistance to this pathogen (Penninckx et al., 1998). However, increased expression of *PDF1.2* does not necessarily correlate with resistance to *B. cinerea* as susceptible mutants displayed normal expression levels of *PDF1.2* (Ferrari et al., 2003; Veronese et al., 2004). *Cir1* has shown constitutive expression of *PDF1.2* (Murray et al., 2002) and to determine what effect the double mutants would have on its expression, this gene was included in the quantitative real-time PCR experiments (Fig. 4.16).

PDF1.2 did not qualify as a defence-related gene in the study of Glazebrook et al. (2003) and our results correlate with these findings as the *Pst* DC3000-treated Col-0 sample did not display expression levels different from wildtype (Fig. 4.16A). Comparable to *PR-2*, *PDF1.2* expression in *cir1* is also regulated through the activation of the SA, JA and ET signalling pathways. However, the regulation of *PDF1.2* expression in *cir1* regarding the SA signalling

pathway fluctuates from that of *PR-2* in that only NPR1, and not EDS1 or PAD4, are required for induced expression.

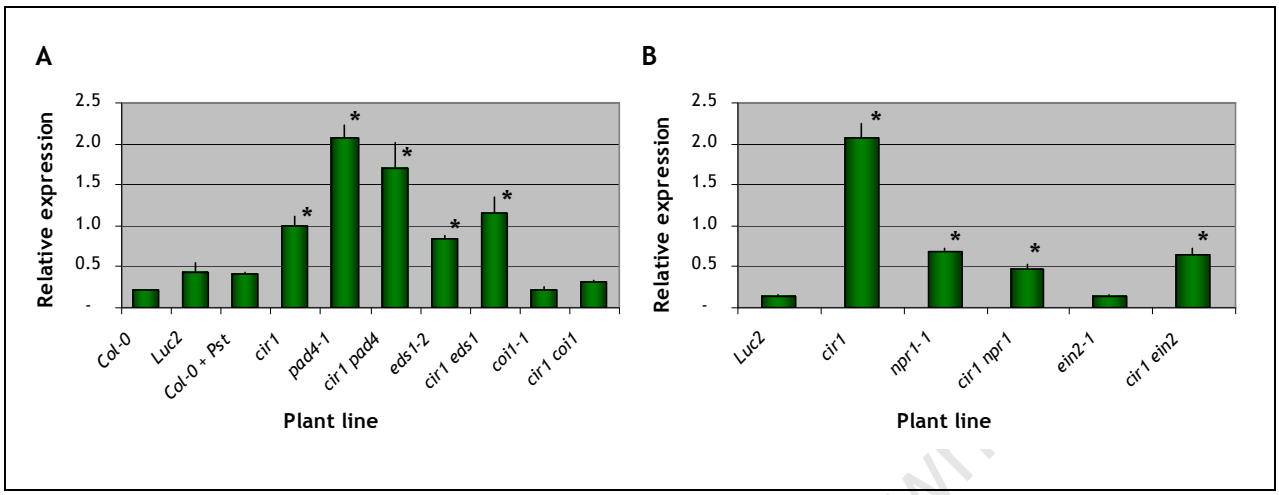

Figure 4.16. Relative expression of *PDF1.2* in *cir1* and *cir1* double mutant lines.
Total RNA was extracted from leaves of four-week-old (**A**) Col-0, *Luc*2, Col-0 infected with *Pst* DC3000 and harvested 24 h post infection, *cir1*, *pad4-1*, *cir1 pad4*, *eds1-2*, *cir1 eds1*, *coi1-1*, *cir1 coi1* and (**B**) *Luc2*, *cir1*, *npr1-1*, *cir1 npr1*, *ein2-1*, *cir1 ein2* plants. cDNA was reverse transcribed from total RNA and equal amounts were used as templates for quantitative real-time PCR. The level of expression was quantified with Corbett RotorGene software (version 6.0, built 38) using a standard curve of pooled cDNA samples. Bars represent the relative expression obtained by normalizing expression to that of actin-2 (At3g18780) or the ubiquitin ligase (At5g25760). Error bars represent the standard error between values at the 95% confidence level. Asterisks indicate a significant difference in relative gene expression compared to expression levels in *Luc2* plants (Student's *t*-test, $P < 0.05$).

Confirming earlier studies (Murray et al., 2002), *cir1* had significantly higher *PDF1.2* expression than *Luc*2 (Fig. 4.16A and B) and likewise, the *cir1 pad4* and *cir1 eds1* double mutants displayed *PDF1.2* expression levels similar to *cir1* (Fig. 4.16A), suggesting that the induced expression in *cir1* is not dependent on EDS1 and PAD4. As previously shown (Murray et al., 2002), the induced expression of *PDF1.2* was drastically reduced by the introduction of *npr1-1* and *ein2-1* in the *cir1* background (Fig. 4.16B), demonstrating that NPR1 and EIN2 are both necessary for enhanced *PDF1.2* expression. Furthermore, *cir1 coi1* had dramatically lower *PDF1.2* expression levels than *cir1*, indicating that induced *PDF1.2* expression in *cir1* is also dependent on COI1.

Genes not activated or down regulated by *cir1*

The expression of the following genes was either not induced or was down regulated in the *cir1* mutant background. It has to be noted that the relative expression of the selected genes was determined only at a single time point and that the regulation of their expression might occur at different times. Therefore, it is possible that the regulation of certain genes

might be missed at the selected time point. *At2g14560* which was recently described as *LURP1* (Knoth et al., 2007) as it shows a pattern of late up regulation in response to *H. parasitica* infection where it has a role in disease resistance mediated by *RPP4*, *RPP7* and *RPP8* as well as in basal resistance against virulent isolates (Eulgem et al., 2004; Knoth et al., 2007). The relative expression levels of *LURP1* obtained through quantitative real-time PCR analyses is presented in Fig. 4.17.

Interestingly, expression levels were higher in the *Pst* DC3000-infected Col-0 sample, signifying that LURP1 could also be involved in basal resistance against *P. syringae* (Fig. 4.17A). Although these results are problematic and need to be repeated, it appears that *LURP1* is up regulated in *cir1* as both experiments displayed a similar trend. *LURP1* was significantly up regulated in *cir1* compared to the *Luc2* sample in the first experiment (Fig. 4.17A) and *cir1* displayed increased expression in the second experiment (Fig. 4.17B). However, gene expression was variable in the second experiment and hence no statistical significant difference between the relative expression levels of *cir1* and *Luc2* could be established (Fig. 4.17B). *LURP1* expression in *cir1 npr1* and *cir1 ein2* were higher than wildtype (Fig. 4.17B) and not significantly different from that of *cir1* (statistics not shown), suggesting that neither NPR1 nor EIN2 are not involved in the regulation of *LURP1* expression in *cir1*. Furthermore, the expression levels of *cir1 pad4*, *cir1 eds1* and *cir1 coi1* were not significantly different from wild-type levels (Fig. 4.17A) suggesting that the high relative expression of *LURP1* in *cir1* requires PAD4, EDS1 and COI1. Therefore, the data is suggestive that the JA- and SA-dependent but NPR1-independent signalling pathways are activated by *cir1* to regulate the expression of *LURP1*.

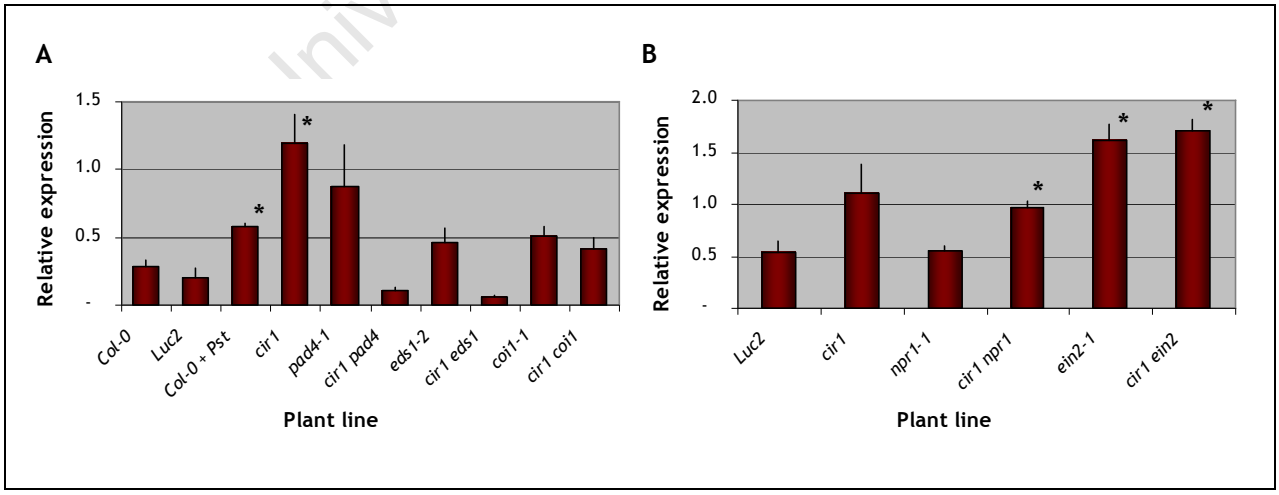

Figure 4.17. Relative expression of *LURP1* in *cir1* and *cir1* double mutant.

Total RNA was extracted from leaves of four-week-old (**A**) Col-0, *Luc2*, Col-0 infected with *Pst* DC3000 and harvested 24 h post infection, *cir1*, *pad4-1*, *cir1 pad4*, *eds1-2*, *cir1 eds1*, *coi1-1*, *cir1 coi1* and (**B**) *Luc2*, *cir1*, *npr1-1*, *cir1 npr1*, *ein2-1*, *cir1 ein2* plants. cDNA was reverse transcribed from total RNA and equal amounts were used as templates for quantitative real-time PCR. The level of expression

was quantified with Corbett RotorGene software (version 6.0, built 38) using a standard curve of pooled cDNA samples. Bars represent the relative expression obtained by normalizing expression to that of actin-2 (At3g18780) or the ubiquitin ligase (At5g25760). Error bars represent the standard error between values at the 95% confidence level. Asterisks indicate a significant difference in relative gene expression compared to expression levels in *Luc2* plants (Student's *t*-test, $P < 0.05$).

The following two genes were grouped together as they displayed similar expression patterns. Very little information is currently available on the first gene, *At1g10140*. According to "The Arabidopsis Information Resource" (TAIR, http://www.arabidopsis.org), it encodes an unknown protein of which the molecular function and biological processes that it could be involved in are yet to be determined. The second gene, *CYP91A2* (cytochrome P450 monooxygenase 91A2; also known as *CYP81F1*) belongs to the group of haem-containing proteins that catalyse a variety of oxidative reactions (Chapple, 1998). Cytochrome P450s have important roles in higher plants where they are involved in the biosynthesis of various endogenous compounds such phytoalexins and fatty acids (Donaldson and Luster, 1991; Bolwell et al., 1994). It is known that *CYP91A2* expression was unchanged after infection with *A. brassicicola* or *Alternaria alternata* (Narusaka et al., 2004). Both *At1g10140* and *CYP91A2* have possible roles in plant defence responses as treatment with virulent *P. syringae* resulted in drastically induced expression (Fig. 4.18A and C; Glazebrook et al., 2003). Yet these genes are some of the few defence-related genes which were not up regulated in *cir1* since expression levels in *cir1* were not significantly different from those of *Luc2* (Fig. 4.18A to D). As the expression of *At1g10140* and *CYP91A2* were not up regulated in *cir1*, their expression patterns do not provide information regarding the signalling pathways activated in the *cir1* mutant and therefore the additional results presented in Fig. 4.18 will not be discussed.

Unfortunately, consistent results could not be obtained regarding the expression of *BG-3* in *cir1* and the double mutant lines (results not shown). Hence the results will not be discussed and *BG-3* has been excluded from the quantitative real-time PCR analysis.

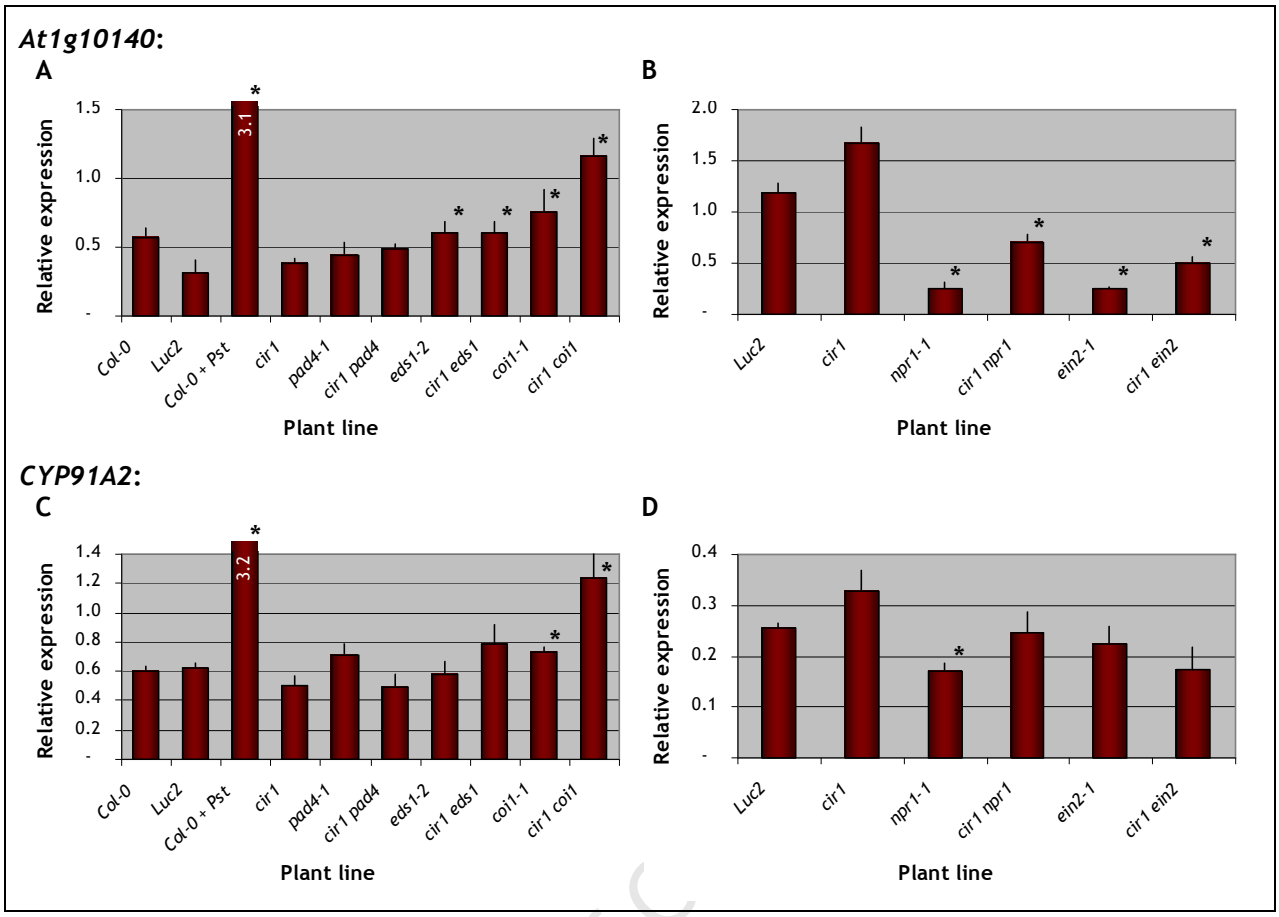

Figure 4.18. Relative expression of *At1g10140* and *CYP91A2* in *cir1* and *cir1* double mutant lines. Total RNA was extracted from leaves of four-week-old (**A, C**) Col-0, *Luc2*, Col-0 infected with *Pst* DC3000 and harvested 24 h post infection, *cir1*, *pad4-1*, *cir1 pad4*, *eds1-2*, *cir1 eds1*, *coi1-1*, *cir1 coi1* and (**B, D**) *Luc2*, *cir1*, *npr1-1*, *cir1 npr1*, *ein2-1*, *cir1 ein2* plants. cDNA was reverse transcribed from total RNA and equal amounts were used as templates for quantitative real-time PCR. The level of expression was quantified with Corbett RotorGene software (version 6.0, built 38) using a standard curve of pooled cDNA samples. Bars represent the relative expression obtained by normalizing expression to that of actin-2 (At3g18780) or the ubiquitin ligase (At5g25760). Error bars represent the standard error between values at the 95% confidence level. Asterisks indicate a significant difference in relative gene expression compared to expression levels in *Luc2* plants (Student's *t*-test, $P < 0.05$).

Three of the selected genes were down regulated in *cir1* at the tested time point. One of these is ACD6 (accelerated cell death 6) which has been described as a positive regulator of the defence network, possibly through the modulation of the SA-dependent signalling pathway (Lu et al., 2005). The relative expression levels of *ACD6* in *cir1* and the *cir1* double mutant lines are presented in Fig. 4.19. In this case *ACD6* expression behaved in an unexpected manner. It is known that the expression of *ACD6* is induced by SA together with light and by *P. syringae* or *H. parasitica* infections (Eulgem et al., 2004; Lu et al., 2005). However, based on our quantitative real-time PCR results, *ACD6* expression was notably

decreased in *Pst* DC3000-treated Col-0 (Fig. 4.19A) and *cir1* (Fig. 4.19A and B). The results suggest that COI1 might be involved in the regulation of *ACD6* expression since expression levels in *cir1 coi1* resembles that of wildtype (Fig. 4.19A) and not of *cir1* (statistics not shown). Although the difference between *cir1* and *cir1 coi1* is not significant, it appears that COI1 has a suppressing effect on *ACD6* expression in *cir1* suggesting that the JA signalling pathway somehow regulates expression of *ACD6* in the *cir1* mutant background, possibly through inhibiting the SA signalling pathway.

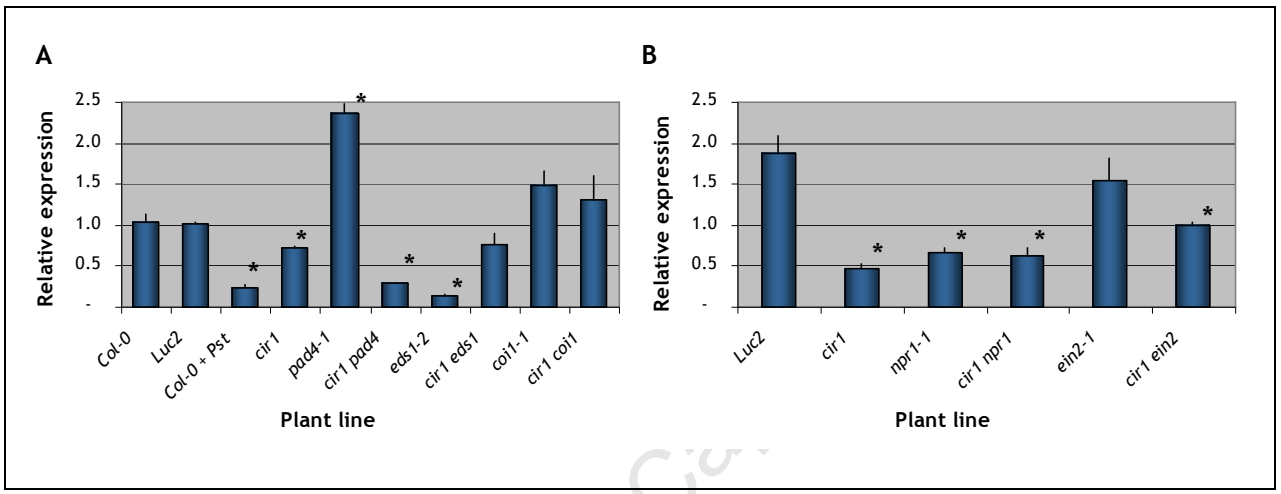

Figure 4.19. Relative expression of *ACD6* in *cir1* and *cir1* double mutant lines.
Total RNA was extracted from leaves of four-week-old (**A**) Col-0, *Luc2*, Col-0 infected with *Pst* DC3000 and harvested 24 h post infection, *cir1*, *pad4-1*, *cir1 pad4*, *eds1-2*, *cir1 eds1*, *coi1-1*, *cir1 coi1* and (**B**) *Luc2*, *cir1*, *npr1-1*, *cir1 npr1*, *ein2-1*, *cir1 ein2* plants. cDNA was reverse transcribed from total RNA and equal amounts were used as templates for quantitative real-time PCR. The level of expression was quantified with Corbett RotorGene software (version 6.0, built 38) using a standard curve of pooled cDNA samples. Bars represent the relative expression obtained by normalizing expression to that of actin-2 (At3g18780) or the ubiquitin ligase (At5g25760). Error bars represent the standard error between values at the 95% confidence level. Asterisks indicate a significant difference in relative gene expression compared to expression levels in *Luc2* plants (Student's *t*-test, $P < 0.05$).

PER50 (peroxidase 50) is a member of the classical class III family of peroxidases that are targeted via the endoplasmic reticulum either extracellularly or to the vacuole. There they function in various roles such as defence, stress and developmentally related processes (Welinder et al., 2002). The quantitative real-time PCR results for *PER50* is presented in Fig. 4.20. In this case, the induction of *PER50* by virulent *P. syringae* was not significantly different from wildtype (Fig. 4.20A). The expression of *PER50* was notably reduced in *cir1* (Fig. 4.20A and B) and *cir1 pad4* compared to *Luc2* (Fig. 4.20A). Since *cir1 pad4* resembled expression levels obtained in *cir1* (statistics not shown), these results suggest that *PER50* expression in *cir1* occurs independently of PAD4. In contrast, *PER50* expression in the *cir1 eds1* and *cir1 coi1* double mutant lines resembled wildtype (Fig. 4.20A) and was

significantly higher than *cir1* (statistics not shown) indicating that EDS1 and COI1 have a negative effect on *PER50* expression in *cir1*, consequently resulting in expression levels notably lower than wildtype (Fig. 4.20A and B). Interestingly, this is one of two occasions where EDS1 and PAD4 function independently of one another in the down regulation of gene expression in *cir1*. Both *cir1 npr1* and *cir1 ein2* displayed markedly diminished expression levels compared to *Luc2* (Fig. 4.20B) and *cir1* (statistics not shown) which suggests that NPR1 and EIN2 act positively on *PER50* expression in *cir1*.

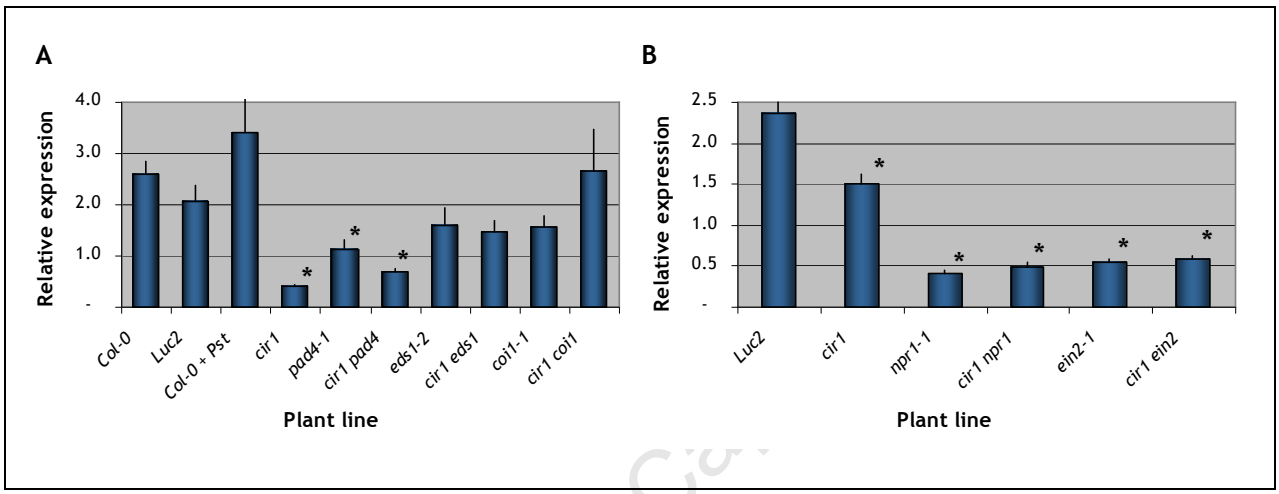

Figure 4.20. Relative expression of *PER50* in *cir1* and *cir1* double mutant.
Total RNA was extracted from leaves of four-week-old (**A**) Col-0, *Luc2*, Col-0 infected with *Pst* DC3000 and harvested 24 h post infection, *cir1*, *pad4-1*, *cir1 pad4*, *eds1-2*, *cir1 eds1*, *coi1-1*, *cir1 coi1* and (**B**) *Luc2*, *cir1*, *npr1-1*, *cir1 npr1*, *ein2-1*, *cir1 ein2* plants. cDNA was reverse transcribed from total RNA and equal amounts were used as templates for quantitative real-time PCR. The level of expression was quantified with Corbett RotorGene software (version 6.0, built 38) using a standard curve of pooled cDNA samples. Bars represent the relative expression obtained by normalizing expression to that of actin-2 (At3g18780) or the ubiquitin ligase (At5g25760). Error bars represent the standard error between values at the 95% confidence level. Asterisks indicate a significant difference in relative gene expression compared to expression levels in *Luc2* plants (Student's *t*-test, $P < 0.05$).

Very little information is available on *At3g47960*, encoding a proton-dependent oligopeptide transport family protein. It is known to have transporter activity and is involved in the biological process of transporting oligopeptides (TAIR, http://www.arabidopsis.org). Fig. 4.21 presents the relative expression levels of *At3g47960* in *cir1* and the *cir1* double mutant lines. The expression of *At3g47960* was dramatically induced in the Col-0 sample infected with *Pst* DC3000 thereby confirming that it is a defence-related gene (Fig. 4.21A; Glazebrook et al., 2003). Few examples exist where defence-related genes were uninduced in *cir1* (Fig. 4.18) but this is only confirmed defence-related gene with expression levels lower in *cir1* than *Luc2* (Fig. 4.21A and B). *At3g47960* expression levels in *cir1 pad4*, *cir1 npr1* and *cir1 ein2* were all lower than that of *Luc2* (Fig. 4.21A and B) and did not show a

notable difference from levels in *cir1* (statistics not shown), demonstrating that *At3g47960* expression in *cir1* occurs independently of PAD4, NPR1 and EIN2. The expression levels in *cir1 eds1* and *cir1 coi1* were significantly higher than *cir1* (statistics not shown), indicating that EDS1 and COI1 have a suppressing effect on the expression of *At3g47960* in *cir1*. Notably, this was the other occasion where the regulatory functions of PAD4 and EDS1 were separated from each other.

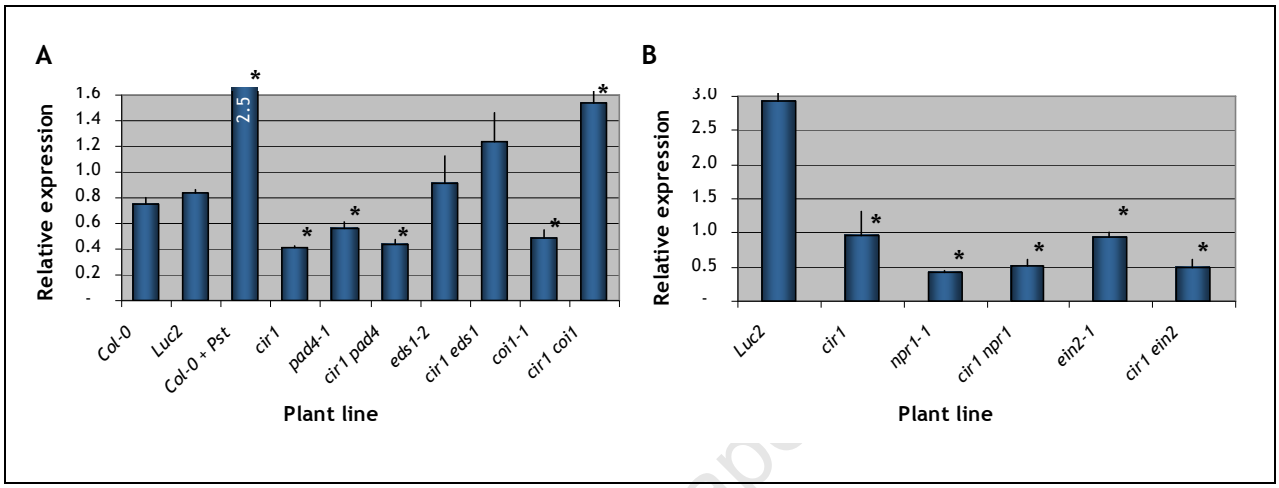

Figure 4.21. Relative expression of *At3g47960* in *cir1* and *cir1* double mutant lines.
Total RNA was extracted from leaves of four-week-old (**A**) Col-0, *Luc2*, Col-0 infected with *Pst* DC3000 and harvested 24 h post infection, *cir1*, *pad4-1*, *cir1 pad4*, *eds1-2*, *cir1 eds1*, *coi1-1*, *cir1 coi1* and (**B**) *Luc2*, *cir1*, *npr1-1*, *cir1 npr1*, *ein2-1*, *cir1 ein2* plants. cDNA was reverse transcribed from total RNA and equal amounts were used as templates for quantitative real-time PCR. The level of expression was quantified with Corbett RotorGene software (version 6.0, built 38) using a standard curve of pooled cDNA samples. Bars represent the relative expression obtained by normalizing expression to that of actin-2 (At3g18780) or the ubiquitin ligase (At5g25760). Error bars represent the standard error between values at the 95% confidence level. Asterisks indicate a significant difference in relative gene expression compared to expression levels in *Luc2* plants (Student's *t*-test, $P < 0.05$).

To summarize, *cir1* activates at least three signalling pathways to up regulate the expression of several defence-related genes (Fig. 4.22.). In the first case, the activation of the SA signalling pathway leads to the induced expression of *At5g10760* (presented in blue, Fig. 4.22). Secondly, *cir1* regulates the SA and ET signalling pathways in concert resulting in the amplified expression of the *At2g31880*, *At4g03450*, *NIMIN-2*, *ZAT7*, *AtLEA5*, *PR-1* and probably *AtGSTF3* (presented in red, Fig. 4.22). These genes are further divided based on the effect of COI1 and the JA signalling pathway on their expression. The expression of *At2g31880*, *At4g03450*, *NIMIN-2* and *AtGSTF3* is unaffected by COI1 whereas *ZAT7*, *AtLEA5*, *PR-1* and *At3g16530* expression is inhibited by COI1 in the *cir1* mutant background. *At3g16530* has also been placed in this group as its regulation by *cir1* is similar to that of *ZAT7*, *AtLEA5* and *PR-1* being dependent on NPR1 and the ET signalling pathway. Lastly, the

SA, ET and JA signalling pathways are concurrently activated by *cir1* to regulate the expression of *PR-2* and *PDF1.2* (presented in green, Fig. 4.22). *PDF1.2* expression is however only dependent on NPR1 and not necessarily on the SA signalling pathway. It is possible that a fourth method, relying on the activation of the unknown and ET signalling pathways for enhanced *AtGSTF3* expression, could exist in *cir1* however at this stage no distinction could be made between the regulation of gene expression by the SA or the unknown signalling pathways.

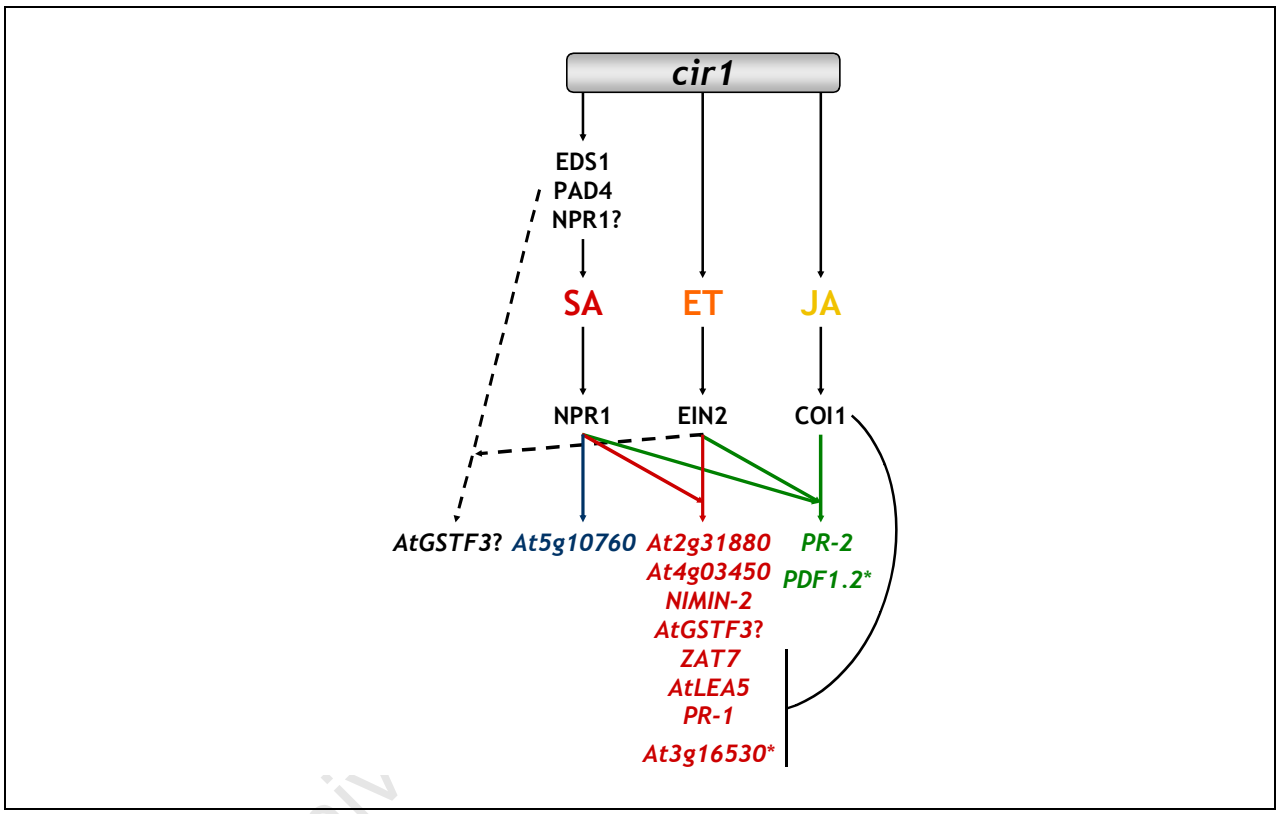

Figure 4.22. A proposed model of *cir1* regulation of the defence signalling pathways leading to induced gene expression.

Based on the quantitative real-time PCR results, genes that were induced in *cir1* could be arranged into three main clusters. In the first cluster (**blue**), the activation of only the SA signalling pathway (**blue line**) by *cir1* leads to the induced expression of *At5g10760* and its expression is dependent on EDS1, PAD4 and NPR1. The second cluster (**red**) consists of several genes whose amplified expression are regulated by *cir1* through both the SA and ET signalling pathways (**red lines**). The expression of these genes require EDS1, PAD4, NPR1 and EIN2 but not COI1. The genes in this cluster can be divided into two groups. The expression of first group, consisting of *At2g31880*, *At4g03450*, *NIMIN-2* and *AtGSTF3*, is unaffected by COI1 and the JA signalling pathway. *ZAT7*, *AtLEA5*, *PR-1* and *At3g16530* belong to the second group whose expression is inhibited by COI1. The asterisk next to *At3g16530* indicates that its expression varies from the rest of the genes in this cluster as it is dependent on NPR1 and EIN2, but not on EDS1 or PAD4. The induced expression of *PR-2* in the third cluster (**green**) are regulated by *cir1* through the combined activity of the SA, ET and JA signalling pathways (**green lines**). EDS1, PAD4, NPR1, EIN2 and COI1 are necessary for augmented expression of this genes. The

asterisk represent an exception to this rule since the expression of *PDF1.2* is dependent on NPR1, EIN2 and COI1 but not on EDS1 or PAD4. *AtGSTF3* occurs twice in the proposed model as it is yet unclear if it is regulated by the ET and unknown signalling pathways (**dashed lines**) or by the SA and ET signalling pathways (**red lines**). *ATGSTF3* could be a member of a potential fourth cluster but further experiments are needed to determine if the unknown signalling pathway indeed plays a role in its regulation. Only genes significantly up regulated in *cir1* and regulatory genes represented by mutants used in this study were included in this model. Arrows signify activation whereas bars indicate repression.

The results obtained through these quantitative real-time PCR experiments highlight the complexity of defence gene regulation. The different signalling pathways function in a very complex plant defence network as these pathways act in distinct combinatorial manners to activate subsets of gene expression. Therefore, as all three signalling pathways are activated by *cir1*, the effect on gene expression depends on the specific gene involved. In addition, very few genes in *cir1* are simply regulated by a single signalling pathway which also points to the complicated interactions between different components of the defence network.

Since all three signalling pathways are activated in the *cir1* mutant background, CIR1 presumably could act as a negative regulator or general repressor of defence signalling. CIR1 might have a similar function to RIN4 (RPM1 interacting 4), another negative regulator of basal defence responses in Arabidopsis (Mackey et al., 2002). Plants overexpressing *RIN4* are inhibited in basal defence responses, while these responses are enhanced in plants lacking *RIN4* (Kim et al., 2005). Similar to *cir1*, the *rin4* (RPM1 interacting 4) mutant displays increased resistance to virulent pathogens and constitutively expresses *PR-1* and *PR-5* (Mackey et al., 2002) which are likely to contribute to the enhanced basal defence of *rin4*.

The genes tested by quantitative real-time PCR were selected based on either their differential expression during previous microarray analyses (S. L. Murray, personal communication) or their induction upon virulent *P. syringae* infection (Glazebrook et al., 2003). Of the seven genes identified through the microarray experiments as being induced in *cir1* (S. L. Murray, personal communication), quantitative real-time PCR established that *ZAT7*, *At2g31880*, *PR-1*, *PR-2* and *AtLEA5* were up regulated in the *cir1* background (Fig. 4.12A and B; 4.13 and 4.15). Of these genes *ZAT7*, *PR-1*, *PR-2* and *AtLEA5* were classified as defence-related genes as their expression was amplified upon virulent *P. syringae* treatment (Fig. 4.13 and 4.15). Ten described defence-related genes were selected (Glazebrook et al., 2003), however only seven of these were induced in response to *Pst* DC3000 treatment under our conditions (Fig. 4.12C, E, G; 4.13E; 4.18A; 4.18C and 4.21A). In the Glazebrook et al. (2003) study, virulent *P. syringae* pv. *maculicola* ES4326 (*Psm* ES4326) was used to infect plants and therefore it appears that certain genes may

respond differently to infection by *Psm* ES4326 compared to *Pst* DC3000. Additionally, gene expression was analysed at only one time-point after the initial infection and therefore discrepancies in gene expression could arise as the induction of certain genes may occur transiently at earlier or later time-points. The concentration of bacteria utilised during the inoculations could also affect the timing of infection, resulting in varying gene expression between the two experiments.

The previously untested *cir1 pad4* and *cir1 eds1* double mutants were included in the quantitative real-time PCR analyses to determine the effect of these mutations on *cir1* gene expression. Based on their known positions and interactions in the SA signalling pathway, *npr1-1*, *pad4-1* and *eds1-2* are all defective in SA-dependent signalling and therefore it was expected that *cir1 pad4* and *cir1 eds1* would generally display similar gene expression profiles to *cir1 npr1*. NPR1 and PAD4 are additionally involved in the unknown signalling pathway (Glazebrook et al., 2003), and based on the known interactions between EDS1 and PAD4 (Feys et al., 2001; Feys et al., 2005), EDS1 is probably also involved in the unknown signalling pathway. Of the eleven genes found to be up regulated in *cir1*, eight displayed equivalent expression patterns in *cir1 npr1*, *cir1 pad4* and *cir1 eds1* (Fig. 4.12A to F; 4.13; 4.14 and 4.16). Furthermore, the expression of *BG-3* (results not shown) and *CYP91A2* (Fig. 4.18C and D), which are both uninduced in *cir1*, behaved similarly in *cir1 npr1*, *cir1 pad4* and *cir1 eds1* as did the down regulated genes, *ACD6* (Fig. 4.19) and *At3g47960* (Fig. 4.21). However, there were exceptions such as *PR-2*, which showed reduced expression in *cir1 npr1* compared to the wild-type levels of *cir1 eds1* and *cir1 pad4* (Fig. 4.15). The *npr1-1* mutant fails to express PR proteins (Cao et al., 1994) and therefore this mutation could have had a more profound effect on *PR-2* expression in the *cir1* background than the *pad4-1* and *eds1-2* mutations. Furthermore, two genes behaved differently in *cir1 npr1* than in *cir1 pad4* and *cir1 eds1* by either displaying levels less (Fig. 4.11) or more than (Fig. 4.12G and H) in *cir1 pad4* and *cir1 eds1*. These differences might be due to experimental variation which could be clarified by repeating the experiments or it could be indicative of the genuine involvement of different components in additional and specific regulatory mechanisms.

4.5 EDS1 protein accumulation in *cir1*, *cir1 eds1* and *cir1 pad4*

It has been shown that the EDS1 protein is essential for resistance to biotrophic pathogens and the accumulation of SA, which in turn enhances the defences of a plant by inducing the synthesis of PR proteins (Wiermer et al., 2005). In addition, EDS1 interacts with the PAD4 protein in unchallenged and pathogen-challenged plant tissues. Upon pathogen attack, both proteins increase in abundance of which a proportion of the proteins are incorporated into EDS1-PAD4 complexes (Feys et al., 2001). It is believed that basal resistance to virulent pathogens is wielded by the potentiating activities of the EDS1-PAD4 complexes, which would

ultimately result in the accumulation of SA and the activation of defence responses (Feys et al., 2001).

As concluded from previous results in this study, *cir1*-mediated resistance to the biotrophic pathogens *Pst* DC3000 and *H. parasitica* Noco2, as well as much *cir1*-dependent gene expression, was dependent on functional EDS1 and PAD4 proteins (Fig. 4.4, 4.5 and 4.8). To determine whether *cir1* affects the accumulation of these proteins, Western Blot analysis with EDS1 and PAD4 antiserum (kindly provided by J. E. Parker, Max-Planck Institute for Plant Breeding Research; Feys et al., 2001) was performed on *cir1*, *cir1 eds1* and *cir1 pad4* before and after infection with *H. parasitica* Noco2. After various attempts, no conclusive results could be obtained from the PAD4 Western Blot analysis (results not shown), whereas the results of the EDS1 Western Blot analysis are presented in Fig. 4.23.

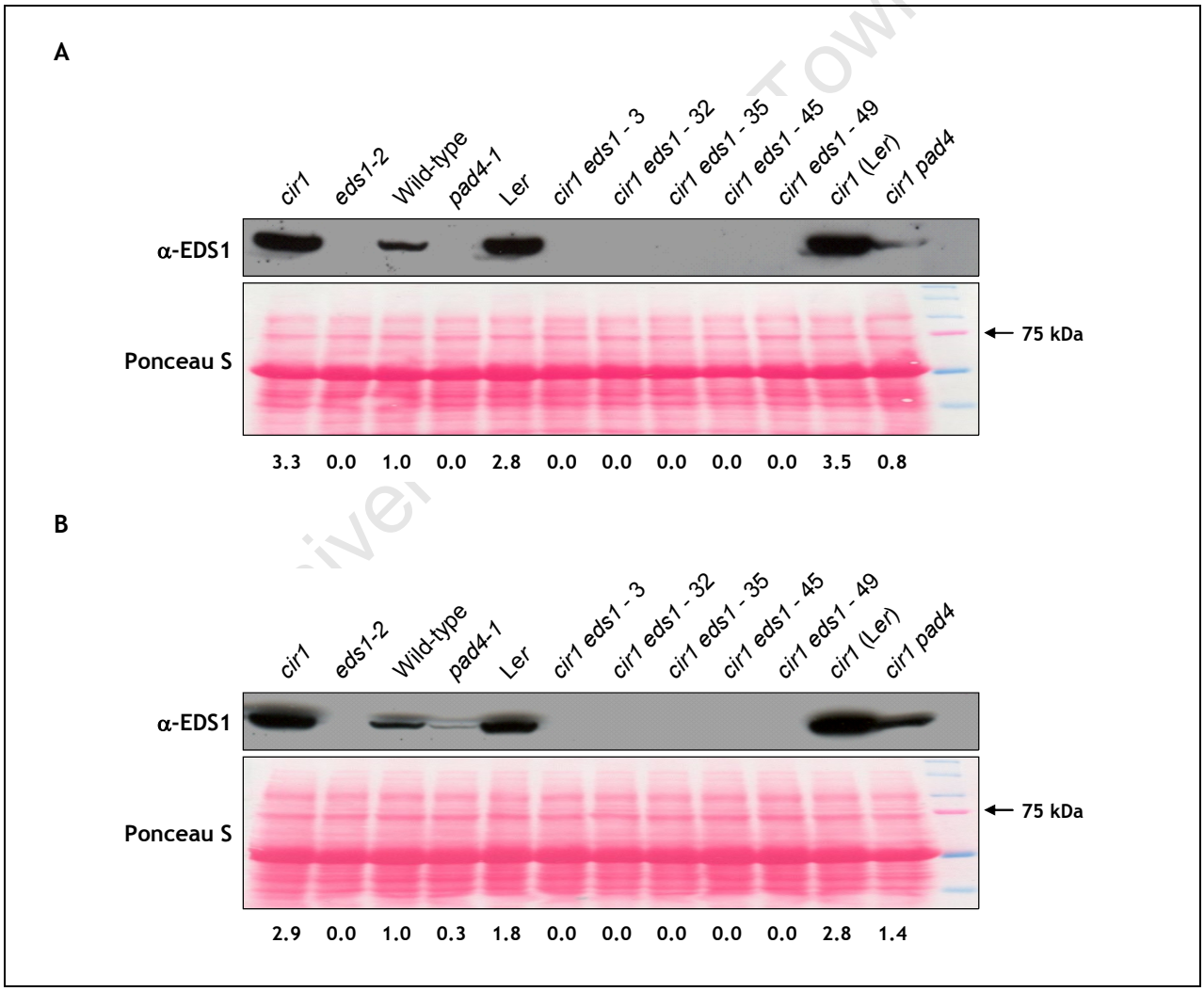

Figure 4.23. Western Blot analysis investigating the accumulation of the EDS1 protein in *cir1*, *cir1 eds1* and *cir1 pad4*.

The accumulation of the EDS1 protein was determined in *cir1*, *eds1-2* (negative control), wild-type (*Luc2* transgenic Col-0 line; positive control), *pad4-1*, L*er* (positive control), five homozygous *cir1 eds1* lines, *cir1* (L*er*) (*cir1* in L*er* background control) and a homozygous *cir1 pad4* line. Total protein

extracts were derived from (**A**) uninfected 4-week-old leaves and (**B**) 4-week-old leaves infected with *H. parasitica* Noco2 and harvested 6 days post infection. Equal loading is shown by Ponceau S staining of the membrane. Western Blot analysis was performed with EDS1 antiserum diluted 1:500 and by utilising a protein molecular weight marker, which was loaded onto each gel, it was established that the bands corresponded to the correct size of approximately 71.5 kDa. Numbers below each blot represent the band intensities relative to the EDS1 signal obtained for the wild-type samples which were set to a value of 1.0, as measured by ImageJ software (version 1.38x; http://rsb.info.nih.gov/ij; Abramoff et al., 2004).

The untreated *cir1* and *cir1* (L*er*) samples displayed a significant increase in the accumulation of the EDS1 protein, as levels were approximately three times higher than that observed in the Col-0 wild-type sample (Fig. 4.23A). As expected from a null mutant which does not express *EDS1*, no bands were visible in *eds1-2* (Feys et al., 2005) or in any of the homozygous *cir1 eds1* samples (Fig. 4.23A) indicating that EDS1 protein levels were significantly reduced in these samples compared to both the Col-0 and L*er* wild-type. EDS1 levels were notably depleted in the *pad4-1* sample (Fig. 4.23A) corresponding to previous results where the EDS1 protein levels were 75% less in a *pad4-1* background than in a Col-0 background (Feys et al., 2005). In this case, the membrane was exposed for only 5 min and the lack of a visible band in the *pad4-1* sample was due to the low exposure time (Fig. 4.23A). Subsequently the same membrane was exposed for 30 min whereupon a faint band in comparison to the wild-type Col-0 sample was observed in *pad4-1* (results not shown). The depletion of the EDS1 protein in this sample indicated that PAD4 has an effect on the expression or accumulation of EDS1 and that the EDS1 protein is stabilized by its interacting partner, PAD4 (Feys et al., 2001). The EDS1 protein is approximately four times less abundant in *cir1 pad4* compared to *cir1*, but more abundant than in *pad4-1* (Fig. 4.23A). Therefore, the *cir1* mutation increases the steady-state levels of the EDS1 protein as the levels of EDS1 accumulation in *cir1* and *cir1 pad4* are more abundant than wildtype and *pad4-1*, respectively (Fig. 4.23A). However, PAD4 is still required for full stability of the EDS1 protein.

A similar scenario regarding the accumulation of the EDS1 protein was observed in the *H. parasitica* Noco2 infected samples (Fig. 4.23B). Again both the *cir1* and *cir1* (L*er*) samples displayed a considerable increase in EDS1 levels which were roughly three times more abundant than that of the wild-type sample (Fig. 4.23B). Again the EDS1 levels in both the *cir1* and *cir1* (L*er*) samples were roughly three times higher than that of the wild-type sample (Fig. 4.23B). Similarly, no visible bands were detected in the *eds1-2* or *cir1 eds1* double mutant lines, indicating a substantial decline in EDS1 protein levels compared to both of the wild-type samples (Fig. 4.23B). Previous findings have shown that EDS1 protein levels increase in *H. parasitica* Noco2 infected tissue at 6 dpi (Feys et al., 2001). A noticeable

increase in EDS1 protein levels was observed in the *pad4-1* sample, where a faint band was detected after 5 min of exposure (Fig. 4.23B). However, the intensity of this band corresponded only to approximately 30% of the band present in the wild-type sample, again suggesting that EDS1 accumulation requires its partner PAD4 (Feys et al., 2005). Additionally, an increase in EDS1 protein accumulation was also observed in the *cir1 pad4* samples after exposure of 5 min (Fig. 4.23B). The level of accumulation was still two times less than that of the *cir1* sample but it remained roughly five times higher than in *pad4-1* (Fig. 4.23B), suggesting that PAD4 is required for the fully augmented levels of EDS1 but that *cir1* still increases the stability of EDS1 in the absence of PAD4.

The resistance phenotype of *cir1* mutant plants to certain biotrophs is therefore associated with considerably increased levels of the EDS1 protein compared to wild-type plants (Fig. 4.23). As the EDS1 protein is vital for SA accumulation (Wiermer et al., 2005), the increase in EDS1 accumulation could evidently be key to the activation of the SA signalling pathway in the *cir1* mutant background, resulting in the regulation of certain defence-related genes and resistance to *H. parasitica* Noco2 (see section 4.6.3).

In a manner that is yet unknown, the *cir1* mutation partially relieved the requirement for PAD4 to accumulate the EDS1 protein in the *cir1 pad4* line, thereby allowing for higher levels of EDS1 accumulation in the double mutant than in *pad4-1*. However, the residual EDS1 protein present in the double mutant was not enough to prevent infection by virulent pathogens as *cir1 pad4* and *pad4-1* displayed similar levels of disease severity (Fig. 4.5 and 4.8). Although it has been suggested that the full expression of basal resistance requires either sustained EDS1 threshold levels or the induction of EDS1 (Feys et al., 2005), the loss of PAD4 could also disable basal resistance (Rustérucci et al., 2001; Mateo et al., 2004). PAD4 does not only structurally stabilize the EDS1 protein, but it is also involved in the signalling activity of the EDS1-PAD4 complexes present in the plant (Feys et al., 2005). By removing PAD4 through mutation, EDS1 levels are reduced, the transduction of signals is compromised and basal defence against virulent pathogens diminished (Feys et al., 2005).

4.6 Discussion

The characterization of the *cir1* mutant through the analysis of epistatic interactions with other well-characterized mutants, camalexin accumulation after pathogen infection, accumulation of the EDS1 protein, induced expression of defence-related genes and its disease resistance profile to pathogens has enabled the development of a proposed model of the role *cir1* plays in the Arabidopsis defence network (Fig. 4.24). The central themes of this model will be discussed in the following sections.

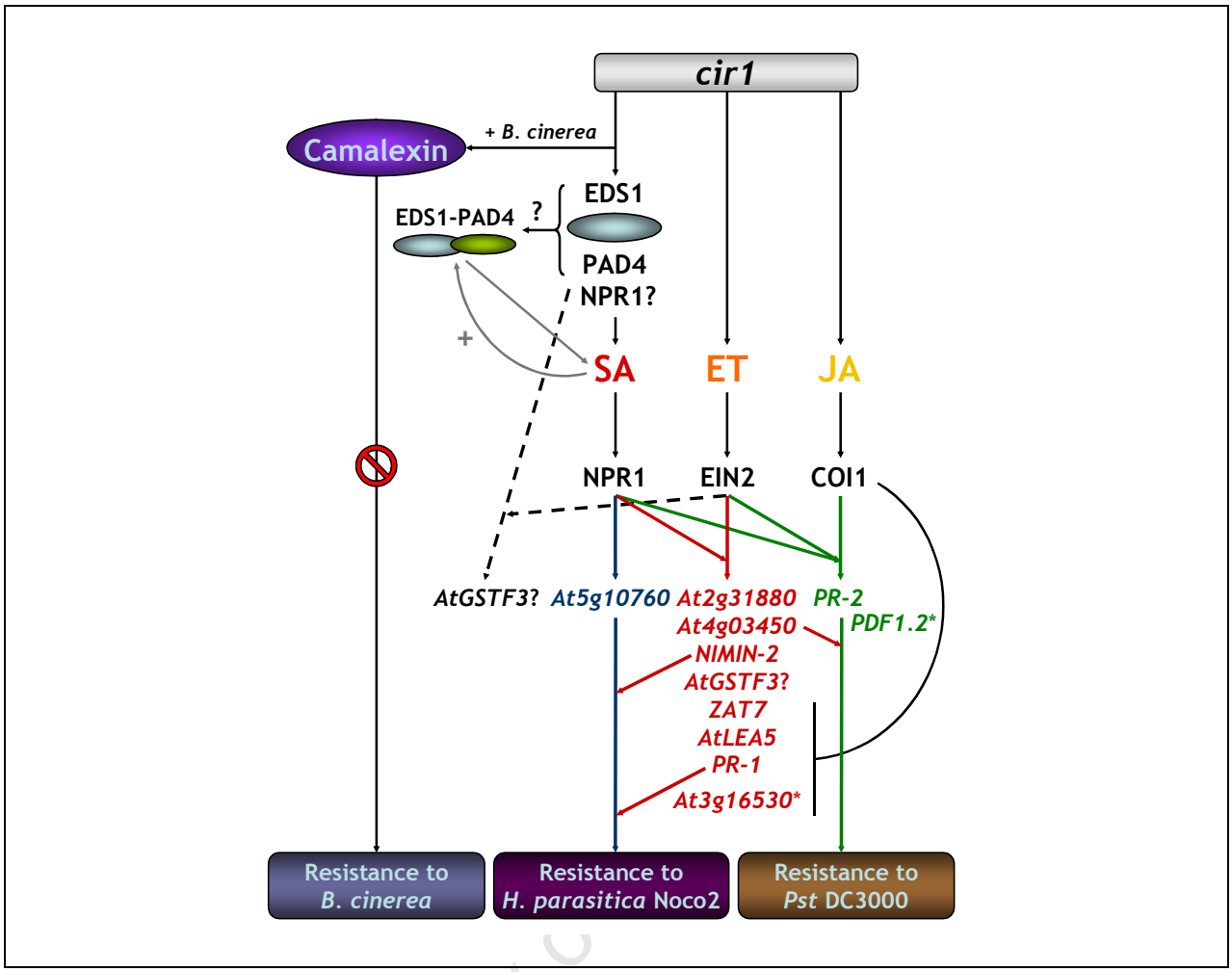

Figure 4.24. A proposed model of the role of *cir1* in the Arabidopsis defence network.

Cir1 acts upstream of EDS1, PAD4, NPR1, EIN2 and COI1 as well as SA, ET and JA accumulation in the defence network (this study; Murray, 2000; Murray et al., 2002). *Cir1* activates the accumulation of camalexin in a PAD4-independent manner after infection by *Botrytis cinerea*, however the high levels of camalexin do not result in resistance to *B. cinerea*. The *cir1* mutation activates the SA signalling pathway (**blue line**) resulting in induced expression of *At5g10760* (in **blue**) and resistance to *Hyaloperonospora parasitica* Noco2 infection (in **purple**) which is dependent on EDS1, PAD4 and NPR1. Induced expression of *At5g10760* (in **blue**) as well as *NIMIN-2* and *PR-1*, regulated by the SA and ET signalling pathways (**red lines**), is correlated with *cir1*-mediated resistance to *H. parasitica* Noco2. During the activation of the SA signalling pathway, the steady-state levels of the EDS1 protein are increased where it requires the PAD4 protein for stabilization. The concept of pre-existing EDS1-PAD4 complexes which lead to enhanced SA accumulation and the involvement of SA in a positive feedback loop resulting in further expression of both genes, was previously described by Feys et al. (2001) and Xing and Chen (2006). The simultaneous activation of the SA and ET signalling pathways (**red lines**) by *cir1* results in induced expression of the **red** defence-related genes which are dependent on EDS1, PAD4, NPR1 and EIN2. The asterisk next to *At3g16530* indicates that its expression varies from the rest of the genes in this cluster as it is dependent on NPR1 and EIN2, but not on EDS1 or PAD4. For the enhanced expression of the **green** defence-related genes and resistance to *Pseudomonas syringae* pv. *tomato* DC3000 (in **brown**), *cir1* activates all three the SA, ET and JA signalling pathways (**green lines**)

in an EDS1, PAD4, NPR1, EIN2 and COI1 dependent manner. The asterisk represents an exception to this rule since the expression of *PDF1.2* is dependent on NPR1, EIN2 and COI1 but not on EDS1 or PAD4. Induced expression of *PR-2* and *At4g03450* is related to *cir1*-mediated resistance to *Pst* DC3000. It is yet unclear if the expression of *AtGSTF3* in *cir1* is regulated by the ET and unknown signalling pathways (**dashed lines**) or by the SA and ET signalling pathways (**red lines**), hence it has been assigned two tentative positions. Only regulatory genes represented by mutants used in this study and genes significantly up regulated in *cir1* were included in this model. Arrows indicate activation whereas bars represent inhibition.

4.6.1 *coi1*, *eds1* and *pad4* are epistatic to *cir1*

Previous epistasis analysis determined that *cir1* operates upstream of the *npr1*, *ein2* and *jar1* mutations (Murray et al., 2002). To further assess the relative position(s) of *cir1* in the SA, ET and JA signalling pathways, additional epistatic relationships between *cir1* and other defence-related mutants were examined. *Coi1-1* was selected for the analysis of the JA signalling pathway since, unlike JAR1, COI1 is required for all major JA-dependent responses (Lorenzo and Solano, 2005). For analysis of the SA signalling pathway, *eds1-2* and *pad4-1* were employed since both exhibit enhanced susceptibility to virulent pathogens including *Pst* DC3000 (Feys et al., 2001) and *H. parasitica* Noco2 (Feys et al., 2005). Given the loss of resistance to *Pst* DC3000 observed in *cir1 coi1*, *cir1 eds1* and *cir1 pad4* (Fig. 4.3, 4.4 and 4.5), it has been concluded that *coi1*, *eds1* and *pad4* are epistatic to *cir1* and are likely to act downstream of the *cir1* mutation (Fig. 4.24). Furthermore, the position of *cir1* relative to *eds1* and *pad4* was confirmed by the *H. parasitica* Noco2 infection assay which indicated that functional EDS1 and PAD4 are required for *cir1*-induced resistance (Fig. 4.8). In addition it has been shown that the induced expression of various defence-related genes in *cir1* is dependent on a combination of functional EDS1, PAD4, NPR1, EIN2 and COI1 (Fig. 4.12 to 4.22), indicating that these loci operate downstream of CIR1 (Fig. 4.24).

4.6.2 Camalexin accumulation is not correlated with *cir1* resistance

Depending on which pathogen interactions are being analysed, camalexin accumulation is regulated by PAD4-dependent and -independent pathways (Glawischnig, 2007). The induction of camalexin biosynthesis in response to *B. cinerea* occurs independently of PAD4 since *cir1 pad4* displayed levels of camalexin similar to *cir1* (Fig. 4.2B). This signifies that camalexin accumulation in *cir1* is regulated by the PAD4-independent pathway. In the proposed model of *cir1* function (Fig. 4.24), camalexin accumulation is positioned upstream of EDS1, PAD4 and NPR1 to represent the PAD4-independent pathway, however the dependence of camalexin biosynthesis on EDS1 (and possibly NPR1) is yet unknown. It has been reported that the *eds1* mutant accumulated significantly less camalexin compared to wildtype in response to avirulent *H. parasitica*, signifying that EDS1 is involved in the

signalling of camalexin biosynthesis (Mert-Türk et al., 2003). However, the role of EDS1 in camalexin accumulation after *B. cinerea* infection has not been determined in wild-type or *cir1* plants. Consequently, the regulation of camalexin biosynthesis in this case is only in relation to PAD4.

Not all *B. cinerea* isolates display the same tolerance to camalexin with sensitive isolates exhibiting reduced hyphal growth and spore germination, while the more resistant isolates are less affected by camalexin (Kliebenstein et al., 2005b). The isolate utilized in our study, GLUK-1, has been shown to be sensitive to camalexin (Kliebenstein et al., 2005b) suggesting that the accumulation of camalexin in *cir1* would result in reduced hyphal growth and spore germination of GLUK-1. However, the high levels of camalexin in *cir1* did not reduce infection by GLUK-1 as the lesion diameters of *cir1* and wildtype were not significantly different (Fig. 4.2A). Although *cir1* accumulates camalexin after infection, the levels of accumulated camalexin are perhaps not sufficiently high enough to have a dramatic effect on the growth of GLUK-1. It is also possible that the some of the signalling pathways activated by *cir1* might somehow facilitate necrotrophic pathogen growth by, for instance, repressing JA- and ET-dependent defence responses.

Interestingly, although *cir1* is resistant to infection by *Pst* DC3000, the camalexin levels remained the same as wildtype after treatment with this pathogen (Fig. 4.6), indicating that camalexin does not form part of the *cir1*-induced defence response to *Pst* DC3000. This lack of importance for camalexin in defence responses to *Pst* DC3000 has been seen before as the camalexin deficient mutant, *pad3*, did not show altered sensitivity to infection by *Pst* DC3000 (Glazebrook and Ausubel, 1994). Furthermore, it appears that camalexin biosynthesis in *cir1* depends on the type of pathogen interaction as camalexin accumulated to higher levels than wildtype in response to a necrotrophic, fungal pathogen (*B. cinerea*; Fig. 4.2B) but not to a biotrophic, bacterial pathogen (*Pst* DC3000; Fig. 4.6).

4.6.3 EDS1 protein accumulation plays a role in *cir1*-mediated basal resistance

The *cir1* mutant accumulates approximately three times more EDS1 protein compared to wildtype in uninfected (Fig. 4.23A) and pathogen-treated samples (Fig. 4.23B). This accumulation is presented with a light blue oval in the model of *cir1* function (Fig. 4.24). It is known that the EDS1 protein is stabilized by PAD4, which acts as its interacting partner (Feys et al., 2001; Feys et al., 2005). The scenario is quite different when PAD4 was absent as the *pad4-1* mutant displayed depleted EDS1 levels before (Fig. 4.23A) and after pathogen infection (Fig. 4.23B). Although the interactions between EDS1 (light blue oval) and PAD4 (light green oval) have not been specifically tested in the *cir1* background, the EDS1-PAD4 complex has been included in the model as it would be unlikely that EDS1 could accumulate to such high levels in *cir1* in the absence of the PAD4 protein. Additionally, it has been shown that an increase in EDS1 protein after pathogen infection is correlated with an

increase in PAD4 protein as well as increased detection of co-immunoprecipitable PAD4 and therefore an increase in the EDS1-PAD4 complexes (Feys et al., 2001). Interestingly, the level of EDS1 accumulation was significantly higher in *cir1 pad4* than in *pad4-1* in uninfected (Fig. 4.23A) and pathogen-treated samples (Fig. 4.23B) indicating that the *cir1* mutation somehow increases the steady-state levels of the EDS1 protein. These results suggest that PAD4 is required for the fully augmented EDS1 levels observed in *cir1* but that *cir1* also has a stabilizing effect on the EDS1 protein in the absence of PAD4. EDS1 and PAD4 interact to form EDS1-PAD4 complexes (Feys et al., 2001) but the molecular associations and biochemical activities of EDS1 and PAD4 need more comprehensive examination (Feys et al., 2005). Possibly *cir1* also acts as an interacting partner to EDS1 to promote the stability of the protein, however any mechanistic links between *cir1* activity and EDS1 accumulation remain unknown.

Consistent with the pre-existing EDS1-PAD4 protein complexes in uninfected plant tissues, it is believed that the combined potentiating activities of EDS1 and PAD4 contribute to basal resistance. Upon virulent pathogen infection, the EDS1-PAD4 activities result in the accumulation of SA and the subsequent activation of defence responses (Feys et al., 2001). SA forms part of a positive feedback loop acting as a contributing factor to the expression of both *EDS1* and *PAD4* (presented in grey, Fig. 4.24), resulting in the further amplification of defence-related responses (Falk et al., 1999; Jirage et al., 1999; Feys et al., 2005; Xing and Chen, 2006). It is therefore possible that the high EDS1 levels observed in the *cir1* mutant background could be a result of an activated SA signalling pathway where SA acts in the positive feedback loop (presented in grey, Fig. 4.24), contributing to EDS1 accumulation via increased EDS1 mRNA accumulation. To test this hypothesis, it would be necessary to determine the EDS1 protein levels in a double mutant consisting of *cir1* and an SA-deficient mutant, such as *eds5*, *sid2* or *NahG*. Furthermore, the gene expression pattern of *EDS1* in the *cir1* background has not yet been determined. Hence it is unclear if the EDS1 protein accumulation in *cir1* is related to an increase in *EDS1* gene expression or a post-transcriptional effect.

EDS1 is essential in basal defence to biotrophic and hemi-biotrophic pathogens and the abundance of EDS1 protein increases upon pathogen attack (Feys et al., 2001). The resistance phenotype of *cir1* to certain biotrophic and hemi-biotrophic pathogens is correlated with increased EDS1 protein levels (Fig. 4.23). It possible that EDS1 contributes to *cir1*-induced basal resistance by incorporating a proportion of accumulated EDS1 proteins into the EDS1-PAD4 complexes, whose potentiating activities results in SA accumulation which in turn activates various defence responses, including defence-related gene expression. CIR1 has been predicted to act as a negative regulator of disease resistance (Murray et al., 2002) making it tempting to speculate that CIR1 might inhibit EDS1

accumulation or render the protein inactive, possibly through direct interaction, which would result in the reduction of basal resistance.

4.6.4 Multiple defence signalling pathways contribute to *cir1*-induced resistance

Based on the results obtained through quantitative real-time PCR analyses, it has been established that all of the signalling mutants utilized in this study affected gene expression in *cir1*. Hence, the *cir1* mutation activates multiple signalling pathways. As indicated in the proposed model, synergistic cross-talk between the SA and ET signalling pathways (presented in red, Fig. 4.24) or between the SA, JA and ET pathways (presented in green, Fig. 4.24) leads to induced expression of a range of defence-related genes. Several genes, including all Cluster A genes, required not only the SA signalling pathway but a combination of the SA and ET signalling pathways for enhanced expression in *cir1* (presented in red, Fig. 4.24). Former microarray studies found similar results as several defence-related genes were induced by the SA and ET signalling pathways functioning in concert (Schenk et al., 2000). Interestingly, the expression of these genes is regulated differently by these three signalling pathways (SA, JA and ET). Half of the induced genes (presented in red) did not reach maximal expression in *cir1* as their expression was affected by the antagonistic effect of the activated JA signalling pathway on the SA signalling pathway (presented by black inhibition bar, Fig. 4.24), whereas the expression of the remaining genes was unaffected.

The quantitative real-time PCR data further indicated that the regulation of the selected genes in Clusters A to D in the *cir1* background did not always correlate with that established by Glazebrook et al. (2003) (Fig. 4.10). For example, *PR-2* is a known SA marker (Uknes et al., 1992) however induced *PR-2* expression in *cir1* requires the simultaneous activation of all three signalling pathways (presented in green, Fig. 4.24). The expression of the JA and ET marker, *PDF1.2*, is dependent on NPR1 as well as the ET and JA signalling pathways in *cir1* (presented in green, Fig. 4.24). Interestingly, a similar situation exists in the *hrl1* (hypersensitive response-like lesions 1; Devadas et al., 2002) where constitutive *PDF1.2* expression in this mutant was reduced in the absence of NPR1 (Devadas et al., 2002). To determine if *PDF1.2* expression requires SA, a *PDF1.2* expression profile in a double mutant comprised of *cir1* and *sid2*, or another mutant that is affected in SA accumulation, needs to be established.

The discrepancies in the regulation of certain genes could be contributed to the fact that the regulatory model was based on the expression of Cluster A to D genes in response to virulent *P. syringae* infection, whereas the methods of regulation of these genes in *cir1* was determined utilizing uninfected plant material from the single and double mutants lines. Glazebrook et al. (2003) also noted that their model could not be applied to all defence-related genes as some displayed expression patterns different from those of the Cluster A to D genes.

An interesting phenomenon occurs in the regulation of *PER50* and the other Cluster D gene, *At3g47960*, in *cir1* as these were the only cases where the regulatory roles of EDS1 and PAD4 were uncoupled from each other (Fig. 4.20 and 4.21). The expression of both genes was suppressed by EDS1 and COI1, resulting in significantly lower expression in *cir1* than in wildtype (Fig. 4.20 and 4.21). The exact reasons for the separation of EDS1 and PAD4 during the regulation of *At3g47960* and *PER50* remain unclear, but other examples exist where EDS1 and PAD4 have different functions within the defence network. EDS1 exerts an early role in TIR-NBS-LRR type R protein mediated resistance functioning independently of PAD4 which is necessary for oxidative burst upstream of the local HR. The second function recruits PAD4 and drives amplification of R protein-mediated and basal defences (Feys et al., 2001). Another study showed that *EDS1*, but not *PAD4*, is necessary for an HR-associated oxidative burst after *RPP1*- or *RPS4*-mediated pathogen recognition (Rustérucci et al., 2001). Interestingly, recent studies established that the PAD4-mediated defence in Arabidopsis against the green peach aphid is uncoupled from EDS1 (Pegadaraju et al., 2007).

Glazebrook et al. (2003) found that the expression of Cluster A genes was augmented in the *coi1-1* and/or *ein2-1* mutants which compromise the JA and/or ET signalling pathways, indicating that the JA and/or ET signalling pathways have an inhibitory effect on SA signalling. In the *cir1 ein2* and *cir1 coi1* double mutant lines, not all Cluster A genes were up regulated compared to wildtype (Fig. 4.12A to F; 4.13E and F), actually *PR-1* was the only Cluster A gene where COI1, and the JA signalling pathway, had an inhibitory effect on its expression in *cir1* (Fig. 4.13E and F). Furthermore, the expression of Cluster D genes was higher in the SA signalling mutants (*pad4-1*, *eds1-2* and *npr1-1*) in the study of Glazebrook et al. (2003) as the inhibitory effect of the SA signalling pathway on JA-dependent gene expression was removed in these mutants. In contrast to these expectations, the expression of *CYP91A2* was not increased in *cir1 pad4*, *cir1 eds1* or *cir1 npr1* compared to wildtype (Fig. 4.18C and D). Although *ACD6* is not a Cluster D gene, its expression in *cir1* is also regulated only by the JA signalling pathway and *ACD6* expression in *cir1 pad4*, *cir1 eds1* and *cir1 npr1* was also not higher than wildtype (Fig. 4.19). These results suggest that the inhibitory effect of SA signalling on JA-dependent gene expression seems to be negligible in this mutant background.

To further elucidate the role of the SA, JA and ET signalling pathways in *cir1*-mediated resistance, it would be meaningful to determine the levels of each of these signalling compounds in the *cir1* mutant. It is also clear that defence gene regulation is very complex as various signalling pathways act in an intricate network where diverse combinations in the network could lead to very different outputs. Complicated results become exceedingly more difficult to interpret, demonstrating the importance of systems biology approaches whereby the results from gene regulatory studies could be mathematically modelled and perturbations

of the system (such as mutants or transgenic plants) simulated to predict the outcome. Experimental testing of these predictions would be used to validate the models. Such a systems biology approach therefore seems essential in untangling the plant defence network.

4.6.5 Correlation between induced gene expression and *H. parasitica* Noco2 and *Pst* DC3000 resistance profiles in *cir1*

To identify genes whose expression is correlated with the *cir1* resistance profile against *H. parasitica* Noco2 and *Pst* DC3000, gene expression patterns were investigated for induced expression in the resistant *cir1* mutant and reduced or wildtype expression in the relevant susceptible double mutant lines.

The expression patterns of *At5g10760*, *NIMIN-2* and *PR-1* might be related to the disease resistance profile of *cir1* against *H. parasitica* Noco2 infection (presented in purple, Fig. 4.24). The *cir1 eds1*, *cir1 pad4* and *cir1 npr1* double mutant lines were susceptible to *H. parasitica* infection and had reduced *At5g10760*, *NIMIN-2* and *PR-1* expression compared to *cir1*, whereas *cir1*, *cir1 ein2* and *cir1 coi1* displayed expression levels significantly higher than wildtype (Fig. 4.11; 4.12E and F; 4.13E and F). Notably, several recessive mutants with increased *PR-1* expression, such as *mpk4* (Petersen et al., 2000), *rin4* (Mackey et al., 2002) and *ssi2* (Shah et al., 2001), are also more resistant than wildtype to infection by virulent strains of *H. parasitica*. These identified genes could be useful as potential candidates in a plant biotechnology approach, and it would be interesting to establish if their overexpression results in increased resistance to *H. parasitica*. Interestingly, *LURP1* which shows a pattern of late up regulation in response to virulent *H. parasitica* infection (Eulgem et al., 2004; Knoth et al., 2007), does not correlate with *cir1*-mediated resistance to *H. parasitica* Noco2. Resistance of *cir1* to this pathogen is dependent on PAD4, EDS1 and NPR1 whereas *LURP1* expression in *cir1* was dependent on PAD4, EDS1 and COI1 (Fig. 4.17A). In addition, the results suggest that NPR1 is not involved in the regulation of *LURP1* in *cir1* (Fig. 4.17B). If there was a correlation between *LURP1* expression and resistance to *H. parasitica* Noco2, *cir1 npr1* would have displayed reduced *LURP1* expression compared to wildtype and *LURP1* expression in *cir1* would have been independent of COI1.

At4g03450 and *PR-2* were the only genes whose expression patterns could be clearly correlated with *cir1*-mediated resistance to *Pst* DC3000 (presented in brown, Fig. 4.24). It is known that *PR-2* expression increases upon *Pst* DC3000 infection (Mishina and Zeier, 2007) and *At4g03450* has been described as an SA-dependent defence-related gene (Glazebrook et al., 2003). *Cir1* exhibited considerably higher expression levels of *At4g03450* (Fig. 4.12C and D) and *PR-2* (Fig. 4.15) than wildtype and all the relevant susceptible double mutant lines displayed significantly reduced *At4g03450* and *PR-2* expression compared to *cir1*. These results suggest that *At4g03450* and *PR-2* act as markers for the activation of defence pathways that lead to *cir1*-induced resistance to *Pst* DC3000.

There are certain limitations in identifying expressed genes which are related to a specific phenotype when using this approach. It is possible that the different combinations of genes in the various double mutant lines are in reality responsible for their phenotypes. Furthermore, some genes might be up regulated in the double mutants to compensate for the lack of expression of others. In addition, not all genes in the genome were targeted in this study hence many genes whose expression profiles correlate with disease resistance may not have been tested.

Cir1 is not the only mutant that relies on the activation of multiple signalling pathways for resistance to pathogens. Others include the *hrl1* mutant, which displays constitutive expression of SA and JA/ET responsive defence-related genes and has enhanced resistance to infection by *Pst* DC3000 and virulent *H. parasitica*. Furthermore, resistance to both these pathogens is mediated by the simultaneous activation of the SA and ET signalling pathways (Devadas et al., 2002). Epistasis analyses between mutants disrupted in the SA, JA and ET pathways and *cpr5* (Bowling et al., 1997) and *cpr6* (Clarke et al., 1998), that constitutively activate these signalling pathways, were conducted. The aim of these experiments was to investigate the relationship between the SA-, JA- and ET-mediated defence responses, and it was found that the SA- and JA/ET-related defence responses function together in the *cpr* mutants to confer resistance to virulent pathogens (Clarke et al., 2000b).

Interestingly, no correlation between the expression of defence-related genes, such *PR-1*, *PR-2*, *PR-5* and *PDF1.2*, and resistance to virulent *Psm* ES4326 and *H. parasitica* Noco2 could be established in the *cpr* mutants (Clarke et al., 2000b). Only five of the induced defence-related genes in *cir1* could be correlated to resistance to *Pst* DC3000 and *H. parasitica* Noco2 (Fig. 4.24). It is possible that the increased expression of a single gene is not sufficient in providing resistance. As previously mentioned, multiple signalling pathways are required for *cir1*-mediated defence responses and therefore it is more likely that combinations of genes contribute substantially toward resistance to virulent *P. syringae* and *H. parasitica* Noco2. Moreover, different combinations of genes could possibly have the same end result on *cir1* resistance in which case the involvement of certain genes in defence could go undetected.

It is clear that *cir1*-mediated resistance to biotrophs is regulated in a complex manner. Furthermore, the activated defence responses in *cir1* are not totally effective against all biotrophs and *cir1*-mediated resistance is probably also dependent on the mode of pathogenicity. *G. orontii* is a biotrophic fungal pathogen and although the mutation does have a limiting effect on the spread of the fungus to uninfected parts of the plant (Table 4.4.), *cir1* is not significantly more resistant to fungal growth (Fig. 4.9). Several Arabidopsis mutants highly susceptible to *P. syringae* infection were screened for their

susceptibility to *G. orontii* and the majority of these mutants were not susceptible to infection by *G. orontii* (Reuber et al., 1998). These results suggest that *G. orontii* does not induce the same components of defence signalling pathways as *P. syringae* or that the defence-related products which are necessary for restraining *P. syringae* infection, are not effective in limiting *G. orontii* growth (Reuber et al., 1998). Another mutant resistant to *G. orontii*, *pmr5* (powdery mildew resistance 5; Vogel et al., 2004), is susceptible to infection by *Pst* DC3000 and *H. parasitica* Emco5 (Vogel et al., 2004). Notably, *pmr5*-induced resistance did not require the activation of the SA, JA or ET signalling pathways, suggesting that its defence mechanisms are not linked to known defence signalling pathways (Vogel et al., 2004). Alternatively, it is possible that *cir1* is not resistant to fungal growth irrespective of the fungus being biotrophic, such as *G. orontii*, or necrotrophic like *B. cinerea*. This might be due to the mode of infection utilized by fungal pathogens compared to that of bacterial pathogens.

4.6.6 Possible *cir1* involvement in additional plant defence responses

Given the role of *cir1* in basal defence, it is likely that it is also involved in non-host resistance. Non-host resistance relies on pre-formed barriers as well as the induction of PTI (Nürnberger and Lipka, 2005) and has been described as the successful control of pathogen growth by basal resistance since similar defence systems and signalling pathways are utilized by both defence mechanisms (Ingle et al., 2006). The overlap between basal and non-host resistance is illustrated by the isolation of mutants defective in both pathways. For example, the *eds1* mutant shows enhanced susceptibility to virulent isolates of *H. parasitica* and *P. syringae* (Parker et al., 1996; Aarts et al., 1998) and supported growth of the non-host pathogen, barley powdery mildew (Zimmerli et al., 2004), indicating that EDS1 has roles in basal and non-host resistance. Furthermore, the overlap was also highlighted in expression studies as it was found that sets of genes were co-regulated during basal and non-host resistance in Arabidopsis (Truman et al., 2006).

As previously mentioned, PTI contributes to PAMP-triggered and basal resistance. Results in this chapter highlight the importance of *cir1*-mediated defence signalling in basal defence systems against virulent *H. parasitica* and *P. syringae* infection. Furthermore, *cir1* displays induced expression of genes possibly involved in PAMP-triggered resistance. *At2g31880* displays rapid induction after treatment with a known PAMP, flg22 (Navarro et al., 2004) and *At3g16530* is up regulated in response to chitin, a PAMP derived from the cell walls of fungi (Zhang et al., 2002). Both genes displayed significantly increased expression in the *cir1* mutant background (Fig. 4.12A and B; 4.14), suggesting that *cir1* does not only directly affect basal resistance but also has an additional regulatory role in defence signalling mediated by PAMP recognition. It would therefore be interesting to determine whether *cir1* has increased resistance to non-host pathogens of Arabidopsis.

The colonization of plant roots by certain non-pathogenic rhizobacteria confers resistance to bacterial and fungal infection in the aerial parts of the plant. This form of disease resistance is called ISR (Pieterse et al., 1998). ISR in Arabidopsis has been shown to function independently of SA and *PR* gene expression (Pieterse et al., 1996), but requires JA and ET signalling components since mutations that interfere with either JA or ET signalling block the expression of ISR (Pieterse et al., 1998; Ton et al., 2001). ISR additionally requires NPR1 at a point downstream of the requirement of ET, which in turn lies downstream of the requirement of JA in the ISR signalling pathway (Pieterse et al., 1998). NPR1 therefore functions downstream of either SA or JA and ET where it acts as an important regulator of induced defence responses according to the upstream signals (Durrant and Dong, 2004). ISR-expressing plants display enhanced expression of certain JA-responsive genes when challenged with a pathogen, signifying that ISR-expressing tissue is primed to activate JA-inducible genes more rapidly or to a higher level upon pathogen attack (van Wees et al., 1999). Interestingly, *cir1* might have a role in ISR since the expression of *PDF1.2* in the *cir1* background was regulated similarly to that of ISR. Induced *PDF1.2* expression required JA and ET as well as NPR1, but not EDS1 or PAD4 (Fig. 4.16). Notably, the ISR trait co-segregates with high basal resistance to virulent *P. syringae*, indicating that ISR is intimately related to basal resistance (Ton et al., 1999). Furthermore, ISR is another example of a JA-dependent response that is not inhibited by SA signalling (van Wees et al., 2000).

In summary, homozygous *cir1 coi1*, *cir1 eds1* and *cir1 pad4* double mutant lines were constructed to help clarify the function of *cir1* in the Arabidopsis basal defence network. Based on the disease resistance profiles of these double mutant lines, it was established that *cir1*-mediated resistance to *Pst* DC3000 is dependent on COI1, EDS1 and PAD4, indicating that *coi1*, *eds1* and *pad4* are epistatic to *cir1*. The resistance of *cir1* to *H. parasitica* Noco2 requires EDS1 and PAD4, which confirmed the position of *cir1* relative to *eds1* and *pad4*. Interestingly, although *cir1* accumulates high camalexin levels after infection with *B. cinerea*, it does not result in resistance to this necrotroph. Additionally, *cir1* is not totally effective against the biotroph *G. orontii*. Quantitative real-time PCR experiments established that the simultaneous activation of multiple signalling pathways resulted in induced defence-related gene expression, of which the expression of some genes could be correlated to *cir1*'s enhanced resistance to virulent pathogens. Furthermore, it was found that *cir1* may have a stabilizing effect on the EDS1 protein, a finding which may explain how *cir1* exerts its effects on SA-mediated signalling.

Chapter 5: General Discussion

In spite of inhabiting environments full of potential disease-causing agents, plants are surprisingly healthy. Disease-causing phytopathogen infections are effectively curbed by a sophisticated and multifaceted immune system consisting of two interconnected branches, ETI and PTI (Jones and Dangl, 2006). ETI has received more attention from the research community in past years, resulting in the cloning of a plethora of *R* and *Avr* genes (Martin et al., 2003) and the collection of a large body of information on the basis of ETI (Nürnberger and Lipka, 2005). In contrast, knowledge on PTI lags behind. Advances in the characterization of PAMP-triggered, non-host and basal defence responses and signalling cascades are key to deciphering the mechanisms underlying PTI (Abramovitch and Martin, 2004; Jones and Takemoto, 2004; Mysore and Ryu, 2004). Our understanding of how plants defend themselves against certain pathogens has been greatly enhanced by the analysis of defence-associated mutants in the model plant, *Arabidopsis thaliana*. This study attempted to decipher mechanisms underlying basal defence against virulent pathogens by utilizing the Arabidopsis *cir1* mutant. Phenotypic and molecular analyses of *cir1* provided new insights into the various components of the defence signalling network involved in *cir1*-mediated basal resistance, thereby further dissecting the layers of PTI.

5.1 *CIR1* maps to chromosome IV

Since the sequencing of the Arabidopsis Col-0 genome at the end of 2000, the biological or biochemical function of countless annotated genes has not yet been determined (The Arabidopsis Genome Initiative, 2000). Through genomic mapping of a mutation, the specific sequence change that is responsible for a mutant phenotype can be identified in a cloned gene, aiding in the assignment of a fundamental function to an annotated gene. In addition, genomic mapping is a forward genetics approach where mutants are used to identify genes involved in specific biological processes, such as disease resistance. Detailed phenotypic analysis of the relevant mutant and the characterization of the corresponding gene can illuminate the underlying mechanisms of the associated process (Østergaard and Yanofsky, 2004). It was therefore necessary to identify the defence-associated *CIR1* gene through genomic mapping to elucidate the underlying mechanisms of *cir1*-induced disease resistance.

Genomic mapping results established that the *CIR1* locus is located in a 309.10 kb region on the lower arm of chromosome IV (Table 3.3). Notably, it appears that chromosome IV is linked to plant disease resistance as several *R* genes reside on the lower arm of chromosome IV (Parker et al., 1997; Young, 2000; van der Biezen et al., 2002; Meyers et al., 2003). Genetic and molecular data have shown that the NBS-LRR class of *R* genes and other *R* gene-like sequences are frequently grouped in clusters in the Arabidopsis genome (Michelmore and

Meyers, 1998) and these clusters are known as major recognition complexes (MRCs) (Holub, 1997; Speulman et al., 1998). MRCs may span millions of base pairs and can consist of dozens of *R* gene sequences (Young, 2000). It is thought that this clustering is involved in both the maintenance, as well as generation, of *R* gene diversity, as it helps to maintain resistance while allowing for novel specificities to evolve (Suwabe et al., 2006).

One of these clusters, termed MRC-H, stretches over a 4.6 Mb region located in the central part of chromosome IV and contains approximately 26 NBS-LRR sequences (Holub, 1997; Mewes et al., 1999; Meyers et al., 1999; Noël et al., 1999). Some of these NBS-LRR sequences encode several *RPP* genes, which confer resistance to various strains of *Hyaloperonospora parasitica*, as well as *RPS* genes necessary for resistance to *Pseudomonas syringae* (Slusarenko and Schlaich, 2003; Suwabe et al., 2006). *RPP5* and its orthologue *RPP4* mapped to the MRC-H cluster (van der Biezen et al., 2002), both falling within a genetic interval on the lower arm of chromosome IV that constituted eight NBS-LRR genes over a 90 kb region (Noël et al., 1999). Interestingly, both *RPP4* and *RPP5* were situated on the centromeric side of the g4539 PCR-based marker and as the MRC-H cluster covers approximately 4.6 Mb of chromosome IV (Mewes et al., 1999), it is possible that the *CIR1* locus also resides within this *R* gene cluster. Other cloned *R* genes found in MRC-H include *RPP2*, *RPP12*, *RPP18* and *RPS2* (Michelmore and Meyers, 1998; Slusarenko and Schlaich, 2003).

Although *CIR1* could not be cloned in this study, it has been identified through complementation studies as one of eight possible candidate genes (Fig. 3.13, Fig. 3.14 and Table 3.6). Once *CIR1* has been identified, characterization of the gene and analysis of the predicted protein structure should reveal the likely function of the CIR1 protein, thereby providing additional information regarding the basis of the enhanced basal resistance phenotype of the *cir1* mutant.

5.2 The possible roles of *CIR1* in Arabidopsis defence

5.2.1 *CIR1* involvement in initial defence signalling events

The SA, JA and ET signalling pathways are activated simultaneously to up regulate the expression of several defence-related genes in *cir1* (Fig. 4.12 to 4.22). This suggests that *CIR1* may encode a negative regulator of defence signalling and that the activity of CIR1 suppresses defence signalling pathways and subsequent expression of defence-related genes. Through the removal of *CIR1*, the suppression is lifted resulting in the activation of the signalling pathways, increased expression of defence-related genes and ultimately in enhanced disease resistance. Additionally, the simultaneous activation of defence pathways by *cir1* further indicates that *CIR1* functions at an early position in the defence signalling network where it either acts prior to, or directly affects, the branching point between these

three signalling pathways. Consistent with this theory, the results obtained from the *Pseudomonas syringae* pv. *tomato* DC3000 (*Pst* DC3000) and *Hyaloperonospora parasitica* Noco2 disease resistance assays (Fig. 4.3, 4.4, 4.5 and 4.8) established that *cir1* functions upstream of *EDS1* and *PAD4* in the SA signalling pathway (Fig. 4.24). Based on results from previous studies, EDS1 and PAD4 activities are positioned downstream of pathogen recognition but upstream of SA accumulation in the defence signalling network (Falk et al., 1999; Jirage et al., 1999; Petersen et al., 2000; Feys et al., 2001; Rustérucci et al., 2001; Kunkel and Brooks, 2002; Thatcher et al., 2005). Furthermore, it has also been shown that *cir1* operates upstream of JA and ET accumulation (Murray et al., 2002). Therefore, it appears that CIR1 activity is located within the initial events of the defence signalling network which would involve the detection of pathogens or the activation and/or regulation of early defence responses, such as synthesis of callose, calcium and ion fluxes and the activation of MAPKs.

It is likely that the recessive *cir1* mutation is a loss-of-function mutation, in which case the eradication of CIR1 activity would result in the defence-related phenotypes of *cir1*. Interestingly, several examples exist where the loss of a function in certain early defence responses results in enhanced disease resistance. For example, the *pmr4* mutant has a mutation in a callose synthase gene and therefore displays a significant reduction in pathogen-inducible callose production. Although the synthesis of callose is generally regarded as a early defence response, the *pmr4* mutant displayed enhanced resistance to *Erysiphe cichoracearum, Golovinomyces orontii* and *H. parasitica* in a SA signalling pathway dependent manner (Vogel and Somerville, 2000; Jacobs et al., 2003; Nishimura et al., 2003). Similar to the predictions regarding the role of *CIR1*, it is believed that *PMR4* is involved in the negative regulation of defence responses and that the removal of the PMR4 protein results in the activation of defence signalling pathways and consequently in increased disease resistance (Nishimura et al., 2003). Furthermore, the disruption of a cyclic nucleotide-gated ion channel results in the activation of broad-spectrum disease resistance (Clough et al., 2000). *DND1* (defense, no death 1; also known as *AtCNGC2*) encodes a cyclic nucleotide-gated ion channel that allows passage of Ca^{2+}, K^{+} and other ions (Leng et al., 1999). The recessive *dnd1* mutation results in the activation of defence responses including high levels of SA and constitutively increased expression of *PR-1* and *β-glucanase*, rendering plants more resistant to infection by avirulent *P. syringae* as well as virulent *P. syringae*, *H. parasitica* and *G. orontii* pathogens (Yu et al., 1998). *DND1* appears to negatively regulate the increase of defence responses as it is expressed constitutively in normal plant leaves but is suppressed upon pathogen infection (Yu et al., 1998; Köhler et al., 2001). Loss-of-function mutants in MAPK cascades include *mpk4* and *edr1* (enhanced disease resistance 1) which both show elevated resistance to several pathogens (Petersen et al., 2000; Frye et al., 2001). *Mpk4*

mutant plants exhibit constitutive SAR with increased SA levels, enhanced resistance to virulent pathogens and constitutive *PR* gene expression. Hence, it appears that MPK4 is negative regulator of SA-mediated defences (Petersen et al., 2000). The Arabidopsis *edr1* mutant shows elevated resistance to virulent *E. cichoracearum* which is dependent on SA perception and synthesis. *EDR1* encodes a putative MAPKKK and it has been proposed that EDR1 functions at the start of a MAPK cascade which negatively regulates defence responses (Frye et al., 2001). Although both MPK4 and EDR1 seem to act as negative regulators of plant defence responses, *mpk4* and *edr1* display distinguishable phenotypes, signifying that it is unlikely that MPK4 would be the downstream MAPK of EDR1 (Zhang and Klessig, 2001). Furthermore, the activities of MPK4 and EDR1 differ to some extent from the proposed function of CIR1, since MPK4 also acts as a positive regulator of JA- and ET-dependent gene expression whereas JA- and ET-induced responses do not contribute to *edr1*-mediated resistance and are therefore not regulated by EDR1 (Frye et al., 2001; Brodersen et al., 2006). The activation of MAPK cascades are generally associated with the induction of defence responses, however these results indicate that there are at least two antagonistic MAPK pathways that play a regulatory role in plants defence responses.

As the *cir1* mutation led to the induced expression of several defence-related genes (Fig. 4.12 to 4.22), it is quite possible that the loss of *CIR1* could be involved either directly or indirectly in the activation of various transcription factors such as the WRKY, Whirly, Myb and ERF transcription factors which affect the regulation of defence-related genes. This could result in fundamental transcriptional reprogramming and in the expression of defence-related genes as part of early defence responses which might be distinct from those mentioned above.

Moreover, even though one of the candidate genes (At4g11170) identified in Chapter 3 is a putative TIR-NBS-LRR type R protein (Table 3.6), it is unlikely that CIR1 would function as a *R* gene involved in the recognition of pathogens as it is improbable that the loss of an R protein would result in the constitutive defence phenotypes of *cir1*. The *ssi4* (suppressor of salicylic acid insensitivity of *npr1-5*; Shirano et al., 2002) and *snc1* (suppressor of *npr1-1*, constitutive 1; Zhang et al., 2003b) mutations, located in two different *R* genes, resulted in the constitutive activation of R proteins and *R* gene-mediated disease resistance responses. These mutants were resistance to virulent *P. syringae* and *H. parasitica* infections and hence displayed similar defence-related phenotypes than *cir1*, however both possessed gain-of-function mutations (Shirano et al., 2002; Zhang et al., 2003b). That said, more recent evidence demonstrates that the possibility of *CIR1* encoding a disease resistance gene-like protein cannot be completely ruled out. Surprisingly, the Arabidopsis *LOV1* gene is a member of the CC-NBS-LRR type R proteins but also confers disease susceptibility to infection by the fungus *Cochliobolus victoriae* (Lorang et al., 2007). Previously, it was believed that NBS-LRR

proteins are only involved in conditioning plant disease resistance but these results suggest that *R* genes could also have a role in disease susceptibility. Perhaps *CIR1* also encodes an *R* gene which confers disease susceptibility and once the function of the gene is disrupted by a mutation, disease susceptibility is lost which subsequently results in disease resistance.

Notably, a number of reports have suggested that R proteins are under negative regulation which plays a crucial role in *R* gene–mediated resistance (reviewed by Rathjen and Moffetty, 2003). Therefore, an alternative role for CIR1 in the defence signalling network might be as a negative regulator of *R* genes. Such is the case with RIN4, a negative regulator of basal defence responses. *PR-1*, *PR-5* and other defence-related genes are constitutively expressed in the *rin4* mutant which is likely to contribute to its enhanced resistance to virulent *H. parasitica* and *P. syringae* infection (Mackey et al., 2002). In addition to its role in basal defence, RIN4 also acts as a negative regulator of the *R* gene, *RPS2*, maintaining it in an inactive state in the absence of the bacterial effector protein AvrRpt2. Once AvrRpt2 is delivered to the plant cell, it eliminates RIN4, resulting in the destabilization of a RPS2-RIN4-containing complex. This in turn leads to the activation of RPS2, the subsequent onset of HR and ultimately in disease resistance (Axtell and Staskawicz, 2003; Mackey et al., 2003; Day et al., 2005). Another example of such negative regulation occurs between the *R* gene, *SNC1*, and its negative regulator, *BON1* (bonzai 1; Zhang et al., 2003b; Yang and Hua, 2004). Through a loss-of-function mutation in *BON1* that derepresses *SNC1*, SNC1-dependent defense responses are constitutively activated resulting in an enhanced disease resistance phenotype to virulent pathogens (Hua et al., 2001; Jambunathan et al., 2001; Jambunathan and McNellis, 2003).

Although the exact purpose of CIR1 in the initial stages of defence signalling is yet unknown and its abovementioned roles are only hypotheses, its function should become apparent once the *CIR1* gene has been identified and characterized. However, additional epistasis studies with mutants upstream of EDS1 could also elucidate the possible position and function of CIR1 in the defence signalling network (to be discussed in section 5.3.2)

5.2.2 CIR1 interactions with EDS1 and other plant proteins

The *cir1* mutant accumulates significantly more EDS1 protein compared to wildtype in untreated and pathogen-treated samples (Fig. 4.23). As the amount of EDS1 protein increases upon pathogen attack and it has been recognized as an essential role-player in basal defence (Feys et al., 2001), it seems that *cir1*-mediated resistance to virulent pathogens could be associated with these increased EDS1 protein levels. The EDS1 protein is stabilized by its interacting partner, PAD4 (Feys et al., 2001; Feys et al., 2005), as demonstrated by the low EDS1 levels present in *pad4-1* mutant plants (Fig. 4.23). However, even though the levels of EDS1 accumulation were less than in *cir1*, the *cir1 pad4* double mutant displayed appreciably higher levels of accumulation than that of the *pad4-1* mutant

(Fig. 4.23). This signifies that the *cir1* mutation results in EDS1 accumulation in a PAD4-dependent manner and that *cir1* somehow affects the stability of the EDS1 protein, which became evident in the absence of PAD4, resulting in an increase in the steady-state levels of the EDS1 protein.

To date, interacting partners of the EDS1 protein have been identified as PAD4 and SAG101 (senescence-associated gene 101) (Zhou et al., 1998; Feys et al., 2001; Feys et al., 2005). Similar to PAD4, SAG101 also interacts with EDS1 to form EDS1-SAG101 complexes in the nucleus of the plant cell and contributes significantly to EDS1-dependent *R* gene-mediated as well as basal resistance pathways, where its function is partly redundant to that of PAD4. It was shown that EDS1, PAD4 and SAG101 proteins have common stabilizing effects on their interacting partners, however as EDS1–SAG101 and EDS1–PAD4 form separate complexes, PAD4 and SAG101 have minimal effect on each other's accumulation (Feys et al., 2005). PAD4 and SAG101 play additive roles in EDS1 accumulation by structurally stabilizing the EDS1 protein through direct interactions. As EDS1 is essential for the stabilization and subsequent accumulation of both PAD4 and SAG101, it indicates that EDS1 may function as an adaptor for these two components to ensure the integrity of the signalling complexes and to facilitate appropriate signal transduction (Park et al., 2003; Feys et al., 2005). The functions of PAD4 and SAG101 stretch further than stabilizing EDS1, as it was concluded that they supply fundamental signalling activity to the EDS1 complexes in which they exist and that all three components are vital for signal transduction (Feys et al., 2005).

For maximal EDS1 accumulation in *cir1*, functional PAD4 is indispensable however the requirement for PAD4 was partially alleviated by the *cir1* mutation in the *cir1 pad4* line (Fig. 4.23). This prompts the theory that perhaps *cir1* has a similar role to PAD4 and SAG101 in the stabilization of the EDS1 protein and that through possible interactions and/or the formation of complexes with EDS1, the EDS1 protein would accumulate in *cir1* mutant plants. Alternatively, the *cir1* protein may not be involved in any EDS1 complexes but could affect the molecular character of EDS1 in such a way that it promotes binding of its interacting partners, thereby increasing its stability and consequently its level of accumulation.

Since the *cir1* mutation results in high levels of EDS1 accumulation, it is likely that CIR1 would suppress the accumulation of EDS1, suggesting that the EDS1 protein is possibly under negative regulation by CIR1. The EDS1-PAD4 complexes are essential for basal resistance to virulent pathogens as its potentiating activities result in SA accumulation and the activation of defence responses (Feys et al., 2001). In addition, EDS1 complexes with PAD4 and SAG101 are important in relaying defence signals (Feys et al., 2005) and disruption thereof by affecting one of the components could influence downstream defence responses. CIR1 may well inhibit EDS1 production and/or accumulation, compromising the transduction of signals and eliminating basal defence against virulent pathogens which would be consistent with its

possible function as a negative regulator of the disease resistance signalling network. In addition, CIR1 may not only negatively regulate EDS1 but could also regulate EDS1 indirectly by suppressing its interacting partners, PAD4 and SAG101. This would result in the destabilization of the EDS1 protein which could negatively affect its accumulation and subsequent downstream signalling. However, it is yet unclear if the *cir1* mutation affects PAD4 and SAG101 accumulation since the Western blot analysis with PAD4 antiserum was unsuccessful (results not shown) and SAG101 accumulation in *cir1* has not been assessed. As the possibility exists that CIR1 interacts with EDS1, CIR1 may have similar inhibitory effects on other yet undetermined proteins involved in disease resistance, however this remains to be tested.

5.3 Future work

In order to increase our understanding of the mechanisms of *cir1* resistance, a wider range of techniques and different approaches need to be employed. Some of these are discussed in the following sections.

5.3.1 Identifying *CIR1* on chromosome IV

The results from the complementation studies based on luciferase and *Pst* DC3000 infection assays that identified JAtY68P03 and JAtY63F16 as the complementing JAtY clones, were preliminary and require confirmation. The results obtained were inconsistent in some cases (Fig. 3.13 and 3.14) which was attributed to the testing of only a few independently transformed lines. The isolation of independently transformed T_2 lines was problematic as only one or two lines representing *cir1* + JAtY63F16 and *cir1* + JAtY68P03, respectively, could be isolated. Poor transformation rates with JAtY clones have been reported as *Agrobacterium* harbouring JAtY clones are on occasion incapable of transforming Arabidopsis plants, as was the case with the JAtY73H06 clone. Therefore, to conclusively establish if the JAtY68P03 and JAtY63F16 clones complemented the *cir1* mutation, additional *cir1* plants have to be transformed with these clones. This would allow for the isolation of supplementary independently transformed lines to be tested with luciferase and *Pst* DC3000 infection assays. Furthermore, verification of the identity and status of the JAtY clones in the relevant transformed lines is also required.

Based on the theory that the JAtY68P03 and JAtY63F16 clones complement *cir1*, eight potential candidate genes have been identified (Table 3.6). Future studies need to determine which of the candidate genes is *CIR1* and identify the specific sequence change responsible for the *cir1* phenotypes. This can be achieved through complementation studies with the individual candidate genes as well as the subsequent sequencing of the relevant complementing candidate gene as described in section 3.7.4.

Experiments relevant to some of the *CIR1* candidate genes could be conducted to assist in identifying *CIR1*. For example, RDR2 is involved in the generation of endogenous siRNAs and the removal of RDR2 results in a reduction in siRNAs (Xie et al., 2004; Gasciolli et al., 2005). Determining the abundance of endogenous siRNAs in the *cir1* mutant background might indicate that *RDR2* is *CIR1*. However the aforementioned complementation studies with individual genes would be indispensable to provide conclusive proof that *CIR1* has been identified.

5.3.2 Further investigations of *cir1* in the defence signalling network

To clarify the position of *CIR1* in the defence signalling network, epistasis analyses with additional mutants in defence network could promote our understanding of *cir1* resistance. Results have indicated that *CIR1* is located upstream of *EDS1* and *PAD4* (Fig. 4.3, 4.4, 4.5 and 4.8), however its precise position is yet unknown. Several other defence-related mutants located upstream of EDS1 and PAD4 activities have been isolated to date, including the *mpk4* mutant which confers resistance to virulent isolates of *P. syringae* and *H. parasitica*, constitutive expression of several *PR* genes and increased SA accumulation (Petersen et al., 2000; Brodersen et al., 2006). Although *cir1* and *mpk4* share many phenotypes, their phenotypes regarding the induction of JA- and ET-responsive genes are opposed. The *cir1* mutation activates the JA and ET signalling pathways and displays constitutive expression of *PDF1.2* (Fig. 4.16; Murray et al., 2002) while *mpk4* blocks these signalling pathways resulting in impaired *PDF1.2* expression (Petersen et al., 2000; Brodersen et al., 2006). By examining JA- and/or ET-dependent phenotypes of these mutants, the position of *cir1* relative to *mpk4* can be established.

Additional mutants located upstream of EDS1 and PAD4 which could be utilized in potential epistasis studies include, amongst others, the *cpr* (constitutive expressor of *PR* genes) mutants (recessive *cpr1* and *cpr5* as well as dominant *cpr6* (Bowling et al., 1994; Bowling et al., 1997; Clarke et al., 1998)). These mutants share several phenotypes with *cir1*, such as enhanced resistance to virulent bacterial and oomycete pathogens as well as the constitutive expression of *PR* genes (Bowling et al., 1994; Bowling et al., 1997; Clarke et al., 1998). However, there are some phenotypic differences. For instance, *cpr1* and *cpr6* plants are significantly dwarfed compared to wild-type plants whereas *cir1* is not (Bowling et al., 1994; Clarke et al., 1998; Murray et al., 2002). Unlike *cir1*, the *cpr5* mutant has abnormal trichomes and forms spontaneous lesion in the absence of pathogens (Bowling et al., 1997; Boch et al., 1998). Therefore, epistasis studies between *cir1* and the *cpr* mutants to determine where *cir1* functions in relation to *cpr1*, *cpr5* and *cpr6*, could be designed on these individual phenotypes. If these phenotypes are dependent on CIR1, it is likely that the *cpr* mutants are positioned upstream of *CIR1*. Another potential candidate is the *ssi4* mutant which contains a gain-of-function mutation in a TIR-NBS-LRR type *R* gene. (Shirano et al.,

2002). This mutant displays similar phenotypes to *mpk4*, however the *ssi4* mutant also displays several morphological abnormalities, including stunted growth, severe chlorosis and the formation of spontaneous lesions, not found in *cir1* that could be investigated in epistasis analysis (Shirano et al., 2002).

The *cir1* mutant is not more resistant to infection by the fungal necrotroph, *Botrytis cinerea* (Fig. 4.1; Murray et al., 2005) or the biotrophic fungus, *Golovinomyces orontii* (Fig. 4.9). At this stage it is unclear if *cir1*-mediated resistance is ineffective against all fungi or only against necrotrophic pathogens. Therefore, it would be interesting to conduct additional pathogen infection studies to clarify this matter. Future fungal infection studies with biotrophic fungi, such as *Erysiphe chicoracearum*, and necrotrophic fungi, for example *Alternaria brassicicola*, *Pythium irregulare* or *Sclerotinia sclerotiorum*, should ascertain if *cir1*-mediated resistance is futile against fungal infections in general, while pathogen studies with the necrotrophic bacteria, *Erwinia carotovora*, and necrotrophic fungi are necessary to determine if the lack of *cir1* resistance is specific to necrotrophic pathogens.

5.3.3 After identification of *CIR1*

A theory has been proposed that CIR1 possibly interacts with EDS1, PAD4 or SAG101 to increase the stability of the EDS1 protein, thereby increasing the steady-state levels of EDS1 in *cir1* and *cir1 pad4* (Fig. 4.23). Further experiments are needed to test this hypothesis and to test the prospect that CIR1 might also interact with other defence-related proteins. However, these experiments can only be executed after *CIR1* has been identified and cloned.

PAD4 was identified as an EDS1 interactor through a yeast two-hybrid assay (Feys et al., 2001). Similarly, CIR1 can be used as bait to screen an Arabidopsis cDNA yeast two-hybrid library constructed from *P. syringae* or *H. parasitica* infected leaves to ascertain if EDS1 interacts with CIR1 and to identify any other putative interacting partners of CIR1 during pathogen defence. This experiment would also be useful in determining if CIR1 perhaps functions as a negative regulator of R proteins, as any possible interactions between CIR1 and R proteins should also become apparent. The identification of putative CIR1 interacting proteins, both upstream and downstream of CIR1, may position CIR1 in a signalling pathway not previously coupled to CIR1 function. Thereafter, protein interactions and presence of complex formation should be confirmed *in planta*. For example, to confirm the presence of CIR1-EDS1 complexes, co-immunoprecipitation experiments can be conducted. Immunoprecipitation of CIR1 proteins from plant extracts using an anti-CIR1 antibody, followed by Western blot analysis using anti-EDS1 antiserum, would determine if CIR1 and EDS1 protein interact in plant tissue. Furthermore, this should be performed before and after pathogen challenge.

An alternative possibility is that the accumulation of EDS1 in *cir1* is due to increased binding of EDS1 to its interacting partners, resulting in increased stability and accumulation. Through Westerns blot analyses utilizing PAD4 and SAG101 antibodies, the PAD4 and SAG101 accumulation levels in *cir1* could be assessed, establishing if *cir1* positively affects only the accumulation of EDS1 or also of its interacting partners. In addition, it has been shown that EDS1 is essential for accumulation of its interactors (Feys et al., 2005), therefore the level of CIR1 protein accumulation in the *eds1* mutant background should be evaluated to ascertain if the loss of EDS1 would affect CIR1 accumulation. As the EDS1 protein is localized either in the nucleus or the cytosol (Feys et al., 2005), subcellular localization of the CIR1 protein might also prove useful. Once these abovementioned experiments have been conducted, the mechanisms of negative regulation by CIR1 might be easier to unravel.

Once *CIR1* has been cloned, expression studies of *CIR1* in defence-related mutants and in plants infected with various pathogens can be performed to further elucidate the role of *CIR1* in the defence network. Quantitative real-time PCR has greatly contributed to gene expression studies as many samples can be analysed in a relatively short time. In addition, Western blot analysis with a CIR1 antibody would establish under what conditions and in which defence-related mutants the CIR1 protein accumulates. Since the proposed function of CIR1 is a negative regulator of the disease resistance signalling network, it would be interesting to assess if CIR1 accumulates to high levels in mutants susceptible to pathogen infections. Furthermore, the analysis of the CIR1 protein structure might identify certain domains with specific functions such as kinase domains, membrane spanning domains, nucleotide-binding domains and those involved in protein-protein interactions.

The *cir1* mutation manipulates all three the defence signal transduction pathways in PTI, resulting in a variety of defence responses. Furthermore, the *cir1* mutant does not display altered plant development such as stunted growth or spontaneous lesion formation, frequently associated with mutants displaying constitutive defence responses. Hence, as *cir1* activates multi-component disease resistance which could provide a broad spectrum of pathogen control, it could be useful to identify *CIR1* homologues in agriculturally important crops. Often genes isolated in one plant species share similar sequences or represent members of widespread gene families, allowing for the identification of homologues in other plant species. The inactivation or manipulation of *CIR1* homologues in crop plants may contribute to the protection of those plants, thereby benefiting the agricultural biotechnology sector.

5.4 Conclusion

Through the genomic mapping of *cir1*, significant progress has been made in locating the *CIR1* locus on chromosome IV and eight possible *CIR1* candidate genes has been identified. Potential additional roles of these eight annotated genes in disease resistance have been highlighted, contributing to one of the general goals of the plant scientific community which is to assign function to annotated genes (Østergaard and Yanofsky, 2004). In an attempt to elucidate the mechanisms of *cir1* resistance, it was established that *CIR1* functions upstream of *EDS1*, *PAD4* and *COI1* in the defence signalling network. Additionally, *cir1*-mediated basal resistance is associated with increased EDS1 protein accumulation and the simultaneous activation of multiple defence signalling pathways that results in the enhanced expression of numerous defence-related genes. Therefore, it is proposed that CIR1 functions as a negative regulator of the disease resistance signalling network. The findings of this study have contributed to the understanding of the Arabidopsis defence signalling network involved in resistance to pathogen infection.

Chapter 6: References

Aarts, N., Metz, M., Holub, E., Staskawicz, B. J., Daniels, M. J. and Parker, J. E. (1998) Different requirements for EDS1 and NDR1 by disease resistance genes define at least two *R* gene-mediated signaling pathways in *Arabidopsis*. Proc. Natl. Acad. Sci. USA **95**: 10306–10311.

Able, A. J., Sutherland, M. W. and Guest, D. I. (2003) Production of reactive oxygen species during non-specific elicitation, non-host resistance and field resistance expression in cultured tobacco cells. Func. Plant Biol. **30**: 91-99.

Abramoff, M. D., Magelhaes, P. J. and Ram, S. J. (2004) Image processing with ImageJ. Biophotonics International **11**: 36-42.

Abramovitch, R. B., Anderson, J. C. and Martin, G. B. (2006) Bacterial elicitation and evasion of plant innate immunity. Nature Rev. Mol. Cell Biol. **7**: 601-611.

Abramovitch, R. B. and Martin, G. B. (2004) Strategies used by bacterial pathogens to suppress plant defenses. Curr. Opin. Plant Biol. **7**: 356-364.

AbuQamar, S., Chen, X., Dhawan, R., Bluhm, B., Salmeron, J., Lam, S., Dietrich, R. A. and Mengiste, T. (2006) Expression profiling and mutant analysis reveals complex regulatory networks involved in Arabidopsis response to *Botrytis* infection. Plant J. **48**: 28-44.

Adams, D. O. and Yang, S. F. (1979) Ethylene biosynthesis: identification of 1-aminocyclopropane-1-carboxylic acid as an intermediate in the conversion of methionine to ethylene. Proc. Natl. Acad. Sci. USA **76**: 170-174.

Agorio, A. and Vera, P. (2007) ARGONAUTE4 is required for resistance to *Pseudomonas syringae* in *Arabidopsis*. Plant Cell **19**: 3778-3790.

Agrios, G. N. (2005) How plants defend themselves against pathogens. In: *Plant Pathology*. Agrios, G. N. (eds.). Academic Press, San Diego.

Alonso-Blanco, C. and Koornneef, M. (2000) Naturally occurring variation in Arabidopsis: an underexploited resource for plant genetics. Trends Plant Sci. **5**: 22-29.

Alonso-Blanco, C., Peeters, A. J., Koornneef, M., Lister, C., Dean, C., van den Bosch, N., Pot, J. and Kuiper, M. T. (1998) Developmet of an AFLP based linkage map of Ler, Col and Cvi *Arabidopsis thaliana* ecotypes and construction of a Ler/Cvi recombinant inbred line population. Plant J. **14**: 259-271.

Alonso, J. M., Hirayama, T., Roman, G., Nourizadeh, S. and Ecker, J. R. (1999) EIN2, a bifunctional transducer of ethylene and stress responses in *Arabidopsis*. Science **284**: 2148-2152.

Anderson, J. P., Badruzsaufari, E., Schenk, P. M., Manners, J. M., Desmond, O. J., Ehlert, C., Maclean, D. J., Ebert, P. R. and Kazan, K. (2004) Antagonistic interaction between abscisic acid and jasmonate-ethylene signaling pathways modulates defense gene expression and disease resistance in Arabidopsis. Plant Cell **16**: 3460-3479.

Apel, K. and Hirt, H. (2004) Reactive oxygen species: metabolism, oxidative stress, and signal transduction. Annu. Rev. Plant Biol. **55**: 373-399.

Asai, T., Tena, G., Plotnikova, J., Willmann, M. R., Chiu, W.-L., Gomez-Gomez, L., Boller, T., Ausubel, F. M. and Sheen, J. (2002) MAP kinase signalling cascade in *Arabidopsis* innate immunity. Nature **415**: 977-983.

Athman, R. and Philpott, D. J. (2004) Innate immunity via Toll-like receptors and Nod proteins. Curr. Opin. Microbiol. **7**: 25-32.

Auh, C.-K. and Murphy, T. M. (1995) Plasma membrane redox enzyme is involved in the synthesis of O^{2-} and H_2O_2 by *Phytophthora* elicitor-stimulated rose cells. Plant Physiol. **107**: 1241-1247.

Ausubel, F. M. (2005) Are innate immune signaling pathways in plants and animals conserved? Nature Immunol. **6**: 973-979.

Axtell, M. J. and Staskawicz, B. (2003) Initiation of RPS2-specified disease resistance in Arabidopsis is coupled to the AvrRpt2-directed elimination of RIN4. Cell **112**: 369-377.

Bauer, Z., Gómez-Gómez, L., Boller, T. and Felix, G. (2001) Sensitivity of different ecotypes and mutants of *Arabidopsis thaliana* toward the bacterial elicitor flagellin correlates with the presence of receptor-binding sites. J. Biol. Chem. **276**: 45669-45676.

Becerra, C., Jahrmann, T., Puigdomènecha, P. and Vicient, C. M. (2004) Ankyrin repeat-containing proteins in *Arabidopsis*: characterization of a novel and abundant group of genes coding ankyrin-transmembrane proteins. Gene **340**: 111–121.

Bell, C. J. and Ecker, J. R. (1994) Assignment of 30 microsatellite loci to the linkage map of Arabidopsis. Genomics **19**: 137-144.

Bender, C. L., Alarcon-Chaidez, F. and Gross, D. C. (1999) *Pseudomonas syringae* phytotoxins: mode of action, regulation, and biosynthesis by peptide and polypeptide synthetases. Microbiol. Mol. Biol. Rev. **63**: 266-292.

Bent, A. F., Innes, R. W., Ecker, J. R. and Staskawicz, B. J. (1992) Disease development in ethylene-insensitive *Arabidopsis thaliana* infected with virulent and avirulent *Pseudomonas* and *Xanthomonas* pathogens. Mol. Plant-Microbe Interact. **5**: 372-378.

Berger, S. (2002) Jasmonate-related mutants of *Arabidopsis* as tools for studying stress signaling. Planta **214**: 497-504.

Berrocal-Lobo, M., Molina, A. and Solano, R. (2002) Constitutive expression of ETHYLENE-RESPONSE-FACTOR1 in Arabidopsis confers resistance to several necrotrophic fungi. Plant J. **29**: 23-32.

Bittel, P. and Robatzek, S. (2007) Microbe-associated molecular patterns (MAMPs) probe plant immunity. Curr. Opin. Plant Biol. **10**: 335-341.

Blee, K. A., Yang, K.-Y. and Anderson, A. J. (2004) Activation of defense pathways: synergism between reactive oxygen species and salicylic acid and consideration of field applicability. Eur. J. Plant Pathol. **110**: 203-212.

Blume, B., Nürnberger, T., Nass, N. and Scheel, D. (2000) Receptor-mediated increase in cytoplasmic free calcium required for activation of pathogen defense in parsley. Plant Cell **12**: 1425-1440.

Boch, J., Verbsky, M. L., Robertson, T. L., Larkin, J. C. and Kunkel, B. N. (1998) Analysis of resistance gene-mediated defense responses in *Arabidopsis thaliana* plants carrying a mutation in *cpr5*. Mol. Plant-Microbe Interact. **11**: 1196-1206.

Boller, T. (1991) Ethylene in pathogenesis and disease resistance. In: *The Plant Hormone Ethylene*. Mattoo, A. K. and Suttle, J. C. (eds.). CRC Press, Boca Raton.

Bolwell, G. P., Bozak, K. and Zimmerlin, A. (1994) Plant cytochrome P450. Phytochemistry **37**: 1491-1506.

Bonas, U. and Lahaye, T. (2002) Plant disease resistance triggered by pathogen-derived molecules: refined models of specific recognition. Curr. Opin. Microbiol. **5**: 44-50.

Booij-James, I. S., Dube, S. K., Jansen, M. A. K., Edelman, M. and Mattoo, A. K. (2000) Ultraviolet-B radiation impacts light-mediated turnover of the photosystem II reaction center heterodimer in Arabidopsis mutants altered in phenolic metabolism. Plant Physiol. **124**: 1275-1283.

Bostock, R. M. (2005) Signal crosstalk and induced resistance: straddling the line between cost and benefit. Annu. Rev. Phytopathol. **43**: 545-580.

Boter, M., Ruíz-Rivero, O., Abdeen, A. and Prat, S. (2004) Conserved MYC transcription factors play a key role in jasmonate signaling both in tomato and Arabidopsis. Genes Dev. **18**: 1577-1591.

Bowling, S. A., Clarke, J. D., Liu, Y., Klessig, D. F. and Dong, X. (1997) The *cpr5* mutant of Arabidopsis expresses both NPR1-dependent and NPR1-independent resistance. Plant Cell **9**: 1573-1584.

Bowling, S. A., Guo, A., Cao, H., Gordon, S., Klessig, D. F. and Dong, X. (1994) A mutation in Arabidopsis that leads to constitutive expression of systemic acquired resistance. Plant Cell **6**: 1845-1857.

Bowman, J. L., Smyth, D. R. and Meyerowitz, E. M. (1991) Genetic interactions among floral homeotic genes of *Arabidopsis*. Development **112**: 1-20.

Bradley, D. J., Kjellbom, P. and Lamb, C. J. (1992) Elicitor- and wound-induced oxidative cross-linking of a proline-rich plant cell wall protein: a novel, rapid defense response. Cell **70**: 21-30.

Braun, U. (1999) Some critical notes on the classification and the generic concept of the *Erysiphaceae*. Schlechtendalia **3**: 48-54.

Brenner, W. G., Romanov, G. A., Kollmer, I., Burkle, L. and Schmulling, T. (2005) Immediate-early and delayed cytokinin response genes of *Arabidopsis thaliana* identified by genome-wide expression profiling reveal novel cytokinin-sensitive processes and suggest cytokinin action through transcriptional cascades. Plant J. **44**: 314-333.

Brodersen, P., Petersen, M., Nielsen, H. B., Zhu, S., Newman, M.-A., Shokat, K. M., Rietz, S., Parker, J. E. and Mundy, J. (2006) Arabidopsis MAP kinase 4 regulates salicylic acid- and jasmonic/ethylene-dependent responses via EDS1 and PAD4. Plant J. **47**: 532-546.

Brooks, D. M., Bender, C. L. and Kunkel, B. N. (2005) The *Pseudomonas syringae* phytotoxin coronatine promotes virulence by overcoming salicylic acid-dependent defences in *Arabidopsis thaliana*. Mol. Plant Pathol. **6**: 629-640.

Brown, I., Trethowan, J., Kerry, M., Mansfield, J. and Bolwell, G. P. (1998) Localization of components of the oxidative cross-linking of glycoproteins and of callose synthase in papillae formed during the interaction between non-pathogenic strains of *Xanthomonas campestris* and French bean mesophyll cells. Plant J. **15**: 333-343.

Brown, R. L., Kazan, K., McGrath, K. C., Maclean, D. J. and Manners, J. M. (2003) A role for the GCC-box in jasmonate-mediated activation of the *PDF1.2* gene of Arabidopsis. Plant Physiol. **132**: 1020–1032.

Browning, K. S. (2004) Plant translation initiation factors: it is not easy to be green. Biochem. Soc. Trans. **32**: 589-591.

Brunner, F., Rosahl , S., Lee, J., Rudd, J. J., Geiler, C., Kauppinen, S., Rasmussen, G., Scheel, D. and Nürnberger, T. (2002) Pep-13, a plant defense-inducing pathogen-associated pattern from *Phytophthora* transglutaminases. EMBO J. **21**: 6681-6688.

Bussink, H. J. and Oliver, R. (2001) Identification of two highly divergent catalase genes in the fungal tomato pathogen, *Cladosporium fulvum*. Eur. J. Biochem. **268**: 15-24.

Cao, H., Bowling, S. A., Gordon, A. S. and Dong, X. N. (1994) Characterization of an *Arabidopsis* mutant that is nonresponsive to inducers of systemic acquired resistance. Plant Cell **6**: 1583-1592.

Cao, H., Li, X. and Dong, X. (1998) Generation of broad-spectrum disease resistance by overexpression of an essential regulatory gene in systemic acquired resistance. Proc. Natl. Acad. Sci. USA **95**: 6531-6536.

Cao, J., Duan, X., McElroy, D. and Wu, R. (1992) Regeneration of herbicide resistant transgenic rice plants following microprojectile-mediated transformation of suspension culture cells. Plant Cell Rep. **11**: 586-591.

Cary, A. J., Liu, W. and Howell, S. H. (1995) Cytokinin action is coupled to ethylene in its effects on the inhibition of root and hypocotyl elongation in *Arabidopsis thaliana* seedlings. Plant Physiol. **107**: 1075–1082.

Chagué, V., Danit, L.-V., Siewers, V., Schulze-Gronover, C., Tudzynski, P., Tudzynski, B. and Sharon, A. (2006) Ethylene sensing and gene activation in *Botrytis cinerea*: a missing link in ethylene regulation of fungus-plant interactions? Mol. Plant-Microbe Interact. **19**: 33-42.

Chang, C. (2003) Ethylene signaling: the MAPK module has finally landed. Trends Plant Sci. **8**: 365-368.

Chang, C., Bowman, J. L., DeJohn, A. W., Lander, E. S. and Meyerowitz, E. M. (1988) Restriction fragment length polymorphism linkage map for *Arabidopsis thaliana*. Proc. Natl. Acad. Sci. USA **85**: 6856-6860.

Chang, C., Kwok, S. F., Bleecker, A. B. and Meyerowitz, E. M. (1993) Arabidopsis ethylene response gene ETR1: similarity of product to two-component regulators. Science **262**: 539-544.

Chapple, C. C. S. (1998) Molecular-genetic analysis of plant cytochrome P450-dependent monooxygenases. Annu. Rev. Plant Physiol. Plant Mol. Biol. **49**: 311-343.

Chapple, C. C. S., Vogt, T., Ellis, B. E. and Somerville, C. R. (1992) An *Arabidopsis* mutant defective in the general phenylpropanoid pathway. Plant Cell **4**: 1413-1424.

Chen, C. and Chen, Z. (2002) Potentiation of developmentally regulated plant defense response by AtWRKY18, a pathogen-induced Arabidopsis transcription factor. Plant Physiol. **129**: 706-716.

Cheong, J.-J. and Choi, Y. D. (2003) Methyl jasmonate as a vital substance in plants. Trends Genet. **19**: 409-413.

Cheong, Y. H., Chang, H.-S., Gupta, R., Wang, X., Zhu, T. and Luan, S. (2002) Transcriptional profiling reveals novel interactions between wounding, pathogen, abiotic stress, and hormonal responses in *Arabidopsis*. Plant Physiol. **129**: 661-667.

Chinchilla, D., Bauer, Z., Regenass, M., Boller, T. and Felix, G. (2005) The *Arabidopsis* receptor kinase FLS2 binds flg22 and determines the specificity of flagellin perception. Plant Cell **18**: 465-476.

Chinchilla, D., Zipfel, C., Robatzek, S., Kemmerling, B., Nürnberger, T., Jones, J. D. G., Felix, G. and Boller, T. (2007) A flagellin-induced complex of the receptor FLS2 and BAK1 initiates plant defence. Nature **448**: 497-501.

Chini, A., Fonseca, S., Fernández, G., Adie, B., Chico, J. M., Lorenzo, O., García-Casado, G., López-Vidriero, I., Lozano, F. M., Ponce, M. R., Micol, J. L. and Solano, R. (2007) The JAZ family of repressors is the missing link in jasmonate signalling. Nature **448**: 666-671.

Chisholm, S. T., Coaker, G., Day, B. and Staskawicz, B. J. (2006) Host-microbe interactions: shaping the evolution of plant immune responses. Cell **124**: 803-814.

Chomczynski, P. and Sacchi, N. (1987) Single step method of RNA isolation by acid guanidinium thiocyanate-phenol-chloroform extraction. Anal. Biochem. **162**: 156-159.

Church, G. M. and Gilbert, W. (1984) Genomic sequencing. Proc. Natl. Acad. Sci. USA **81**: 1991-1995.

Ciftci-Yilmaz, S., Morsy, M. R., Song, L., Coutu, A., Krizek, B. A., Lewis, M. W., Warren, D., Cushman, J., Connolly, E. L. and Mittler, R. (2007) The EAR-motif of the Cys2/His2-type zinc finger protein Zat7 plays a key role in the defense response of *Arabidopsis* to salinity stress. J. Biol. Chem. **282**: 9260-9268.

Clarke, A., Desikan, R., Hurst, R. D., Hancock, J. T. and Neill, S. J. (2000a) NO way back: nitric oxide and programmed cell death in *Arabidopsis thaliana* suspension cells. Plant Journal **24**: 667-677.

Clarke, J. D., Aarts, N., Feys, B. J., Dong, X. and Parker, J. E. (2001) Constitutive disease resistance requires *EDS1* in the *Arabidopsis* mutants *cpr1* and *cpr6* and is partially *EDS1*-dependent in *cpr5*. Plant J. **26**: 409-420.

Clarke, J. D., Liu, Y., Klessig, D. F. and Dong, X. (1998) Uncoupling *PR* gene expression from NPR1 and bacterial resistance: Characterization of the dominant Arabidopsis *cpr6-1* mutant. Plant Cell **10**: 557-569.

Clarke, J. D., Volko, S. M., Ledford, H., Ausubel, F. M. and Dong, X. (2000b) Roles of Salicylic Acid, Jasmonic Acid, and Ethylene in *cpr*-Induced Resistance in Arabidopsis. Plant Cell **12**: 2175-2190.

Clough, S. J. and Bent, A. F. (1998) Floral dip: a simplified method for *Agrobacterium*-mediated transformation of *Arabidopsis thaliana*. Plant J. **16**: 735-743.

Clough, S. J., Fengler, K. A., Yu, I.-c., Lippok, B., Smith, R. K., Jr and Bent, A. F. (2000) The Arabidopsis *dnd1* "defense, no death" gene encodes a mutated cyclic nucleotide-gated ion channel. Proc. Natl. Acad. Sci. USA **97**: 9323-9328.

Coego, A., Ramirez, V., Gil, M. J., Flors, V., Mauch-Mani, B. and Vera, P. (2005) An Arabidopsis homeodomain transcription factor, *OVEREXPRESSOR OF CATIONIC PEROXIDASE 3*, mediates resistance to infection by necrotrophic pathogens. Plant Cell **17**: 2123-2137.

Conrath, U., Pieterse, C. M. and Mauch-Mani, B. (2002) Priming in plant-pathogen interactions. Trends Plant Sci. **7**: 210-216.

Crawford, N. M. and Guo, F. M. (2005) New insights into nitric oxide metabolism and regulatory functions. Trends Plant Sci. **4**: 195-200.

Creelman, R. A. and Mullet, J. E. (1997) Biosynthesis and action of jasmonates in plants. Annu. Rev. Plant Physiol. Plant Mol. Biol. **48**: 355-381.

da Cunha, L., McFall, A. J. and Mackey, D. (2006) Innate immunity in plants: a continuum of layered defenses. Microbes Infect. **8**: 1372-1381.

da Cunha, L., Sreerekha, M.-V. and Mackey, D. (2007) Defense suppression by virulence effectors of bacterial phytopathogens. Curr. Opin. Plant Biol. **10**: 349-357.

Dangl, J. L. and Jones, J. D. G. (2001) Plant pathogens and integrated defence responses to infection. Nature **411**: 826-833.

Dardick, C. and Ronald, P. (2006) Plant and animal pathogen recognition receptors signal through non-RD kinases. PLoS Pathog. **2**: e2.

Day, B., Dahlbeck, D., Huang, J., Chisholm, S. T., Li, D. and Staskawicz, B. J. (2005) Molecular basis for the RIN4 negative regulation of RPS2 disease resistance. Plant Cell **17**: 1292–1305.

Delaney, T. P., Friedrich, L. and Ryals, J. A. (1995) Arabidopsis signal transduction mutant defective in chemically and biologially induced disease resistance. Proc. Natl. Acad. Sci. USA **92**: 6602-6606.

Delledonne, M. (2005) NO news is good news for plants. Curr. Opin. Plant Biol. **8**: 390-396.

Delledonne, M., Xia, Y., Dixon, R. and Lamb, C. (1998) Nitric oxide functions as a signal in plant disease resistance. Nature **394**: 585-588.

Delledonne, M., Zeier, J., Marocco, A. and Lamb, C. (2001) Signal interactions between nitric oxide and reactive oxygen intermediates in the plant hypersensitive disease resistance response. Proc. Natl. Acad. Sci. USA **98**: 13454-13459.

Dempsey, D. M. A., Shah, J. and Klessig, D. F. (1999) Salicylic acid and disease resistance in plants. Crit. Rev. Plant. Sci. **18**: 547-575.

Denby, K. J., Jason, L. J. M., Murray, S. L. and Last, R. L. (2005) *ups1*, an *Arabidopsis thaliana* camalexin accumulation mutant defective in multiple defence signalling pathways. Plant J. **41**: 673-684.

Denby, K. J., Kumar, P. and Kliebenstein, D. J. (2004) Identification of *Botrytis cinerea* susceptibility loci in *Arabidopsis thaliana*. Plant J. **38**: 473-486.

Desikan, R., Hancock, J. T., Bright, J., Harrison, J., Weir, I., Hooley, R. and Neill, S. J. (2005) A role for ETR1 in hydrogen peroxide signaling in stomatal guard cells. Plant Physiol. **137**: 831-834.

Desikan, R., Hancock, J. T., Ichimura, K., Shinozaki, K. and Neill, S. J. (2001) Harpin induces activation of the *Arabidopsis* mitogen-activated protein kinases AtMPK4 and AtMPK6. Plant Physiol. **126**: 1579-1587.

Deslandes, L., Olivier, J., Peeters, N., Feng, D. X., Khounlotham, M., Boucher, C., Somssich, I., Genin, S. and Marco, Y. (2003) Physical interaction between RRS1-R, a protein conferring resistance to bacterial wilt, and PopP2, a type III effector targeted to the plant nucleus. Proc. Natl. Acad. Sci. USA **100**: 8024-8029.

Despres, C., Chubak, C., Rochon, A., Clark, R., Bethune, T., Desveaux, D. and Fobert, P. R. (2003) The *Arabidopsis* NPR1 disease resistance protein is a novel cofactor that confers redox regulation of DNA binding activity to the basic domain/leucine zipper transcription factor TGA1. Plant Cell **15**: 2181-2191.

Desveaux, D., Maréchal, A. and Brisson, N. (2005) Whirly transcription factors: defense gene regulation and beyond. Trends Plant Sci. **10**: 95-102.

Desveaux, D., Subramaniam, R., Després, C., Mess, J.-N., Lévesque, C., Fobert, P. R., Dangl, J. L. and Brisson, N. (2004) A "Whirly" transcription factor is required for salicylic acid-dependent disease resistance in *Arabidopsis*. Dev. Cell **6**: 229-240.

Dettmer, J., Hong-Hermesdorf, A., Stierhof, Y.-D. and Schumacher, K. (2006) Vacuolar H^+-ATPase activity is required for endocytic and secretory trafficking in *Arabidopsis*. Plant Cell **18**: 715-730.

Dettmer, J., Schubert, D., Calvo-Weimar, O., Stierhof, Y.-D., Schmidt, R. and Schumacher, K. (2005) Essential role of the V-ATPase in male gametophyte development. Plant J. **41**: 117–124.

Devadas, S. K., Enyedi, A. and Raina, R. (2002) The Arabidopsis *hrl1* mutation reveals novel overlapping roles for salicylic acid, jasmonic acid and ethylene signalling in cell death and defence against pathogens. Plant J. **30**: 467-480.

Dever, T. E. (2002) Gene-specific regulation by general translation factors. Cell **108**: 545-556.

Devoto, A., Ellis, C., Magusin, A., Chang, H.-S., Chilcott, C., Zhu, T. and Turner, J. G. (2005) Expression profiling reveals *COI1* to be a key regulator of genes involved in wound- and methyl jasmonate-induced secondary metabolism, defence, and hormone interactions. Plant Mol. Biol. **58**: 497-513.

Devoto, A. and Turner, J. G. (2003) Regulation of jasmonate-mediated plant responses in Arabidopsis. Ann. Bot. **92**: 329-337.

Devoto, A. and Turner, J. G. (2005) Jasmonate-regulated Arabidopsis stress signalling network. Physiol. Plant. **123**: 161-172.

Diaz, J., ten Have, A. and van Kan, J. A. (2002) The role of ethylene and wound signaling in resistance of tomato to *Botrytis cinerea*. Plant Physiol. **129**: 1341-1351.

Diévart, A. and Clark, S. E. (2003) Using mutant alleles to determine the structure and function of leucine-rich repeat receptor-like kinases. Curr. Opin. Plant Biol. **6**: 507-516.

Dinka, S. J. and Raizada, M. N. (2006) Inexpensive fine mapping and positional cloning in plants using visible, mapped transgenes. Can. J. Bot. **84**: 179–188.

Dixon, R. A. (2001) Natural products and plant disease resistance. Nature **411**: 843-847.

Doke, N. (1983) Generation of superoxide anion by potato tuber protoplasts during the hypersensitive response to hyphal cell wall components of *Phytophthora infestans* and specific inhibition of the reaction by suppressors of hypersensitivity. Physiol. Plant Pathol. **23**: 359-367.

Donaldson, R. P. and Luster, D. G. (1991) Multiple forms of plant cytochromes P450. Plant Physiol. **96**: 669-674.

Dong, X. (1998) SA, JA, ethylene, and disease resistance in plants. Curr. Opin. Plant Biol. **1**: 316-323.

Dong, X. (2001) Genetic dissection of systemic acquired resistance. Curr. Opin. Plant Biol. **4**: 309-314.

Dong, X. (2004) NPR1, all things considered. Curr. Opin. Plant Biol. **7**: 547-552.

Dong, X., Mindrinos, M., Davis, K. R. and Ausubel, F. M. (1991) Induction of *Arabidopsis* defense genes by virulent and avirulent *Pseudomonas syringae* strains and by a cloned avirulence gene. Plant Cell **3**.

Donofrio, N. M. and Delaney, T. P. (2001) Abnormal callose response phenotype and hypersusceptibility to *Peronospora parasitica* in defense-compromised Arabidopsis *nim1-1* and salicylate hydroxylase-expressing plants. Mol. Plant-Microbe Interact. **14**: 439-450.

Drenkard, E., Richter, B. G., Rozen, S., Stutius, L. M., Angell, N. A., Mindrinos, M., Cho, R. J., Oefner, P. J., Davis, R. W. and Ausubel, F. M. (2000) A simple procedure for the analysis of single nucleotide polymorphisms facilitates map-based cloning in Arabidopsis. Plant Physiol. **124**: 1483-1492.

Drouaud, J., Camilleri, C., Bourguignon, P.-Y., Canaguier, A., Bérard, A., Vezon, D., Giancola, S., Brunel, D., Colot, V., Prum, B., Quesneville, H. and Mézard, C. (2006) Variation in crossing-over rates across chromosome 4 of *Arabidopsis thaliana* reveals the presence of meiotic recombination "hot spots". Genome Research **16**: 106-114.

Durner, J., Wendehenne, D. and Klessig, D. F. (1998) Defense gene induction in tobacco by nitric oxide, cyclic GMP and cyclic ADP ribose. Proc. Natl. Acad. Sci. USA **95**: 10328-10333.

Durrant, W. E. and Dong, X. (2004) Systemic acquired resistance. Annu. Rev. Phytopathol. **42**: 185-209.

Durrett, R. T., Chen, K.-Y. and Tanksley, S. D. (2002) A simple formula useful for positional cloning. Genetics **160**: 353-355.

Ecker, J. R. (2004) Re-entry of the ethylene MPK6 module. Plant Cell **16**: 3169-3173.

Edwards, K., Johnstone, C. and Thompson, C. (1991) A simple and rapid method for the preparation of plant genomic DNA for PCR analysis. Nucleic Acids Res. **19**: 1349.

Elad, Y. (1993) Regulators of ethylene biosynthesis or activity as a tool for reducing susceptibility of host plant tissues to infection by *Botrytis cinerea*. Neth. J. Plant Pathol. **99**: 105-113.

Ellis, C., Karafyllidis, I. and Turner, J. G. (2002) Constitutive activation of jasmonate signaling in an *Arabidopsis* mutant correlates with enhanced resistance to *Erysiphe cichoracearum*, *Pseudomonas syringae*, and *Myzus persicae*. Mol. Plant-Microbe Interact. **15**: 1025-1030.

Ellis, C. and Turner, J. G. (2001) The Arabidopsis mutant *cev1* has constitutively active jasmonate and ethylene signal pathways and enhanced resistance to pathogens. Plant Cell **13**: 1025-1033.

Espinosa, A. and Alfano, J. R. (2004) Disabling surveillance: bacterial type III secretion system effectors that suppress innate immunity. Cell. Microbiol. **6**: 1027–1040.

Eulgem, T. (2005) Regulation of the *Arabidopsis* defense transcriptome. Trends Plant Sci. **10**: 71-78.

Eulgem, T., Rushton, P. J., Schmelzer, E., Hahlbrock, K. and Somssich, I. E. (1999) Early nuclear events in plant defense: rapid gene activation by WRKY transcription factors. EMBO J. **18**: 4689-4699.

Eulgem, T. and Somssich, I. E. (2007) Networks of WRKY transcription factors in defense signaling. Curr. Opin. Plant Biol. **10**: 366-371.

Eulgem, T., Weigman, V. J., Chang, H.-S., McDowell, J. M., Holub, E. B., Glazebrook, J., Zhu, T. and Dangl, J. L. (2004) Gene expression signatures from three genetically separable resistance gene signaling pathways for downy mildew resistance. Plant Physiol. **135**: 1129-1144.

Fabri, C. O. and Schaffner, A. R. (1994) An Arabidopsis thaliana RFLP mapping set to localize mutations to chromosomal regions. Plant J. **5**: 149-156.

Falk, A., Feys, B. J., Frost, L. N., Jones, J. D. G., Daniels, M. J. and Parker, J. E. (1999) *EDS1*, an essential component of *R* gene-mediated disease resistance in *Arabidopsis* has homology to eukaryotic lipases. Proc. Natl. Acad. Sci. USA **96**: 3292-3297.

Farmer, E. E., Almeras, E. and Krishnamurthy, V. (2003) Jasmonates and related oxylipins in plant responses to pathogenesis and herbivory. Curr. Opin. Biotechnol. **6**: 372-378.

Feechan, A., Kwon, E., Yun, B.-W., Wang, Y., Pallas, J. A. and Loake, G. J. (2005) A central role for *S*-nitrosothiols in plant disease resistance. Proc. Natl. Acad. Sci. USA **102**: 8054–8059.

Felix, G. and Boller, T. (2003) Molecular sensing of bacteria in plants. The highly conserved RNA-binding motif RNP-1 of bacterial cold shock proteins is recognized as an elicitor signal in tobacco. J. Biol. Chem. **278**: 6201-6208.

Felix, G., Duran, J., Volko, S. and Boller, T. (1999) Plants have a sensitive perception system for the most conserved domain of bacterial flagellin. Plant J. **18**: 265-276.

Fellbrich, G., Romanski, A., Varet, A., Blume, B., Brunner, F., Engelhardt, S., Felix, G., Kemmerling, B., Krzymowska, M. and Nürnberger, T. (2002) NPP1, a *Phytophthora*-associated trigger of plant defence in parsley and *Arabidopsis*. Plant J. **32**: 375-390.

Ferrari, S., Plotnikova, J. M., De Lorenzo, G. and Ausubel, F. M. (2003) Arabidopsis local resistance to *Botrytis cinerea* involves salicylic acid and camalexin and requires *EDS4* and *PAD2*, but not *SID2*, *EDS5* or *PAD4*. Plant J. **35**: 193-205.

Feys, B. J., Benedetti, C. E., Penfold, C. N. and Turner, J. G. (1994) Arabidopsis mutants selected for resistance to the phytotoxin coronatine are male-sterile, insensitive to methyl jasmonate, and resistant to a bacterial pathogen. Plant Cell **6**: 751-759.

Feys, B. J., Moisan, L. J., Newman, M.-A. and Parker, J. E. (2001) Direct interaction between the *Arabidopsis* disease resistance signalling proteins, EDS1 and PAD4. EMBO J. **20**: 5400-5411.

Feys, B. J., Wiermer, M., Bhat, R. A., Moisan, L. J., Medina-Escobar, N., Neu, C., Cabral, A. and Parker, J. E. (2005) Arabidopsis SENESCENCE-ASSOCIATED GENE101 stabilizes and signals with an ENHANCED DISEASE SUSCEPTIBILITY1 complex in plant innate immunity. Plant Cell **17**: 2601-2613.

Flor, H. H. (1971) Current status of the gene-for-gene concept. Annu. Rev. Phytopathol. **9**: 275-296.

Fobert, P. R. and Després, C. (2005) Redox control of systemic acquired resistance. Curr. Opin. Plant Biol. **8**: 378-382.

Foissner, I. D., Wendehenne, D., Langebartels, C. and Durner, J. (2000) *In vivo* imaging of an elicitor-induced nitric oxide burst in tobacco. Plant J. **23**: 817-824.

Friedrich, L., Lawton, K., Dietrich, R., Willits, M., Cade, R. and Ryals, J. (2001) NIM1 overexpression in Arabidopsis potentiates plant disease resistance and results in enhanced effectiveness of fungicides. Mol. Plant-Microbe Interact. **14**: 1114-1124.

Fritz-Laylin, L. K., Krishnamurthy, N., Tör, M., Sjolander, K. V. and Jones, J. D. G. (2005) Phylogenomic analysis of the receptor-like proteins of rice and Arabidopsis. Plant Physiol. **138**: 611-623.

Frye, C. A., Tang, D. and Innes, R. W. (2001) Negative regulation of defense responses in plants by a conserved MAPKK kinase. Proc. Natl. Acad. Sci. USA **98**: 373-378.

Fujimoto, S. Y., Ohta, M., Usui, A., Shinshi, H. and Ohme-Takagi, M. (2000) Arabidopsis ethylene-responsive element binding factors act as transcriptional activators or repressors of GCC box mediated gene expression. Plant Cell **12**: 393-404.

Gasciolli, V., Mallory, A. C., Bartel, D. P. and Vaucheret, H. (2005) Partially redundant functions of *Arabidopsis* DICER-like enzymes and a role for DCL4 in producing trans-acting siRNAs. Curr. Biol. **15**: 1494-1500.

Gfeller, A. and Farmer, E. E. (2004) Keeping the leaves green above us. Science **306**: 1515-1516.

Gigardin, S. E. and Philpott, D. J. (2004) Mini-review: the role of peptidoglycan recognition in innate immunity. Eur. J. Immunol. **34**: 1777-1782.

Girardin, S. E., Sansonetti, P. J. and Philpott, D. J. (2002) Intracellular vs extracellular recognition of pathogens - common concepts in mammals and flies. Trends Microbiol. **10**: 193-199.

Glawischnig, E. (2007) Molecules of interest: Camalexin. Phytochemistry **68**: 401-406.

Glawischnig, E., Hansen, B. G., Olsen, C. E. and Halkier, B. A. (2004) Camalexin is synthesized from indole-3-acetaldoxime, a key branching point between primary and secondary metabolism in Arabidopsis. Proc. Natl. Acad. Sci. USA **101**: 8245-8250.

Glazebrook, J. (1999) Genes controlling expression of defense responses in Arabidopsis. Curr. Opin. Plant Biol. **2**: 280-286.

Glazebrook, J. (2001) Genes controlling expression of defense responses in *Arabidopsis* - 2001 status. Curr. Opin. Plant Biol. **4**: 301-308.

Glazebrook, J. (2005) Contrasting mechanisms of defense against biotrophic and necrotrophic pathogens. Annu. Rev. Phytopathol. **43**: 205–227.

Glazebrook, J. and Ausubel, F. M. (1994) Isolation of phytoalexin-deficient mutants of *Arabidopsis thaliana* and characterization of their interactions with bacterial pathogens. Proc. Natl. Acad. Sci. USA **91**: 8955-8959.

Glazebrook, J., Chen, W., Estes, B., Chang, H.-S., Nawrath, C., Metraux, J.-P., Zhu, T. and Katagiri, F. (2003) Topology of the network integrating salicylate and jasmonate signal transduction derived from global expression phenotyping. Plant J. **34**: 217-228.

Glazebrook, J., Rogers, E. E. and Ausubel, F. M. (1996) Isolation of Arabidopsis mutants with enhanced disease susceptibility by direct screening. Genetics **143**: 973-982.

Gómez-Gómez, L. (2004) Plant perception systems for pathogen recognition and defence. Mol. Immunol. **41**: 1055–1062.

Gómez-Gómez, L., Bauer, Z. and Boller, T. (2001) Both the extracellular leucine-rich repeat domain and the kinase activity of FLS2 are required for flagellin binding and signalling in *Arabidopsis*. Plant Cell **13**: 1155-1163.

Gómez-Gómez, L. and Boller, T. (2000) FLS2: an LRR receptor-like kinase involved in the perception of the bacterial elicitor flagellin in *Arabidopsis*. Mol. Cell **5**: 1003-1011.

Gómez-Gómez, L. and Boller, T. (2002) Flagellin perception: a paradigm for innate immunity. Trends Plant Sci. **7**: 251-256.

Gómez-Gómez, L., Felix, G. and Boller, T. (1999) A single locus determines sensitivity to bacterial flagellin in *Arabidopsis thaliana*. Plant J. **18**: 277-284.

Govrin, E. M. and Levine, A. (2000) The hypersensitive response facilitates plant infection by the necrotrophic pathogen *Botrytis cinerea*. Curr. Biol. **10**: 751-757.

Grant, J. J., Yun, B.-Y. and Loake, G. J. (2000a) Oxidative burst and cognate redox signalling reported by luciferase imaging: identification of a redox signalling network that functions independently of ethylene, SA and Me-JA but is dependent on MAPKK activity. Plant J. **24**: 569-582.

Grant, M., Brown, I., Adams, S., Knight, M., Ainslie, A. and Mansfield, J. (2000b) The RPM1 plant disease resistance gene facilitates a rapid and sustained increase in cytosolic calcium that is necessary for the oxidative burst and hypersensitive cell death. Plant J. **23**: 441-450.

Grant, M., Godiard, L., Straube, E., Ashfield, T., Lewald, J., Sattler, A., Innes, R. W. and Dangl, J. L. (1995) Structure of the Arabidopsis *Rpm1* gene enabling dual-specificity disease resistance. Science **269**: 843-846.

Greenberg, J. (1997) Programmed cell death in plant-pathogen interactions. Annu. Rev. Plant Physiol. Plant Mol. Biol. **48**: 525-545.

Greenberg, J. T. and Yao, N. (2004) The role and regulation of programmed cell death in plant-pathogen interactions. Cell. Microbiol. **6**: 201-211.

Griffiths, A. J. F., Miller, J. H., Suzuki, D. T., Lewontin, R. C. and Gelbart, W. M. (2004) Basic eukaryotic chromosome mapping. In: *An Introduction to Genetic Analysis*. Griffiths, A. J. F. (eds.). Freeman, W H and Co., New York.

Grubb, C. D. and Abel, S. (2006) Glucosinolate metabolism and its control. Trends Plant Sci. **11**: 89-100.

Gu, Y.-Q., Wildermuth, M. C., Chakravarthy, S., Loh, Y.-T., Yang, C., He, X., Han, Y. and Martin, G. B. (2002) Tomato transcription factors Pti4, Pti5, and Pti6 activate defense responses when expressed in Arabidopsis. Plant Cell **14**: 817-831.

Guo, H. and Ecker, J. R. (2004) The ethylene signaling pathway: new insights. Curr. Opin. Plant Biol. **7**: 40-49.

Gupta, V., Willits, M. G. and Glazebrook, J. (2000) *Arabidopsis thaliana EDS4* contributes to salicylic acid (SA)-dependent expression of defense responses: evidence for inhibition of jasmonic acid signaling by SA. Mol. Plant-Microbe Interact. **13**: 503-511.

Gutterson, N. and Reuber, T. L. (2004) Regulation of disease resistance pathways by AP2/ERF transcription factors. Curr. Opin. Plant Biol. **7**: 465–471.

Guzman, P. and Ecker, J. R. (1990) Exploiting the triple response of *Arabidopsis* to identify ethylene-related mutants. Plant Cell **2**: 513-523.

Halkier, B. A. and Gershenson, J. (2006) Biology and biochemistry of glucosinolates. Annu. Rev. Plant Biol. **57**: 303-333.

Hammerschmidt, R. (1999) Phytoalexins: What have we learned after 60 years? Annu. Rev. Phytopathol. **37**: 285-306.

Hammond-Kosack, K. E. and Parker, J. E. (2003) Deciphering plant-pathogen communication: fresh perspectives for molecular resistance breeding. Curr. Opin. Biotechnol. **14**: 177-193.

Heath, M. (2000) Nonhost resistance and nonspecific plant defenses. Curr. Opin. Plant Biol. **3**: 315-319.

Hemm, M. R., Ruegger, M. O. and Chapple, C. C. S. (2003) The Arabidopsis *ref2* mutant is defective in the gene encoding CYP83A1 and shows both phenylpropanoid and glucosinolate phenotypes. Plant Cell **15**: 179–194.

Higuchi, M., Pischke, M. S., Mahonen, A. P., Miyawaki, K., Hashimoto, Y., Seki, M., Kobayashi, M., Shinozaki, K., Kato, T., Tabata, S., Helariutta, Y., Sussman, M. R. and Kakimoto, T. (2004) *In planta* functions of the Arabidopsis cytokinin receptor family. Proc. Natl. Acad. Sci. USA **101**: 8821-8826.

Hirt, H. (2000) Results and problems in cell differentiation: MAP kinases in plant signal transduction. Springer, Heidelberg.

Holsters, M., Silva, B., van Vliet, F., Genetello, C., de Block, M., Dhaese, P., Depicker, A., Inzé, D., Engler, G., Villarroel, R., van Montagu, M. and Schell, J. (1980) The functional organization of the nopaline *A. tumefaciens* plasmid pTiC58 Plasmid **3**: 212-230.

Holub, E. B. (1997) Organization of resistance genes in Arabidopsis. In: *The Gene-for-Gene Relationship in Plant-Parasite Interactions*. Crute, I. R., Holub, E. B. and Burdon, J. J. (eds.). CAB International, Wallingford.

Holub, E. B., Beynon, J. L. and Crute, I. R. (1994) Phenotypic and genotypic characterization of interactions between isolates of *Peronospora parasitica* and accessions of *Arabidopsis thaliana*. Mol. Plant-Microbe Interact. **7**: 223-239.

Hua, J., Chang, C., Sun, Q. and Meyerowitz, E. M. (1995) Ethylene sensitivity conferred by Arabidopsis ERS gene. Science **269**: 1712-1714.

Hua, J., Grisafi, P., Cheng, S. H. and Fink, G. R. (2001) Plant growth homeostasis is controlled by the *Arabidopsis BON1* and *BAP1* genes. Genes Dev. **15**: 2263-2272.

Hua, J., Sakai, H., Nourizadeh, S., Chen, Q. G., Bleecker, A. B., Ecker, J. R. and Meyerowitz, E. M. (1998) EIN4 and ERS2 are members of the putative ethylene receptor family in Arabidopsis. Plant Cell **10**: 1321-1332.

Huang, X., Stettmaier, K., Michel, C., Hutzler, P., Mueller, M. J. and Durner, J. (2004) Nitric oxide is induced by wounding and influences jasmonic acid signaling in *Arabidopsis thaliana*. Planta **218**: 938-946.

Hückelhoven, R., Dechert, C. and Kogel, K.-H. (2001) Non-host resistance of barley is associated with a hydrogen peroxide burst at sites of attempted penetration by wheat powdery mildew fungus. Mol. Plant Pathol. **2**: 199-205.

Huitema, E., Vleeshouwers, G. A. A., Francis, D. M. and Kamoun, S. (2003) Active defence responses associated with nonhost resistance of *Arabidopsis thaliana* to the oomycete pathogen *Phytophthora infestans*. Mol. Plant Pathol. **4**: 487-500.

Hull, A. K., Vij, R. and Celenza, J. L. (2000) *Arabidopsis* cytochrome P450s that catalyze the first step of tryptophan-dependent indole-3-acetic acid biosynthesis. Proc. Natl. Acad. Sci. USA **97**: 2379-2384.

Ingle, R. A., Carstens, M. and Denby, K. J. (2006) PAMP recognition and the plant–pathogen arms race. BioEssays **28**: 880–889.

Jacobs, A. K., Lipka, V., Burton, R. A., Panstruga, R., Strizhov, N., Schulze-Lefert, P. and Fincher, G. B. (2003) An Arabidopsis callose synthase, GSL5, is required for wound and papillary callose formation. Plant Cell **15**: 2503-2513.

Jakoby, M., Weisshaar, B., Droge-Laser, W., Vicente-Carbajosa, J., Tiedemann, J., Kroj, T. and Parcy, F. (2002) bZIP transcription factors in Arabidopsis. Trends Plant Sci. **7**: 106-111.

Jambunathan, N. and McNellis, T. W. (2003) Regulation of *Arabidopsis COPINE 1* gene expression in response to pathogens and abiotic stimuli. Plant Physiol. **132**: 1370-1381.

Jambunathan, N., Siani, J. M. and McNellis, T. W. (2001) A humidity-sensitive *Arabidopsis* copine mutant exhibits precocious cell death and increased disease resistance. Plant Cell **13**: 2225-2240.

Jander, G., Norris, S. R., Rounsley, S. D., Bush, D. F., Levin, I. M. and Last, R. L. (2002) Arabidopsis map-based cloning in the post-genome era. Plant Physiol. **129**: 440-450.

Jia, Y., MacAdams, S. A., Bryan, G. T., Hershey, H. P. and Valent, B. (2000) Direct interaction of resistance gene and avirulence gene products confers rice blast resistance. EMBO J. **19**: 4004-4014.

Jih, P. J., Chen, Y. C. and Jeng, S. T. (2003) Involvement of hydrogen peroxide and nitric oxide in expression of the ipomoelin gene from sweet potato. Plant Physiol. **132**: 381-389.

Jirage, D., Tootle, T. L., Reuber, T. L., Frost, L. N., Feys, B. J., Parker, J. E., Ausubel, F. M. and Glazebrook, J. (1999) *Arabidopsis thaliana PAD4* encodes a lipase-like gene that is important for salicylic acid signaling. Proc. Natl. Acad. Sci. USA **96**: 13583-13588.

Jirage, D., Zhou, N., Cooper, B., Clarke, J. D., Dong, X. and Glazebrook, J. (2001) Constitutive salicylic acid-dependent signaling in *cpr1* and *cpr6* mutants requires PAD4. Plant J. **26**: 395-407.

Jones, A. M., Thomas, V., Bennett, M. H., Mansfield, J. and Grant, M. (2006) Modifications to the Arabidopsis defense proteome occur prior to significant transcriptional change in response to inoculation with *Pseudomonas syringae*. Plant Physiol. **142**: 1603-1620.

Jones, D. A. and Takemoto, D. (2004) Plant innate immunity – direct and indirect recognition of general and specific pathogen-associated molecules. Curr. Opin. Immunol. **16**: 48–62.

Jones, J. D. G. and Dangl, J. L. (2006) The plant immune system. Nature **444**: 323-329.

Journot-Catalino, N., Somssich, I. E., Roby, D. and Kroj, T. (2006) The transcription factors WRKY11 and WRKY17 act as negative regulators of basal resistance in *Arabidopsis thaliana*. Plant Cell **18**: 3289-3302.

Kachroo, P., Shanklin, J., Shah, J., Whittle, E. J. and Klessig, D. F. (2001) A fatty acid desaturase modulates the activation of defense signaling pathways in plants. Proc. Natl. Acad. Sci. USA **98**: 9448-9453.

Kalde, M., Barth, M., Somssich, I. E. and Lippok, B. (2003) Members of the *Arabidopsis* WRKY group III transcription factors are part of different plant defense signaling pathways. Mol. Plant-Microbe Interact. **16**: 295-305.

Kandoth, P. K., Ranf, S., Pancholi, S. S., Jayanty, S., Walla, M. D., Miller, W., Howe, G. A., Lincoln, D. E. and Stratmann, J. W. (2007) Tomato MAPKs LeMPK1, LeMPK2 and LeMPK3 function in the systemin-mediated defense response against herbivorous insects. Proc. Natl. Acad. Sci. USA **104**: 12205-12210.

Kang, L., Li, J., Zhao, T., Xiao, F., Tang, X., Thilmony, R., He, S. Y. and Zhou, J.-M. (2003) Interplay of the Arabidopsis nonhost resistance gene *NHO1* with bacterial virulence. Proc. Natl. Acad. Sci. USA **18**: 3519-3524.

Karniol, B., Yahalom, A., Kwok, S., Tsuge, T., Matsui, M., Deng, X. W. and Chamovitz, D. A. (1998) The Arabidopsis homologue of an eIF3 complex subunit associates with the COP9 complex. FEBS Lett. **439**: 173-179.

Karpinski, S., Gabrys, H., Mateo, A., Karpinska, B. and Mullineaux, P. M. (2003) Light perception in plant disease defense signalling. Curr. Opin. Plant Biol. **6**: 390-396.

Kasschau, K. D., Fahlgren, N., Chapman, E. J., Sullivan, C. M., Cumbie, J. S., Givan, S. A. and Carrington, J. C. (2007) Genome-wide profiling and analysis of *Arabidopsis* siRNAs. PLoS Biology **5**: 0479-0493.

Katagiri, F., Thilmony, R. and He, S. Y. (2002) The *Arabidopsis thaliana-Pseudomonas syringae* interaction. In: *The Arabidopsis Book*. Somerville, C. R. and Meyerowitz, E. M. (eds.). Am. Soc. Plant Biologists, Rockville.

Katiyar-Agarwal, S., Morgan, R., Dahlbeck, D., Borsani, O., Villegas, A., Jr, Zhu, J.-K., Staskawicz, B. J. and Jin, H. (2006) A pathogen-inducible endogenous siRNA in plant immunity. Proc. Natl. Acad. Sci. USA **103**: 18002-18007.

Kempema, L. A., Cui, X., Holzer, F. M. and Walling, L. L. (2007) Arabidopsis transcriptome changes in response to phloem-feeding silverleaf whitefly nymphs. Similarities and distinctions in responses to aphids. Plant Physiol. **143**: 849-865.

Kende, H. (1993) Ethylene biosynthesis. Annu. Rev. Plant Physiol. Plant Mol. Biol. **44**: 283-307.

Kieber, J. J., Rothenberg, M., Roman, G., Feldmann, K. A. and Ecker, J. R. (1993) CTR1, a negative regulator of the ethylene response pathway in Arabidopsis, encodes a member of the RAF family of protein kinases. Cell **72**: 427-441.

Kim, K.-C., Fan, B. and Chen, Z. (2006) Pathogen-induced Arabidopsis WRKY7 is a transcriptional repressor and enhances plant susceptibility to *Pseudomonas syringae*. Plant Physiol. **142**: 1180-1192.

Kim, M. G., da Cunha, L., McFall, A. J., Belkhadir, Y., DebRoy, S., Dangl, J. L. and Mackey, D. (2005) Two *Pseudomonas syringae* type III effectors inhibit RIN4-regulated basal defense in *Arabidopsis*. Cell **121**: 749-759.

King, E. O., Ward, M. K. and Raney, D. E. (1954) Two simple media for the demonstration of phycocynin and fluorescein. J. Lab. Clin. Med. **44**: 301-307.

Klessig, D. F., Durner, J., Noad, R., Navarre, D. A., Wendehenne, D., Kumar, D., Zhou, J. M., Shah, J., Zhang, S., Kachroo, P., Trifa, Y., Pontier, D., Lam, E. and Silva, H. (2000) Nitric oxide and salicylic acid signaling in plant defense. Proc. Natl. Acad. Sci. USA **97**: 8849-8855.

Kliebenstein, D. J., Kroymann, J. and Mitchell-Olds, T. (2005a) The glucosinolate-myrosinase system in an ecological and evolutionary context. Curr. Opin. Plant Biol. **8**: 264-271.

Kliebenstein, D. J., Rowe, H. C. and Denby, K. J. (2005b) Secondary metabolites influence Arabidopsis/*Botrytis* interactions: variation in host production and pathogen sensitivity. Plant J. **44**: 25-36.

Kliebenstein, D. J., West, M. A., van Leeuwen, H., Loudet, O., Doerge, R. W. and St Clair, D. A. (2006) Identification of QTLs controlling gene expression networks defined a priori. BMC Bioinformatics **7**: 308.

Kloek, A. P., Verbsky, M. L., Sharma, S. B., Schoelz, J. E., Vogel, J., Klessig, D. F. and Kunkel, B. N. (2001) Resistance to *Pseudomonas syringae* conferred by an *Arabidopsis thaliana* coronatine-insensitive (*coi1*) mutation occurs through two distinct mechanisms. Plant J. **26**: 509-522.

Knoester, M., van Loon, L. C., van den Heuvel, J., Hennig, J., Bol, J. F. and Linthorst, H. J. M. (1998) Ethylene-insensitive tobacco lacks nonhost resistance against soil-borne fungi. Proc. Natl. Acad. Sci. USA **95**: 1933-1937.

Knoth, C., Ringler, J., Dangl, J. L. and Eulgem, T. (2007) *Arabidopsis* WRKY70 is required for full *RPP4*-mediated disease resistance and basal defense against *Hyaloperonospora parasitica*. Mol. Plant-Microbe Interact. **20**: 120-128.

Koch, E. and Slusarenko, A. (1990) Arabidopsis is susceptible to infection by a Downy Mildew Fungus. Plant Cell **2**: 437-445.

Köhler, C., Merkle, T., Roby, D. and Neuhaus, G. (2001) Developmentally regulated expression of a cyclic nucleotide-gated ion channel from *Arabidopsis* indicates its involvement in programmed cell death. Planta **213**: 327-332.

Konieczny, A. and Ausubel, F. M. (1993) A procedure for mapping *Arabidopsis* mutations using co-dominant ecotype-specific PCR-based markers. Plant J. **4**: 403-410.

Koornneef, M. and Hanhart, C. (1983) Linkage marker stocks of *Arabidopsis thaliana*. Arabidopsis Inf. Serv. **20**: 89-92.

Koornneef, M., van Eden, J., Hanhart, C. J., Stam, P., Braaksma, F. J. and Feenstra, W. J. (1983) Linkage map of *Arabidopsis thaliana*. J Hered. **74**: 265-272.

Kovtun, Y., Chiu, W. L., Tena, G. and Sheen, J. (2000) Functional analysis of oxidative stress-activated mitogen-activated protein kinase cascade in plants. Proc. Natl. Acad. Sci. USA **97**: 2940-2945.

Krause, M. and Durner, J. (2004) Harpin inactivates mitochondria in Arabidopsis suspension cells. Mol. Plant-Microbe Interact. **17**: 131-139.

Kroj, T., Rudd, J. J., Nürnberger, T., Gabler, Y., Lee, J. and Scheel, D. (2003) Mitogen-activated protein kinases play an essential role in oxidative burst-independent expression of pathogenesis-related genes in parsley. J. Biol. Chem. **278**: 2256-2264.

Kumar, D. and Klessig, D. F. (2000) Differential induction of tobacco MAP kinases by the defense signals nitric oxide, salicylic acid, ethylene, and jasmonic acid. Mol. Plant-Microbe Interact. **3**: 347-351.

Kunkel, B. N. and Brooks, D. M. (2002) Cross talk between signaling pathways in pathogen defense. Curr. Opin. Plant Biol. **5**: 325–331.

Kunze, G., Zipfel, C., Robatzek, S., Niehaus, K., Boller, T. and Felix, G. (2004) The N terminus of bacterial elongation factor Tu elicits innate immunity in *Arabidopsis* plants. Plant Cell **16**: 3496-3507.

Laloi, C., Apel, K. and Danon, A. (2004) Reactive oxygen signalling: the latest news. Curr. Opin. Plant Biol. **7**: 323-328.

Lamb, C. and Dixon, R. A. (1997) The oxidative burst in plant disease resistance. Annu. Rev. Plant Physiol. Plant Mol. Biol. **48**: 251-275.

Lamotte, O., Gould, K., Lecourieux, D., Sequeira-Legrand, A., Lebrun-Garcia, A., Durner, J., Pugin, A. and Wendehenne, D. (2004) Analysis of nitric oxide signaling functions in tobacco cells challenged by the elicitor cryptogein. Plant Physiol. **135**: 516-529.

Landry, L. G., Chapple, C. C. S. and Last, R. L. (1995) Arabidopsis mutants lacking phenolic sunscreens exhibit enhanced ultraviolet-B injury and oxidative damage. Plant Physiol. **109**: 1159-1166.

Lawton, K., Weymann, K., Friedrich, L., Vernooij, B., Uknes, S. and Ryals, J. (1995) Systemic acquired resistance in *Arabidopsis* requires salicylic acid but not ethylene. Mol. Plant-Microbe Interact. **8**: 863-870.

Lawton, K. A., Potter, S. L., Uknes, S. and Ryals, J. (1994) Acquired resistance signal transduction in *Arabidopsis* is ethylene independent. Plant Cell **6**: 581-588.

Lecourieux, D., Lamotte, O., Bourque , S., Wendehenne, D., Mazars, C., Ranjeva, R. and Pugin, A. (2005) Proteinaceous and oligosaccharidic elicitors induce different calcium signatures in the nucleus of tobacco cells. Cell Calcium **38**: 527-538.

Leng, Q., Mercier, R. W., Yao, W. and Berkowitz, G. A. (1999) Cloning and first functional characterization of a plant cyclic nucleotide-gated cation channel. Plant Physiol. **121**: 753-761.

Leon, J. and Sanchez-Serrano, J. J. (1999) Molecular biology of jasmonic acid biosynthesis in plants. Plant Physiol. Biochem. **37**: 373-380.

Li, H., Lin, H., Zhang, W., Zou, Y., Zhang, J., Tang, X. and Zhou, J.-M. (2005) Flagellin induces innate immunity in nonhost interactions that is suppressed by *Pseudomonas syringae* effectors. Proc. Natl. Acad. Sci. USA **102**: 12990–12995.

Li, J., Brader, G. and Palva, E. T. (2004) The WRKY70 transcription factor: a node of convergence for jasmonate-mediated and salicylate-mediated signals in plant defense. Plant Cell **16**: 319-331.

Li, J., Wen, J., Lease, K. A., Doke, J. T., Tax, F. E. and Walker, J. C. (2002) BAK1, an Arabidopsis LRR receptor-like protein kinase, interacts with BRI1 and modulates brassinosteroid signaling. Cell **110**: 213-222.

Li, X., Clarke, J. D., Zhang, Y. and Dong, X. (2001) Activation of an EDS1-mediated R-gene pathway in the *snc1* mutant leads to constitutive, NPR1-independent pathogen resistance. Mol. Plant-Microbe Interact. **14**: 1131–1139.

Lieberherr, D., Wagner, U., Dubuis, P.-H., Métraux, J.-P. and Mauch, F. (2003) The rapid induction of glutathione *S*-transferases *AtGSTF2* and *AtGSTF6* by avirulent *Pseudomonas syringae* is the result of combined salicylic acid and ethylene signaling. Plant Cell Physiol. **44**: 750-757.

Lin, W.-C., Lu, C.-F., Wu, J.-W., Cheng, M.-L., Lin, Y.-M., Yang, N.-S., Black, L., Green, S. K., Wang, J.-F. and Cheng, C.-P. (2004) Transgenic tomato plants expressing the *Arabidopsis NPR1* gene display enhanced resistance to a spectrum of fungal and bacterial diseases. Transgenic Res. **13**: 567-581.

Lindermayr, C., Saalbach, G. and Durner, J. (2005) Proteomic identification of *S*-nitrosylated proteins in Arabidopsis. Plant Physiol. **137**: 921-930.

Lister, C. and Dean, C. (1993) Recombinant inbred lines for mapping RFLP and phenotypic markers in *Arabidopsis thaliana*. Plant J. **4**: 745-750.

Liu, L., Hausladen, A., Zeng, M., Que, L., Heitman, J. and Stamler, J. S. (2001) A metabolic enzyme for *S*-nitrosothiol conserved from bacteria to humans. Nature **410**: 490-494.

Liu, Y.-G., Liu, H., Chen, L., Qiu, W., Zhang, J., Wu, H., Yang, C., Su, J., Wang, Z., Tian, D. and Mei, M. (2002) Development of new transformation-competent artificial chromosome vectors and rice genomic libraries for efficient gene cloning. Gene **282**: 247-255.

Liu, Y.-G., Shirano, Y., Fukaki, H., Yanai, Y., Tasaka, M., Tabata, S. and Shibata, D. (1999) Complementation of plant mutants with large genomic DNA fragments by a transformation-competent artificial chromosome vector accelerates positional cloning. Proc. Natl. Acad. Sci. USA **96**: 6535-6540.

Lorang, J. M., Sweat, T. A. and Wolpert, T. J. (2007) Plant disease susceptibility conferred by a "resistance" gene. Proc. Natl. Acad. Sci. USA **104**: 14861-14866.

Lorenzo, O., Chico, J. M., Sanchez-Serrano, J. J. and Solano, R. (2004) JASMONATE-INSENSITIVE1 encodes a MYC transcription factor essential to discriminate between different jasmonate-regulated defense responses in Arabidopsis. Plant Cell **16**: 1938-1950.

Lorenzo, O., Piqueras, R., Sánchez-Serrano, J. J. and Solano, R. (2003) ETHYLENE RESPONSE FACTOR1 integrates signals from ethylene and jasmonate pathways in plant defense. Plant Cell **15**: 165–178.

Lorenzo, O. and Solano, R. (2005) Molecular players regulating the jasmonate signalling network. Curr. Opin. Plant Biol. **8**: 1-9.

Loridon, K., Cournoyer, B., Goubely, C., Depeiges, A. and Picard, G. (1998) Length polymorphism and allele structure of trinucleotide microsatellites in natural accessions of *Arabidopsis thaliana*. Theor. Appl. Genet. **97** 591–604.

Lu, C., Kulkarni, K., Souret, F. F., MuthuValliappan, R., Tej, S., Poethig, R. S., Henderson, I. R., Jacobsen, S. E., Wang, W., Green, P. J. and Meyers, B. C. (2006) MicroRNAs and other small RNAs enriched in the *Arabidopsis* RNA-dependent RNA polymerase-2 mutant. **16**: 1276–1288.

Lu, H., Liu, Y. and Greenberg, J. T. (2005) Structure–function analysis of the plasma membrane-localized Arabidopsis defense component ACD6. Plant J. **44**: 798-809.

Lu, H., Rate, D. N., Song, J. T. and Greenberg, J. T. (2003) ACD6, a novel ankyrin protein, is a regulator and an effector of salicylic acid signaling in the Arabidopsis defense response. Plant Cell **15**: 2408–2420.

Lu, M., Tang, X. and Zhou, J.-M. (2001) Arabidopsis NHO1 is required for general resistance against *Pseudomonas* bacteria. Plant Cell **13**: 437-447.

Ludwig, A. A., Saitoh, H., Felix, G., Freymark, G., Miersch, O., Wasternack, C., T, B., Jones, J. D. and Romeis, T. (2005) Ethylene-mediated cross-talk between calcium-dependent protein kinase and MAPK signaling controls stress responses in plants. Proc. Natl. Acad. Sci. USA **102**: 10736-10741.

Lukowitz, W., Gillmor, C. S. and Scheible, W.-R. (2000) Positional cloning in Arabidopsis. Why it feels good to have a genome initiative working for you. Plant Physiol. **123**: 795-805.

Lund, S. T., Stall, R. E. and Klee, H. J. (1998) Ethylene regulates the susceptible response to pathogen infection in tomato. Plant Cell **10**: 371-382.

Mackey, D., Belkhadir, Y., Alonso, J. and Ecker, J. R. (2003) *Arabidopsis* RIN4 is a target of the type III virulence effector AvrRpt2 and modulates RPS2-mediated resistance. Cell **112**: 379-389.

Mackey, D., Holt, B. F., III, Wiig, A. and Dangl, J. L. (2002) RIN4 interacts with *Pseudomonas syringae* type III effector molecules and is required for RPM1-mediated resistance in *Arabidopsis*. Cell **108**: 743-754.

Mackey, D. and McFall, A. J. (2006) MAMPs and MIMPs: proposed classification for inducers of innate immunity. Mol. Microbiol. **61**: 1365-1371.

Martin, G. B., Bogdanove, A. J. and Sessa, G. (2003) Understanding the functions of plant disease resistance proteins. Annu. Rev. Plant Biol. **54**: 23–61.

Mateo, A., Mühlenbock, P., Rustérucci, C., Chang, C. C.-C., Miszalski, Z., Karpinska, B., Parker, J. E., Mullineaux, P. M. and Karpinski, S. (2004) *LESION SIMULATING DISEASE 1* is required for acclimation to conditions that promote excess excitation energy. Plant Physiol. **136**: 2818-2830.

Mauch-Mani, B. and Slusarenko, A. J. (1993) *Arabidopsis* as a model host for studying plant-pathogen interactions. Trends Microbiol. **1**: 265.

Mauch-Mani, B. and Slusarenko, A. J. (1996) Production of salicylic acid precursors is a major function of phenylalanine ammonia-lyase in the resistance of Arabidopsis to *Peronospora parasitica*. Plant Cell **8**: 203-212.

Mauch, F., Mauch-Mani, B., Gaille, C., Kull, B., Haas, D. and Reimmann, C. (2001) Manipulation of salicylate content in *Arabidopsis thaliana* by the expression of an engineered bacterial salicylate synthase. Plant J. **25**: 62-77.

McConn, M. and Browse, J. (1996) The critical requirement for linolenic acid is pollen development, not photosynthesis, in an *Arabidopsis* mutant. Plant Cell **8**: 403-416.

McDowell, J. M., Cuzick, A., Can, C., Beynon, J., Dangl, J. L. and Holub, E. B. (2000) Downy mildew (*Peronospora parasitica*) resistance genes in Arabidopsis vary in functional requirements for *NDR1*, *EDS1*, *NPR1* and salicylic acid accumulation. Plant J. **22**: 523-529.

Meinke, D. W., Cherry, J. M., Dean, C., Rounsley, S. D. and Koornneef, M. (1998) *Arabidopsis thaliana*: A model plant for genome analysis. Science **282**: 662-668.

Mellersh, D. G. and Heath, M. C. (2003) An investigation into the involvement of defense signaling pathways in components of the nonhost resistance of *Arabidopsis thaliana* to rust fungi also reveals a model system for studying rust fungal compatibility. Mol. Plant-Microbe Interact. **16**: 398-404.

Melotto, M., Underwood, W., Koczan, J., Nomura, K. and He, S. (2006) The innate immune function of plant stomata against bacterial invasion. Cell **126**: 969-980.

Mengiste, T., Chen, X., Salmeron, J. and Dietrich, R. (2003) The *BOTRYTIS SUSCEPTIBLE1* gene encodes an R2R3MYB transcription factor protein that is required for biotic and abiotic stress responses in Arabidopsis. Plant Cell **15**: 2551-2565.

Menke, F. L. H., van Pelt, J., Pieterse, C. M. J. and Klessig, D. F. (2004) Silencing of the mitogen-activated protein kinase MPK6 compromises disease resistance in Arabidopsis. Plant Cell **16**: 897-907.

Mert-Türk, F., Bennett, M. H., Mansfield, J. W. and Holub, E. B. (2003) Camalexin accumulation in *Arabidopsis thaliana* following abiotic elicitation or inoculation with virulent or avirulent *Hyaloperonospora parasitica*. Physiol. Mol. Plant Pathol. **62**: 137–145.

Mewes, H. W., Heumann, K., Kaps, A., Mayer, K., Pfeiffer, F., Stocker, S. and Frishman, D. (1999) MIPS: a database for genomes and proteins sequences. Nucleic Acids Res. **27**: 44-48.

Meyers, B. C., Dickermann, A. W., Michelmore, R. W., Sivaramakrishnan, S., Sobral, B. W. and Young, N. D. (1999) Plant disease resistance genes encode members of an ancient and diverse protein family within the nucleotide binding superfamily. Plant J. **20**: 317-332.

Meyers, B. C., Kozik, A., Griego, A., Kuang, H. and Michelmore, R. W. (2003) Genome-wide analysis of NBS-LRR–encoding genes in Arabidopsis. Plant Cell **15**: 809–834.

Mézard, C. (2006) Meiotic recombination hotspots in plants. Biochem. Soc. Trans. **34**: 531-534.

Michelmore, R. W. and Meyers, B. C. (1998) Clusters of resistance genes in plants evolve by divergent selection and a birth-and-death process. Genome Research **8**: 1113-1130.

Mikkelsen, M. D., Hansen, C. H., Wittstock, U. and Halkier, B. A. (2000) Cytochrome P450 CYP79B2 from *Arabidopsis* catalyzes the conversion of tryptophan to indole-3-acetaldoxime, a precursor of indole glucosinolates and indole-3-acetic acid. J. Biol. Chem. **275**: 33712-33717.

Mikkelsen, M. D., Petersen, B. L., Glawischnig, E., Jensen, A. B., Andreasson, E. and Halkier, B. A. (2003) Modulation of CYP79 genes and glucosinolate profiles in Arabidopsis by defense signaling pathways. Plant Physiol. **131**: 298-308.

Mishina, T. E. and Zeier, J. (2007) Pathogen-associated molecular pattern recognition rather than development of tissue necrosis contributes to bacterial induction of systemic acquired resistance in Arabidopsis. Plant J. **50**: 500–513.

Mittler, R., Vanderauwera, S., Gollery, M. and van Breusegem, F. (2004) Reactive oxygen gene network of plants. Trends Plant Sci. **9**: 490-498.

Mizutani, M., Ward, E. and Ohta, D. (1998) Cytochrome P450 superfamily in *Arabidopsis thaliana*: isolation of cDNAs, differential expression, and RFLP mapping of multiple cytochromes P450. Plant Mol. Biol. **37**: 39-52.

Moffat, A. S. (2001) Finding new ways to fight plant diseases. Science **298**: 1702-1704.

Morris, K., Mackerness, S. A.-H., Page, T., John, C. F., Murphy, A. M., Carr, J. P. and Buchanan-Wollaston, V. (2000) Salicylic acid has a role in regulating gene expression during leaf senescence. Plant J. **23**: 677-685.

Mou, Z., Fan, W. and Dong, X. (2003) Inducers of plant systemic acquired resistance regulate NPR1 function through redox changes. Cell **113**: 935-944.

Mowla, S. B., Cuypers, A., Driscoll, S. P., Kiddle, G., Thomson, J., Foyer, C. H. and Theodoulou, F. L. (2006) Yeast complementation reveals a role for an *Arabidopsis thaliana* late embryogenesis abundant (LEA)-like protein in oxidative stress tolerance. Plant J. **48**: 743-756.

Mur, L. A. J., Kenton, P., Atzorn, R., Miersch, O. and Wasternack, C. (2006) The outcome of concentration-specific interactions between salicylate and jasmonate signaling include synergy, antagonism, and oxidative stress leading to cell death. Plant Physiol. **140**: 249-262.

Murashige, T. and Skoog, F. (1962) A revised medium for rapid growth and bio assays with tobacco tissue cultures. Physiol. Plant. **15**: 473-497.

Murray, S. L. (2000) Identification and characterisation of *Arabidopsis* systemic acquired resistance mutants isolated by luciferase imaging. PhD thesis. University of Edinburgh, Edinburgh, UK.

Murray, S. L., Adams, N., Kliebenstein, D. J., Loake, G. J. and Denby, K. J. (2005) A constitutive *PR-1::luciferase* expression screen identifies Arabidopsis mutants with differential disease resistance to both biotrophic and necrotrophic pathogens. Mol. Plant Pathol. **6**: 31-41.

Murray, S. L., Ingle, R. A., Petersen, L. N. and Denby, K. J. (2007) Basal resistance against *Pseudomonas syringae* in Arabidopsis involves WRKY53 and a protein with homology to a nematode resistance protein. Mol. Plant-Microbe Interact. **20**: 1431-1438.

Murray, S. L., Thomson, C., Chini, A., Read, N. D. and Loake, G. J. (2002) Characterization of a novel, defense-related Arabidopsis mutant, *cir1*, isolated by luciferase imaging. Mol. Plant-Microbe Interact. **15**: 557-566.

Mylne, J. and Botella, J. R. (1998) Binary vectors for sense and antisense expression of Arabidopsis ESTs. Plant Mol. Biol. Rep. **16**: 257-262.

Mysore, K. S. and Ryu, C.-M. (2004) Nonhost resistance: how much do we know? Trends Plant Sci. **9**: 97-104.

Nakano, T., Suzuki, K., Fujimura, T. and Shinshi, H. (2006) Genome-wide analysis of the ERF gene family in Arabidopsis and rice. Plant Physiol. **140**: 411–432.

Nam, K. H. and Li, J. (2002) BRI1/BAK1, a receptor kinase pair mediating brassinosteroid signalling. Cell **110**: 203-212.

Nandi, A., Kachroo, P., Fukushige, H., Hidebrand, D., Klessig, D. F. and Shah, J. (2003) Ethylene and jasmonic acid signaling affect the NPR1-independent expression of defense genes without

impacting resistance to *Pseudomonas syringae* and *Peronospora parasitica* in the *Arabidopsis ssi1* mutant. Mol. Plant-Microbe Interact. **16**: 588-599.

Narusaka, Y., Narusaka, M., Seki, M., Umezawa, T., Ishida, J., Nakajima, M., Enju, A. and Shinozaki, K. (2004) Crosstalk in the responses to abiotic and biotic stresses in *Arabidopsis*: Analysis of gene expression in *cytochrome P450* gene superfamily by cDNA microarray. Plant Mol. Biol. **55**: 327-342.

Naur, P., Petersen, B. L., Mikkelsen, M. D., Bak, S., Rasmussen, H., Olsen, C. E. and Halkier, B. A. (2003) CYP83A1 and CYP83B1, two nonredundant cytochrome P450 enzymes metabolizing oximes in the biosynthesis of glucosinolates in Arabidopsis. Plant Physiol. **133**: 63-72.

Navarro, L., Zipfel, C., Rowland, O., Keller, I., Robatzek, S., Boller, T. and Jones, J. D. G. (2004) The transcriptional innate immune response to flg22. Interplay and overlap with Avr gene-dependent defense responses and bacterial pathogenesis. Plant Physiol. **135**: 1113–1128.

Nawrath, C. and Metraux, J. P. (1999) Salicylic acid induction-deficient mutants of Arabidopsis express PR-2 and PR-5 and accumulate high levels of camalexin after pathogen inoculation. Plant Cell **11**: 1393-1404.

Ndamukong, I., Abdallat, A. A., Thurow, C., Fode, B., Zander, M., Weigel, R. and Gatz, C. (2007) SA-inducible Arabidopsis glutaredoxin interacts with TGA factors and suppresses JA-responsive *PDF1.2* transcription. Plant J. **50**: 128-139.

Nelson, N. (2003) A journey from mammals to yeast with vacuolar H^+-ATPase (V-ATPase). J. Bioenerg. Biomembr. **35**: 281–289.

Nimchuk, Z., Eulgem, T., Holt, B. F., III and Dangl, J. L. (2003) Recognition and response in the plant immune system. Annu. Rev. Genet. **37**: 579–609.

Nishi, T. and Forgac, M. (2002) The vacuolar (H^+)-ATPases — Nature's most versatile proton pumps. Nat. Rev. Mol. Cell Biol. **3**: 94–103.

Nishimura, C., Ohashi, Y., Sato, S., Kato, T., Tabata, S. and Ueguchi, C. (2004) Histidine kinase homologs that act as cytokinin receptors possess overlapping functions in the regulation of shoot and root growth in Arabidopsis. Plant Cell **16**: 1365-1377.

Nishimura, M. T., Stein, M., Hou, B. H., Vogel, J. P., Edwards, H. and Somerville, S. C. (2003) Loss of a callose synthase results in salicylic acid-dependent disease resistance. Science **301**: 969-972.

Noël, L., Moores, T. L., van der Biezen, E. A., Parniske, M., Daniels, M. J., Parker, J. E. and Jones, J. D. G. (1999) Pronounced intraspecific haplotype divergence at the *RPP5* complex disease resistance locus of *Arabidopsis*. Plant Cell **11**: 2099-2111.

Nomura, K., Melotto, M. and He, S.-Y. (2005) Suppression of host defense in compatible plant-*Pseudomonas syringae* interactions. Curr. Opin. Plant Biol. **8**: 361-368.

Norman-Setterblad, C., Vidal, S. and Palva, E. T. (2000) Interacting signal pathways control defense gene expression in *Arabidopsis* in response to cell wall-degrading enzymes from *Erwinia carotovora*. Mol. Plant-Microbe Interact. **13**: 430-438.

Nürnberger, T., Brunner, F., Kemmerling, B. and Piater, L. (2004) Innate immunity in plants and animals: striking similarities and obvious differences. Immunol. Rev. **198**: 249–266.

Nürnberger, T. and Lipka, V. (2005) Non-host resistance in plants: new insights into an old phenomenon. Mol. Plant Pathol. **6**: 335-345.

O'Donnell, P. J., Jones, J. B., Antoine, F. R., Ciardi, J. and Klee, H. J. (2001) Ethylene-dependent salicylic acid regulates an expanded cell death response to a plant pathogen. Plant J. **25**: 315-323.

O'Donnell, P. J., Schmelz, E. A., Moussatche, P., Lund, S. T., Jones, J. B. and Klee, H. J. (2003) Susceptible to intolerance-a range of hormonal actions in a susceptible *Arabidopsis* pathogen response. Plant J. **33**: 245-257.

O'Donnell, P. J., Schmelz, E., Block, A., Miersch, O., Wasternack, C., Jones, J. B. and Klee, H. J. (2003) Multiple hormones act sequentially to mediate a susceptible tomato pathogen defense response. Plant Physiol. **133**: 1181-1189.

Ochsenbein, C., Przybyla, D., Danon, A., Landgraf, F., Göbel, C., Imboden, A., Feussner, I. and Apel, K. (2006) The role of *EDS1* (enhanced disease susceptibility) during singlet oxygen-mediated stress responses of Arabidopsis. Plant J. **47**: 445–456.

Ohme-Takagi, M. and Shinshi, H. (1995) Ethylene-inducible DNA binding proteins that interact with an ethylene-responsive element. Plant Cell **7**: 173-182.

Onate-Sanchez, L. and Singh, K. B. (2002) Identification of *Arabidopsis* ethylene-responsive element binding factors with distinct induction kinetics after pathogen infection. Plant Physiol. **128**: 1313-1322.

Orozco-Cárdenas, M. L. and Ryan, C. A. (2002) Nitric oxide negatively modulates wound signaling in tomato plants. Plant Physiol. **130**: 487-493.

Østergaard, L. and Yanofsky, M. F. (2004) Establishing gene function by mutagenesis in *Arabidopsis thaliana*. Plant J. **39**: 682–696.

Ow, D. W., Wood, K. V., DeLuca, M., De Wit, J. R., Helinksi, D. R. and Howell, S. H. (1986) Transient and stable expression of the firefly luciferase gene in plant cells and trangenic plants. Science **234**: 856-859.

Pagnussat, G. C., Lanteri, M. L., Lombardo, M. C. and Lamattina, L. (2004) Nitric oxide mediates the indole-acetic acid activation of a mitogen-activated protein kinase cascade involved in adventitious root formation. Plant Physiol. **135**: 279-286.

Pajerowska, K. M., Parker, J. E. and Gebhardt, C. (2005) Potato homologs of *Arabidopsis thaliana* genes functional in defense signaling — identification, genetic mapping, and molecular cloning. Mol. Plant-Microbe Interact. **18**: 1107-1119.

Pan, Q., Wendel, J. and Fluhr, R. (2000) Divergent evolution of plant NBS-LRR resistance gene homologues in dicot and cereal genomes. J. Mol. Evol. **50**: 203–213.

Pan, X., Liu, H., Clarke, J., Jones, J., Bevan, M. and Stein, L. (2003) ATIDB: *Arabidopsis thaliana* insertion database. Nucleic Acids Res. **31**: 1245-1251.

Panter, S. N. and Jones, D. A. (2002) Age-related resistance to plant pathogens. Adv. Bot. Res. **38**: 251-280.

Park, S. H., Zarrinpar, A. and Lim, W. A. (2003) Rewiring MAP kinase pathways using alternative scaffold assembly mechanisms. Science **299**: 1061-1064.

Parker, J. E., Coleman, M. J., Szabo, V., Frost, L. N., Schmidt, R., van der Biezen, E. A., Moores, T., Dean, C., Daniels, M. J. and Jones, J. D. G. (1997) The Arabidopsis downy mildew resistance gene RPP5 shares similarity to the Toll and Interleukin-1 receptors with *N* and *L6*. Plant Cell **9**: 879-894.

Parker, J. E., Holub, E. B., Frost, L. N., Falk, A., Gunn, N. D. and Daniels, M. J. (1996) Characterization of *eds1*, a mutation in Arabidopsis suppressing resistance to *Peronospora parasitica* specified by several different *RPP* genes. Plant Cell **8**: 2033-2046.

Parker, J. E., Szabo, V., Staskawicz, B. J., Lister, C., Dean, C., Daniels, M. J. and Jones, J. D. G. (1993) Phenotypic characterization and molecular mapping of the *Arabidopsis thaliana* locus *RPP5*, determining disease resistance to *Peronospora parasitica*. Plant J. **4**: 821-831.

Patnaik, D. and Khurana, P. (2003) Genetic transformation of Indian bread (*T. aestivum*) and pasta (*T. durum*) wheat by particle bombardment of mature embryo-derived calli. BMC Plant Biology **3**: 5.

Peck, S. C. (2003) Early phosphorylation events in biotic stress. Curr. Opin. Plant Biol. **6**: 334-338.

Pegadaraju, V., Louis, J., Singh, V., Reese, J. C., Bautor, J., Feys, B. J., Cook, G., Parker, J. E. and Shah, J. (2007) Phloem-based resistance to green peach aphid is controlled by Arabidopsis *PHYTOALEXIN DEFICIENT4* without its signaling partner *ENHANCED DISEASE SUSCEPTIBILITY1*. Plant J. **52**: 332-341.

Peña-Cortés, H., Albrecht, T., Prat, S., Weiler, E. W. and Willmitzer, L. (1993) Aspirin prevents wound-induced gene expression in tomato leaves by blocking jasmonic acid biosynthesis. Planta **191**: 123-128.

Penninckx, I. A. M. A., Eggermont, K., Terras, F. R. G., Thomma, B. P. H. J., De Samblanx, G. W., Buchala, A., Métraux, J.-P., Manners, J. M. and Broekaert, W. F. (1996) Pathogen-induced systemic activation of a plant defensin gene in Arabidopsis follows a salicylic acid-independent pathway. Plant Cell **8**: 2309-2323.

Penninckx, I. A. M. A., Thomma, B. P. H. J., Buchala, A., Métraux, J.-P. and Broekaert, W. F. (1998) Concomitant activation of jasmonate and ethylene response pathways is required for induction of a plant defensin gene in Arabidopsis. Plant Cell **10**: 2103-2113.

Pestova, T. V., Lomakin, I. B., Lee, J. H., Choi, S. K., Dever, T. E. and Hellen, C. U. T. (2000) The joining of ribosomal subunits in eukaryotes requires eIF5B. Nature **403**: 332-335.

Peters, J. L., Cnudde, F. and Gerats, T. (2003) Forward genetics and map-based cloning approaches. Trends Plant Sci. **8**: 484-491.

Petersen, M., Brodersen, P., Naested, H., Andreasson, E., Lindhart, U., Johansen, B., Nielsen, H. B., Lacy, M., Austin, M. J., Parker, J. E., Sharma, S. B., Klessig, D. F., Martienssen, R., Mattsson, O., Jensen, A. B. and Mundy, J. (2000) *Arabidopsis* MAP kinase 4 negatively regulates systemic acquired resistance. Cell **103**: 1111-1120.

Pieterse, C. M. J. and van Loon, L. C. (1999) Salicylic acid-independent plant defence pathways. Trends Plant Sci. **4**: 1360-1385.

Pieterse, C. M. J., van Wees, S. C. M., Hoffland, E., van Pelt, J. A. and van Loon, L. C. (1996) Systemic resistance in Arabidopsis induced by biocontrol bacteria is independent of salicylic acid accumulation and pathogenesis-related gene expression. Plant Cell **8**: 1225-1237.

Pieterse, C. M. J., van Wees, S. C. M., van Pelt, J. A., Knoester, M., Laan, R., Gerrits, H., Wiesbeek, P. J. and van Loon, L. C. (1998) A novel signaling pathway controlling induced systemic resistance in *Arabidopsis*. Plant Cell **10**: 1571-1580.

Plotnikova, J. M., Reuber, T. L., Ausubel, F. M. and Pfister, D. H. (1998) Powdery mildew pathogenesis of *Arabidopsis thaliana*. Mycologia **90**: 1009-1016.

Polverari, A., Molesini, B., Pezzotti, M., Buonaurio, R., Marte, M. and Delledonne, M. (2003) Nitric oxide-mediated transcriptional changes in *Arabidopsis thaliana*. Mol. Plant-Microbe Interact. **16**: 1094-1105.

Ponce, M. R., Robles, P. and Micol, J. L. (1999) High-throughput genetic mapping in *Arabidopsis thaliana*. Mol. Gen. Genet. **261**: 408-415.

Pozo, M., van Loon, L. C. and Pieterse, C. M. J. (2005) Jasmonates - signals in plant-microbe interactions. Plant Growth Regul. **23**: 211-222.

Pugin, A., Frachisse, J. M., Tavernier, E., Bligny, R., Gout, E., Douce, R. and Guern, J. (1997) Early events induced by the elicitor cryptogein in tobacco cells: Involvement of a plasma membrane

NADPH oxidase and activation of glycolysis and the pentose phosphate pathway. Plant Cell **9**: 2077-2091.

Ramonell, K., Berrocal-Lobo, M., Koh, S., Wan, J., Edwards, H., Stacey, G. and Somerville, S. (2005) Loss-of-function mutations in chitin responsive genes show increased susceptibility to the powdery mildew pathogen *Erysiphe cichoracearum*. Plant Physiol. **138**: 1027-1036.

Rashotte, A. M., Mason, M. G., Hutchison, C. E., Ferreira, F. J., Schaller, G. E. and Kieber, J. J. (2006) A subset of Arabidopsis AP2 transcription factors mediates cytokinin responses in concert with a two-component pathway. Proc. Natl. Acad. Sci. USA **103**: 11081-11085.

Rathjen, J. P. and Moffetty, P. (2003) Early signal transduction events in specific plant disease resistance. Curr. Opin. Plant Biol. **6**: 300-306.

Reignault, P., Frost, L. N., Richardson, H., Daniels, M. J., Jones, J. D. G. and Parker, J. E. (1996) Four *Arabidopsis RPP* loci controlling resistance to the Noco2 isolate of *Peronospora parasitica* map to regions known to contain other *RPP* recognition specificities. Mol. Plant-Microbe Interact. **9**: 464-473.

Reiter, R. S., Williams, J. G. K., Feldmann, K. A., Rafalski, J. A., Tingey, S. V. and Scolnik, P. A. (1992) Global and local genome mapping in *Arabidopsis thaliana* by using recombinant inbred lines and random amplified polymorphic DNAs. Proc. Natl. Acad. Sci. USA **89**: 1477-1481.

Rentel, M. C., Lecourieux, D., Ouaked, F., Usher, S. L., Petersen, L., Okamoto, H., Knight, H., Peck, S. C., Grierson, C. S., Hirt, H. and Knight, M. R. (2004) OXI1 kinase is necessary for oxidative burst-mediated signalling in *Arabidopsis*. Nature **427**: 858-861.

Reuber, T. L., Plotnikova, J. M., Dewdney, J., Rogers, E. E., Wood, W. and Ausubel, F. M. (1998) Correlation of defense gene induction defects with powdery mildew susceptibility in *Arabidopsis* enhanced disease susceptibility mutants. Plant J. **16**: 473-485.

Robatzek, S., Chinchilla, D. and Boller, T. (2006) Ligand-induced endocytosis of the pattern recognition receptor FLS2 in *Arabidopsis*. Genes Dev. **20**: 537-542.

Rojo, E., Solano, R. and Sánchez-Serrano, J. J. (2003) Interactions between signaling compounds involved in plant defense. J. Plant Growth Regul. **22**: 82-98.

Roman, G., Lubarsky, B., Kieber, J. J., Rothenberg, M. and Ecker, J. R. (1995) Genetic analysis of ethylene signal transduction in *Arabidopsis thaliana*: five novel mutant loci integrated into a stress response pathway. Genetics **139**: 1393-1409.

Romeis, T., Piedras, P., Zhang, S., Klessig, D. F., Hirt, H. and Jones, J. D. G. (1999) Rapid Avr9- and Cf-9-dependent activation of MAP kinases in tobacco cell cultures and leaves: convergence of resistance gene, elicitor, wound, and salicylate responses. Plant Cell **11**: 273-287.

Romero-Puertas, M. C., Perazzolli, M., Zago, E. D. and Delledonne, M. (2004) Nitric oxide signalling functions in plant–pathogen interactions. Cell. Microbiol. **6**: 795-803.

Ron, M. and Avni, A. (2004) The receptor for the fungal elicitor ethylene-inducing xylanase is a member of a resistance-like gene family in tomato. Plant Cell **16**: 1604-1615.

Rozen, S. and Skaletsky, H. J. (2000) Primer3 on the WWW for general users and for biologist programmers. In: *Bioinformatics Methods and Protocols: Methods in Molecular Biology*. Krawetz, S. and Misener, S. (eds.). Humana Press, Totowa.

Ruegger, M. O. and Chapple, C. (2001) Mutations that reduce sinapoylmalate accumulation in *Arabidopsis thaliana* define loci with diverse roles in phenylpropanoid matabolism. Genetics **159**: 1741-1749.

Rushton, P. J. and Somssich, I. E. (1998) Transcriptional control of plant genes responsive to pathogens. Curr. Opin. Plant Biol. **1**: 311-315.

Rustérucci, C., Aviv, D. H., Holt, B. F., III, Dangl, J. L. and Parker, J. E. (2001) The disease resistance signaling components *EDS1* and *PAD4* are essential regulators of the cell death pathway controlled by *LSD1* in Arabidopsis. Plant Cell **13**: 2211-2224.

Rustérucci, C., Espunya, M. C., Díaz, M., Chabannes, M. and Martínez, M. C. (2007) *S*-Nitrosoglutathione reductase affords protection against pathogens in Arabidopsis, both locally and systemically. Plant Physiol. **143**: 1282-1292.

Ryals, J., Neuenschwander, U. H., Willits, M. G., Molina, A., Steiner, H.-Y. and Hunt, M. D. (1996) Systemic acquired resistance. Plant Cell **8**: 1809-1819.

Sakai, H., Hua, J., Chen, Q. G., Chang, C., Medrano, L. J., Bleecker, A. B. and Meyerowitz, E. M. (1998) ETR2 is an ETR1-like gene involved in ethylene signaling in Arabidopsis. Proc. Natl. Acad. Sci. USA **95**: 5812-5817.

Sambrook, J., Fritsch, E. F. and Maniatis, T. (1989) Molecular cloning: a laboratory manual. Cold Spring Harbor Laboratory Press, Cold Spring Harbor, New York.

Schaller, G. E. and Kieber, J. J. (2002) Ethylene. In: *The Arabidopsis Book*. Somerville, C. R. and Meyerowitz, E. M. (eds.). Am. Soc. Plant Biologists, Rockville.

Schenk, P. M., Kazan, K., Wilson, I., Anderson, J. P., Richmond, T., Somerville, S. C. and Manners, J. M. (2000) Co-ordinated plant defense responses in Arabidopsis revealed by microarray analysis. Proc. Natl. Acad. Sci. USA **97**: 11655-11660.

Schuhegger, R., Nafisi, M., Mansourova, M., Petersen, B. L., Olsen, C. E., Svatos, A., Halkier, B. A. and Glawischnig, E. (2006) CYP71B15 (PAD3) catalyzes the final step in camalexin biosynthesis. Plant Physiol. **141**: 1248-1254.

Schuhegger, R., Rauhut, T. and Glawischnig, E. (2007) Regulatory variability of camalexin biosynthesis. J. Plant Physiol. **164**: 636-644.

Serino, L., Reimmann, C., Baur, H., Beyeler, M., Visca, P. and Haas, D. (1995) Structural genes for salicylate biosynthesis from chorismate in *Pseudomonas aeruginosa*. Mol. Gen. Genet. **249**: 217-228.

Shah, J., Kachroo, P. and Klessig, D. F. (1999) The Arabidopsis *ssi1* mutation restores pathogenesis-related gene expression in *npr1* plants and renders defensin gene expression salicylic acid dependent. Plant Cell **11**: 191-206.

Shah, J., Kachroo, P., Nandi, A. and Klessig, D. F. (2001) A recessive mutation in the *Arabidopsis SSI2* gene confers SA- and *NPR1*-independent expression of *PR* genes and resistance against bacterial and oomycete pathogens. Plant J. **25**: 563-574.

Shah, J., Tsui, F. and Klessig, D. F. (1997) Characterization of a salicylic acid–insensitive mutant (*sai1*) of *Arabidopsis thaliana*, identified in a selective screen utilizing the SA-inducible expression of the *tms2* gene. Mol. Plant-Microbe Interact. **10**: 69-78.

Shirano, Y., Kachroo, P., Shah, J. and Klessig, D. F. (2002) A gain-of-function mutation in an Arabidopsis Toll Interleukin1 Receptor–Nucleotide Binding Site–Leucine-Rich Repeat type R gene triggers defense responses and results in enhanced disease resistance. Plant Cell **14**: 3149–3162.

Shirasu, K., Nakajima, H., Rajasekhar, V. K., Dixon, R. A. and Lamb, C. J. (1997) Salicylic acid potentiates an agonist-dependent gain control that amplifies pathogen signals in the activation of defense mechanisms. Plant Cell **9**: 261-270.

Shiu, S. H. and Bleecker, A. B. (2001) Receptor-like kinases from *Arabidopsis* form a monophyletic gene family related to animal receptor kinases. Proc. Natl. Acad. Sci. USA **98**: 10763-10768.

Shoji, T., Nakajima, H. and Hashimoto, T. (2000) Ethylene suppresses jasmonate-induced gene expression in nicotine biosynthesis. Plant Cell Physiol. **41**: 1072-1076.

Slusarenko, A. J. and Schlaich, N. L. (2003) Downy mildew of *Arabidopsis thaliana* caused by *Hyaloperonospora parasitica* (formerly *Peronospora parasitica*). Mol. Plant Pathol. **4**: 159-170.

Solano, R., Stepanova, A., Chao, Q. and Ecker, J. R. (1998) Nuclear events in ethylene signaling: a transcriptional cascade mediated by ETHYLENE-INSENSITIVE3 and ETHYLENE-RESPONSE-FACTOR1. Genes Dev. **12**: 3703-3714.

Speulman, E., Bouchez, D., Holub, E. B. and Beynon, J. L. (1998) Disease resistance gene homologs correlate with disease resistance loci of *Arabidopsis thaliana*. Plant J. **14**: 467-474.

Spoel, S. H., Koornneef, A., Claessens, S. M., Korzelius, J. P., van Pelt, J. A., Mueller, M. J., Buchala, A. J., Metraux, J. P., Brown, R., Kazan, K., van Loon, L. C., Dong, X. and Pieterse, C. M. (2003) NPR1 modulates cross-talk between salicylate- and jasmonate-dependent defense pathways through a novel function in the cytosol. Plant Cell **15**: 760-770.

Stamler, J. S., Jaraki, O., Osborne, J., Simon, D. I., Keaney, K., Vita, J., Singel, D., Valeri, C. R. and Loscalzo, J. (1992) Nitric oxide circulates in mammalian plasma primarily as an *S*-nitroso adduct of serum albumin. Proc. Natl. Acad. Sci. USA **89**: 7674-7677.

Stamler, J. S., Lamas, S. and Fang, F. C. (2001) Nitrosylation: The prototypic redox-based signaling mechanism. Cell **106**: 675–683.

Staswick, P. E., Su, W. P. and Howell, S. H. (1992) Methyl jasmonate inhibition of root-growth and induction of a leaf protein are decreased in an *Arabidopsis thaliana* mutant. Proc. Natl. Acad. Sci. USA **89**: 6837-6840.

Staswick, P. E. and Tiryaki, I. (2004) The oxylipin signal jasmonic acid is activated by an enzyme that conjugates it to isoleucine in Arabidopsis. Plant Cell **16**: 2117-2127.

Staswick, P. E., Tiryaki, I. and Rowe, M. L. (2002) Jasmonate response locus *JAR1* and several related Arabidopsis genes encode enzymes of the Firefly luciferase superfamily that show activity on jasmonic, salicylic, and indole-3-acetic acids in an assay for adenylation. Plant Cell **14**: 1405-1415.

Staswick, P. E., Yuen, G. Y. and Lehman, C. C. (1998) Jasmonate signaling mutants of *Arabidopsis* are susceptible to the soil fungus *Pythium irregulare*. Plant J. **15**: 747-754.

Stintzi, A. and Browse, J. (2000) The Arabidopsis male-sterile mutant, *opr3*, lacks the 12-oxophytodienoic acid reductase required for jasmonate synthesis. Proc. Natl. Acad. Sci. USA **97**: 10625-10630.

Stracke, R., Werber, M. and Weisshaar, B. (2001) The R2R3-MYB gene family in *Arabidopsis thaliana*. Curr. Opin. Plant Biol. **4**: 447-456.

Strompen, G., Dettmer, J., Stierhof, Y.-D., Schumacher, K., Jürgens, G. and Mayer, U. (2005) Arabidopsis vacuolar H^+-ATPase subunit E isoform 1 is required for Golgi organization and vacuole function in embryogenesis. Plant J. **41**: 125–132.

Stutius, L. M., Volko, S. M. and Ausubel, F. M. (2000). Physiological and genetic analyses of *edr5*, an *Arabidopsis* enhanced disease resistance mutant. 11th International conference on Arabidopsis research, Madison, USA.

Sun, W., Dunning, F. M., Pfund, C., Weingarten, R. and Bent, A. F. (2006) Within-species flagellin polymorphism in *Xanthomonas campestris* pv. *campestris* and its impact on elicitation of *Arabidopsis FLAGELLIN SENSING2*-dependent defenses. Plant Cell **18**: 764-779.

Suwabe, K., Tsukazaki, H., Iketani, H., Hatakeyama, K., Kondo, M., Fujimura, M., Nunome, T., Fukuoka, H., Hirai, M. and Matsumoto, S. (2006) Simple sequence repeat-based comparative genomics between *Brassica rapa* and *Arabidopsis thaliana*: the genetic origin of clubroot resistance. Genetics **173**: 309-319.

Sze, H., Schumacher, K., Müller, M. L., Padmanaban, S. and Taiz, L. (2002) A simple nomenclature for a complex proton pump: VHA genes encode the vacuolar H^+-ATPase. Trends Plant Sci. **7**: 157-161.

Tada, Y., Mori, T., Shinogi, T., Yao, N., Takahashi, S., Betsuyaku, S., Sakamoto, M., Park, P., Nakayashiki, H., Tosa, Y. and Mayama, S. (2004) Nitric oxide and reactive oxygen species do not elicit hypersensitive cell death but induce apoptosis in the adjacent cells during the defense response of oat. Mol. Plant-Microbe Interact. **17**: 245-253.

Takahashi, F., Yoshida, R., Ichimura, K., Mizoguchi, T., Seo, S., Yonezawa, M., Maruyama, K., Yamaguchi-Shinozaki, K. and Shinozaki, K. (2007) The mitogen-activated protein kinase cascade MKK3-MPK6 is an important part of the jasmonate signal transduction pathway in *Arabidopsis*. Plant Cell **19**: 805-818.

Tao, Y., Xie, Z., Chen, W., Glazebrook, J., Chang, H.-S., Han, B., Zhu, T., Zou, G. and Katagiri, F. (2003) Quantitative nature of Arabidopsis responses during compatible and incompatible interactions with the bacterial pathogen *Pseudomonas syringae*. Plant Cell **15**: 317-330.

Thatcher, L. F., Anderson, J. P. and Singh, K. B. (2005) Plant defence responses: what have we learnt from *Arabidopsis*? Func. Plant Biol. **32**: 1-19.

The Arabidopsis Genome Initiative (2000) Analysis of the genome sequence of the flowering plant *Arabidopsis thaliana*. Nature **408**: 796-815.

Thilmony, R., Underwood, W. and He, S. Y. (2006) Genome-wide transcriptional analysis of the *Arabidopsis thaliana* interaction with the plant pathogen *Pseudomonas syringae* pv. *tomato* DC3000 and the human pathogen *Escherichia coli* O157:H7. Plant J. **46**: 34-53.

Thines, B., Katsir, L., Melotto, M., Niu, Y., Mandaokar, A., Liu, G., Nomura, K., He, S. Y., Howe, G. A. and Browse, J. (2007) JAZ repressor proteins are targets of the SCF^{COI1} complex during jasmonate signalling. Nature **448**: 661-665.

Thomma, B. P. H. J., Eggermont, K., Broekaert, W. F. and Cammue, B. P. A. (2000) Disease development of several fungi on *Arabidopsis* can be reduced by treatment with methyl jasmonate. Plant Physiol. Biochem. **38**.

Thomma, B. P. H. J., Eggermont, K., Penninckx, I. A. M. A., Mauch-Mani, B., Vogelslang, R., Cammue, B. P. A. and Broekaert, W. F. (1998) Separate jasmonate-dependent and salicylate-dependent defense-response pathways in *Arabidopsis* are essential for resistance to distinct microbial pathogens. Proc. Natl. Acad. Sci. USA **95**: 15107-15111.

Thomma, B. P. H. J., Eggermont, K., Tierens, K. F. and Broekaert, W. F. (1999a) Requirement of functional *ethylene-insensitive 2* gene for efficient resistance of *Arabidopsis* to infection by *Botrytis cinerea*. Plant Physiol. **121**: 1093-1102.

Thomma, B. P. H. J., Nelissen, I., Eggermont, K. and Broekaert, W. F. (1999b) Deficiency in phytoalexin production causes enhanced susceptibility of *Arabidopsis thaliana* to the fungus *Alternaria brassicicola*. Plant J. **19**: 163-171.

Thomma, B. P. H. J., Penninckx, I. A. M. A., Broekaert, W. F. and Cammue, B. P. A. (2001) The complexity of disease signaling in Arabidopsis. Curr. Opin. Immunol. **13**: 63-68.

Thordal-Christensen, H. (2003) Fresh insights into processes of nonhost resistance. Curr. Opin. Plant Biol. **6**: 351–357.

Ton, J., Davison, S., van Wees, S. C. M., van Loon, L. C. and Pieterse, C. M. J. (2001) The Arabidopsis *ISR1* locus controlling Rhizobacteria-mediated induced systemic resistance is involved in ethylene signaling. Plant Physiol. **125**: 652-661.

Ton, J., de Vos, M., Robben, C., Buchala, A. J., Metraux, J. P., Van Loon, L. C. and Pieterse, C. M. J. (2002) Characterisation of Arabidopsis-enhanced disease susceptibility mutants that are affected in systemically induced resistance. Plant J. **29**: 11-21.

Ton, J., Jakab, G., Toquin, V., Flors, V., Iavicoli, A., Maeder, M. N., Metraux, J. P. and Mauch-Mani, B. (2005) Dissecting the β-aminobutyric acid-induced priming phenomenon in Arabidopsis. Plant Cell **17**: 987-999.

Ton, J., Pieterse, C. M. J. and van Loon, L. C. (1999) Identification of a locus in *Arabidopsis* controlling both the expression of rhizobacteria-mediated induced systemic resistance (ISR) and basal resistance against *Pseudomonas syringae* pv. *tomato*. Mol. Plant-Microbe Interact. **12**: 911-918.

Torres, M. A. and Dangl, J. L. (2005) Functions of the respiratory burst oxidase in biotic interactions, abiotic stress and development. Curr. Opin. Plant Biol. **8**: 397-403.

Torres, M. A., Dangl, J. L. and Jones, J. D. G. (2002) *Arabidopsis gp91^{phox}* homologues *AtrbohD* and *AtrbohF* are required for accumulation of reactive oxygen intermediates in the plant defense response. Proc. Natl. Acad. Sci. USA **99**: 517-522.

Torres, M. A., Jones, J. D. G. and Dangl, J. L. (2006) Reactive oxygen species signaling in response to pathogens. Plant Physiol. **141**: 373-378.

Truman, W., Bennett, M. H., Kubigsteltig, I., Turnbull, C. and Grant, M. (2007) Arabidopsis systemic immunity uses conserved defense signaling pathways and is mediated by jasmonates. Proc. Natl. Acad. Sci. USA **104**: 1075-1080.

Truman, W., Torres de Zabala, M. and Grant, M. (2006) Type III effectors orchestrate a complex interplay between transcriptional networks to modify basal defence responses during pathogenesis and resistance. Plant J. **46**: 14-33.

Tsuji, J., Jackson, E. P., Gage, D. A., Hammerschmidt, R. and Somerville, S. C. (1992) Phytoalexin accumulation in *Arabidopsis thaliana* during the hypersensitive reaction to *Pseudomonas syringae* pv *syringae*. Plant Physiol. **98**: 1304-1309.

Turner, J. G., Ellis, C. and Devoto, A. (2002) The jasmonate signal pathway. Plant Cell Suppl. **2002**: S153-S164.

Tzafrir, I., Pena-Muralla, R., Dickerman, A., Berg, M., Rogers, R., Hutchen, S., Sweeney, T. C., McElver, J., Aux, G., Patton, D. and Meinke, D. (2004) Identification of genes required for embryo development in *Arabidopsis*. Plant Physiol. **135**: 1206–1220.

Uguillas, C., Letelier, I., Blanco, F., Jordana, X. and Holuigue, L. (2004) NPR1-independent activation of immediate early salicylic acid-responsive genes in Arabidopsis. Mol. Plant-Microbe Interact. **17**: 34-42.

Uknes, S., Mauch-Mani, B., Moyer, M., Potter, S., Williams, S., Dincher, S., Chandler, D., Slusarenko, A., Ward, E. and Ryals, J. A. (1992) Acquired resistance in *Arabidopsis*. Plant Cell **4**: 645-656.

Underhill, D. M. and Ozinsky, A. (2002) Toll-like receptors: key mediators of microbe detection. Curr. Opin. Immunol. **14**: 103-110.

van Camp, W., van Montagu, M. and Inze, D. (1998) H_2O_2 and NO: redox signals in disease resistance. Trends Plant Sci. **3**: 330-334.

van der Biezen, E. A., Freddie, C. T., Kahn, K., Parker, J. E. and Jones, J. D. G. (2002) *Arabidopsis RPP4* is a member of the *RPP5* multigene family of TIR-NB-LRR genes and confers downy mildew resistance through multiple signalling components. Plant J. **29**: 439-451.

van der Biezen, E. A. and Jones, J. D. G. (1998) Plant disease resistance proteins and the gene-for-gene concept. Trends Biochem. Sci. **23**: 454-456.

van Hulten, M., Pelser, M., van Loon, L. C., Pieterse, C. M. J. and Ton, J. (2006) Costs and benefits of priming for defense in *Arabidopsis*. Proc. Natl. Acad. Sci. USA **103**: 5602–5607.

van Kan, J. A. L. (2006) Licensed to kill: the lifestyle of a necrotrophic plant pathogen. Trends Plant Sci. **11**: 247-253.

van Loon, L. C. (1997) Induced resistance in plants and the role of pathogenesis-related proteins. Eur. J. Plant Pathol. **103**: 753-765.

van Loon, L. C. and Bakker, P. A. H. M. (2005) Induced systemic resistance as a mechanism of disease suppression by rhizobacteria. In: *PGPR: Biocontrol and Biofertilization*. Siddiqui, Z. A. (eds.). Springer, Heidelberg.

van Loon, L. C., Geraats, B. P. J. and Linthorst, H. J. M. (2006) Ethylene as a modulator of disease resistance in plants. Trends Plant Sci. **11**: 184-191.

van Loon, L. C. and van Strien, E. A. (1999) The families of pathogenesis-related proteins, their activities, and comparative analysis of PR-1 type proteins. Physiol. Mol. Plant Pathol. **55**: 85-97.

van Wees, S. C. M., de Swart, E. A. M., van Pelt, J. A., van Loon, L. C. and Pieterse, C. M. J. (2000) Enhancement of induced disease resistance by simultaneous activation of salicylate- and jasmonate-dependent defense pathways in *Arabidopsis thaliana*. Proc. Natl. Acad. Sci. USA **97**: 8711-8716.

van Wees, S. C. M., Luijendijk, M., Smoorenburg, I., van Loon, L. C. and Pieterse, C. M. J. (1999) Rhizobacteria-mediated induced systemic resistance (ISR) in *Arabidopsis* is not associated with a direct effect on known defense-genes but stimulates the expression of the jasmonate-inducible gene *Atvsp* upon challenge. Plant Mol. Biol. **41**: 537-549.

Vandenabeele, S., der Kelen, K. V. and Dat, J. (2003) A comprehensive analysis of hydrogen peroxide-induced gene expression in tobacco. Proc. Natl. Acad. Sci. USA **100**: 16113-16118.

Verberne, M. C., Verpoorte, R., Bol, J. F., Mercado-Blanco, J. and Linthorst, H. J. (2000) Overproduction of salicylic acid in plants by bacterial transgenes enhances pathogen resistance. Nat. Biotechnol. **18**: 779-783.

Veronese, P., Chen, X., Bluhm, B., Salmeron, J., Dietrich, R. A. and Mengiste, T. (2004) The BOS loci of Arabidopsis are required for resistance to *Botrytis cinerea* infection. Plant J. **40**: 558-574.

Veronese, P., Nakagami, H., Bluhm, B., AbuQmar, S., Chen, X., Salmeron, J., Dietrich, R. A., Hirt, H. and Mengiste, T. (2006) The membrane-anchored *BOTRYTIS-INDUCED KINASE1* plays distinct roles in *Arabidopsis* resistance to necrotrophic and biotrophic pathogens. Plant Cell **18**: 257-273.

Verwoerd, T. C., Dekker, B. M. M. and Hoekema, A. (1989) A small-scale procedure for the rapid isolation of plant RNAs. Nucl. Acids Res. **17**: 2362.

Vijayan, P., Shockey, J., Levesque, C. A., Cook, R. J. and Browse, J. (1998) A role for jasmonate in pathogen defense of *Arabidopsis*. Proc. Natl. Acad. Sci. USA **95**: 7209-7214.

Vogel, J., Raab, T. K., Somerville, C. R. and Somerville, S. C. (2004) Mutations in *PMR5* result in powdery mildew resistance and altered cell wall composition. Plant J. **40**: 968-978.

Vogel, J. and Somerville, S. (2000) Isolation and characterization of powdery mildew-resistant *Arabidopsis* mutants. Proc. Natl. Acad. Sci. USA **97**: 1897-1902.

Volko, S. M. (1998) Isolation and characterization of *Arabidopsis* mutants with altered disease susceptibility. PhD thesis. University of Basel, Basel, Switzerland.

von Arnim, A. G. (2003) On again – off again: COP9 signalosome turns the key on protein degradation. Curr. Opin. Plant Biol. **6**: 520–529.

Vorwerk, S., Somerville, S. and Somerville, C. R. (2004) The role of plant cell wall polysaccharide composition in disease resistance. Trends Plant Sci. **9**: 203-209.

Wagner, U., Edwards, R., Dixon, D. P. and Mauch, F. (2002) Probing the diversity of the Arabidopsis glutathione *S*-transferase gene family. Plant Mol. Biol. **49**: 515-532.

Wan, J., Zhang, S. and Stacey, G. (2004) Activation of a mitogen-activated protein kinase pathway in *Arabidopsis* by chitin. Mol. Plant Pathol. **5**: 125-135.

Wang, D., Amornsiripanitch, N. and Dong, X. (2006) A genomic approach to identify regulatory nodes in the transcriptional network of systemic acquired resistance in plants. PLoS Pathog. **2**: e123.

Wang, D., Weaver, N. D., Kesarwani, M. and Dong, X. (2005) Induction of protein secretory pathway is required for systemic acquired resistance. Science **308**: 1036-1040.

Wang, K. L., Li, H. and Ecker, J. R. (2002) Ethylene biosynthesis and signaling networks. Plant Cell Suppl. **14**: S131-S151.

Wang, M.-B. and Metzlaff, M. (2005) RNA silencing and antiviral defense in plants. Curr. Opin. Plant Biol. **8**: 216-222.

Weigel, R. R., Bäuscher, C., Pfitzner, A. J. P. and Pfitzner, U. M. (2001) NIMIN-1, NIMIN-2 and NIMIN-3, members of a novel family of proteins from *Arabidopsis* that interact with NPR1/NIM1, a key regulator of systemic acquired resistance in plants. Plant Mol. Biol. **46**: 143-160.

Welinder, K. G., Justesen, A. F., Kjærsgård, I. V. H., Jensen, R. B., Rasmussen, S. K., Jespersen, H. M. and Duroux, L. (2002) Structural diversity and transcription of class III peroxidases from *Arabidopsis thaliana*. Eur. J. Biochem. **269**: 6063-6081.

Whalen, M. C., Innes, R. W., Bent, A. F. and Staskawicz, B. J. (1991) Identification of *Pseudomonas syringae* pathogens of *Arabidopsis* and a bacterial locus determining avirulence on both *Arabidopsis* and soybean. Plant Cell **3**: 49-59.

Wiermer, M., Feys, B. J. and Parker, J. E. (2005) Plant immunity: the EDS1 regulatory node. Curr. Opin. Plant Biol. **8**: 383–389.

Wojtaszek, P. (1997) Oxidative burst: an early plant response to pathogen infection. Biochem. J. **322**: 681-692.

Woodward, A. W. and Bartel, B. (2005) Auxin: regulation, action, and interaction. Ann. Bot. **95**: 707-735.

Xiao, S. Y., Calis, O., Patrick, E., Zhang, G., Charoenwattana, P., Muskett, P. R., Parker, J. E. and Turner, J. G. (2005) The atypical resistance gene, *RPW8*, recruits components of basal defence for powdery mildew resistance in Arabidopsis. Plant J. **42**: 95-110.

Xie, D.-X., Feys, B. J., James, S., Nieto-Rostro, M. and Turner, J. G. (1998) COI1: an Arabidopsis gene required for jasmonate-regulated defense and fertility. Science **280**: 1091-1094.

Xie, Z., Johansen, L. K., Gustafson, A. M., Kasschau, K. D., Lellis, A. D., Zilberman, D., Jacobsen, S. E. and Carrington, J. C. (2004) Genetic and functional diversification of small RNA pathways in plants. PLoS Biology **2**: 0642-0652.

Xing, D. and Chen, Z. (2006) Effects of mutations and constitutive overexpression of *EDS1* and *PAD4* on plant resistance to different types of microbial pathogens. Plant Sci. **171**: 251-262.

Xu, Y., Chang, P., Liu, D., Narasimhan, M. L., Raghothama, K. G., Hasegawa, P. M. and Bressan, R. A. (1994) Plant defense genes are synergistically induced by ethylene and methyl jasmonate. Plant Cell **6**: 1077-1085.

Yamamoto, A., Katou, S., Yoshioka, H., Doke, N. and Kawakita, H. (2003) Nitrate reductase, a nitric oxide-producing enzyme: induction by pathogen signals. J. Gen. Plant Pathol. **69**: 218-229.

Yamasaki, H. (2000) Nitrite-dependent nitric oxide production pathway: implications for involvement of active nitrogen species in photoinhibition *in vivo*. Philos. Trans. R Soc. Lond. B Biol. Sci. **355**: 1477-1488.

Yang, S. and Hua, J. A. (2004) Haplotype-specific resistance gene regulated by BONZAI1 mediates temperature-dependent growth control in *Arabidopsis*. Plant Cell **4**: 1060-1071.

Young, N. D. (2000) The genetic architecture of resistance. Curr. Opin. Plant Biol. **3**: 285-290.

Yu, D., Chen, C. and Chen, Z. (2001) Evidence for an important role of WRKY DNA binding proteins in the regulation of *NPR1* gene expression. Plant Cell **13**: 1527-1539.

Yu, I.-c., Parker, J. E. and Bent, A. F. (1998) Gene-for-gene disease resistance without the hypersensitive response in *Arabidopsis dnd1* mutant. Proc. Natl. Acad. Sci. USA **95**: 7819-7824.

Yun, B.-W., Atkinson, H. A., Gaborit, C., Greenland, A., Read, N. D., Pallas, J. A. and Loake, G. J. (2003) Loss of actin cytoskeletal function and EDS1 activity, in combination, severely compromises non-host resistance in *Arabidopsis* against wheat powdery mildew. Plant J. **34**: 768-777.

Zeidler, D., Zähringer, U., Gerber, I., Dubery, I., Hartung, T., Bors, W., Hutzler, P. and Durner, J. (2004) Innate immunity in *Arabidopsis thaliana*: lipopolysaccharides activate nitric oxide synthase (NOS) and induce defense genes. Proc. Natl. Acad. Sci. USA **101**: 15811-15816.

Zeier, J., Delledonne, M., Mishina, T., Severi, E., Sonoda, M. and Lamb, C. (2004) Genetic elucidation of nitric oxide signaling in incompatible plant-pathogen interactions. Plant Physiol. **136**: 2875-2886.

Zhang, B., Ramonell, K., Somerville, S. and Stacey, G. (2002) Characterization of early, chitin-induced gene expression in *Arabidopsis*. Mol. Plant-Microbe Interact. **15**: 963-970.

Zhang, C., Czymmek, K. J. and Shapiro, A. D. (2003a) Nitric oxide does not trigger early programmed cell death events but may contribute to cell-to-cell signaling governing progression of the Arabidopsis hypersensitive response. Mol. Plant-Microbe Interact. **16**: 962-972.

Zhang, S. and Klessig, D. F. (2001) MAPK cascades in plant defense signaling. Trends Plant Sci. **6**: 520-527.

Zhang, Y., Goritschnig, S., Dong, X. and Li, X. (2003b) A gain-of-function mutation in a plant disease resistance gene leads to constitutive activation of downstream signal transduction pathways in *suppressor of npr1-1, constitutive 1*. Plant Cell **15**: 2636–2646.

Zhang, Y. and Li, X. (2005) A putative nucleoporin 96 is required for both basal defense and constitutive resistance responses mediated by *suppressor of npr1-1, constitutive 1*. Plant Cell **17**: 1306-1316.

Zhang, Y., Tessaro, M. J., Lassner, M. and Li, X. (2003c) Knockout analysis of Arabidopsis transcription factors TGA2, TGA5 and TGA6 reveals their redundant and essential roles in systemic acquired resistance. Plant Cell **15**: 2647-2653.

Zhao, J., Davis, L. C. and Verpoorte, R. (2005) Elicitor signal transduction leading to production of plant secondary metabolites. Biotechnol Adv. **23**: 283-333.

Zhao, J. and Last, R. L. (1996) Coordinate regulation of the tryptophan biosynthetic pathway and indolic phytoalexin accumulation in Arabidopsis. Plant Cell **8**: 2235-2244.

Zhao, Y., Thilmony, R., Bender, C. L., Schaller, A., He, S. Y. and Howe, G. A. (2003) Virulence systems of *Pseudomonas syringae* pv. *tomato* promote bacterial speck disease in tomato by targeting the jasmonate signaling pathway. Plant J. **36**: 485-499.

Zhou, N., Tootle, T. L. and Glazebrook, J. (1999) Arabidopsis PAD3, a gene required for camalexin biosynthesis, encodes a putative cytochrome P450 monooxygenase. Plant Cell **11**: 2419-2428.

Zhou, N., Tootle, T. L., Tsui, F., Klessig, D. F. and Glazebrook, J. (1998) *PAD4* functions upstream from salicylic acid to control defense responses in Arabidopsis. Plant Cell **10**: 1021–1030.

Zimmerli, L., Stein, M., Lipka, V., Schulze-Lefert, P. and Somerville, S. (2004) Host and nonhost pathogens elicit different jasmonate/ethylene responses in *Arabidopsis*. Plant J. **40**: 633-646.

Zimmermann, P., Hirsch-Hoffmann, M., Hennig, L. and Gruissem, W. (2004) GENEVESTIGATOR. Arabidopsis Microarray Database and Analysis Toolbox. Plant Physiol. **136**: 2621-2632.

Zimmermann, S., Nürnberger, T., Frachisse, J.-M., Wirtz, W., Guern, J., Hedrich, R. and Scheel, D. (1997) Receptor-mediated activation of a plant Ca^{2+}-permeable ion channel involved in pathogen defense. Proc. Natl. Acad. Sci. USA **94**: 2751-2755.

Zipfel, C. and Felix, G. (2005) Plants and animals: a different taste for microbes? Curr. Opin. Plant Biol. **8**: 353-360.

Zipfel, C., Kunze, G., Chinchilla, D., Caniard, A., Jones, J. D. G., Boller, T. and Felix, G. (2006) Perception of the bacterial PAMP EF-Tu by the receptor EFR restricts *Agrobacterium*-mediated transformation. Cell **125**: 749-760.

Zipfel, C., Robatzek, S., Navarro, L., Oakeley, E. J., Jones, J. D. G., Felix, G. and Boller, T. (2004) Bacterial disease resistance in *Arabidopsis* through flagellin perception. Nature **428**: 764-767.

Table 3.3 Recombination frequencies at specific marker positions on chromosome IV of 36 *cir1* homozygous plants

Markers with their corresponding annotation units and positions are shown. "C" and "L" indicates plants that are homozygous for Col-0 and L*er* respectively, while "H" is indicative of heterozygous plants. Some results could not be determined ("u").

Plant name	**nga8** T32A17[a] 5628810[b]	**F28M11a** F28M11 6342494	**Det1.1** T9A4 6346227	**F7L13a** F7L13 6452209	**T12H20a** T12H20 6589456	**T22B4a** T22B4 6732662	**F8L21a** F8L21 6898630	**F25E4a** F25E4 6955144	**T26M18a** T26M18 7157376	**T4C9a** T4C9 7342625	**T20K18a** T20K18 7485905	**CIW6** T6G15 7892620	**F18A5a** F18A5 8008121	**CM4-3** FCAALL 8046530	**g4539** FCAALL 9631258
2	H	C	C	C	C	C	C	C	C	C	C	C	C	C	C
4	C	C	C	C	C	C	C	C	C	C	C	C	C	C	C
7	C	C	C	C	C	C	C	C	C	C	C	C	C	C	C
11	C	C	C	C	C	C	C	C	C	C	C	C	C	C	C
14	C	C	C	C	C	C	C	C	C	C	C	C	C	C	C
15	C	C	C	C	C	C	C	C	C	C	C	H	H	H	C
16	C	C	u	C	C	C	C	C	C	C	C	C	C	C	u
20	C	C	C	C	C	C	C	C	C	C	C	C	C	C	H
23	C	C	C	C	C	C	C	C	C	C	C	C	C	C	C
27	C	C	C	C	C	C	C	C	C	C	C	C	C	C	C
29	C	C	C	C	C	C	C	C	C	C	C	C	C	C	C
33	C	C	C	C	C	C	C	C	C	C	C	C	C	C	u
34	C	C	C	C	C	C	C	C	C	C	C	C	C	C	H
37	H	C	C	C	C	C	C	C	C	C	C	C	C	u	H
38	C	C	C	C	C	C	C	C	C	C	C	C	C	C	C
40	C	C	C	C	C	C	C	C	C	C	C	C	C	C	C
41	C	C	C	C	C	C	C	C	C	C	C	C	C	C	C
46	C	C	C	C	C	C	C	C	C	C	C	C	H	H	H
48	C	C	C	C	C	C	C	C	C	C	C	C	C	C	C
76	H	H	H	H	H	H	H	H	H	H	H	H	H	H	H
77	C	C	C	C	C	C	C	C	C	C	C	C	C	C	H
81	C	C	C	C	C	C	C	C	C	C	C	C	C	C	C
87	C	C	C	C	C	C	C	C	C	C	C	C	C	C	H
90	H	C	C	C	C	C	C	C	C	C	C	C	C	C	C

Continued on next page

Table 3.3 **Continued from previous page**

Plant name	nga8 T32A17[a] 5628810[b]	F28M11a F28M11 6342494	Det1.1 T9A4 6346227	F7L13a F7L13 6452209	T12H20a T12H20 6589456	T22B4a T22B4 6732662	F8L21a F8L21 6898630	F25E4a F25E4 6955144	T26M18a T26M18 7157376	T4C9a T4C9 7342625	T20K18a T20K18 7485905	CIW6 T6G15 7892620	F18A5a F18A5 8008121	CM4-3 FCAALL 8046530	g4539 FCAALL 9631258
94	C	C	u	C	C	C	C	C	C	C	C	C	C	u	u
128	C	C	C	C	C	C	C	C	C	C	C	C	C	u	u
130	C	C	C	C	C	C	C	C	C	C	C	C	C	u	u
131	C	C	C	C	C	C	C	C	C	C	C	C	C	u	u
146	C	C	C	C	C	C	C	C	C	C	C	C	C	u	u
151	C	C	C	C	C	C	C	C	H	H	H	H	H	u	u
152	C	C	C	C	C	C	C	C	C	C	C	C	C	u	u
157	C	C	C	C	C	C	C	C	C	C	H	H	H	u	u
159	C	C	C	C	C	C	C	C	C	C	C	C	C	u	u
168	H	H	H	H	H	C	H	H	H	H	H	C	C	u	u
185	C	C	C	C	C	C	C	C	C	H	H	H	C	u	u
195	C	C	C	C	C	C	C	C	C	C	C	C	C	u	u
Total plants	36	36	34	36	36	36	36	36	36	36	36	36	36	23	22
Total chromosomes	72	72	68	72	72	72	72	72	72	72	72	72	72	46	44
% Rec[c]	**6.94**	**2.78**	**2.94**	**2.78**	**2.78**	**1.39**	**2.78**	**2.78**	**4.17**	**5.56**	**6.94**	**6.94**	**6.94**	**6.52**	**15.91**

[a] Annotation unit which corresponds to the TAIR BAC or P1 vector names on which the marker is situated.

[b] Position based on AGI map (The Arabidopsis Genome Initiative, 2000) in bp available from TAIR.

[c] "% Rec" represents percentage recombination and was calculated as number of recombinant chromosomes/total number of tested chromosomes.

A

```
Col-0       aacactcaaaagtagtaacaactaaga**ATG**GAAGATATCATCATCGGCGTGGTGGCTCTCGCCGCGGTTCTCCTTTTCTTCCTCTACCAAAAACCGAAAA  100
cir1_F      aacactcaaaagtagtaacaactaaga**ATG**GAAGATATCATCATCGGCGTGGTGGCTCTCGCCGCGGTTCTCCTTTTCTTCCTCTACCAAAAACCGAAAA
cir1_R      ····************************************************************************************

Col-0       CCAAACGGTACAAGCTACCTCCAGGGCCATCACCACTTCCGGTGATCGGAAACCTCCTTCAGCTTCAGAAGCTTAACCCACAACGCTTCTTCGCTGGATG  200
cir1_F      CCAAACGGTACAAGCTACCTCCAGGGCCATCACCACTTCCGGTGATCGGAAACCTCCTTCAGCTTCAGAAGCTTAACCCACAACGCTTCTTCGCTGGATG
cir1_R      ····************************************************************************************

Col-0       GGCCAAAAAATACGGTCCAATCTTGTCATACAGGATAGGAAGCAGAACAATGGTGGTGATATCTTCAGCTGAGCTAGCTAAAGAGCTTCTCAAGACGCAA  300
cir1_F      GGCCAAAAAATACGGTCCAATCTTGTCATACAGGATAGGAAGCAGAACAATGGTGGTGATATCTTCAGCTGAGCTAGCTAAAGAGCTTCTCAAGACGCAA
cir1_R      ····************************************AGCAGAACAATGGTGGTGATATCTTCAGCTGAGCTAGCTAAAGAGCTTCTCAAGACGCAA

Col-0       GATGTCAACTTTGCGGACCGGCCTCCACATCGTGGCCATGAGTTCATATCCTACGGCAGGCGTGACATGGCATTAAACCACTACACACCGTATTACCGAG  400
cir1_F      GATGTCAACTTTGCGGACCGGCCTCCACATCGTGGCCATGAGTTCATATCCTACGGCAGGCGTGACATGGCATTAAACCACTACACACCGTATTACCGAG
cir1_R      GATGTCAACTTTGCGGACCGGCCTCCACATCGTGGCCATGAGTTCATATCCTACGGCAGGCGTGACATGGCATTAAACCACTACACACCGTATTACCGAG

Col-0       AGATAAGGAAGATGGGGATGAACCACTTGTTCTCACCAACACGTGTGGCCACCTTTAAGCATGTACGAGAGGAAGAGGCTAGGAGGATGATGGATAAGAT  500
cir1_F      AGATAAGGAAGATGGGGATGAACCACTTGTTCTCACCAACACGTGTGGCCACCTTTAAGCATGTACGAGAGGAAGAGGCTAGGAGGATGATGGATAAGAT
cir1_R      AGATAAGGAAGATGGGGATGAACCACTTGTTCTCACCAACACGTGTGGCCACCTTTAAGCATGTACGAGAGGAAGAGGCTAGGAGGATGATGGATAAGAT

Col-0       CAACAAGGCCGCGGATAAATCCGAAGTAGTCGATATAAGTGAGCTTATGTTGACCTTCACGAACTCGGTTGTGTGTAGACAAGCGTTCGGGAAGAAGTAC  600
cir1_F      CAACAAGGCCGCGGATAAATCCGAAGTAGTCGATATAAGTGAGCTTATGTTGACCTTCACGAACTCGGTTGTGTGTAGACAAGCGTTCGGGAAGAAGTAC
cir1_R      CAACAAGGCCGCGGATAAATCCGAAGTAGTCGATATAAGTGAGCTTATGTTGACCTTCACGAACTCGGTTGTGTGTAGACAAGCGTTCGGGAAGAAGTAC

Col-0       AATGAAGATGGAGAAGAGATGAAGAGGTTCATCAAGATTCTTTATGGGACTCAAAGCGTTTTGGGGAAGATCTTTTTCTCTGATTTTTTCCCATATTGTG  700
cir1_F      AATGAAGATGGAGAAGAGATGAAGAGGTTCATCAAGATTCTTTATGGGACTCAAAGCGTTTTGGGGAAGATCTTTTTCTCTGATTT··············
cir1_R      AATGAAGATGGAGAAGAGATGAAGAGGTTCATCAAGATTCTTTATGGGACTCAAAGCGTTTTGGGGAAGATCTTTTTCTCTGATTTTTTCCCATATTGTG

Col-0       GCTTTCTTGATGATTTATCAGGCCTCACAGCTTATATGAAAGAGTGTTTCGAAAGACAAGACACTTATATTCAAGAGGTTGTCAATGAGACGCTTGATCC  800
cir1_F      ····************************************************************************************
cir1_R      GCTTTCTTGATGATTTATCAGGCCTCACAGCTTATATGAAAGAGTGTTTCGAAAGACAAGACACTTATATTCAAGAGGTTGTCAATGAGACGCTTGATCC

Col-0       TAAGAGAGTCAAGCCCGAAACCGAGAGCATGATTGATCTCTTGATGGGGATCTACAAAGAACAACCTTTCGCTTCTGAGTTTACTGTAGATAATGTCAAA  900
cir1_F      ····************************************************************************************
cir1_R      TAAGAGAGTCAAGCCCGAAACCGAGAGCATGATTGATCTCTTGATGGGGATCTACAAAGAACAACCTTTCGCTTCTGAGTTTACTGTAGATAATGTCAAA

Col-0       GCCGTCATCTTG                                                                                        912
cir1_F      ···********
cir1_R      GCCGTCATCTTG
```

B

```
Col-0       GATATTGTAGTGGCGGGAACAGATACTGCAGCTGCGGCGGTTGTGTGGGGGATGACGTATCTAATGAAGTACCCACAAGTGTTGAAGAAAGCTCAAGCAG  100
cir1_F      GATATTGTAGTGGCGGGAACAGATACTGCAGCTGCGGCGGTTGTGTGGGGGATGACGTATCTAATGAAGTACCCACAAGTGTTGAAGAAAGCTCAAGCAG
cir1_R      ····************************************************************************************

Col-0       AAGTGAGAGAGTATATGAAAGAGAAAGGTTCAACGTTCGTTACTGAAGACGATGTCAAGAACCTTCCTTACTTCAGAGCCTTAGTTAAAGAAACCCTAAG  200
cir1_F      AAGTGAGAGAGTATATGAAAGAGAAAGGTTCAACGTTCGTTACTGAAGACGATGTCAAGAACCTTCCTTACTTCAGAGCCTTAGTTAAAGAAACCCTAAG
cir1_R      ····************************************************************************CCTAAG

Col-0       GATCGAACCAGTGATTCCTCTCCTTATCCCTCGTGCTTGCATTCAAGATACCAAGATCGCCGGTTACGACATCCCCGCAGGAACAACGGTCAACGTCAAC  300
cir1_F      GATCGAACCAGTGATTCCTCTCCTTATCCCTCGTGCTTGCATTCAAGATACCAAGATCGCCGGTTACGACATCCCCGCAGGAACAACGGTCAACGTCAAC
cir1_R      GATCGAACCAGTGATTCCTCTCCTTATCCCTCGTGCTTGCATTCAAGATACCAAGATCGCCGGTTACGACATCCCCGCAGGAACAACGGTCAACGTCAAC

Col-0       GCGTGGGCCGTGTCACGTGACGAGAAAGAATGGGGACCGAACCCTGATGAGTTTAGGCCCGAGAGGTTTCTTGAGAAGGAAGTTGACTTCAAAGGCACGG  400
cir1_F      GCGTGGGCCGTGTCACGTGACGAGAAAGAATGGGGACCGAACCCTGATGAGTTTAGGCCCGAGAGGTTTCTTGAGAAGGAAGTTGACTTCAAAGGCACGG
cir1_R      GCGTGGGCCGTGTCACGTGACGAGAAAGAATGGGGACCGAACCCTGATGAGTTTAGGCCCGAGAGGTTTCTTGAGAAGGAAGTTGACTTCAAAGGCACGG

Col-0       ACTACGAGTTTATACCGTTCGGGTCAGGCCGGAGAATGTGCCCGGGAATGCGTCTTGGGGCCGCGATGCTTGAGGTTCCTTATGCGAACCTTCTCCTCAG  500
cir1_F      ACTACGAGTTTATACCGTTCGGGTCAGGCCGGAGAATGTGCCCGGGAATGCGTCTTGGGGCCGCGATGCTTGAGGTTCCTTATGCGAACCTTCTCCTCAG
cir1_R      ACTACGAGTTTATACCGTTCGGGTCAGGCCGGAGAATGTGCCCGGGAATGCGTCTTGGGGCCGCGATGCTTGAGGTTCCTTATGCGAACCTTCTCCTCAG

Col-0       CTTCAACTTTAAACTTCCTAATGGGATGAAACCAGATGATATCAATATGGATGTCATGACTGGTCTTGCTATGCACAAGTCGCAGCATCTCAAGCTTGTT  600
cir1_F      CTTCAACTTTAAACTTCCTAATGGGATGAAACCAGATGATATCAATATGGATGTCATGACTGGTCTTGCTATGCACAAGTCGCAGCATCTCAAGCTTGTT
cir1_R      CTTCAACTTTAAACTTCCTAATGGGATGAAACCAGATGATATCAATATGGATGTCATGACTGGTCTTGCTATGCACAAGTCGCAGCATCTCAAGCTTGTT

Col-0       CCAGAGAAAGTGAACAAGTAT**TAG**ctaatatatatcaataaatctaccttctctgattatatagtatatgttcctccagtgtattctgtttcaatgtttg  700
cir1_F      CCAGAGAAAGTGAACAAGTAT**TAG**ctaatatatatcaataaatctaccttctctgattatatagt····************************
cir1_R      CCAGAGAAAGTGAACAAGTAT**TAG**ctaatatatatcaataaatctaccttctctgattatatagtatatgttcctccagtgtattctgtttcaatgtttg

Col-0       gtttctttcttaaatggcaatcgtctctctatctttctcttcacattttgatatgaaggaagcaaattcacatgatgtcttttgtgatccttatatatttt  800
cir1_F      ····************************************************************************************
cir1_R      gtttctttcttaaatggcaatcgtctctctatctttctcttcacattttgatatgaaggaagcaaattcacatgatgtcttttgtgatccttatatatttt

Col-0       cactgaatggctacaaaaat                                                                              820
cir1_F      ····················
cir1_R      cactgaatggctacaaaaat
```


Figure 3.10. DNA sequence alignment of the two exons of *CYP83A1* (At4g13770) in Col-0 and *cir1*.

The two exons of *CYP83A1* were amplified from *cir1* genomic DNA, sequenced and aligned with the Col-0 sequence available form TAIR. (**A**) The first exon comprise 912 bp including the 5' untranslated region (UTR) which is indicated by small case letters. (**B**) The second exon consists of 820 bp including the 3' UTR which is represented by small case letters. **ATG** and **TAG** represent the start and stop codons of the coding sequence, respectively. Both exons were sequenced using forward and reverse primers, indicated by "F" and "R" respectively.